



**NANYANG  
TECHNOLOGICAL  
UNIVERSITY**

**ASYMMETRIC SYNTHESIS OF CHIRAL PHOSPHINES  
AND ARSINES PROMOTED BY ORGANOMETALLIC  
COMPLEXES**

**LIU FENGLI**

**SCHOOL OF PHYSICAL AND MATHEMATICAL  
SCIENCES**

**2010**



**Asymmetric Synthesis of Chiral Phosphines and Arsines  
Promoted by Organometallic Complexes**

**Liu Fengli**

*(B.Sc., M.Sc.)*

School of Physical and Mathematical Sciences

A thesis submitted to the Nanyang Technological University

In fulfillment of the requirement for the degree of

Doctor of Philosophy in Chemistry

**2010**

## **Acknowledgements**

I would like to express my sincere gratitude to my supervisor, Professor Leung Pak-Hing, whose unquenchable curiosity and love for the subject are probably the most valuable lessons I have learned from this PhD, and his continual support, encouragement and cheerfulness have kept me going over the duration of this project. He has given me enormous freedom to pursue my interests while at the same time providing just the right amount of guidance.

I would like to extend my gratitude to Dr. Li Yongxin for performing the X-ray Crystallography, for Ms. Cheong Shu Qi for the Elemental Analysis and for Ms. Eeling from the NMR lab, their prompt service and dedication helped me a lot.

I am also thankful to Sumod, Ben, Yongxin, Shuli, Lulu, Zhang Yi, Luo Ding, Mengtao, Dingyi, for their kindly suggestions and invaluable discussion on my project and all my juniors Minyi, Mingjun, Yinhua, Deepa, Chen Ke and Cheow for being an inspiration through their enthusiasm in work.

I would also like to acknowledge the Nanyang Technological University for awarding me a research scholarship to pursue my doctorate degree.

Last but not least, my deepest gratitude must go to my family, for their supports in my pursuit of a Ph.D. degree.

## TABLE OF CONTENTS

<b>Acknowledgements</b> .....	i
<b>Nomenclature, X-ray Structural Data, Abbreviations and Symbols</b> .....	ix
<b>Summary</b> .....	xiv
<b>Chapter 1</b>	
<b><i>General Introduction</i></b>	
1.1 Chiral Phosphines.....	1
1.1.1 A Classification of Chiral Phosphines and their Synthesis.....	2
1.1.1.1 <i>P</i> -Chiral Phosphines.....	2
1.1.1.2 Phosphines with Chiral Carbon Backbones.....	13
1.1.2 Chiral Phosphine Transition Metal Complexes in Asymmetric Catalysis..	19
1.1.2.1 Asymmetric Hydrogenation.....	19
1.1.2.2 Asymmetric Hydrosilylation Reaction.....	21
1.1.2.3 Asymmetric Allylic Substitution.....	23
1.1.2.4 Asymmetric Heck Reaction.....	24
1.1.2.5 Other Reactions.....	25
1.2 Arsine Ligands.....	26
1.2.1 Achiral Arsine Ligands.....	26
1.2.2 Chiral Arsines.....	27
1.2.2.1 Preparation of Chiral Arsine Ligands.....	28

1.2.3 Application of Chiral Arsine Ligands.....	31
1.3 The Two Important Chiral Templates Used in the Project.....	34
1.3.1 Asymmetric [2+2] Cycloaddition.....	35
1.3.2 Oxidative Coupling Reaction.....	36
1.3.3 Asymmetric Hydroamination Reaction.....	37
1.3.4 Asymmetric Hydrophosphination Reaction.....	38
1.3.5 Asymmetric Hydroarsination Reaction.....	40
1.4 Aims of the Present Project.....	41

## Chapter 2

### *3-Substituted Furan as Diene in Asymmetric Diels-Alder Reaction*

2.1 Introduction.....	43
2.2 Results and Discussion.....	47
2.2.1 Intramolecular <i>Endo</i> -Diels-Alder Reaction between 3-Diphenylphosphino- furan and Diphenylvinylphosphine.....	47
2.2.1.1 X-ray Structural Analysis of <i>endo</i> - <b>114</b> .....	49
2.2.1.2 Liberation and the Optical Purity of <i>endo</i> - <b>115</b> .....	51
2.2.1.3 Reoordination <i>endo</i> - <b>115</b> to ( <i>R</i> )- <b>117</b> and ( <i>S</i> )- <b>117</b> .....	52
2.2.1.4 X-ray Structural Analysis of <i>endo</i> - <b>116b</b> .....	54
2.2.2 Intramolecular <i>Endo</i> -Diels-Alder Reaction between 3-Diphenylphosphino- furan and Diphenyl[( <i>E</i> )-2-(ethoxycarbonyl)vinyl]phosphine.....	56
2.2.2.1 X-ray Structural Analysis of <i>endo</i> - <b>119</b> .....	58
2.2.2.2 Liberation and the Optical Purity of <i>endo</i> - <b>120</b> .....	60

2.2.3 Intramolecular <i>Endo</i> -Diels-Alder Reaction between 3-Diphenylphosphino- furan and Phenyldivinylphosphine.....	61
2.2.3.1 X-ray Structural Analysis of <i>endo</i> - <b>122a</b> .....	63
2.2.3.2 Preparation of the Dichloro Complex <i>endo</i> - <b>123</b> .....	64
2.2.3.3 X-ray Structural Analysis of <i>endo</i> - <b>123</b> .....	66
2.2.3.4 Liberation and the Optical Purity of <i>endo</i> - <b>124</b> .....	68
2.2.3.5 Preparation of the Dichloro Complex <i>endo</i> - <b>126a,b</b> .....	70
2.2.3.6 X-ray Structural Analysis of <i>endo</i> - <b>126a,b</b> .....	71
2.2.4 Intramolecular <i>Endo</i> -Diels-Alder Reaction between Bis-(3-furyl) phenyl- phosphine And Diphenylvinylphosphine.....	72
2.2.4.1 Preparation of Chloro Complex ( <i>R</i> )- <b>127</b> .....	73
2.2.4.2 Single Crystal X-ray Diffraction Studies on ( <i>R</i> )- <b>127</b> .....	73
2.2.4.3 Asymmetric Diels-Alder Reaction involving ( <i>R</i> )- <b>127</b> and Diphenyl- Vinylphosphine.....	74
2.2.4.4 X-ray Structural Analysis of <i>endo</i> - <b>129</b> .....	76
2.2.4.5 Liberation and the Optical Purity of <i>endo</i> - <b>130</b> .....	79
2.3 Conclusion.....	80
2.4 Experimental Section.....	81
<b>Chapter 3</b>	
<b><i>3-Diphenylphosphinofuran as Dienophile in Asymmetric Diels-Alder Reaction</i></b>	
3.1 Introduction.....	92
3.2 Results and Discussion.....	96

3.2.1 Asymmetric Diels-Alder Reaction involving 3-Diphenylphosphino- furan and 1-phenyl-3,4-dimethylphosphole.....	96
3.2.2 X-ray Structural Analysis of ( $R_C,S_P$ )- <b>138b</b> .....	98
3.2.3 Preparation of Dichloro Complexes for ( $S_P$ )- <b>139</b> and ( $S_P$ )- <b>140</b> .....	100
3.2.4 X-ray Structural Analysis of ( $R_C,S_P$ )- <b>139</b> .....	101
3.2.5 Liberation and the Optical Purity of ( $R_P$ )- <b>141</b> .....	102
3.2.6 X-ray Structural Analysis of ( $S_P$ )- <b>140</b> .....	103
3.2.7 Preparation of the Diiodo Complex ( $S_P$ )- <b>142</b> .....	105
3.2.8 X-ray Structural Analysis of ( $S_P$ )- <b>142</b> .....	105
3.2.9 Liberation and the Optical Purity ( $S_P$ )- <b>140</b> .....	107
3.2.10 The Role of the Platinum Template.....	107
3.3 Conclusion.....	109
3.4 Experimental Section.....	109

## Chapter 4

### *Asymmetric Hydrophosphination Reaction*

4.1 Introduction.....	115
4.2 Results and Discussion.....	116
4.2.1 Hydrophosphination of ( $E$ )-1-Phenyl-3-pyridin-2-yl-propenone.....	116
4.2.1.1 Single Crystal X-ray Structural Analysis of ( $R$ )- <b>146</b> .....	118
4.2.1.2 Liberation and the Optical Purity of ( $R$ )- <b>147</b> .....	120
4.2.2 Hydrophosphination of ( $E$ )-1-naphthyl-3-pyridin-2-yl-propenone.....	121
4.2.2.1 Single Crystal X-ray Structural Analysis of ( $R_C,S_C$ )- <b>148</b> .....	122

4.2.2.2 Liberation and the Optical Purity of ( <i>R</i> )- <b>150</b> .....	124
4.2.3 Hydrophosphination of ( <i>E</i> )-1-Thiophthyl-3-pyridin-2-yl-propenone .....	125
4.2.3.1 Single Crystal X-ray Structural Analysis of ( <i>R<sub>C</sub></i> , <i>S<sub>C</sub></i> )- <b>151</b> .....	125
4.2.3.2 Two Dimensional <sup>1</sup> H- <sup>1</sup> H ROESY NMR of ( <i>R<sub>C</sub></i> , <i>S<sub>C</sub></i> )- <b>151</b> .....	128
4.2.3.3 Liberation and the Optical Purity of ( <i>R</i> )- <b>153</b> .....	129
4.2.4 Hydrophosphination of ( <i>E</i> )-1-Methyl-3-pyridin-2-yl-2-propenoate.....	130
4.2.4.1 Single Crystal X-ray Structural Analysis of ( <i>R<sub>C</sub></i> , <i>S<sub>C</sub></i> )- <b>154</b> .....	131
4.2.4.2 Liberation and the Optical Purity of ( <i>S<sub>C</sub></i> )- <b>156</b> .....	133
4.2.5 Hydrophosphination of ( <i>E</i> )-1-Phenyl-3-quinolin-2-yl-2-propenone.....	134
4.2.5.1 Single Crystal X-ray Structural Analysis of ( <i>R<sub>C</sub></i> , <i>S<sub>C</sub></i> )- <b>157</b> .....	135
4.2.5.2 Liberation and the Optical Purity of ( <i>S<sub>C</sub></i> )- <b>158</b> .....	136
4.2.6 Mechanistic Considerations.....	137
4.3 Experimental Section.....	141

## Chapter 5

### *Asymmetric Hydroarsination Reaction*

5.1. Introduction.....	150
5.2. Results and Discussion.....	151
5.2.1 Hydroarsination of ( <i>E</i> )-1-Phenyl-3-pyridin-2-yl-2-propenone.....	151
5.2.1.1 Single Crystal X-ray Structural Analysis of ( <i>R</i> )- <b>161</b> .....	153
5.2.1.2 Liberation and the Optical Purity of ( <i>R</i> )- <b>162</b> .....	155
5.2.2 Hydroarsination of ( <i>E</i> )-1-Naphthyl-3-pyridin-2-yl-2-propenone.....	156
5.2.2.1 Single Crystal X-ray Structural Analysis of ( <i>R</i> )- <b>164</b> .....	158

5.2.2.2 Liberation and the Optical Purity of ( <i>R</i> )- <b>165</b> .....	159
5.2.3 Hydroarsination of ( <i>E</i> )-1-Methyl-3-pyridin-2-yl-2-propenate.....	160
5.2.3.1 Single Crystal X-ray Structural Analysis of ( <i>R<sub>C</sub>,S<sub>C</sub></i> )- <b>166</b> .....	161
5.2.3.2 Liberation and the Optical Purity of ( <i>S</i> )- <b>168</b> .....	163
5.2.4 Mechanistic Considerations.....	164
5.3. Conclusion.....	167
5.4 Experimental Section.....	167
<b>Chapter 6</b>	
<b>Asymmetric Hydrophosphination Reaction of Phosphinoalkynes</b>	
6.1 Introduction .....	173
6.2 Results and Discussion.....	175
6.2.1 Hydrophosphination of Diphenyl(phenylethynyl)phosphine.....	175
6.2.1.1. Single Crystal X-ray Structural Analysis of ( <i>R<sub>C</sub>,R<sub>P</sub></i> )- <b>173</b> .....	176
6.2.1.2 Preparation of the Dichloro Complex ( <i>S<sub>P</sub></i> )- <b>174</b> .....	178
6.2.1.3 X-ray Structural Analysis of ( <i>S<sub>P</sub></i> )- <b>174</b> .....	178
6.2.1.4 Liberation and the Optical Purity of ( <i>R<sub>P</sub></i> )- <b>175</b> .....	180
6.2.2 Hydrophosphination of Di(phenylethynyl)phenylphosphine .....	181
6.2.2.1 Single Crystal X-ray Structural Analysis of ( <i>R<sub>P</sub>,R<sub>P</sub></i> )- <b>177</b> .....	183
6.2.2.2 Liberation and the Optical Purity of ( <i>S<sub>P</sub>,S<sub>P</sub></i> )- <b>178</b> .....	185
6.3 Conclusion.....	186
6.4 Experimental Section.....	186
<b>References</b> .....	190

<b>Publications</b> .....	213
<b>Appendices</b> .....	214

## Nomenclature

The nomenclature used throughout the thesis conforms to the format adopted by Chemical Abstracts (Chemical Abstracts, 13<sup>th</sup> Collective Index, Index Guide, 1992-1996).

## X-ray Structural Data

The X-ray structural analyses were kindly carried out by Dr. Li Yongxin at the Nanyang Technological University (Division of Chemistry and Biological Chemistry).

## Abbreviations and Symbols

An	anisoyl
Ar	aryl
ax	axial
BICP	(2, 2')-bis(diphenylphosphino)-(1,1')-dicyclopentane
BINAP	2,2'-bis(diphenylphosphino)-1,1'-binaphthyl
Bn	benzyl
Bu	butyl
br	broad
bp	boiling point
<i>ca.</i>	about (Latin <i>circa</i> )
calcd	calculated
CHIRAPHOS	2, 3-bis(diphenylphosphino)butane

cod	cyclooctadiene-1,5-diene
conc.	concentrated
Cy	cyclohexyl
d	doublet, day(s)
dd	doublet of a doublet
dt	doublet of a triplet
de	diastereomeric excess
decomp.	Decomposed
deg	degree(s)
DIOP	2,3- <i>O</i> -isopropylidene-2,3-dihydroxy-1,4-bis(diphenylphosphino) butane
DIPAMP	1,2-bis[( <i>o</i> -methoxyphenyl)phenylphosphino]ethane
dm	decimeter
DMPP	3,4-dimethyl-1-phenylphosphole
dppe	1,2-bis(diphenylphosphino)ethane
Duphos	1,2-bis(2,5-dimethylphospholano)benzene
ee	enantiomeric excess
eq	equatorial
Et-FerroTANE	1,1'-bis-2,4-diethylphosphotano)ferrocene
Et	ethyl
<i>et. al.</i>	and others (Latin <i>alii</i> )
g	gram(s)

h	hour(s)
Hex	hexyl
Hz	hertz
<i>i.e.</i>	that is (Latin <i>id est</i> )
<i>i</i>	iso
Josiphos	1-[2-(diphenylphosphino)ferrocenyl]ethylcyclohexylphosphine ethanol adduct
LDA	lithium diisopropylamide
m	multiplet
<i>m</i>	<i>meta</i>
Me	methyl
Men	menthyl
Meo-PIPHEP	2,2'-bis(diphenylphosphino)-6,6'-dimethoxy-1,1'-biphenyl
min	minute(s)
MONOPHOS	8,9,10,11,12,13,14,15-octahydro-3,5-dioxa-4-(phosphacyclohepta [2,1-a;3,4-a']dinaphthalen-4-yl)dimethylamine
MOP	2-(diphenylphosphino)-2'-methoxy-1,1'-binaphthyl
mp	melting point
<i>n</i>	straight chain
NMR	Nuclear Magnetic Resonance
NOE	Nuclear Overhauser Effect
NORPHOS	2,3-bis(diphenylphosphino)norbornane

<i>o</i>	<i>ortho</i>
<i>p</i>	<i>para</i>
PAMP	( <i>o</i> -methoxyphenyl)methylphenylphosphine
Pr	propyl
Ph	phenyl
<sup>31</sup> P NMR	<sup>31</sup> P { <sup>1</sup> H} NMR
PHOX	phosphinooxazolines
ppm	parts per million
PYRPHOS	bis-(diphenylphosphino)-1-benzylpyrrolidine
q	quartet
qn	quintet
r.t.	room temperature
<i>R</i>	<i>rectus</i> (Latin: right absolute configuration)
ROESY	2D rotating frame Nuclear Overhauser Enhancement
<i>S</i>	<i>sinister</i> (Latin: left absolute configuration)
s	singlet
<i>s</i>	secondary
SEGPPOS	5,5'-bis(diphenylphosphino)-4,4'-bi-1,3-benzodioxole
t	triplet
<i>t</i>	tertiary
THF	tetrahydrofuran
tol	tolyl

$\text{\AA}$	angstrom(s)
$\delta$	NMR chemical shift in ppm
$[\alpha]_D$	specific rotation measured at sodium D line (589 nm)

## Summary

This thesis describes the development of chiral cyclometalated-amine templates promoted asymmetric reactions such as the Diels-Alder, hydrophosphination and hydroarsination reactions for the synthesis of chiral phosphine and chiral arsine ligands.

The [4+2] Diels-Alder reactions involving 3-diphenylphosphinofuran and three phosphine functionalized dienophiles viz. diphenylvinylphosphine, diphenyl[(*E*)-2-(ethoxycarbonyl)vinyl]phosphine and divinylphenylphosphine were carried out by employing platinum complexes containing the *ortho* metalated (*R*)-(1-(dimethylamino)ethyl)naphthalene (*R*)-**86** as the chiral template to generate the *endo*-cycloadducts. In chapter 1 the cycloaddition reaction between diphenylvinylphosphine and di-(3-furyl)phenylphosphine is also presented. The chiral naphthylamine auxiliary in the isolated chelating diphosphine *endo*-cycloadduct metal template complexes could be removed chemoselectively by treatment with concentrated sulfuric acid, during which the oxanorbornene skeleton of the diphosphine metal complexes is inert to the acid treatment. Further ligand liberation from the resultant dichloro complexes using aqueous cyanide gave the free bis(diphenylphosphino)-substituted cycloadduct ligands which are air stable.

The asymmetric [4+2] Diels-Alder reaction involving 3-diphenylphosphinofuran as the dienophile and 3,4-dimethyl-1-phenylphosphole, DMPP, as the cyclic diene was carried out by utilizing the platinum(II) template complex (*R*)-**86** as the chiral

auxiliary. Two (*S<sub>P</sub>*)-*exo* cycloadducts were obtained with high stereoselectivity as P-P bidentate chelates on the platinum template. The chiral naphthylamine auxiliary was subsequently removed by treatment with concentrated hydrochloric acid to form three dichloroplatinum(II) complexes in which two products were from the acid hydrolysis of vinyl ether. Benzoylation of the hemiacetals only gave one product. The absolute configurations and the coordination properties of the *P*-chiral cycloadducts have been established by single-crystal X-ray analysis.

The organopalladium complex (*R*)-**144** as the chiral auxiliary has also been used to promote the asymmetric hydrophosphination reactions of diphenylphosphine with (*E*)-1-phenyl-3-pyridin-2-yl-2-propenone, (*E*)-1-naphthyl-3-pyridin-2-yl-2-propenone, (*E*)-1-thiophenyl-3-pyridin-2-yl-2-propenone, (*E*)-1-methyl-3-pyridin-2-yl-2-propenoate and (*E*)-1-phenyl-3-quinolin-2-yl-2-propenone in high regio- and stereoselectivities under mild conditions. Hydrophosphination of (*E*)-1-phenyl-3-pyridin-2-yl-2-propenone, (*E*)-1-naphthyl-3-pyridin-2-yl-2-propenone, (*E*)-1-thiophenyl-3-pyridin-2-yl-2-propenone with diphenylphosphine generated two stereoisomeric products as five-membered 2-pyridylphosphine P-N bidentate chelates on the chiral naphthylamine palladium template. Using the same chiral metal template, the corresponding hydrophosphination reactions of (*E*)-1-methyl-3-pyridin-2-yl-2-propenoate and (*E*)-1-phenyl-3-quinolin-2-yl-2-propenone only gave one product as a six-membered P-N bidentate chelate. The naphthylamine auxiliary could be removed chemoselectively from the template product by treatment with concentrated hydrochloric acid to form the corresponding

optically pure neutral complexes. Subsequent ligand displacement from the palladium achieved using aqueous potassium cyanide generated the optically pure keto- and ester-functionalized chiral P-N ligands in high yields.

The asymmetric hydroarsination reactions between diphenylarsine and (*E*)-1-phenyl-3-pyridin-2-yl-2-propenone, (*E*)-1-naphthyl-3-pyridin-2-yl-2-propenone and (*E*)-1-methyl-3-pyridin-2-yl-2-propenoate have been achieved by use of the organopalladium complex (*R*)-**144** as the chiral reaction template in high regio- and stereoselectivities under mild conditions. Hydroarsination of (*E*)-1-phenyl-3-pyridin-2-yl-2-propenone and (*E*)-1-naphthyl-3-pyridin-2-yl-2-propenone with diphenylarsine generated two stereoisomeric products in the ratio of 3:1 as five-membered As-N bidentate chelates on the chiral naphthylamine palladium template. Using the same chiral metal template, the corresponding hydrophosphination reaction with (*E*)-1-methyl-3-pyridin-2-yl-2-propenoate only gave one product as a six-membered As-N bidentate chelate. The naphthylamine auxiliary could be removed chemoselectively by treatment with concentrated hydrochloric acid to form the corresponding optically pure neutral complexes. Subsequent ligand displacement from the palladium using aqueous potassium cyanide generated the optically pure keto- and ester-functionalized chiral pyridylarsine ligands.

The application of chiral cyclometalated-amine template for the asymmetric hydrophosphination involving methylphenylphosphine and ethynylphosphines viz. diphenyl(phenylethynyl)phosphine and di(phenylethynyl)phenylphosphine were

established. The reactions resulted in the formation of *P*-chiral diphosphine ligands, while the diastereoselectivity of the reactions was low.

# Chapter 1

## General Introduction

### 1.1 Chiral Phosphines

Biologically active compounds, such as pharmaceuticals, agrochemicals, fragrances, and flavors as well as functional materials, are indispensable in our daily life.<sup>1</sup> Many biological functions of these key molecules arise from specific molecular and chirality recognition. So preparation of optically active substances is a substantial challenging work for chemists in both academia and industry. It is necessary to pile up of optically active building blocks, which must be with suitable configuration, functionality, and conformational rigidity or flexibility to generate the desired stereoselectivity in the target complex.<sup>1</sup> In meeting the demand, asymmetric synthesis has become to the most attractive approach that is on a par with other methods, including optical and enzymatic resolutions.<sup>2</sup>

Enantiomerically pure phosphines have attracted great interest in transition metal catalyzed asymmetric reactions.<sup>3</sup> Phosphine ligands with a lone pair of electrons can be as Lewis bases and ligate to metals. Experience has shown that complexes including “soft” phosphine ligands and “soft” metals such as rhodium, ruthenium, palladium or iridium are sufficiently stable and can act as catalysts. Due to the  $\sigma$ -donating and  $\pi$ -accepting properties of the phosphine ligands, they can be used for electronic “fine tuning” of the catalyst. An important advantage of phosphine ligands over related N- or O-ligands is their facile characterization by <sup>31</sup>P NMR spectroscopy.

This method can give a fast and comprehensive characterization of synthetic intermediates, ligands and metal complexes and even make some insight into the mechanism of catalytic processes possible.<sup>3d</sup>

In 1968 Knowles<sup>4</sup> and Horner<sup>5</sup> reported that asymmetric hydrogenation was possible by replacing the triphenylphosphine ligands of the Wilkinson's catalyst  $[\text{RhCl}(\text{PPh}_3)_3]$  with *P*-chiral monophosphines, albeit with poor enantioselectivity. Following this, numerous enantiomerically pure phosphines have been prepared<sup>6</sup> and asymmetric hydrogenation of alkenes, ketones and imines can be achieved in high enantioselectivity.<sup>3</sup> Apart from hydrogenation, chiral phosphines have also been used successfully in other asymmetric catalytic reactions such as allylic substitution, Hydrosilylation, Heck reaction, hydroboration, hydrogen transfer on ketones et al.<sup>3</sup> The design and synthesis of chiral phosphine ligands have played an important role in the development of asymmetric synthesis.

### **1.1.1 A Classification of Chiral Phosphines and Their Syntheses**

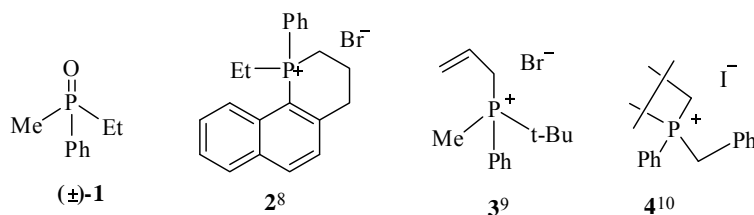
Chiral phosphine ligands can be divided into two groups: phosphines with chiral phosphorus centres and with chiral carbon backbones.

#### **1.1.1.1 *P*-Chiral Phosphines**

##### **A. Preparation by Resolution of Racemates**

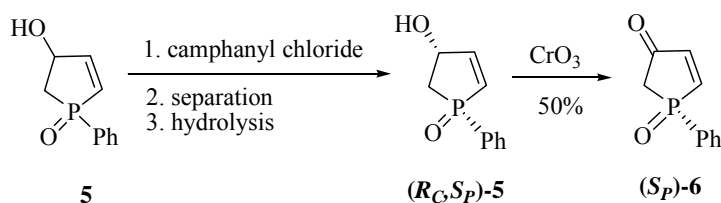
The classical methods to prepare *P*-chiral phosphines usually involve resolution as a critical step. The first known optically active organophosphorus

compound, ethylmethylphenylphosphine oxide (**1**), was obtained by direct resolution with (+)-bromocamphorsulfonic acid to form the separable diastereomeric salts.<sup>7</sup>



Typically, the resolution of phosphonium salts was performed by combining the racemate with the silver salt of a chiral acid, for example, enantiomeric silver menthoxyacetates<sup>8</sup> and silver camphorsulfonates<sup>11</sup>. Phosphonium salts **2-4** are some of the examples that were resolved using this method. Subsequent electrolytic reduction of the resolved phosphonium salts gave the corresponding phosphines with retention of configuration at phosphorus.

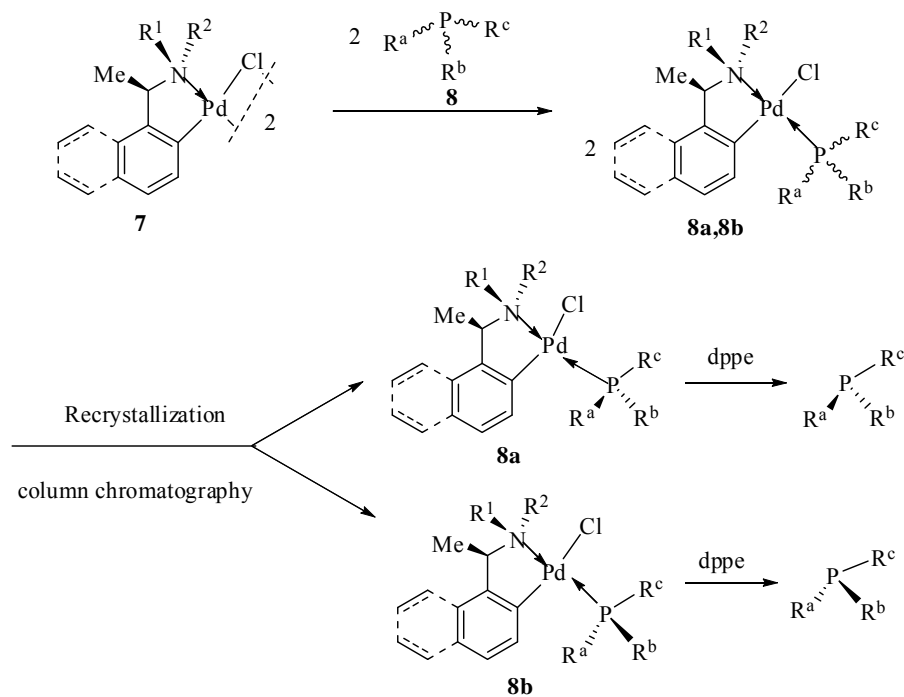
A typical method for the resolution of racemic phosphorus compounds involves the formation of covalent diastereomers. To obtain enantiomeric 4-oxo-1-phenyl-2-phospholene-1-oxide **6**, Bodalski and co-workers<sup>12</sup> resolved its 4-hydroxy precursor **5** via the formation of diastereomeric esters with (-)- $\omega$ -camphanic acid. (*R<sub>C</sub>,S<sub>P</sub>*)-**5** was obtained by fractional crystallization and, by hydrolysis, was subsequently converted into the desired ketophospholene oxide **6** (Scheme 1.1).



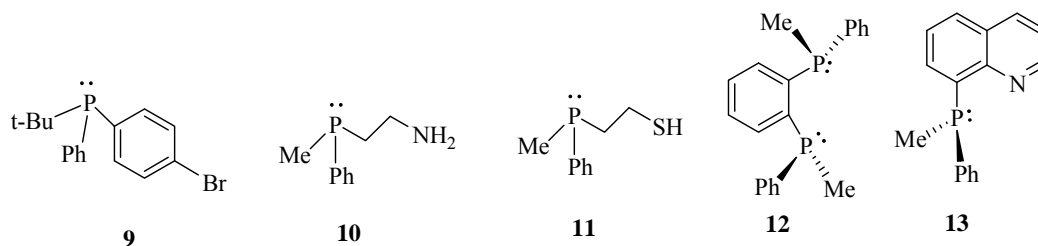
**Scheme 1.1**

Chiral palladium (II) complexes derived from enantiomeric 1-phenylethylamines and 1-naphthylethylamines<sup>13,14</sup> are effective resolving agents for certain types of phosphines.<sup>15</sup> The desired racemic phosphine is made to react with the cyclometallated dimer **7** and gives a pair of mononuclear complexes **8** in 1:1 (sometimes, 0.5 equiv of the resolving agents is used and one enantiomer works while the unreacted excess one remains in solution). Complexes **8** are diastereomeric and can be separated by column chromatography or recrystallization. After separated, the phosphine is displaced from the palladium by means of dppe or another strongly coordinating agent to give the desired enantiomerically pure phosphine. This method has been widely used to resolve monodentate and bidentate phosphines such as **9-13**.

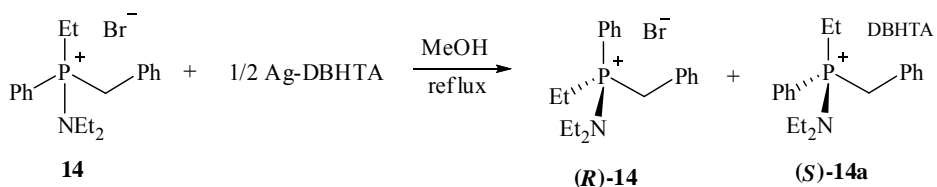
15



Scheme 1.2

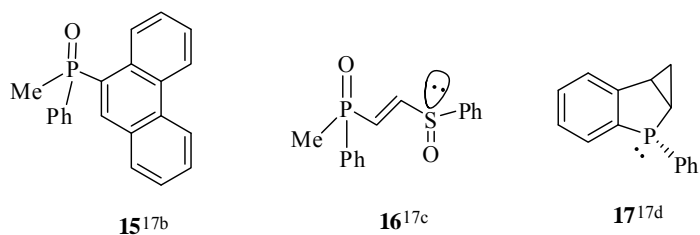


Kinetic resolution of racemic *P*-stereogenic phosphorus compounds has also been studied. Horner and Jordan developed kinetic resolution of a preformed aminophosphonium salt **14** (Scheme 1.3) through the reaction with silver hydrogen dibenzoyltartrate. Due to the less soluble, the unreacted half of the phosphonium hydrogentartrate (**R**)-**14** was successfully isolated.<sup>16</sup> The half of the salt containing exchanged counterion ((*S*)-**14a**) was readily separated being poorly soluble in hydroxylic solvents.



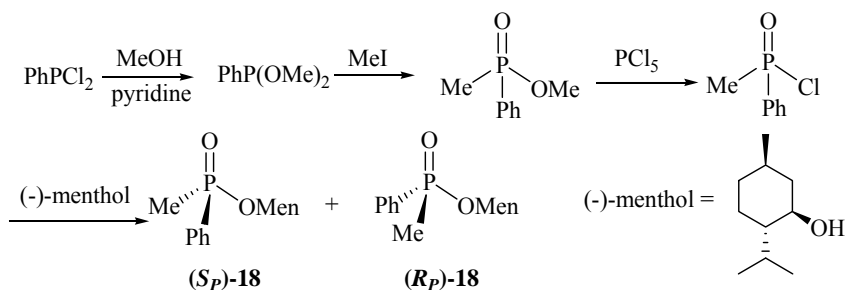
**Scheme 1.3**

With the development of high performance chromatographic techniques and a range of chiral stationary phases (CSPs), chromatographic resolution of racemic phosphorus has become a viable alternative to the existing classical methods of resolutions.<sup>17a</sup> Compounds **15-17** are several chiral phosphorus compounds that have been resolved using various CSPs.

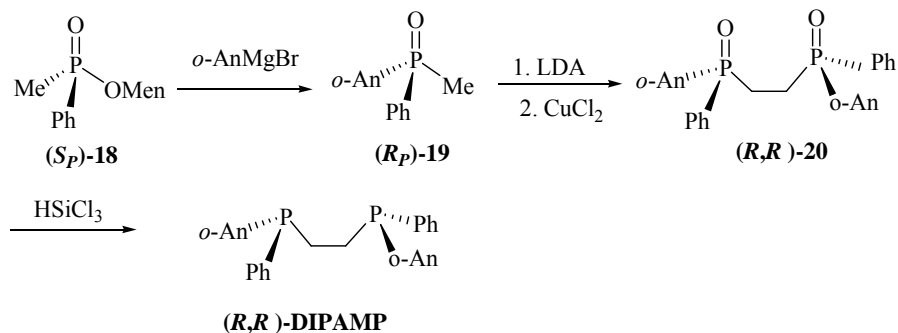


## B. Preparation by Stereoselective Synthesis

Synthetic routes using a stoichiometric amount of a chiral auxiliary was developed due to the lack of flexibility of the methods involving resolutions of racemic mixtures. Nudelman and Cram<sup>18</sup> and Mislow and co-workers<sup>19,20</sup> first explored the idea in the late 1960s, using menthol as a chiral auxiliary. They demonstrated that unsymmetrically substituted menthylphosphinates (**18**, Scheme 1.4) could be obtained as the diastereomeric forms by resolution. The chiral menthylphosphinates could be reacted stereospecifically with Grignard reagents to generate the tertiary phosphine oxides with a high degree of stereospecificity. This procedure was used by Knowles and co-workers in one of the steps of the synthesis of DIPAMP,<sup>21</sup> as depicted in Scheme 1.5.



Scheme 1.4

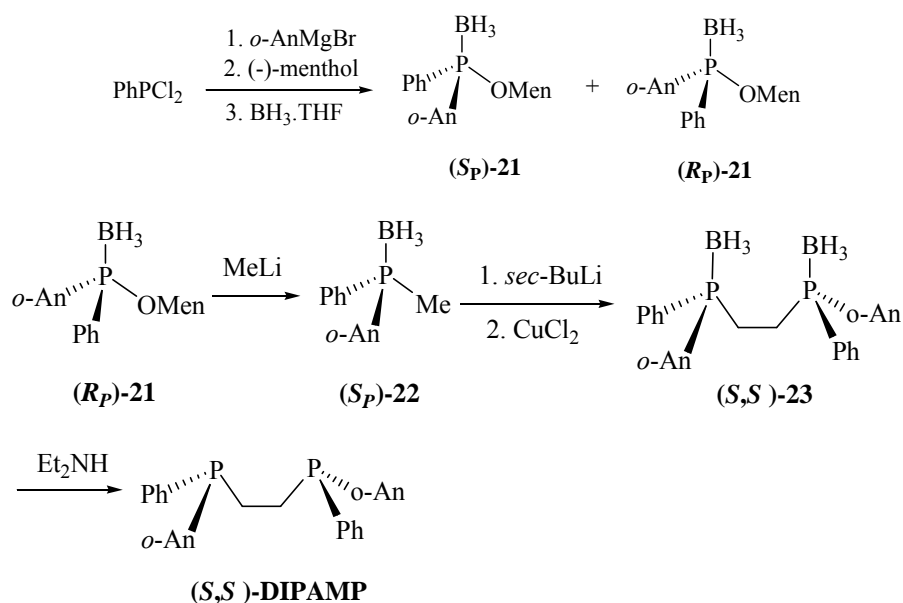


Scheme 1.5

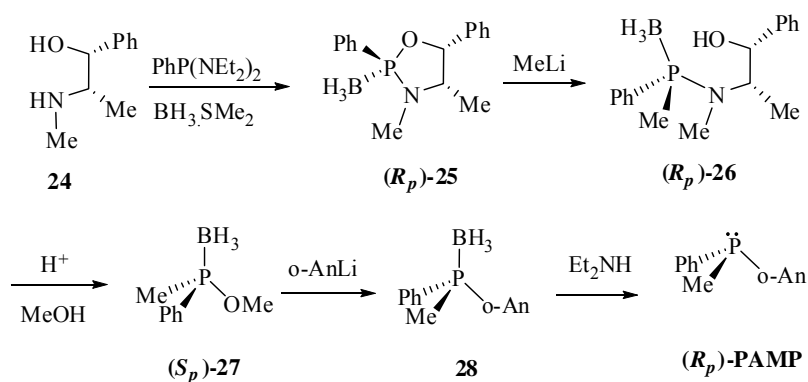
In 1990, Imamoto et al.<sup>22</sup> went a step further in menthol methodology by using phosphine-boranes instead of phosphine oxides. Phosphine-boranes offer some distinct advantages over oxides. They can be conveniently prepared and smoothly cleaved. Owing to the reduction in polarity of the B-H and P-B bonds, they are crystalline and chemically and configurationally stable even under severe conditions (oxidant, acid or basic media). The decomplexation of phosphine-borane complexes is accomplished with retention of configuration by reaction with amine<sup>22</sup> or with strong acids followed by hydrolysis.<sup>23</sup> The diastereomeric phosphinite-boranes **21** were separated by means of chromatography and (*R<sub>P</sub>*)-**21** was then converted to (*S,S*)-DIPAMP as shown in Scheme 1.6.

Optically active ephedrine has also been utilized as chiral auxiliary to synthesize *P*-chiral phosphines by two sequential nucleophilic displacements on phosphorus derivatives (Scheme 1.7).<sup>24</sup> Oxazaphospholidene (*R<sub>P</sub>*)-**25** prepared from (–)-ephedrine(**24**), PhP(NEt<sub>2</sub>)<sub>2</sub> and BH<sub>3</sub>.SMe<sub>2</sub> underwent regio and stereoselective rupture of P-O bond with methyllithium to give the corresponding aminophosphine-borane complex (*R<sub>P</sub>*)-**26**. Subsequent displacement of the

phosphinite-borane adduct (*S<sub>p</sub>*)-**27** with organolithium reagent resulted in the generation of phosphine-borane complexes **28** in 85–100% ee. When required, these products could be further purified to virtually enantiomeric purity by recrystallization. After deboration the respective monophosphines (*R<sub>p</sub>*)-PAMP can be achieved with excellent optical purity.

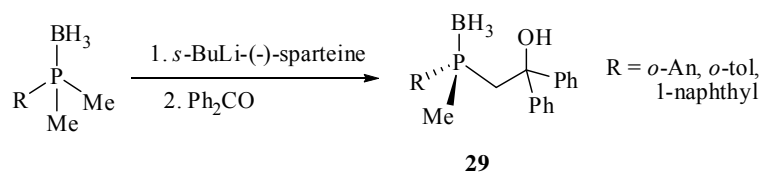


Scheme 1.6



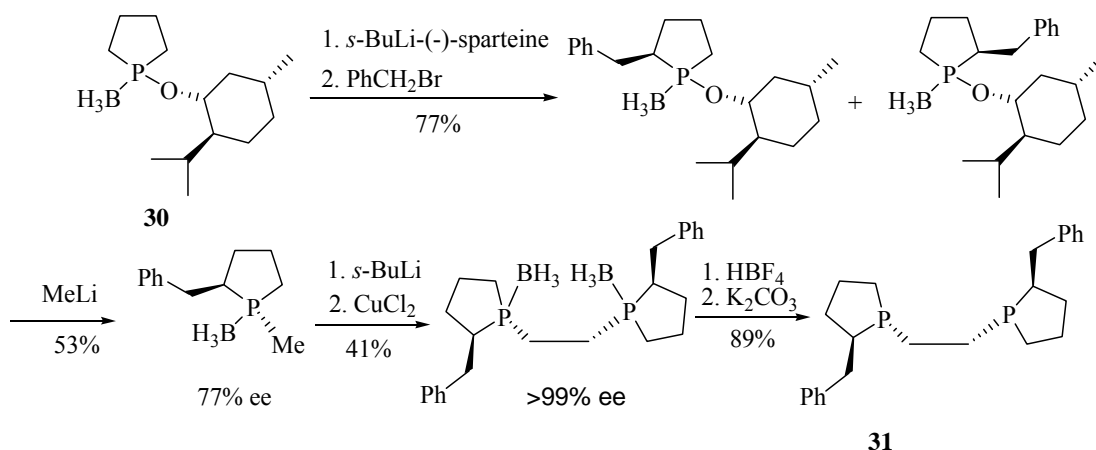
Scheme 1.7

The enantioselective deprotonation and subsequent alkylation of phosphine-boranes or phosphine-sulfides is an important synthetic route to *P*-chiral phosphorus compounds. As the chiral deprotonation agent, the *s*-BuLi/(-)-sparteine reagent system was most frequently employed.<sup>25-28</sup> The generated non-racemic organolithium species reacted with various electrophiles (carbonyl compounds, alkyl halides, oxygen gas, disulfides, carbon dioxide, etc.) to afford their derivatives. For example, the resultant  $\alpha$ -carbanion can subsequently undergo nucleophilic addition to benzophenone to synthesize phosphine-borane adducts (*S<sub>p</sub>*)-**29** in up to 87% ee (Scheme 1.8).<sup>29</sup>

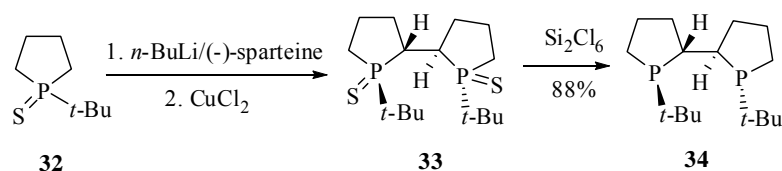


**Scheme 1.8**

On the other hand, 1-menthoxyphospholane-borane (**30**) was used to selective deprotonation with *s*-BuLi/(-)-sparteine and subsequent benzylation to give a mixture of products in a 9:1 ratio. Further elaboration gave *P*-chiral 1,2-bis(phospholano)ethane **31** (Scheme 1.9).<sup>30</sup> Phospholane sulfide **32** was used to deprotonation and oxidative coupling to yield the dimerization product **33** with 95% ee (Scheme 1.10). Subsequent purification by recrystallization, followed by desulfurization, provided biphospholanyl **34** (abbreviated as TangPhos).<sup>31</sup>



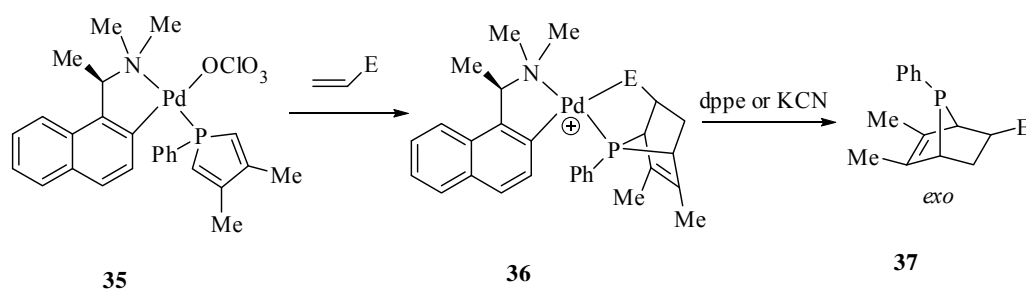
Scheme 1.9



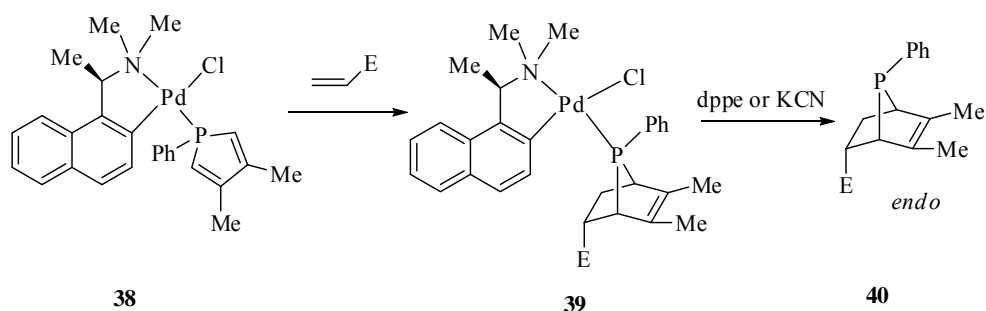
Scheme 1.10

Palladium(II) complexes containing enantiomerically pure forms of orthometallated amines, discussed in 1.1.1.1.A, have been applied by Leung's group<sup>32</sup> to prepare a range of functionalized *P*-chiral phosphines via the Diels–Alder reaction. Although the five-membered heterocycle 3,4-dimethyl-1-phenylphosphole (DMPP) itself is not a reactive cyclic diene, it becomes reactive when it is coordinated to the Pd atom (**35**),<sup>33</sup> as shown in Scheme 1.11. Since the weak and labile perchlorato-palladium bond can be displaced by most electron-rich functionalities in the reacting dienophiles, the addition occurs stereospecifically to yield the pair of *exo*-cycloadducts intramolecularly with prior coordination of the dienophile<sup>34-45</sup> in high stereo- and regioselectivities. The pair of cationic diastereomeric complexes **36**

can then be separated by the usual techniques, yielding only one enantiomer of the final phosphine **37**. Interestingly, the readily available template site in the complex **35** can be blocked by replacing the perchlorate ligand with the chloro counterpart. Thus the weaker donors in most organic dienophiles are not able to cleave the thermodynamically stable and kinetically inert Pd–Cl bond in **38** for interaction with the palladium center, which therefore deters the formation of any bidentate *exo*-cycloadduct. However, the activated DMPP ligand in the chloro complex can undergo an intermolecular *endo*-cycloadduct reaction (Scheme 1.12).<sup>46-50</sup>



Scheme 1.11



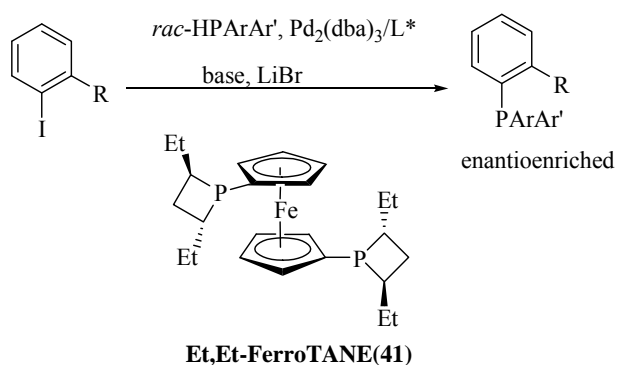
Scheme 1.12

### C. Preparation by Asymmetric Catalysis

The most common synthetic methods towards enantiopure *P*-chiral phosphines

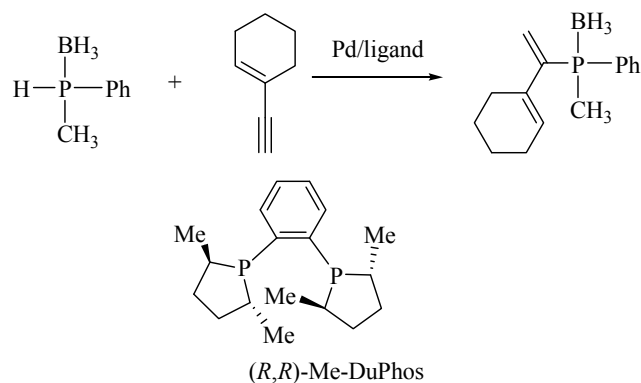
include resolution of the racemic products or reactions in which a stoichiometric amount of chiral auxiliary is used to induce stereoselectivity. Interestingly, several papers have been published quite recently on the application of chiral homogeneous catalysts in the synthesis of these ligands.<sup>51-52</sup>

Helmchen and Korff have synthesized *P*-chiral triarylphosphines by palladium-catalyzed cross-coupling reactions of racemic secondary phosphines and ortho-substituted aryl iodides.<sup>51</sup> Enantiomeric excesses of up to 90% were achieved using *in situ* prepared catalysts modified with the chiral bisphosphetane Et,Et-FerroTANE (**41**) (Scheme 1.13).



**Scheme 1.13**

Gaumont and co-workers have reported the successful hydrophosphination of unactivated alkynes using Pd complexes of various chiral diphosphines as catalyst.<sup>52</sup> The racemic secondary phosphine MePhPH was used as a borane adduct (Scheme 1.14). The tested catalytic systems provided, for the first time, access to enantioenriched *P*-chiral vinylphosphines. The highest enantiomeric excess (42%) was achieved by application of the (*R,R*)-DuPhos ligand.



Scheme 1.14

### 1.1.1.2 Phosphines with Chiral Carbon Backbones

A large number of phosphine ligands with backbone chirality have been developed and successfully used in a range of different metal-catalyzed asymmetric reactions. Generally, these kind of phosphine ligands can be divided into three groups according to the type of chirality present in the side-chain: (1) central chirality; (2) axial chirality; (3) planar chirality.

#### A. C-Chiral Phosphines

Phosphines bearing one or more chiral carbon side chains account for the biggest family in chiral phosphines. Some examples of the phosphines bearing chiral carbon side chains are shown in Figure 1.1.

Phosphines with chiral center(s) in the side-chain are the easiest to prepare since their synthesis mostly starts from a chiral natural product. Treatment of the tosylate (or halide) of the optically active compound with the diphenylphosphide

anion produced the desired chiral phosphines (Scheme 1.15). With this method, numerous phosphines were prepared by Kagan's group. Most of them start from the naturally abundant tartaric acid and hence there is  $C_2$  symmetry in these products. A typical example is the preparation of (*R,R*)-DIOP (Scheme 1.16).<sup>60</sup> The ligand **42** was synthesized from the chiral amino alcohol (Scheme 1.17).<sup>61</sup>

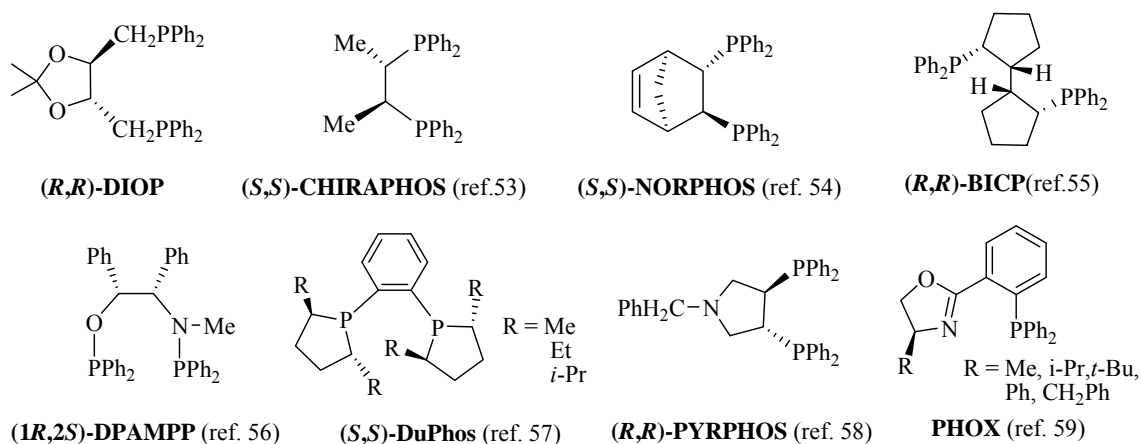
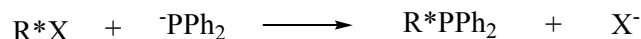
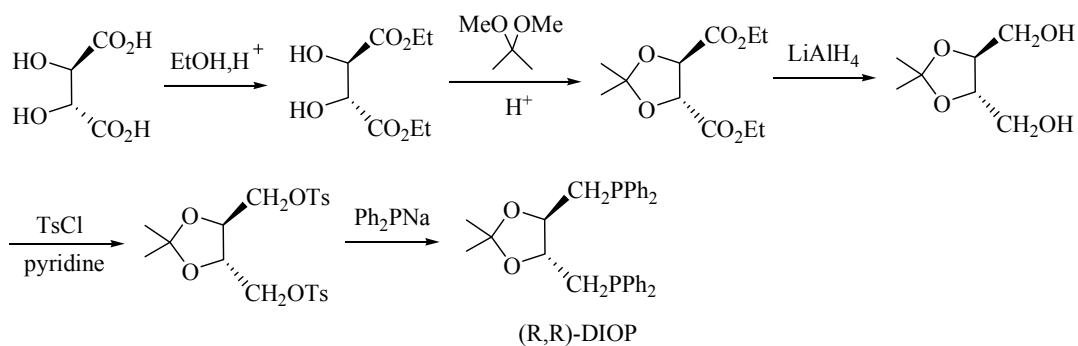


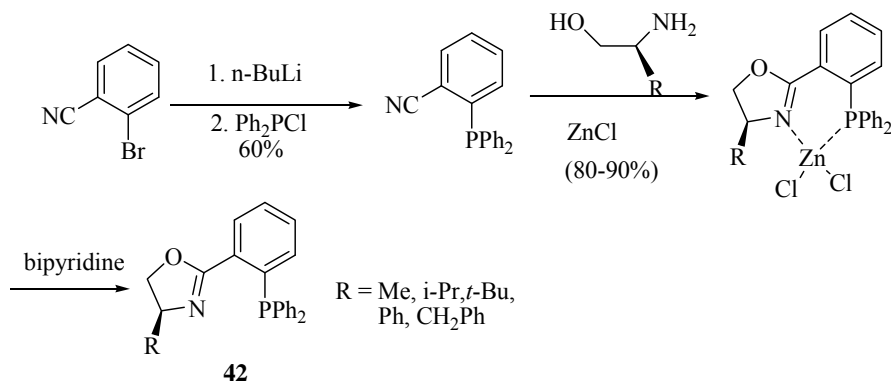
Figure 1.1



Scheme 1.15

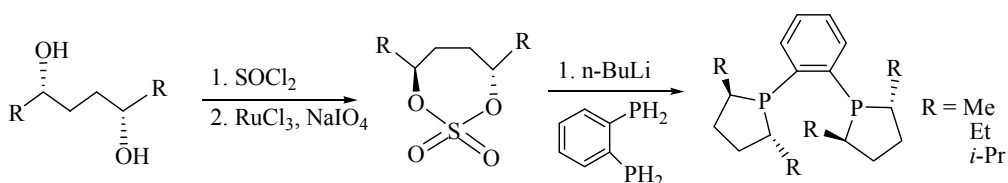


Scheme 1.16



Scheme 1.17

Besides deriving the desired chirality from the natural pool or readily available chiral compounds, C-chiral phosphines can also be obtained by asymmetric reactions. For example, the synthesis of DuPhos involves the use of 1,4-diols to generate 1,4-diol cyclic sulfates.<sup>62</sup> Deprotonation of 1,2-bis(phosphino)benzene with *n*-BuLi (2 equiv) gave dilithium bis(phosphido)benzenes, which were then treated with 1,4-diol cyclic sulfates to afford the DuPhos ligands (Scheme 1.18).



Scheme 1.18

## B. Axial Chiral Phosphines

The diphosphine BINAP of a C<sub>2</sub>-symmetric axially chiral ligand has proven to be one of the most effective ligands in a wide range of enantioselective metal-catalyzed transformations.<sup>63</sup> Inspired by the success of BINAP, analogues with

various biaryl skeleta have been developed and several selected samples are shown in Figure 1.2.

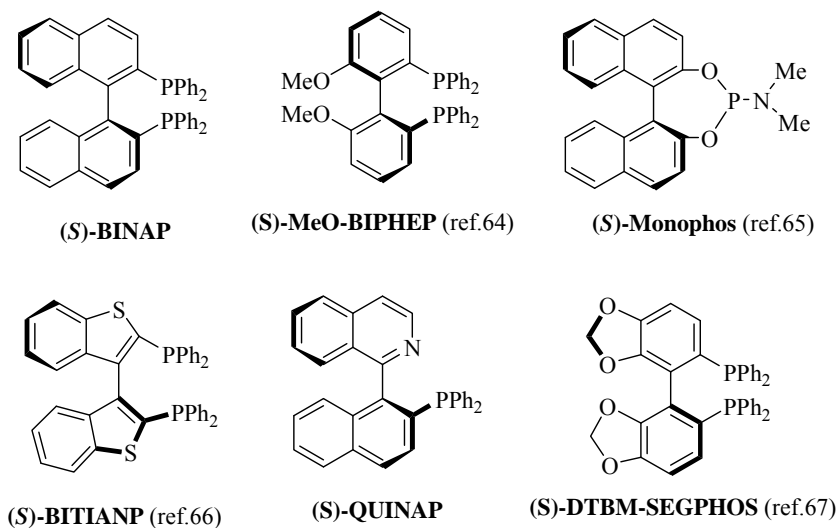
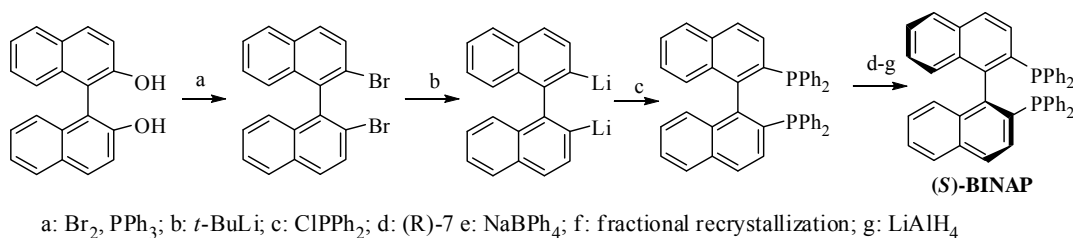


**Figure 1.2**

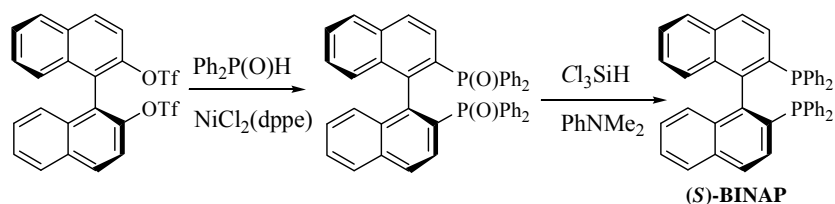
Resolution is often used to obtain axial-chirality biaryl phosphines. The first reliable access to optically pure BINAP was attained by synthesis of the racemate followed by resolution with the optically active cyclopalladated-amine complex **7** (Scheme 1.19).<sup>68</sup>



**Scheme 1.19**

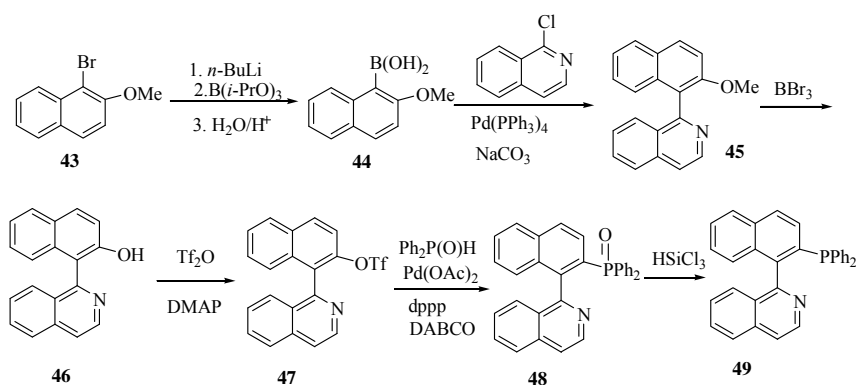
More efficient access to enantiomerically pure BINAP led to synthetic

methods with direct introduction of phosphinyl groups onto an optically active binaphthyl framework (obtained by resolution or asymmetric reactions). Kumobayashi developed a method using the stereospecific Ni-catalyzed coupling between the ditriflate and easy-to-handle diphenylphosphine oxide, giving a mixture of BINAP, its monoxide and its dioxide.<sup>69,70</sup> The mixture was then reduced with trichlorosilane to give BINAP in high yield (Scheme 1.20).



Scheme 1.20

Brown et al. reported the synthesis of 1,1'-(2-diphenylphosphino-1-naphthyl)-isoquinoline (QUINAP) **49** in 1993 (Scheme 1.21).<sup>71</sup> The synthesis of this compound involves two key steps: metal catalyzed coupling of two aryl precursors and introduction of the phosphine moiety to the biaryl backbone. The racemic QUINAP **49** was further subjected to diastereomeric resolution by treatment with chiral (*R*)-palladium-amine-naphthyl complex **7**.



Scheme 1.21

### C. Phosphines with Planar Chirality

Chiral phosphines with planar chirality were synthesized much later than ligands with central and axial chirality. Most of such phosphine ligands are based on the backbone of ferrocene complexes. Some examples of this class of chiral phosphines are given in Figure 1.3.

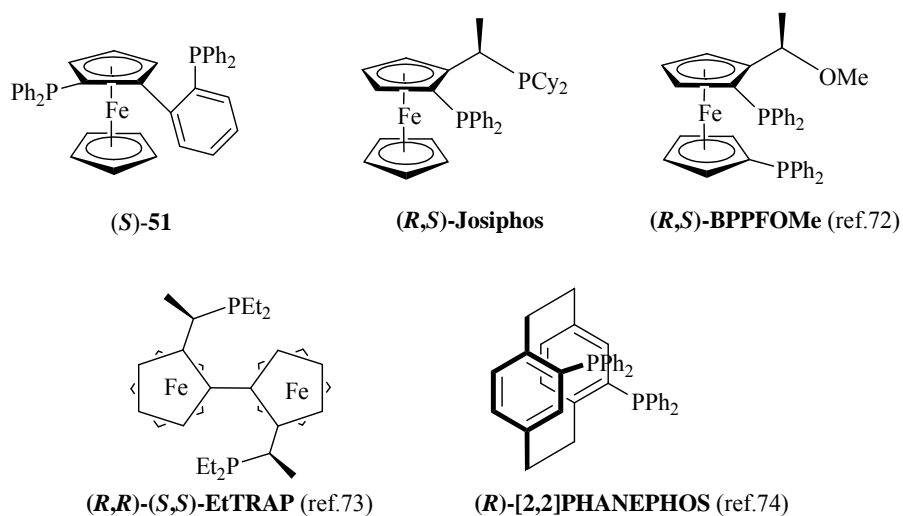
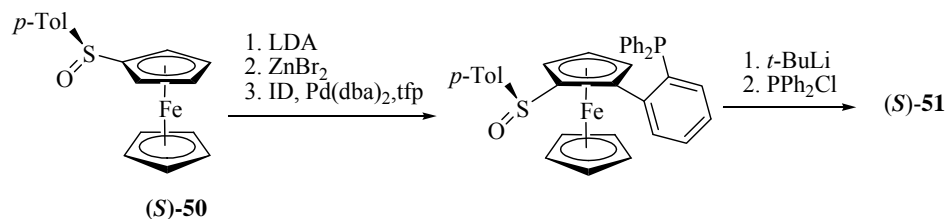


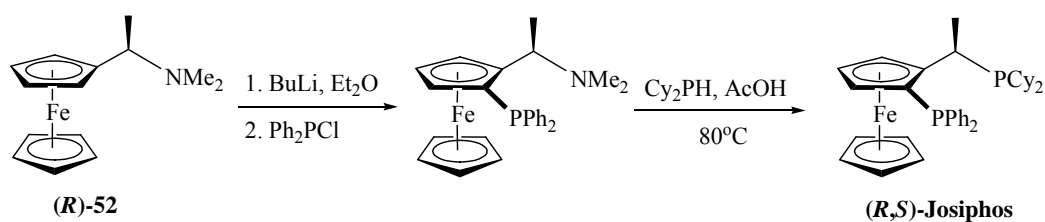
**Figure 1.3**

**(S)-51** was designed by the Knochel group who started from chiral sulfoxide **(S)-50** (Scheme 1.22).<sup>75</sup> Ortho-lithiation of **(S)-50** using LDA followed by transmetallation with  $\text{ZnBr}_2$  furnished the corresponding zinc reagent. Negishi cross-coupling with (2-iodophenyl)diphenylphosphine in the presence of  $\text{Pd}(\text{dba})_2$  and tris-*o*-furylphosphine afforded the chiral sulfoxide in 74% yield. Sulfoxide-lithium exchange with *t*-BuLi and trapping of the lithium intermediate with  $\text{PPh}_2\text{Cl}$  provided **(S)-51** in 81% yield.



Scheme 1.22

Planar chirality can be induced using stereospecific reactions by using the readily available chiral compounds. An example of such methodology is given in Scheme 1.23.<sup>76</sup> The stepwise stereospecific lithiation of commercially available (*R*)-52 enables the introduction of one or two diphenylphosphino groups on the cyclopentadienyl rings. Alternatively, a second phosphino group can be introduced via retentive nucleophilic displacement of the amino group to generate chiral diphosphines.



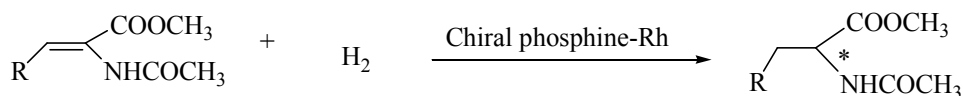
Scheme 1.23

## 1.1.2 Chiral Phosphine Transition Metal Complexes in Asymmetric Catalysis

### 1.1.2.1 Asymmetric Hydrogenation

The development of homogenous asymmetric hydrogenation was initiated by

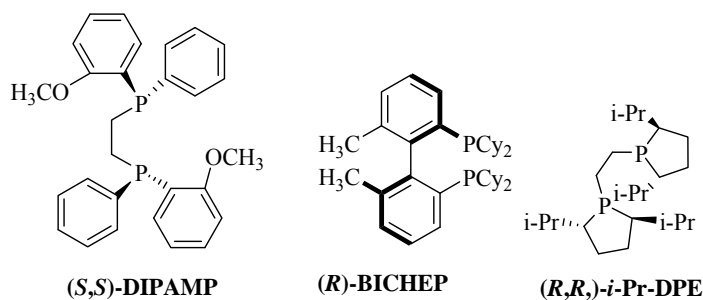
Horner and co-workers<sup>5</sup> and Knowles and Sabacky.<sup>4</sup> These were variants of Wilkinson's catalyst using enantiomerically pure monodentate phosphine ligands, and provide definite, but low, asymmetric induction. In the early 1970s, a breakthrough in this field came when Kagan and Dang prepared the bidentate ligand DIOP, which was found to yield up to 82% ee in the rhodium-catalysed hydrogenation of  $\alpha$ -(acylamino)acrylic acids.<sup>77</sup> Since then, thousands of chiral diphosphines with diverse structures have been developed for asymmetric hydrogenation. Selected chiral phosphines and the corresponding data in asymmetric hydrogenation of amino acid derivatives<sup>3b</sup> are given in Scheme 1.24 and Table 1.1.



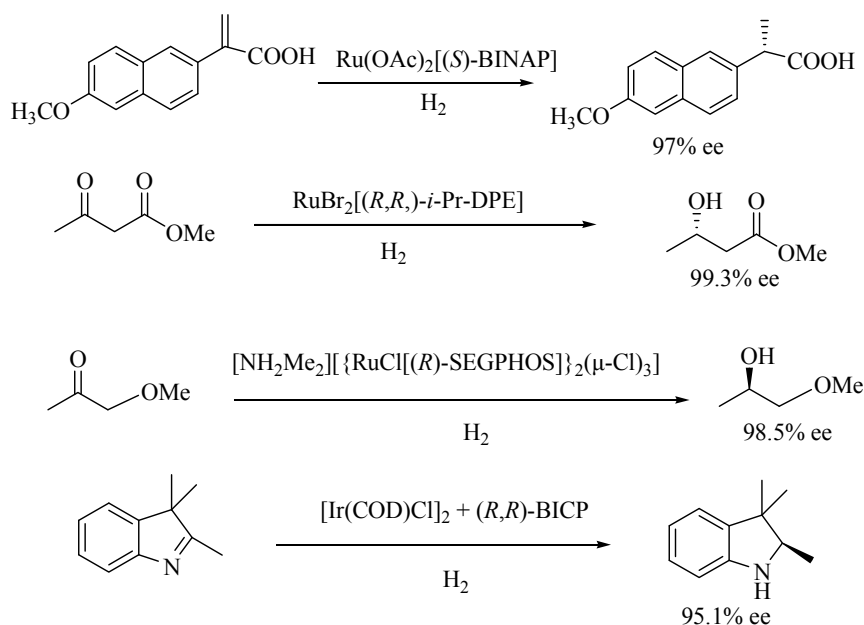
Scheme 1.24

**Table 1.1 Selected chiral phosphines and the corresponding data of asymmetric hydrogenation**

Phosphine ligand	% ee of product (R = Ph)	Phosphine ligand	% ee of product (R = H)
<b>(R,R)-DIPAMP</b>	96( <i>S</i> )	<b>(S,S)-Et-Duphos</b>	>99( <i>R</i> )
<b>(R,R)-PYRPHOS</b>	96.5( <i>S</i> )	<b>(R,R,S,S)-EtTRAP</b>	96( <i>R</i> )
<b>(R)-BICHEP</b>	95( <i>S</i> )	<b>(R)-PHANEPHOS</b>	99.6( <i>R</i> )
<b>(1R,2S)-DPAMPP</b>	97( <i>R</i> )	<b>(S)-MonoPhos</b>	99.6( <i>R</i> )



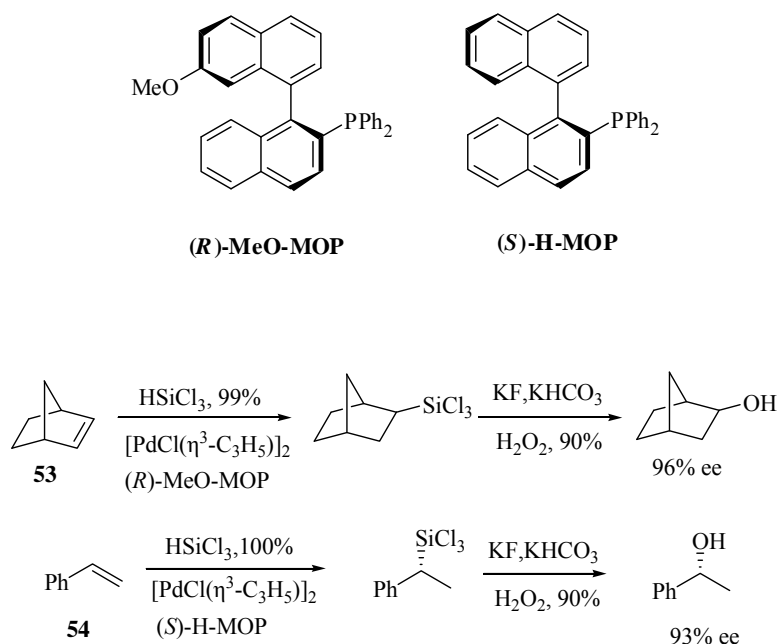
Noyori's research on BINAP-Ru catalysts for asymmetric hydrogenation opened up opportunities for efficient hydrogenations of a variety of substrates.<sup>78</sup> A wide variety of prochiral olefin, ketone and imine substrates were hydrogenated with excellent enantioselectivity. Besides Rh and Ru complexes, chiral phosphine complexes of Ir have also been found to be effective catalysts for asymmetric hydrogenation. Selected examples of metal complexes in these reactions are given in Scheme 1.25.<sup>79</sup>



Scheme 1.25

### 1.1.2.2 Asymmetric Hydrosilylation Reaction

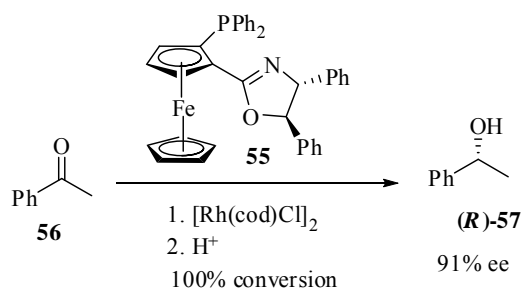
Hydrosilylation is the addition of organic and inorganic silicon hydrides to carbon-carbon, carbon-oxygen and carbon-nitrogen multiple bonds. Palladium complexes with MOP ligands which are monodentate phosphine ligands, including MeO-MOP<sup>80</sup> and H-MOP<sup>81</sup> are very efficient catalysts in the hydrosilylation of olefins with trichlorosilane. For example, norbornene (**53**) and styrene (**54**) are converted into the hydrosilylated derivatives with excellent enantioselectivity. The trichlorosilanes were derivatised into the corresponding alcohols (Scheme 1.26).



**Scheme 1.26**

The rhodium-catalysed hydrosilylation of ketones has received more attention than other metals. Uemura and co-workers have found that rhodium-based oxazolinyferrocene-phosphine (**55**) are effective for catalyzing the asymmetric hydrosilylation of acetophenone (**56**) to provide the (*R*)-alcohol (**57**) as product in 91%

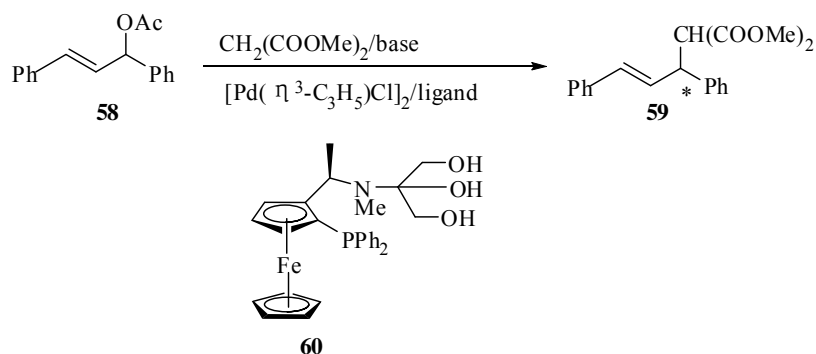
ee (Scheme 1.27).<sup>82</sup>



**Scheme 1.27**

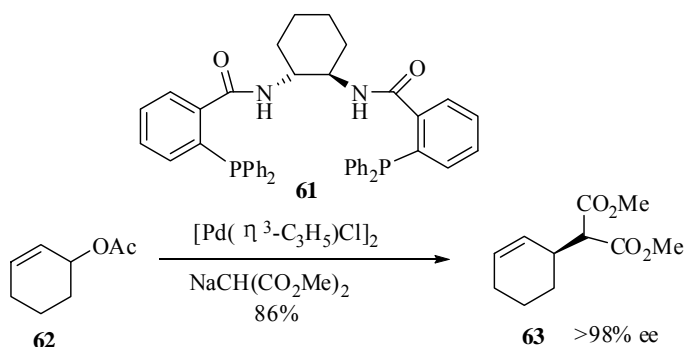
### 1.1.2.3 Asymmetric Allylic Substitution

Enantioselective metal-catalysed allylic substitution reactions have attracted considerable attention. Among metals used, palladium is the most important one in this class of catalytic reactions. The major focus in academia has been on the allylic alkylation of 1,3-diphenyl-2-propenyl acetate (**58**). Many ligands have been used for this reaction, and enantioselectivities in excess of 90% ee have often been achieved.<sup>2c</sup> Hayashi and co-workers designed the first ligand (**60**) to work with this level of selectivity (Scheme 1.28).<sup>83</sup> Other ligands such as QUINAP ligand<sup>84</sup> and Josiphos<sup>85</sup> have also been used successfully.



**Scheme 1.28**

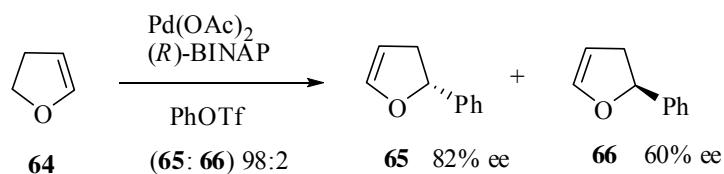
However, most of these ligands give lower enantioselectivities with cyclic substrates. Trost and Bunt developed the ligands (**61**) to be generally applicable to cyclohexenyl acetate (**62**) to give the substitution product (**63**) with excellent selectivity (Scheme 1.29).<sup>86</sup>



Scheme 1.29

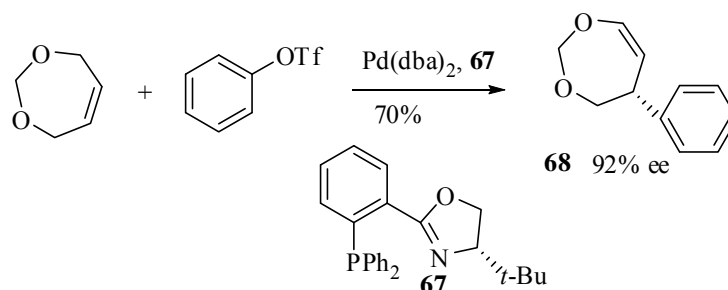
#### 1.1.2.4 Asymmetric Heck Reaction

In general, the Heck reaction is one of the most important C-C coupling reactions in modern organic chemistry. Dihydrofuran (**64**) is a popular substrate for the asymmetric Heck reaction. In 1991, Hayashi and co-workers reported that using a Pd-BINAP catalyst, the first example of an intermolecular asymmetric Heck reaction involving the phenylation of dihydrofuran with phenyl triflate gave different regioisomeric product (**65**) and (**66**) in 82% ee and 60% ee (Scheme 1.30).<sup>87</sup>



Scheme 1.30

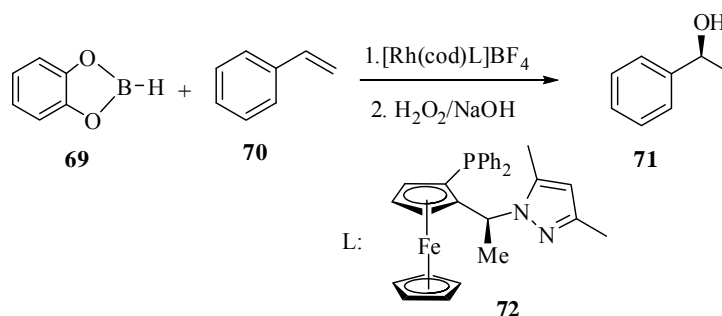
Phosphino-oxazoline ligands, such as compound (**67**) has also been employed successfully to enantioselective Heck reactions, involving the coupling of triflates to give the product (**68**) with excellent stereocontrol (Scheme 1.31).<sup>88</sup>



**Scheme 1.31**

### 1.1.2.5 Other Reactions

Asymmetric hydroboration has been a useful method to introduce functional groups to organic complex. The standard hydroborating agent is catecholborane(**69**). The intermediate boronate can be converted into the corresponding alcohol by hydrogen peroxide oxidation with retention of configuration. In the presence of the pyrazole-containing ligand (**72**) containing rhodium complex,<sup>89,90</sup> reaction of styrene (**70**) and catecholborane formed phenethyl alcohol (**71**) in 95% ee (Scheme 1.32).



**Scheme 1.32**

Asymmetric hydroformylation (addition of hydrogen and carbon monoxide to olefins to give optical active aldehydes) has been provided by using Rh (I) complexes of chiral diphosphines,<sup>91,92</sup> such as BINAP and CHIRAPHOS, to give the products in moderate to high optical purity. Chiral phosphine phosphite ligand containing rhodium complexes also provided good enantioselectivity and regioselectivity across a range of alkenes.<sup>93</sup> Asymmetric coupling reactions between Grignard reagents and organic halide were found to be catalyzed by nickel- and palladium-phosphine complexes efficiently.<sup>94,95</sup> Chiral  $\beta$ -aminophosphine ligands are amongst the best for catalyzing these reactions with good enantioselectivity.<sup>96-98</sup>

Chiral phosphine complexes have also been used as potent asymmetric catalysts in some cases of cycloaddition,<sup>99</sup> Michael addition,<sup>100</sup> hydrovinylation of olefins,<sup>101</sup> hydroboration,<sup>102</sup> Suzuki coupling<sup>103</sup> and epoxidation.<sup>104</sup>

## 1.2 Arsine Ligands

### 1.2.1 Achiral Arsine Ligands

Recently, organoarsenic compounds have been found to play important roles in many aspects of organic synthesis and catalytic reactions.<sup>105</sup> Tertiary arsines have been reported to be effective ligands in certain transition metal-catalyzed organic reactions, for example, Stille<sup>106</sup> and Heck reactions,<sup>107</sup> hydroformylation,<sup>108</sup> Suzuki-Miyaura coupling reaction,<sup>109</sup> carbonylation,<sup>110</sup> norbornene polymerization<sup>111</sup> and Wittig-type olefination of aldehydes,<sup>112</sup> epoxidation,<sup>113</sup> cyclization of an allylic enyne<sup>114</sup> and hydrosilylation.<sup>115</sup>

There are two approaches for the preparation of tertiary arsines: classical arsination and catalytic arsination.<sup>105</sup> The first classical method is the nucleophilic aromatic substitution of aryl halides with highly reducing  $\text{Ph}_2\text{AsM}$  ( $\text{M} = \text{Li}, \text{Na}, \text{K}$ ), which are usually prepared in situ in liquid ammonia.<sup>116,117</sup> In addition, arylarsines can also be achieved by the photoirradiation of ammonia.<sup>118</sup> Another method to prepare tertiary arsines involved the reaction of Grignard or organolithium reagents with haloarsine.<sup>119</sup>

In 1997, Shibasaki and coworkers reported the first nickel-catalyzed arsination of BINOL ditriflate to prepare BINAs ligands in which secondary arsine ( $\text{Ph}_2\text{AsH}$ ) was utilized as the arsinating agent.<sup>120</sup> In 2003, palladium catalyzed  $\text{As-C}(\text{sp}^2)$  bond formation between aryl iodides and  $n\text{-Bu}_3\text{Sn-AsPh}_2$  with limited functional group compatibility ( $-\text{Cl}$  and  $-\text{OMe}$  groups).<sup>121</sup> This  $n\text{-Bu}_3\text{Sn-AsPh}_2$  reagent was synthesized in situ from the  $\text{Ph}_2\text{As}^-$  anion (generated from  $\text{Ph}_3\text{As}$  and Na metal in liquid ammonia) and  $n\text{-Bu}_3\text{SnCl}$ . In 2005,  $\text{Pd}(\text{OAc})_2$  was also used to catalyze solvent-free arsination between functionalized aryl triflates and triphenylarsine in neutral reaction medium.<sup>122</sup> The limitation of this reaction is that heteroatom-substituted 3-pyridyl triflate, 8-quinolyl triflate and 2-formylphenyl triflate did not work.

### 1.2.2 Chiral Arsines

A large number of chiral phosphine ligands have been developed and achieved a highly stereoselective optical yield in various asymmetric reactions. In contrast, the chemistry of analogous chiral arsines is much less developed notwithstanding that

these ligands also show good donor characteristics towards transition metals, as they are able to stabilize transition metal centres in both low and high oxidation states.<sup>123</sup> The uncatalyzed thermal barrier to inversion of tertiary arsines is around 14 kcal mol<sup>-1</sup> more stable than tertiary phosphines, also they are generally less air-sensitive. One of the important objectives of the present study is to further explore the asymmetric synthesis of chiral arsine ligands.

### 1.2.2.1 Preparation of Chiral Arsine Ligands

Based on the standard synthesis of enantiomerically pure compounds, arsine ligands can be prepared *via* three different synthetic methodologies:

#### A. Optical Resolution

Several As-chiral arsine ligands have been resolved successfully by chiral palladium(II) complexes (Figure 1.4).<sup>105</sup> For example, the synthesis of the racemic amino-arsine ligand **73** is shown in Scheme 1.33, the racemic ligands were further resolved using a chiral naphthylamine-Pd (II) template.<sup>124</sup>

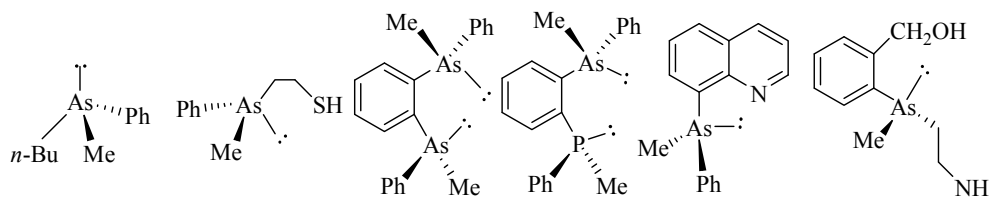
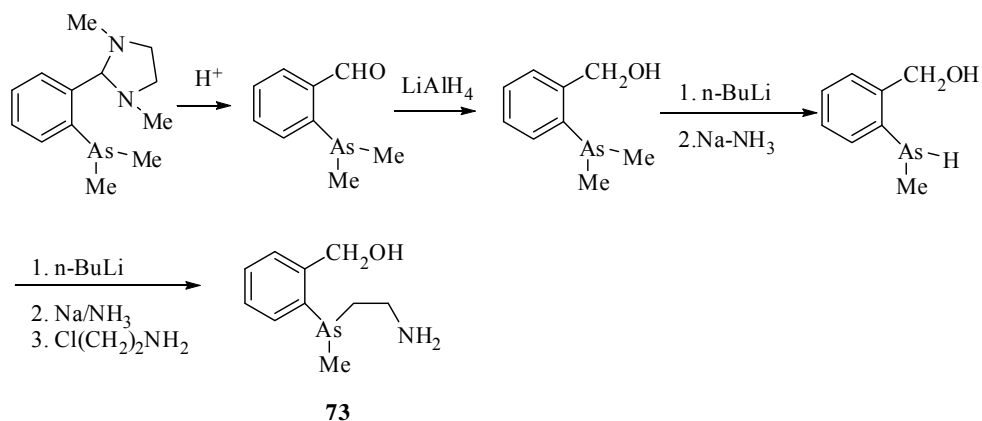


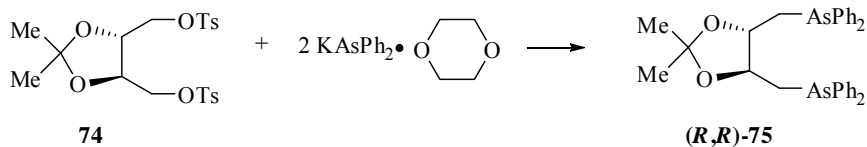
**Figure 1.4**



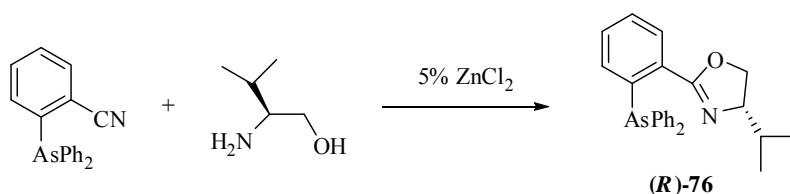
**Scheme 1.33**

## B. Synthesis from Chiral Pools

The use of chiral natural products as the starting material is a classical and convenient approach in preparing a target molecule. The chiral bidentate (*R,R*)-Diarsop **75** was achieved by the reaction of 1,4-ditosyl-2,3-*o*-isopropylidene-*D*-threitol **74** with potassium diphenylarsenide dioxanate (Scheme 1.34).<sup>125</sup> In the presence of 5% ZnCl<sub>2</sub>, (*S*)-2-amino-3-methyl-1-butanol was treated with the *o*-cyanoarsine ligand to give the optical pure oxazoline functionalized As-N heterobidentate ligand (*R*)-**76** (Scheme 1.35).<sup>122</sup>

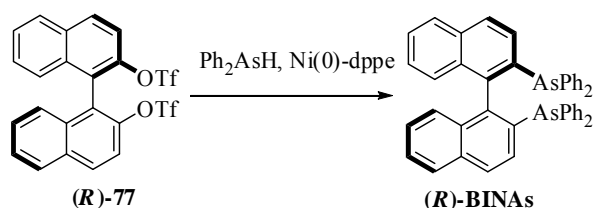


**Scheme 1.34**

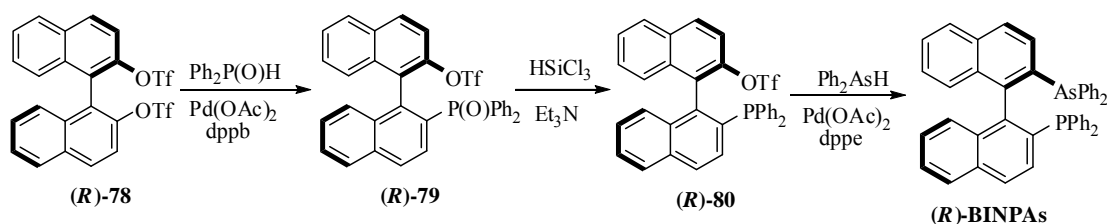


**Scheme 1.35**

Axial chiral arsine 2,2'-bis(diphenylarsino)- 1,1'-binaphthyl (BINAs) was efficiently synthesized by the stereospecific Ni-catalyzed coupling between readily available optically active binaphthol ditriflate (*R*)-**77** and diphenylarsine with retention of configuration (Scheme 1.36).<sup>120</sup> 2-Diphenylarsino-2'-diphenylphosphino-1,1'-binaphthyl (BINAPAs) was also prepared from binaphthol ditriflate. The ditriflate complex was transformed to phosphine oxide **79** by the palladium catalyzed cross-coupling reaction with diphenylphosphine oxide (Scheme 1.37). After reduction of **79** with trichlorosilane, BINAPAs was efficiently synthesized by the stereospecific Pd-catalyzed coupling between readily available optically active triflate and diphenylarsine with retention of configuration.<sup>126</sup>



Scheme 1.36

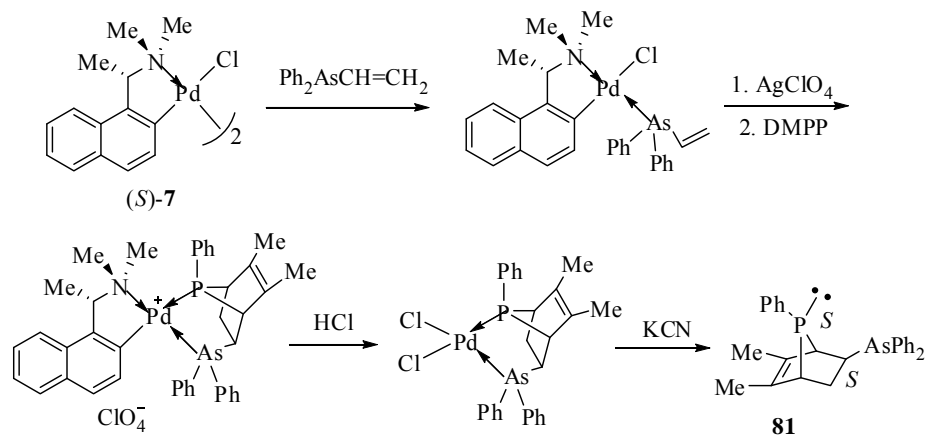


Scheme 1.37

### C. Asymmetric Synthesis

One of the most useful asymmetric synthetic methods involves the utilization of a chiral precursor as an auxiliary. The stereoselectivity of the reaction could be controlled by the steric and electronic factors of the chiral auxiliary. Scheme 1.38

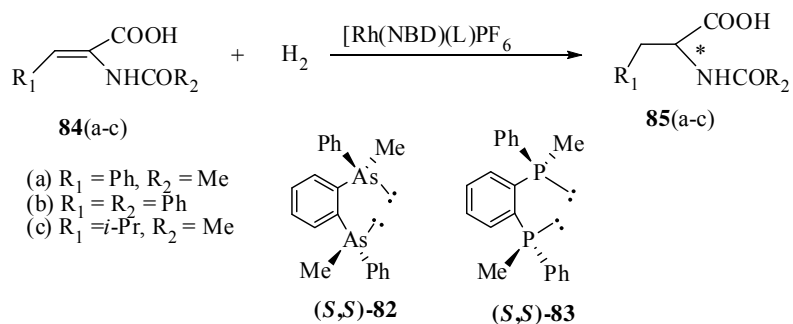
shows an excellent example of the asymmetric synthesis of As-P bidentate ligand **81** promoted by the *ortho*-palladated naphthylamine auxiliary.<sup>43</sup>



**Scheme 1.38**

### 1.2.3 Application of Chiral Arsine Ligands

The rhodium (I) complex containing (*S,S*)-**82** was found to outperform its phosphorus analogue (*S,S*)-**83** in the asymmetric hydrogenation of  $\alpha$ -(acylamino)acrylic acids substrate, which affords the  $\alpha$ -amido acid product (Scheme 1.39 and Table 1.2).<sup>127</sup> In the similar reaction, (*R,R*)-**75** gave a lower enantioselectivity of 39% ee.<sup>125</sup>

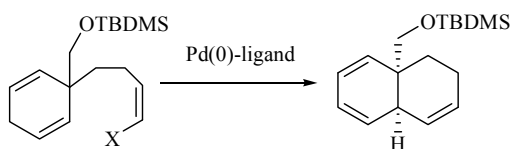


**Scheme 1.39**

**Table 1.2 Enantiomeric excess hydrogenation of prochiral amino acids 85(a-c)**

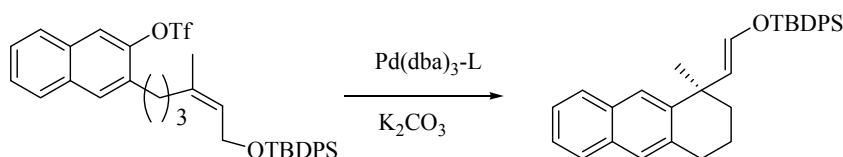
Optical pure product	( <i>S,S</i> )-(-)- <b>82</b>	( <i>S,S</i> )-(-)- <b>83</b>
<b>85a</b>	80%( <i>S</i> )	79%( <i>S</i> )
<b>85b</b>	77%( <i>S</i> )	64%( <i>S</i> )
<b>85c</b>	90%( <i>S</i> )	94%( <i>S</i> )

In the intramolecular asymmetric Heck reaction (Scheme1.40), the results (Table 1.3) obtained when using BINAs in an alkenyl iodide-using system clearly show an increased reaction rate comparing with that seen when using BINAP,<sup>120</sup> and moreover a superior yield (90%) and enantiomeric excess (82%) was obtained. However, for the corresponding alkenyl triflate system (entries 3, 4), BINAs appears to be less effective than BINAP.<sup>126</sup> To overcome this problem, the new ligand BINAPAs was synthesized and it is more effective than BINAP in the intramolecular asymmetric Heck reaction that use aryl triflates (Scheme1.41). As shown in Table 1.3, the asymmetric Heck reaction using BINAPAs appeared to proceed more rapidly than the reaction using BINAP.

**Scheme1.40**

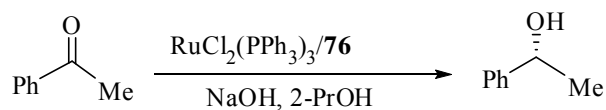
**Table 1.3 Intramolecular Asymmetric Heck Reaction using BINAs and BINAP**

X	Pd-ligand	yield(%)of product	ee(%) of product
I	Pd <sub>2</sub> (dba) <sub>3</sub> -( <i>R</i> )-BINAs	90	82
I	Pd <sub>2</sub> (dba) <sub>3</sub> -( <i>R</i> )-BINAP	55	32
OTf	Pd <sub>2</sub> (dba) <sub>3</sub> -( <i>R</i> )-BINAs	5	82
OTf	Pd <sub>2</sub> (dba) <sub>3</sub> -( <i>R</i> )-BINAP	21	93

**Scheme1.41****Table 1.3 Intramolecular Asymmetric Heck Reaction using BINAPAs and BINAP**

chiral ligand(L)	solvent	Temp(°C)	Time(h)	Yield(%)	Ee(%)
( <i>R</i> )-BINAP	THF	60	48	60	87
( <i>R</i> )-BINAPAs	THF	60	36	86	61
( <i>R</i> )-BINAP	toluene	60	14	78	87
( <i>R</i> )-BINAPAs	toluene	60	14	89	86
( <i>R</i> )-BINAP	toluene	40	46	74	89
( <i>R</i> )-BINAPAs	toluene	40	46	91	88

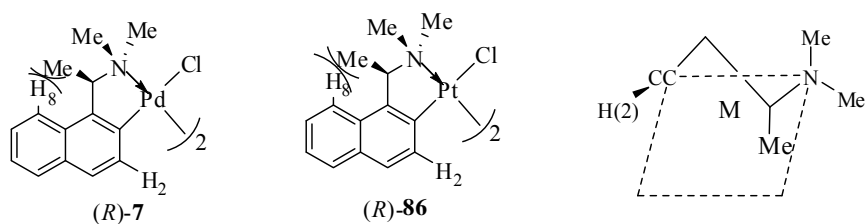
Studies of the complex formed in situ from optically active **76** and RuCl<sub>2</sub>(PPh<sub>3</sub>)<sub>3</sub> in asymmetric transfer hydrogenation of acetophenone with 2-propanol (Scheme1.42) promoted by catalytic amounts of NaOH, revealed slightly higher activity and enantioselectivity in giving 89% yield with 82% ee of (*R*)-1-phenylethanol than its P,N analogue, which gives 83% yield and 73% ee.<sup>128</sup>



Scheme 1.42

### 1.3 The Two Important Chiral Templates Used in the Project

Two chiral templates involving organopalladium complexes containing *ortho*-metalated (*R*)-(1-(dimethylamino)ethyl)naphthalene (*R*)-**7** and its platinum analog (*R*)-**86** were used in this project.



A unique stereochemical feature of the chiral naphthylamine complexes is that there is a strong internal steric repulsion between the methyl substituent on the stereogenic carbon and its neighbouring naphthylene proton  $H_8$ .<sup>129</sup> The crystallographic analysis and 2-dimensional solution NMR studies involving rotating Overhauser effect (ROESY) have confirmed that the five-membered organometallic ring is locked into the static  $\delta$  conformation, both in solid state and in solution.<sup>130</sup> The methyl substituent at the stereogenic carbon adopts an axial disposition in the rigid five-membered ring and the prochiral NMe groups are locked into nonequivalent axial and equatorial positions. In addition, the naphthylene proton  $H_2$  protrudes

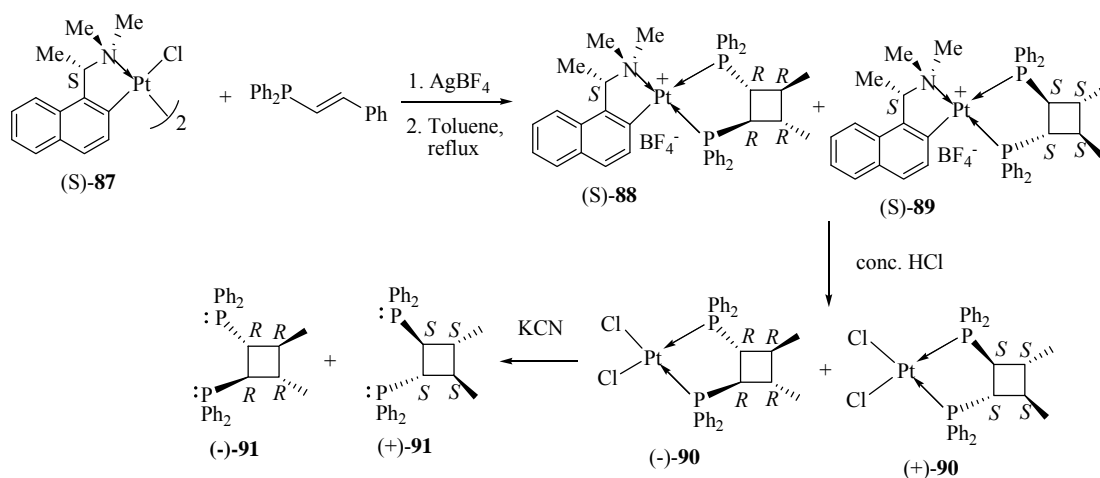
invariably towards the space somewhat above the square plane due to the rigid  $\delta$  conformation and the strict planarity of the naphthylene ring. Besides the steric based control, the auxiliary also influences an electronic control since the  $\sigma$ -donation nitrogen and the  $\pi$ -accepting naphthylene carbon of the organometallic ring control the regioselectivity of the incoming ligands. Ligands with soft donors (like phosphole) prefer to bind *trans* to NMe<sub>2</sub> entity of the auxiliary.<sup>32</sup> It is believed that by systematically varying the steric and electronic properties of the ligands and the nature of the metal centers, chiral cyclometalated complexes can be applied to a wide spectrum of asymmetric reactions.

Our group has successfully applied the chiral *ortho*-metalated-amine complexes to asymmetric Diels-Alder reaction for the synthesis of a range of functionalized *P*-chiral phosphines (see 1.1.1.1).

### 1.3.1 Asymmetric [2+2] Cycloaddition

The organoplatinum complex containing *ortho*-metalated (1-(dimethylamino)ethyl)-naphthalene as the chiral auxiliary has been used efficiently to promote asymmetric [2+2] dimerization of (*E*)-2-(diphenylphosphanyl) styrene.<sup>131</sup> This dimerization reaction proceeds with high stereoselectivity to generate two cycloadducts (*S*)-**88** and (*S*)-**89** in the ratio of 6:1, respectively. As the two cycloadducts generated could not be purified efficiently, the naphthylamine auxiliary was removed by treatment with concentrated hydrochloric acid to generate the corresponding dichloro complexes (Scheme 1.43). Further treatment of the enantiomerically enriched dichloro complexes **90** with aqueous cyanide liberated an

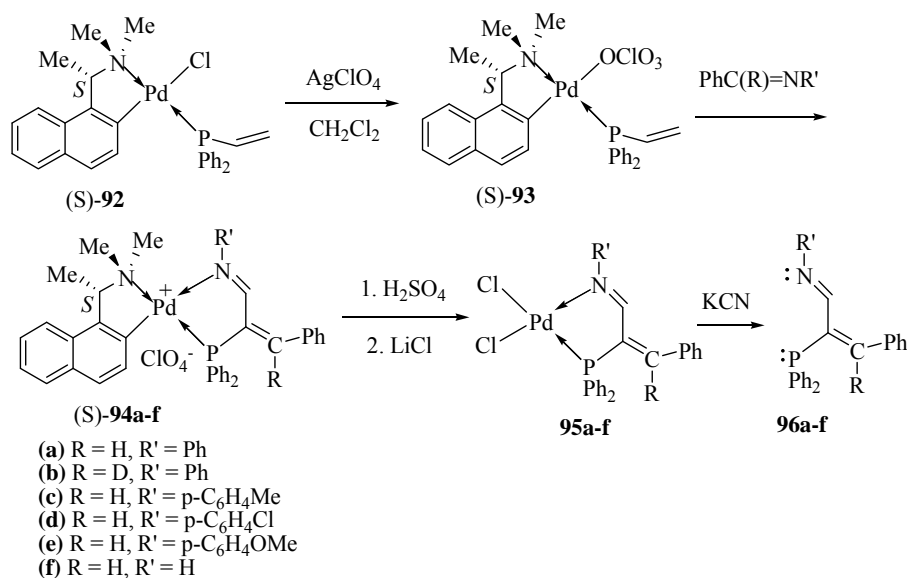
enantiomeric mixture of free diphosphane ligands **91**.



**Scheme 1.43**

### 1.3.2 Oxidative Coupling Reaction

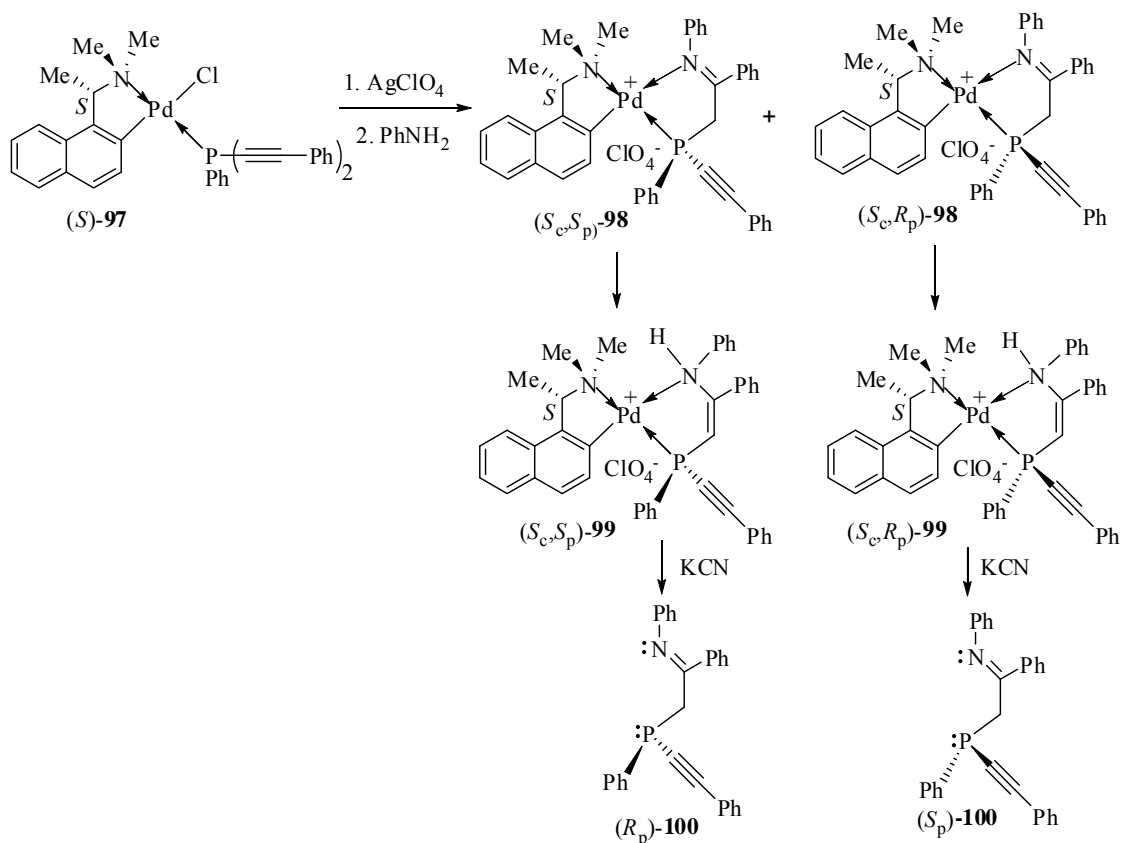
As shown in scheme 1.44, chiral *ortho*-palladated-amine complex has been successfully applied to promote oxidative coupling reaction between  $\text{Ph}_2\text{P}-\text{CH}=\text{CH}_2$  and a series of imines  $\text{PhC}(\text{R})=\text{N}(\text{R}')$  [where  $\text{R} = \text{H}, \text{D}$ ;  $\text{R}' = \text{H}, \text{Ph}, p\text{-Me}(\text{C}_6\text{H}_4), p\text{-Cl}(\text{C}_6\text{H}_4), p\text{-MeO}(\text{C}_6\text{H}_4)$ ] to produce the unexpected imino-phosphine ligands  $(\text{R}')\text{N}=\text{C}-\text{C}(\text{CPhR})\text{PPh}_2$  where the P,N-bidentate chelates to the chiral palladium template.<sup>132</sup> The coupling reactions initially adopted a [2+2] cycloaddition mechanism followed by the ring-opening pathway to generate the acyclic ligands. The naphthylamine moiety in the template complexes can be removed chemoselectively in strong sulfuric acid/LiCl to obtain dichloro complex **95a-f**. Then the imino-phosphines **96a-f** could be liberated from palladium by the treatment with aqueous cyanide.



Scheme 1.44

### 1.3.3 Asymmetric Hydroamination Reaction

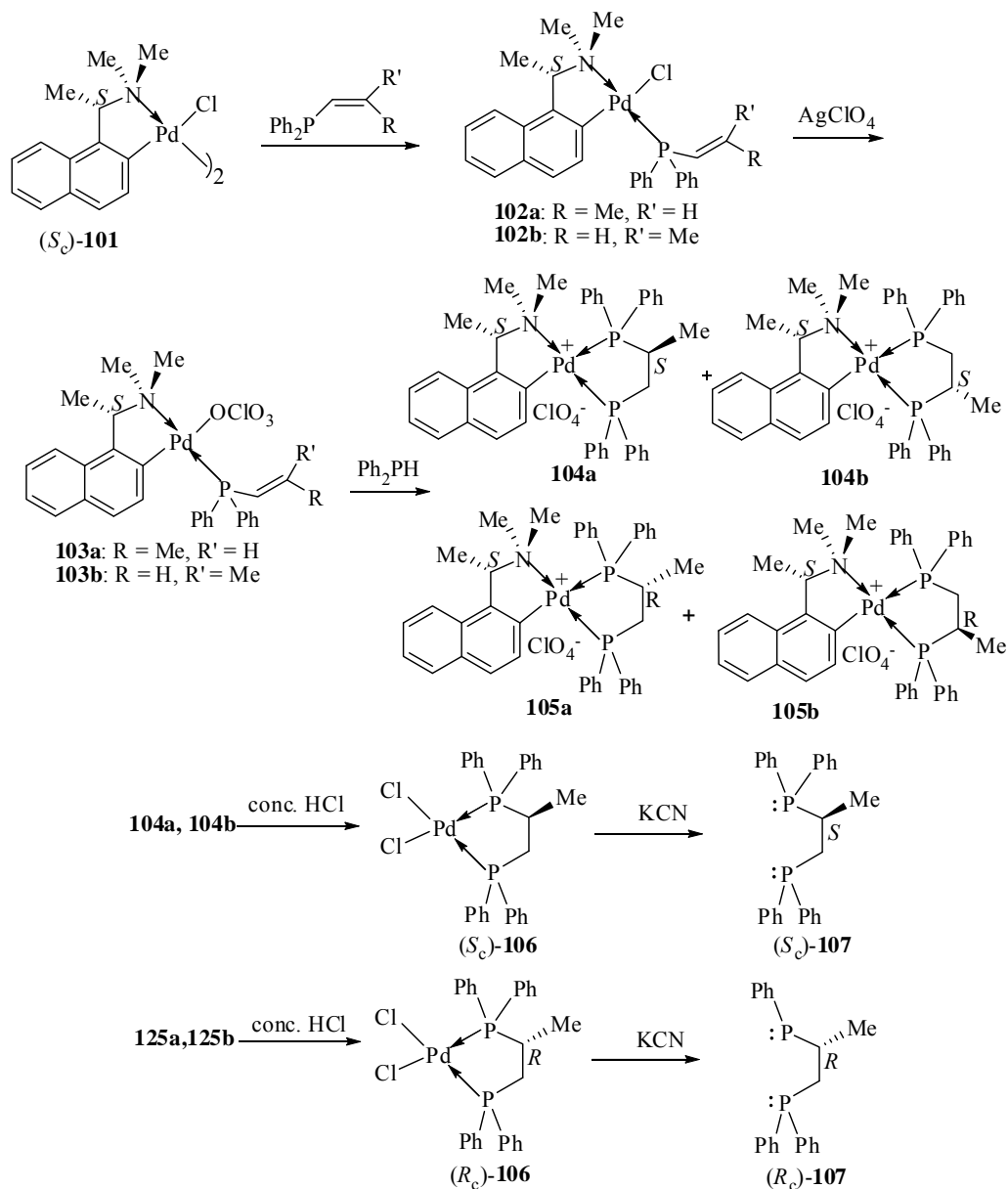
In the presence of the organopalladium template containing the orthometalated (*S*)-(1-(dimethylamino)ethyl)naphthylene auxiliary, di(phenylethynyl) phenylphosphine can be activated toward the asymmetric hydroamination reaction with aniline to give two diastereomeric chelating iminophosphine complexes (*S<sub>c</sub>,S<sub>p</sub>*)-**98** and (*S<sub>c</sub>,R<sub>p</sub>*)-**98** in the ratio 4:1 (Scheme 1.45).<sup>133</sup> Then both *P*-chiral template complexes underwent the tautomerism process in solution and transformed quantitatively into their enamino counterparts (*S<sub>c</sub>,S<sub>p</sub>*)-**99** and (*S<sub>c</sub>,R<sub>p</sub>*)-**99**, respectively. Subsequently treatment of either iminophosphine or enamino phosphine template complexes with KCN a pair of novel and enantiomerically pure *P*-chiral iminophosphines (*R<sub>p</sub>*)-**100** and (*S<sub>p</sub>*)-**100** were obtained in high yields.



Scheme 1.45

### 1.3.4 Asymmetric Hydrophosphination Reaction

The efficiency of the chiral cyclopalladated-amine template promoted asymmetric hydrophosphination reactions between diphenylphosphine and (*E*)- or (*Z*)-diphenyl-1-propenylphosphine in high regio- and stereoselectivities under mild conditions has been illustrated by our group.<sup>134</sup> Hydrophosphination of (*Z*)-diphenyl-1-propenylphosphine with diphenylphosphine gave chiral diphosphine (*S<sub>c</sub>*)-**107** as the major product. Using the same chiral metal template, the corresponding hydrophosphination reaction with (*E*)-diphenyl-1-propenylphosphine gave predominantly chiral diphosphine (*R<sub>c</sub>*)-**107** (Scheme 1.46).

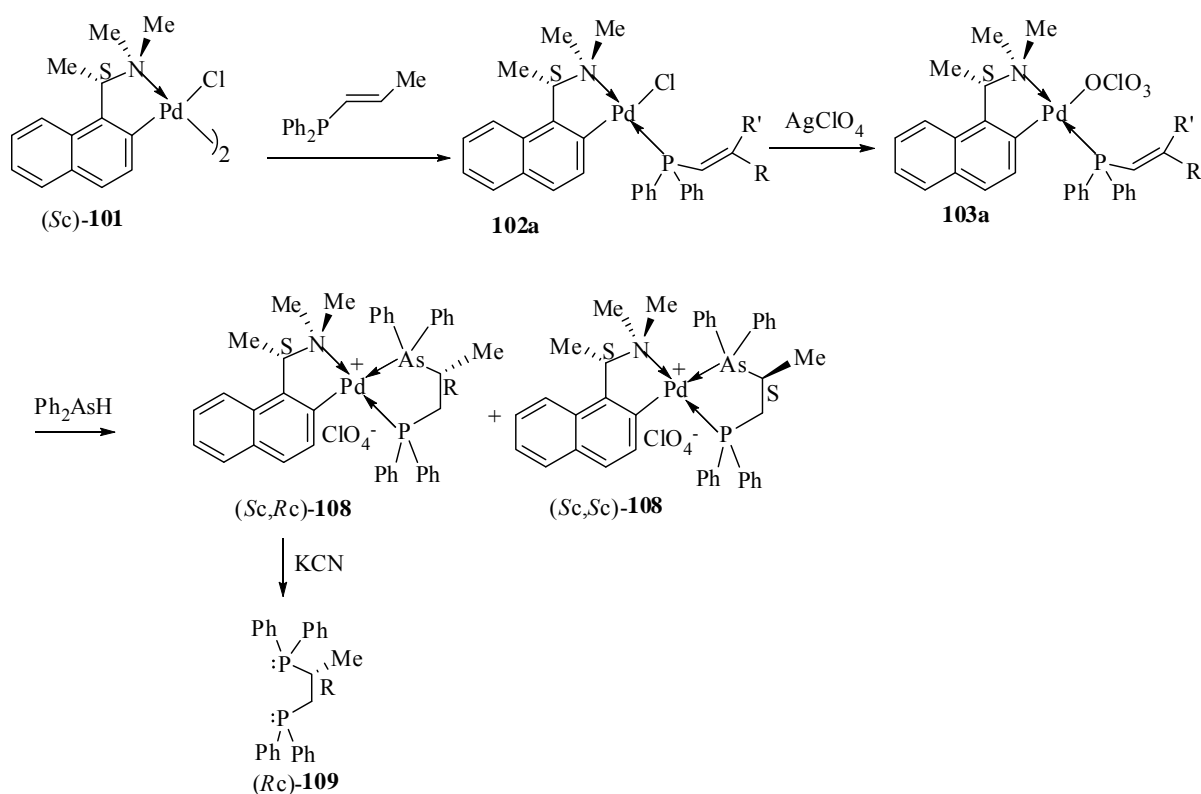


**Scheme 1.46**

Our group also extended the asymmetric hydrophosphination reaction to synthesize functionalized diphosphine ligands with chirality residing on the carbon backbone. Under mild conditions, the alkenols, 3-buten-1-ol and 2-propyn-1-ol, were subjected to direct hydrophosphination to give the corresponding Markovnikov addition products. The phosphine functionalized alkenols thus obtained were subsequently subjected to a second-stage asymmetric hydrophosphination employing

an organopalladium complex containing the orthometalated (*R*)-(1-(dimethylamino)ethyl)naphthalene as a chiral auxiliary and reaction promoter.<sup>135</sup> In the presence of an organopalladium(II) complex derived from (*S*)-*N,N*-dimethyl-1-(1-naphthyl)ethylamine an optically pure *C*<sub>2</sub>-symmetrical diphosphine ligand containing two ester functional groups at the two chiral carbon stereogenic centres was prepared efficiently from the asymmetric hydrophosphination reaction between diphenylphosphine and dimethyl acetylenedicarboxylate.<sup>136</sup>

### 1.3.5 Asymmetric Hydroarsination Reaction



**Scheme 1.47**

Our group has demonstrated that transition-metal complex-promoted asymmetric hydroarsination is a potential synthetic route for the preparation of asymmetric arsenic ligands.<sup>137</sup> As shown in scheme 1.47, The dissymmetrical chiral

bidentate (*R*)-(+)-1-(diphenylphosphino)-2-(diphenylarsino)propane was prepared stereoselectively via the novel asymmetric hydroarsination reaction between diphenylarsine and diphenyl-1-propenyl-(*E*)-phosphine using di- $\mu$ -chlorobis{(*S*)-1-[1-(dimethylamino)ethyl]-2-naphthalenyl-C,N}dipalladium(II) as the chiral reaction promoter. However, the current asymmetric hydroarsination reaction could only be induced effectively in polar solvents, such as methanol.

#### 1.4 Aims of the Present Project

The project aims at contributing to the knowledge and development of synthetic methods involving chiral bidentate phosphines and pyridylphosphines. To date the importance of chiral phosphines in asymmetric catalysis has been well established. This has led to the need for variety of functionalized chiral phosphines with chirality residing either on the P or on the C-backbone or on both. Due to the relatively few known arsine ligands, their catalytic properties are also not well studied. Synthesis of new kinds of chiral As-N ligands is also reported in this work.

Chapter 2 describes the Diels-Alder reactions between 3-diphenylphosphinofuran and various vinylphosphine dienophiles in the presence of the organo-platinum complex to give the *endo*-cycloadducts. This is the first instance of *endo*-cycloadducts being generated in the intramolecular Diels-Alder reaction using the chiral template method. Chapter 3 reports the Diels-Alder reaction between 3-diphenylphosphinofuran and DMPP under the promotion of the organo-platinum complex in which the furan acts as the dienophile. Chapter 4 deals with the

asymmetric hydrophosphination of diphenylphosphine with pyridine and quinoline complexes in the presence of the organo-palladium complex to generate the optically pure keto- and ester-functionalized chiral P-N bidentate ligands. Chapter 5 presents the asymmetric hydroarsination reactions as a new and alternative technique of preparing chiral As-N bidentate ligands promoted by the organo-palladium complex. Chapter 6 describes the asymmetric hydrophosphination between phosphinoalkynes and phenylmethylphosphine in the presence of the organo-palladium complex to generate the *P*-chiral diphosphines.

## Chapter 2

# 3-Substituted Phosphinofurans as Dienes in Asymmetric Diels-Alder Reaction

### 2.1 Introduction

Well-known and extensively studied for many decades, the Diels-Alder reaction remains as one of the most frequently employed synthetic methods for the synthesis of complex molecules<sup>138</sup> such as natural products, antibiotics and prostaglandins.<sup>139-141</sup> It is not only practically favorable but also the best understood reaction theoretically.<sup>142</sup>

Due to the strong aromaticity, furan is a poor diene for the Diels-Alder reaction. However, it still constitutes an important class of dienes for the [4+2] cycloaddition reaction, yielding versatile oxanorbornenes that have been used in the syntheses of numerous complex molecular architectures.<sup>143</sup>

In general, furans can undergo the Diels-Alder reaction with very reactive dienophiles such as activated alkenes, alkynes and allenes.<sup>144-147</sup> For example, phenyl vinylsulfonate worked with furans in excellent yields at room temperature to yield a 5.4:1 mixture of *endo*/*exo* isomers.<sup>148</sup> Phenylsulfonyl allene underwent cycloaddition with furan at 100 °C to give a 58% yield of the *endo* cycloadduct (together with a 3% yield of the corresponding *exo* adduct).<sup>149</sup>

Lewis acid catalysts and high-pressure protocols have been used to improve the yields in such cycloaddition reactions.<sup>150</sup> Lewis acids are commonly used to

catalyze Diels-Alder reactions as, by complexing with the dienophile, the energy gap between the lowest unoccupied molecular orbital (LUMO) of the dienophile and the highest occupied molecular orbital (HOMO) of the diene is reduced, thus decreasing the activation energy required to achieve the cycloaddition. Moreover, as this stabilization is greater for the *endo* transition state, as a result of beneficial enhancement of secondary orbital overlap that is unobtainable in an *exo* mode of reaction, the use of Lewis acids favors an increased ratio of *endo:exo* products.<sup>151</sup> In the cycloaddition of methyl acrylate or acrylonitrile with furan,<sup>13a</sup> catalytic quantities of zinc iodide can greatly accelerate the rate and improve the yield and the resulting 7-oxabicyclo[2.2.1] heptenes were achieved as mixtures of *exo/endo* isomers. For sensitive dienes and dienophiles, Yb(fod)<sub>3</sub> was used as a mild cycloaddition catalyst.<sup>152</sup> In presence of 10 mol-% of Yb(fod)<sub>3</sub>, addition of acrolein to furan afforded a 4:5:1 mixture of *exo/endo* cycloadducts in 40% yield. According to the study, high-pressure furan cycloadditions with monoactivated and deactivated dienophiles, Harwood and coworkers<sup>153</sup> found that 6,6-fused ring systems with *exo*-stereochemistry at the ring junction are readily prepared using high pressure. 7,6-fused ring systems can also be prepared, having a mixture of *endo*- and *exo*-products (Figure2.1).

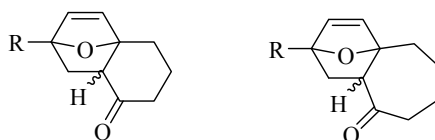
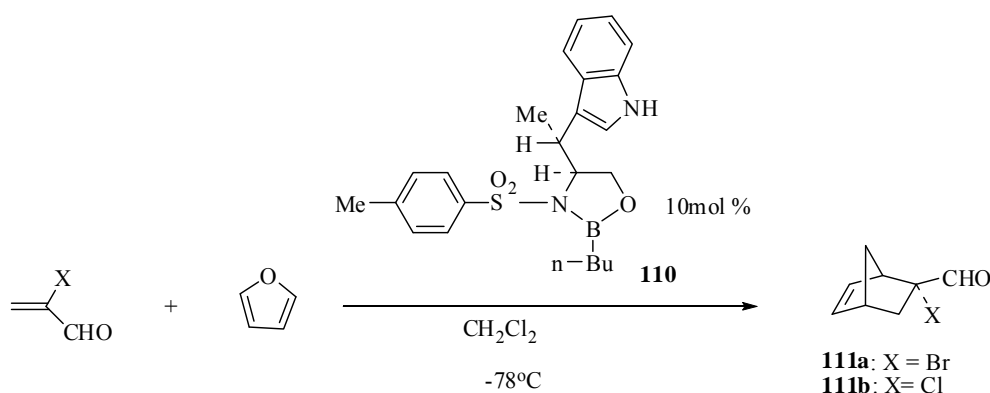


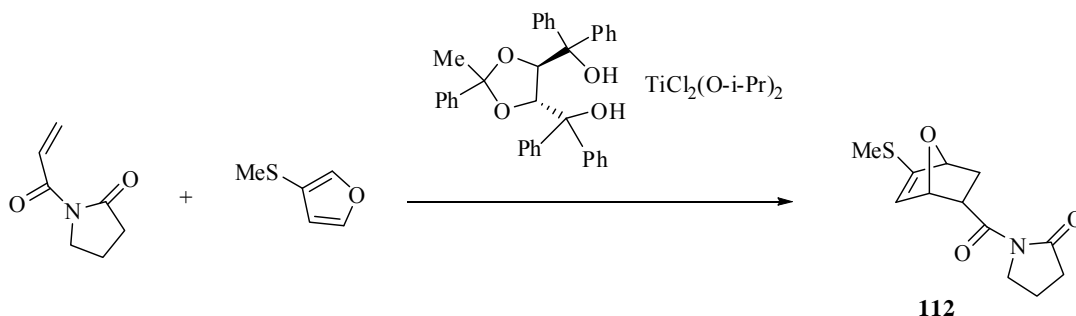
**Figure2.1**

As for the asymmetric furan Diels-Alder reaction, numerous chiral catalysts and

chiral auxiliaries (on the dienophile or diene)<sup>138b</sup> have been applied for the synthesis of optically active cycloadducts. In 1993, Corey first reported the application of an enantioselective catalyst to furan (Scheme 2.1).<sup>154</sup> In the presence of the oxazaborolidine-derived chiral catalyst **110**, cycloaddition of 2-bromo- and 2-chloroacrolein with furan led to the cycloadducts **111a, b** in >98% chemical yield (*exo/endo* 99:1) with 96:4 and 95:5 enantioselectively, respectively. Another example of a catalytic enantioselective furan cycloaddition reaction was reported by Narasaka (Scheme 2.2).<sup>155</sup> The treatment of 3-methylthiofuran with acrylamide in the presence of a chiral titanium catalyst resulted in the formation of cycloadduct **112** (*endo/exo* = 85:15) in 97% combined yield. The enantiomeric excess of the *endo* product **112** was 87%.

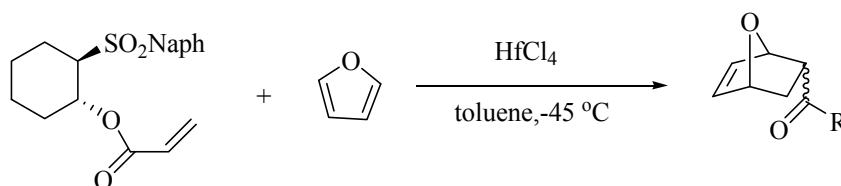


Scheme 2.1



Scheme 2.2

HfCl<sub>4</sub>-mediated Diels-Alder reaction of furan and (-)-(1*R*,2*R*)-2-(naphthalene-2-sulfonyl)cyclohexylacrylate in toluene proceeded at low temperature (-45 °C) to afford the cycloadduct in good yield (83%) with high diastereomeric excess (*endo/exo* = 68/32, *endo* = 87% de, *exo* = 91% de) (Scheme 2.3).<sup>156</sup>



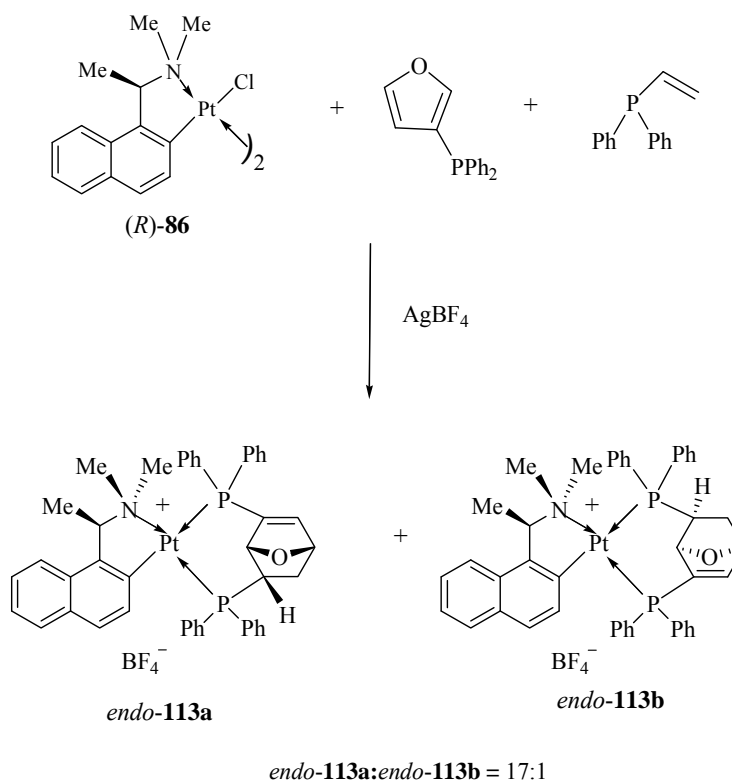
**Scheme 2.3**

Leung and coworkers have reported the use of cyclometalated-amine complexes as efficient chiral templates for the asymmetric synthesis of chiral phosphines and their metal complexes *via* the asymmetric Diels-Alder reaction between heterocyclic dienes, such as 3,4-dimethyl-1-phenylphosphole (DMPP), 3,4-dimethyl-1-phenylarsole (DMPA), 2-diphenylphosphinofuran, and *N*-diphenylphosphinopyrrole, and a range of dienophiles.<sup>157-160</sup> In general, these cyclometalated-amine complexes promoted carbon-carbon bond formation reactions can be related to a common intermediate in which the cyclic diene and the dienophile are co-ordinated simultaneously to the chiral metal template during the course of cycloaddition to give the *exo*-cycloadducts. In these asymmetric syntheses, the chiral metal templates not only activate the substrates and provide the desired stereochemical control for the cycloaddition reaction but also stabilize the resulting cycloadducts. However in these intramolecular reactions, no *endo*-cycloadducts have

been produced. In pursuing our interest and extending the scope of this class of metal template promoted cycloaddition reactions, we hereby present the chiral platinum template promoted cycloaddition reactions, we hereby present the chiral platinum template promoted asymmetric Diels-Alder reaction between 3-diphenylphosphinofuran and diphenylvinylphosphine.

## 2.2 Results and Discussion

### 2.2.1 Intramolecular *Endo*-Diels-Alder Reaction between 3-Diphenylphosphinofuran and Diphenylvinylphosphine



**Scheme 2.4**

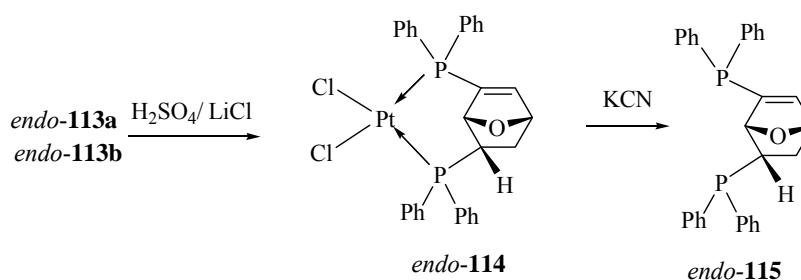
In the absence of a metal template, no reaction was observed between

3-diphenylphosphinofuran and diphenylvinylphosphine, even under prolonged heating. However, the corresponding Diels-Alder reaction could be induced with the use of (*R*)-**86** as the template precursor, to generate diphenylphosphino-substituted cycloadducts which are coordinated as bidentate chelates onto the chiral metal template (Scheme 2.4).

The dimeric complex (*R*)-**86** itself is not an efficient chiral template, as it could not induce the desired Diels-Alder reaction even upon heating. The M-Cl bond that is *trans* to the aromatic carbon is inert to ligand substitution (even with monodentate phosphines).<sup>161-162</sup> Thus the chloro ligand which occupies one of the two essential coordination sites hinders the simultaneous coordination of 3-diphenylphosphinofuran and diphenylvinylphosphine onto the metal template, and no cycloaddition reaction could be observed. However, upon removal of all chloro ligands with stoichiometric amount of silver tetrafluoroborate, (*R*)-**86** activates the desired Diels-Alder reaction.

Stoichiometric amounts of (*R*)-**86**, diphenylvinylphosphine and 3-diphenylphosphinofuran in 1,2-dichloroethane were treated with aqueous silver tetrafluoroborate,<sup>157-158</sup> the corresponding asymmetric Diels-Alder reaction was completed in 7 days at 60 °C. Prior to the purification, the <sup>31</sup>P{<sup>1</sup>H} NMR spectrum of the crude reaction mixture in CDCl<sub>3</sub> exhibited two pairs of doublets indicative of the formation of only two stereochemically distinct products *endo*-**113a** and *endo*-**113b** in the ratio 17:1. The doublets of the major diastereomer were observed at  $\delta$  26.2 ( $J_{PP}$  = 14.5 Hz,  $J_{PtP}$  = 1713 Hz) and -4.6 ( $J_{PP}$  = 14.5 Hz,  $J_{PtP}$  = 3682 Hz).

Treatment of the tetrafluoroborate salts with concentrated sulfuric acid at room temperature removed the naphthylamine auxiliary chemoselectively (Scheme 2.5). Upon addition of excess lithium chloride into the acidic solution, the dichloro complex *endo*-**114** that precipitated out of solution was recrystallized from dichloromethane-diethyl ether as pale yellow prisms in 70% yield,  $[\alpha]_{\text{D}} +34.7^{\circ}$  ( $c$  4,  $\text{CH}_2\text{Cl}_2$ ). The  $^{31}\text{P}\{^1\text{H}\}$  NMR spectrum of the reaction mixture in  $\text{CDCl}_3$  exhibited one pair of doublets at  $\delta$  21.2 ( $J_{\text{PP}}=14.7$  Hz,  $J_{\text{PtP}}=3577$  Hz) and -15.1 ( $J_{\text{PP}}=14.7$  Hz,  $J_{\text{PtP}}=3411$  Hz).



**Scheme 2.5**

### 2.2.1.1 X-ray Structural Analysis of *endo*-**114**

The molecular structure and the absolute configurations of the recrystallized *endo*-**114** were established by a single-crystal X-ray crystallographic analysis. Interestingly, *endo*-**114** crystallized as a pair of crystallographically independent molecules in the unit cell. However, the two molecules have the same absolute stereochemistry and molecular connectivity and differ only slightly in their bond angles. For clarity, only one molecule (molecule 1) is depicted in Figure 2.2.

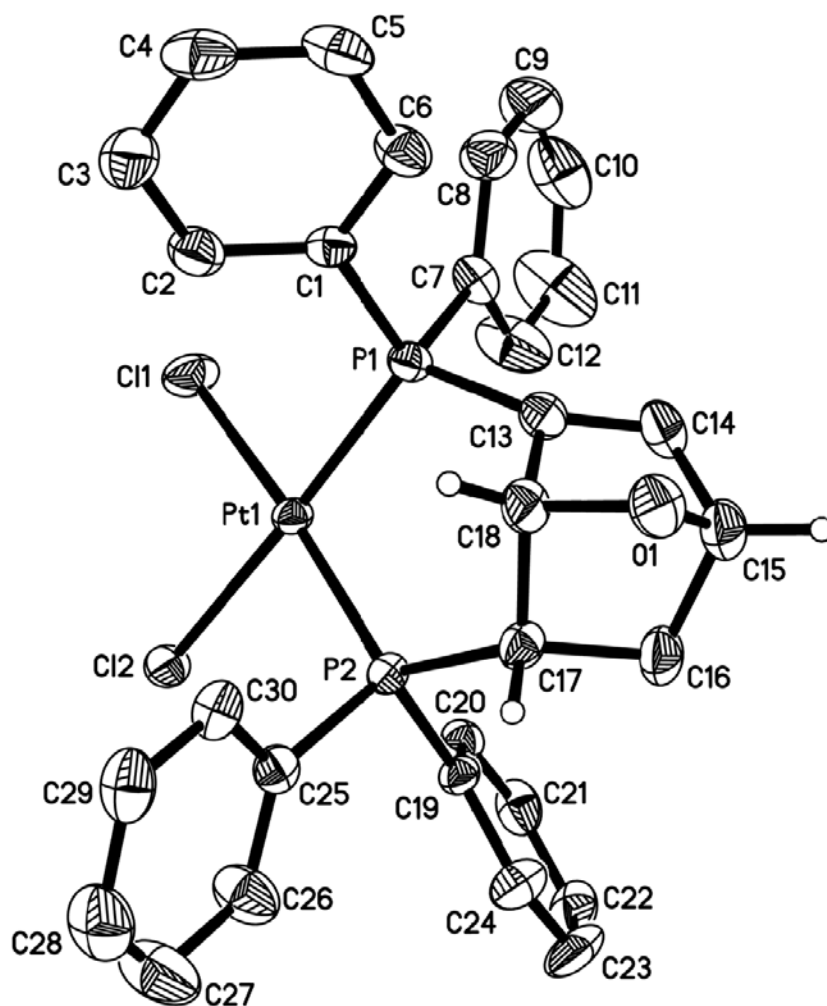


**Figure 2.2** Molecular structure of the dichloro complex *endo*-114 (Molecule 1)

The crystallographic study reveals that the cycloaddition reaction between the coordinated 3-diphenylphosphinofuran and diphenylvinylphosphine has resulted in the formation of the *endo*-phosphine. The chiral ligand coordinates as a bidentate chelate *via* its phosphorus donor atoms to the platinum, with the diphenylphosphino group substituted at the *endo* position at C(27). The geometry at platinum is distorted square planar with angles at platinum in the ranges of 84.9(1)-87.5(1) and 174.5(1)-177.3(1) $^{\circ}$ . The absolute configurations of the three newly generated

stereogenic centers at C(15), C(17), and C(18) are *S*, *S*, and *R*, respectively. Importantly the C-O-C bonds in the oxanorbornene skeleton remained unchanged in the strong sulfuric acid treatment. Selected bond lengths and bond angles are given in Table 2.1 (molecule 1) and Table 2.2 (molecule 2).

**Table 2.1 Selected bond lengths (Å) and angles (deg) for *endo*-114 (Molecule 1)**

Pt(1)–P(1)	2.231(1)	P(1)–Pt(1)–P(2)	97.8(1)
Pt(1)–P(2)	2.240(1)	P(1)–Pt(1)–Cl(2)	177.3(1)
Pt(1)–Cl(2)	2.352(1)	P(2)–Pt(1)–Cl(2)	84.9(1)
Pt(1)–Cl(1)	2.353(1)	P(1)–Pt(1)–Cl(1)	87.5(1)
P(1)–C(13)	1.800(3)	P(2)–Pt(1)–Cl(1)	174.5(1)
P(2)–C(17)	1.859(3)	Cl(2)–Pt(1)–Cl(1)	89.8(1)
C(13)–C(14)	1.320(5)	C(18)–C(13)–P(1)	120.7(2)
C(13)–C(18)	1.526(5)	C(13)–C(14)–C(15)	106.0(3)
C(14)–C(15)	1.513(5)	C(14)–C(15)–C(16)	104.5(3)
C(15)–O(1)	1.435(5)	C(15)–C(16)–C(17)	101.4(3)
C(15)–C(16)	1.539(5)	C(16)–C(17)–C(18)	100.4(3)
C(16)–C(17)	1.543(4)	C(18)–C(17)–P(2)	115.6(2)
C(17)–C(18)	1.558(4)	C(13)–C(18)–C(17)	105.7(3)
C(18)–O(1)	1.428(4)	C(18)–O(1)–C(15)	96.1(2)

### 2.2.1.2 Liberation and the Optical Purity of *endo*-115

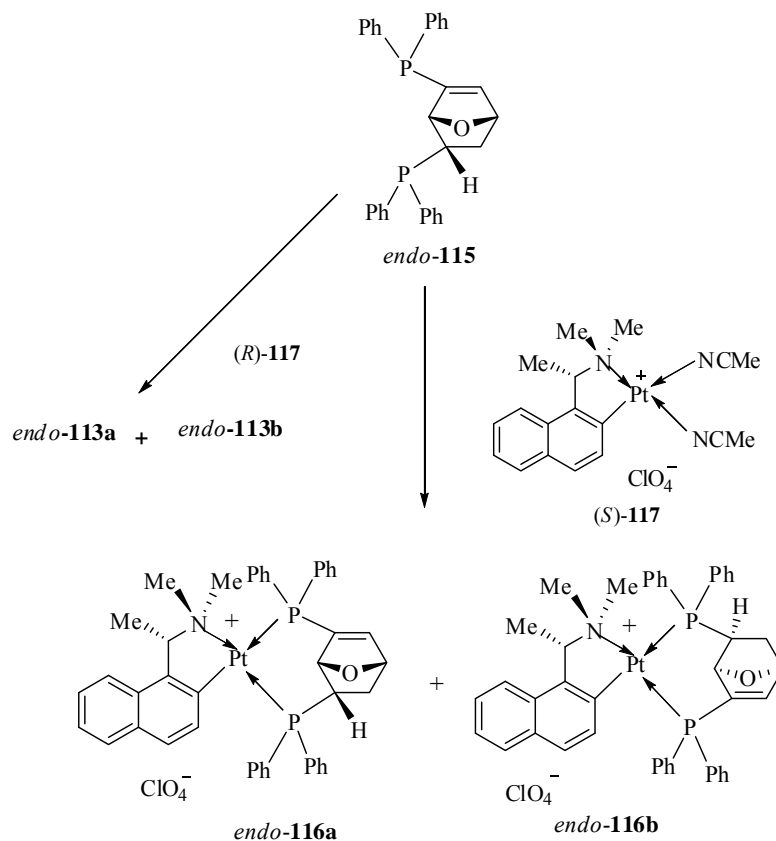
The optically active ligand *endo*-115 can be stereospecifically liberated from the complex *endo*-114 by treatment of the dichloro complex with aqueous potassium cyanide at room temperature (Scheme 2.5). The liberated *endo*-115 was obtained as an air stable white solid in 80% yield,  $[\alpha]_D -37.6^\circ$  (*c* 1.7, CH<sub>2</sub>Cl<sub>2</sub>). The <sup>31</sup>P{<sup>1</sup>H} NMR spectrum of the free ligand in CDCl<sub>3</sub> exhibited two doublets at  $\delta$  -12.5 (*J*<sub>PP</sub> = 77 Hz) and -20.8 (*J*<sub>PP</sub> = 77 Hz).

**Table 2.2 Selected bond lengths (Å) and angles (deg) for *endo*-114 (Molecule 2)**

Pt(2)–P(4)	2.230(1)	P(3)–Pt(2)–Cl(3)	86.5(1)
Pt(2)–P(3)	2.234(1)	P(4)–Pt(2)–Cl(4)	86.2(1)
Pt(2)–Cl(3)	2.348(1)	P(3)–Pt(2)–Cl(4)	175.6(1)
Pt(2)–Cl(4)	2.353(1)	Cl(3)–Pt(2)–Cl(4)	89.5 (1)
P(3)–C(43)	1.837(3)	C(43)–P(3)–Pt(2)	119.9(1)
P(4)–C(47)	1.783(3)	C(47)–P(4)–Pt(2)	112.1(1)
C(43)–C(44)	1.543(4)	C(47)–P(4)–Pt(2)	112.1(1)
C(43)–C(48)	1.545(5)	C(44)–C(43)–C(48)	100.8(3)
C(44)–C(45)	1.549(5)	C(48)–C(43)–P(3)	118.4(2)
C(45)–O(2)	1.422(4)	C(43)–C(44)–C(45)	100.9(3)
C(45)–C(46)	1.522(5)	C(46)–C(45)–C(44)	103.8(3)
C(46)–C(47)	1.347(5)	C(47)–C(46)–C(45)	104.7(3)
C(47)–C(48)	1.523(5)	C(46)–C(47)–C(48)	105.0(3)
C(48)–O(2)	1.426(4)	C(48)–C(47)–P(4)	122.6(2)
P(4)–Pt(2)–P(3)	97.8(1)	C(47)–C(48)–C(43)	105.9(3)
P(4)–Pt(2)–Cl(3)	174.8(1)	C(45)–O(2)–C(48)	96.7(2)

### 2-2.1.3 Reoordination of *endo*-115 to (*R*)-117 and (*S*)-117

In order to determine the enantiomeric purity of *endo*-115 and to establish the identity of the unisolated isomer, the liberated ligand was re-coordinated to the equally accessible (*R*)-117 (Scheme 2.6). This re-coordination process generated two regioisomers in the ratio of 12:1. These two recomplexation products exhibit identical  $^{31}\text{P}\{^1\text{H}\}$  NMR spectra to those recorded for the products generated from the original cycloaddition reaction, so the products *endo*-113 and *endo*-113 generated from the original cycloaddition reaction are identified as regioisomers.



Scheme 2.6

As a further check, *endo*-115 was recomplexed to *(S)*-117 thus generating two regioisomers *endo*-116a and *endo*-116b in the ratio of 7:1. The major isomer showed a pair of doublets at  $\delta$  27.6 ( $J_{\text{PP}} = 14.5$  Hz,  $J_{\text{PtP}} = 1710$  Hz) and -6.2 ( $J_{\text{PP}} = 14.5$  Hz,  $J_{\text{PtP}} = 3677$  Hz). These two recomplexation products exhibit different  $^{31}\text{P}\{^1\text{H}\}$  NMR spectra to those recorded for the two cycloadducts generated directly from the asymmetric cycloaddition reaction thus reaffirming that the liberated ligand is stereochemically pure. Eventually, the major recomplexation product in this instance could be isolated in a diastereomerically pure form by fractional crystallization from dichloromethane-diethyl ether as pale yellow crystals in 85% yield,  $[\alpha]_{\text{D}} -35^{\circ}$  ( $c$  1.0,  $\text{CH}_2\text{Cl}_2$ ). Due to the unique *trans*-electronic influence which originates from the

organoplatinum unit, the larger platinum–phosphorus coupling constant observed for the doublet signal at  $\delta -6.2$  is diagnostic of the  $\text{PPh}_2$  group coordinated *trans* to the  $\sigma$ -donating nitrogen atom.<sup>157,158,160</sup> On the other hand, the doublet at  $\delta 27.6$ , which shows the smaller platinum–phosphorus coupling constant, is unambiguously assigned to the  $\text{PPh}_2$  group that is coordinated *trans* to the strong  $\pi$ -accepting orthometalated carbon atom.

#### 2-2.1.4 X-ray Structural Analysis of *endo-116b*

This crystalline product was confirmed by X-ray crystallography to be complex *endo-116b*, as shown in Figure 2.3. Selected bond lengths and angles are given in Table 2.3. The geometry at platinum is distorted square planar with angles at platinum in the ranges of 84.9(1)-87.5(1) and 174.4(1)-177.2(1)°. The absolute configurations of the four generated stereogenic centers at C(11), C(29), C(31), and C(32) are *S*, *S*, *S*, and *R*, respectively. Along with the significant difference in the two Pt-P coupling constants observed in the  $^{31}\text{P}\{^1\text{H}\}$  NMR spectrum, the Pt-P(1) distance [2.387(2) Å] is clearly longer than the Pt-P(2) bond [2.242(2) Å]. These spectroscopic and structural data thus confirm that the unique *trans*-electronic influences which originate from the organoplatinum unit operate strongly both in the solid state and in solution. From the  $^{31}\text{P}\{^1\text{H}\}$  NMR spectroscopic data of *endo-116b*, the doublet signal at  $\delta -6.2$  is diagnostic of the  $\text{PPh}_2$  group from 3-diphenylphosphinofuran, while the doublet at  $\delta 27.6$  is assigned to the  $\text{PPh}_2$  group from diphenylvinylphosphine. Hence it could be established that complex *endo-113b* is the major component of the mixture

generated directly from the asymmetric Diels-Alder reaction, while complex *endo-113a* is the minor cycloaddition product formed.

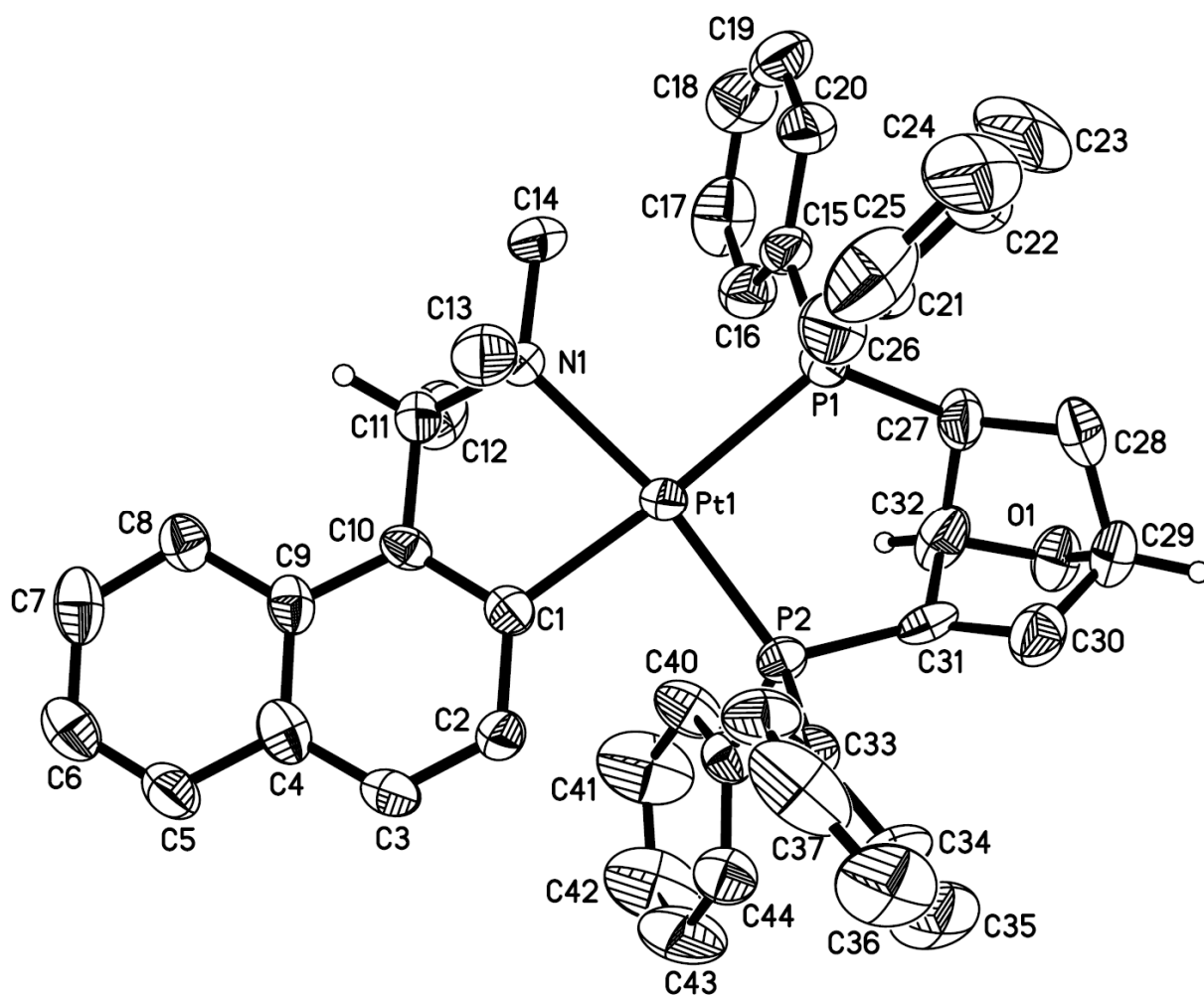


Figure 2.3 Molecular structure and absolute stereochemistry of the cationic complex *endo-116b*

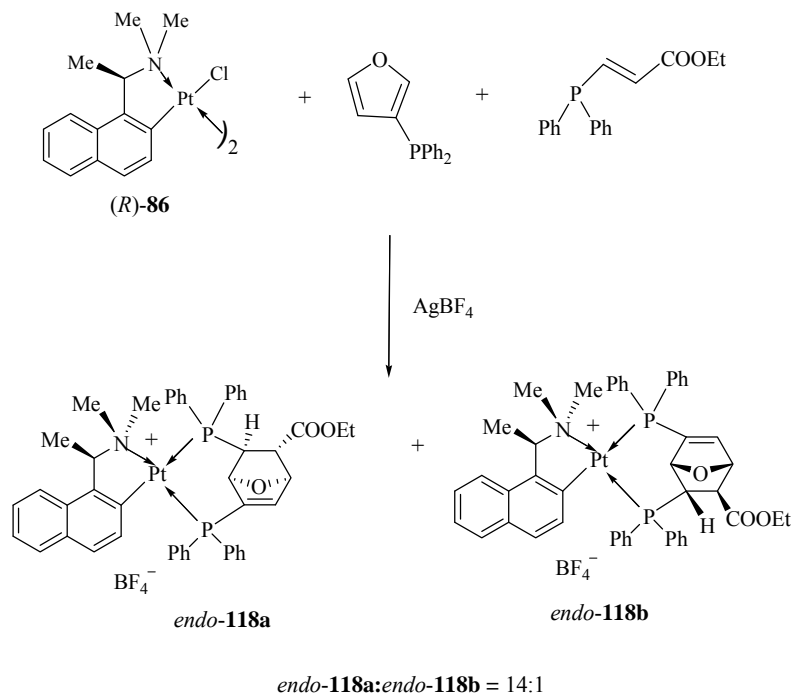
**Table 2.3 Selected bond lengths (Å) and angles (deg) for *endo*-116b**

Pt(1)–C(1)	2.118(8)	N(1)–Pt(1)–P(2)	169.7(2)
Pt(1)–N(1)	2.196(7)	C(1)–Pt(1)–P(1)	175.2(3)
Pt(1)–P(2)	2.242(2)	N(1)–Pt(1)–P(1)	96.5(2)
Pt(1)–P(1)	2.387(2)	P(2)–Pt(1)–P(1)	93.48(8)
C(27)–C(28)	1.513(15)	C(28)–C(27)–C(32)	101.5(9)
C(27)–C(32)	1.539(15)	C(32)–C(27)–P(1)	112.9(6)
C(27)–P(1)	1.946(11)	C(29)–C(28)–C(27)	102.4(9)
C(28)–C(29)	1.496(15)	C(28)–C(29)–C(30)	105.3(9)
C(29)–O(1)	1.447(13)	C(31)–C(30)–C(29)	107.2(10)
C(29)–C(30)	1.496(15)	C(30)–C(31)–C(32)	103.7(9)
C(30)–C(31)	1.331(13)	C(32)–C(31)–P(2)	120.9(7)
C(31)–C(32)	1.550(14)	C(27)–C(32)–C(31)	105.4(9)
C(31)–P(2)	1.784(9)	C(32)–O(1)–C(29)	97.0(7)
C(32)–O(1)	1.414(12)	C(27)–P(1)–Pt(1)	119.1(3)
C(1)–Pt(1)–N(1)	79.4(3)	C(31)–P(2)–Pt(1)	113.6(3)
C(1)–Pt(1)–P(2)	90.7(2)		

### 2-2.2 Intramolecular Endo-Diels-Alder Reaction Between 3-Diphenylphosphinofuran and Diphenyl[(*E*)-2-(ethoxycarbonyl)vinyl]phosphine

When (*R*)-**86**, diphenyl[(*E*)-2-(ethoxycarbonyl)vinyl]phosphine and 3-diphenylphosphinofuran in dichloromethane were treated with aqueous silver tetrafluoroborate (Scheme 2.7), the corresponding asymmetric Diels-Alder reaction was completed in 20 days at room temperature. Prior to purification, the  $^{31}\text{P}\{^1\text{H}\}$  NMR spectrum of the crude reaction mixture in  $\text{CDCl}_3$  exhibited three pairs of doublets indicative of the formation of three stereochemically distinct products in the ratio 14:1:1. The doublets of the major diastereomer *endo*-**118a** were observed at  $\delta$  28.5 ( $J_{\text{PP}}=14.5$  Hz,  $J_{\text{PtP}}=1713$  Hz) and -3.2 ( $J_{\text{PP}}=14.5$  Hz,  $J_{\text{PtP}}=3664$  Hz). Upon comparison to the NMR data from the Diels-Alder reaction of 3-diphenylphosphinofuran and diphenylvinylphosphine, the doublet signal at  $\delta$  -3.2 is

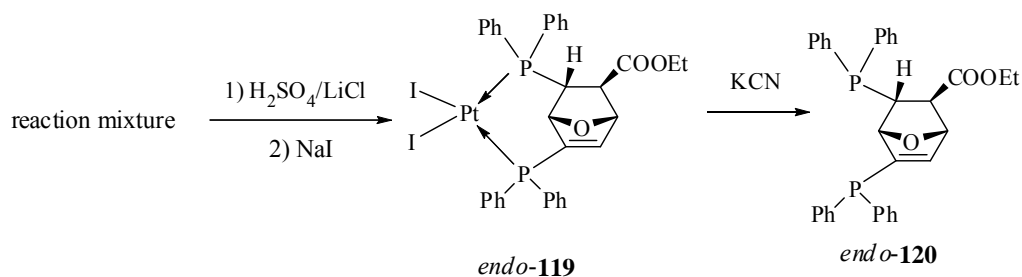
diagnostic of the PPh<sub>2</sub> group from 3-diphenylphosphinofuran, while the doublet at  $\delta$  28.5 is assigned to PPh<sub>2</sub> group from diphenyl[(*E*)-2-(ethoxycarbonyl)vinyl]phosphine.



**Scheme 2.7**

Treatment of the tetrafluoroborate salt with concentrated sulfuric acid at room temperature removed the naphthylamine auxiliary chemoselectively (Scheme 2.8). Upon addition of excess lithium chloride into the acidic solution, the dichloro complexes precipitated from solution as pale yellow solids. Attempts to separate the isomers by crystallization failed. Therefore the dichloro complex was converted into the corresponding diiodo complex which has been found to be readily crystallized. Upon treatment of the dichloro complex with sodium iodide,<sup>163</sup> the <sup>31</sup>P{<sup>1</sup>H} NMR spectrum of the diiodo complexes in CDCl<sub>3</sub> exhibited two pairs of doublets in the ratio of 15:1 and the doublets of the major diastereomer *endo*-119 were observed at  $\delta$

20.5 ( $J_{PP} = 8.9$ ,  $J_{PtP} = 3396$  Hz), -17.9 ( $J_{PP} = 8.9$ ,  $J_{PtP} = 3181$  Hz). The complex was subsequently obtained as yellow crystals from dichloromethane-diethyl ether in 72% yield,  $[\alpha]_D +12.7^\circ$  ( $c$  0.6,  $\text{CH}_2\text{Cl}_2$ ).



**Scheme 2.8**

### 2-2.2.1 X-ray Structural Analysis of *endo-119*

The isolated diiodo complex was shown to be the complex *endo-119* as confirmed by the X-ray crystallographic analysis (Figure 2.4). The crystallographic study further revealed that the cycloaddition reaction between the coordinated 3-diphenylphosphinofuran and diphenyl[(*E*)-2-(ethoxycarbonyl)vinyl]phosphine resulted in the formation of the *endo*-cycloadduct. The chiral ligand coordinates as a bidentate chelate via the phosphorus donor atoms to the platinum. The geometry at platinum is distorted square planar with angles at platinum in the ranges of 86.0(1)-87.2(1) and 173.0(1)-174.1(1)°. The absolute configurations of the four newly generated stereogenic centers at C(15), C(16), C(17), and C(18) are *R*, *R*, *R*, and *S*, respectively, with the diphenylphosphino group being orientated in the *endo* position at C(17). The distances of the two Pt-P bonds are similar (2.238(1) and 2.261(1) Å), and so are the two Pt-I bonds (2.628(1) and 2.643(1) Å). Selected bond lengths and

bond angles are given in Table 2.4. There is a disorder in the arrangement of  $\text{CH}_2\text{CH}_3$  group where two possible orientations are displaced from on another.

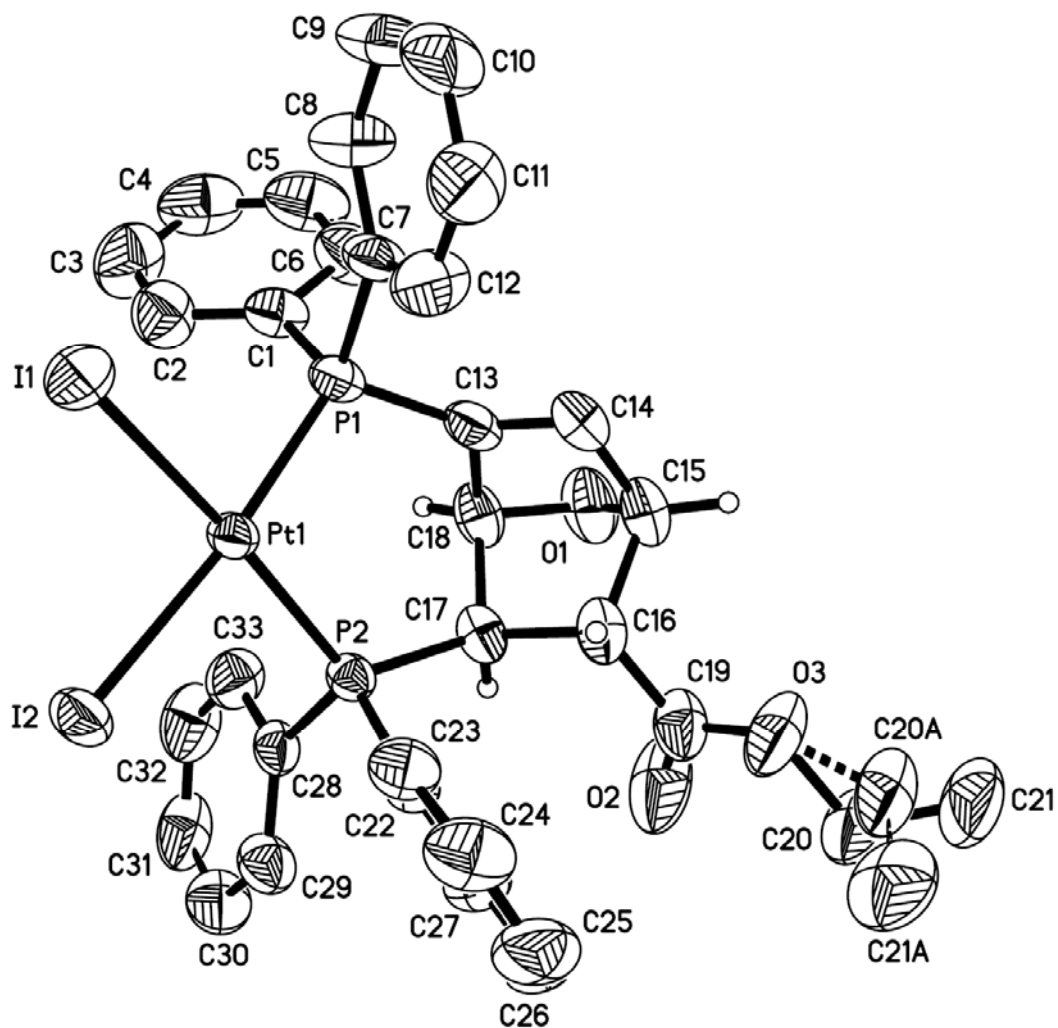


Figure 2.4 Molecular structure and absolute stereochemistry of *endo*-119

**Table 2.4 Selected bond lengths (Å) and angles (deg) for *endo-119***

Pt(1)–P(1)	2.238(1)	C(19)–O(3)	1.302(7)
Pt(1)–P(2)	2.261(1)	P(1)–Pt(1)–P(2)	98.1(1)
Pt(1)–I(1)	2.628(1)	P(1)–Pt(1)–I(1)	87.2(1)
Pt(1)–I(2)	2.643(1)	P(2)–Pt(1)–I(1)	174.1(1)
C(13)–C(14)	1.330(7)	P(1)–Pt(1)–I(2)	173.0(1)
C(13)–C(18)	1.530(6)	P(2)–Pt(1)–I(2)	86.0 (1)
C(13)–P(1)	1.773(5)	I(1)–Pt(1)–I(2)	89.0 (1)
C(14)–C(15)	1.517(7)	C(18)–C(13)–P(1)	121.7(3)
C(15)–O(1)	1.419(6)	C(13)–C(14)–C(15)	105.7(4)
C(15)–C(16)	1.565(6)	C(14)–C(15)–C(16)	104.0(4)
C(16)–C(17)	1.550(6)	C(17)–C(16)–C(15)	100.8(4)
C(17)–C(18)	1.551(6)	C(16)–C(17)–C(18)	100.3(3)
C(17)–P(2)	1.851(4)	C(18)–C(17)–P(2)	115.8(3)
C(18)–O(1)	1.425(5)	C(13)–C(18)–C(17)	106.5(3)
C(19)–O(2)	1.195(6)		

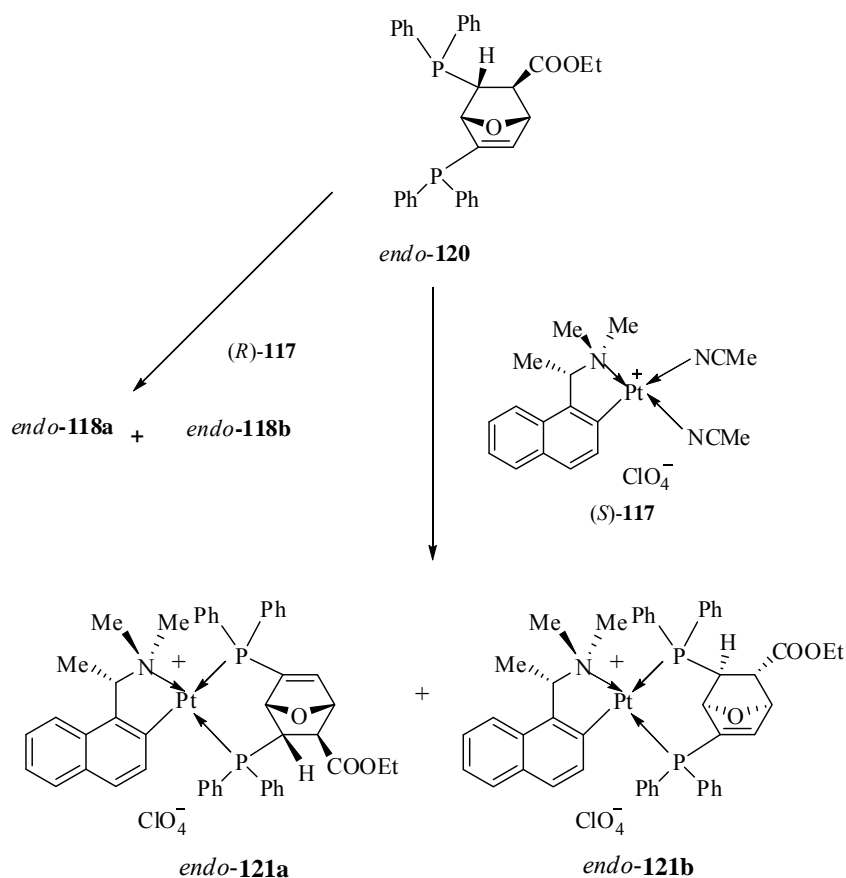
### 2-2.2.2 Liberation and the Optical Purity of *endo-120*

The optically active ligand *endo-120* can be chemoselectively liberated from the complex *endo-119* by treatment of the diiodo complex with aqueous potassium cyanide at room temperature (Scheme 2.9). The liberated *endo-120* was obtained as an air stable white solid in 90% yield,  $[\alpha]_{365} +18^{\circ}$  ( $c$  0.8,  $\text{CH}_2\text{Cl}_2$ ). The  $^{31}\text{P}\{^1\text{H}\}$  NMR spectrum of the free ligand in  $\text{CDCl}_3$  exhibited two doublets at  $\delta$  -12.3 ( $J_{\text{PP}} = 81$  Hz) and -21.4 ( $J_{\text{PP}} = 81$  Hz).

As there is a need to confirm the optical purity of *endo-120*, the liberated ligand was re-coordinated to the equally accessible (*R*)-**117**. This re-coordination process generated two regioisomers in the ratio of 8:1. These two recomplexation products exhibit identical  $^{31}\text{P}\{^1\text{H}\}$  NMR spectra to those recorded for the product generated from the original cycloaddition reaction, so the product *endo-118a* and

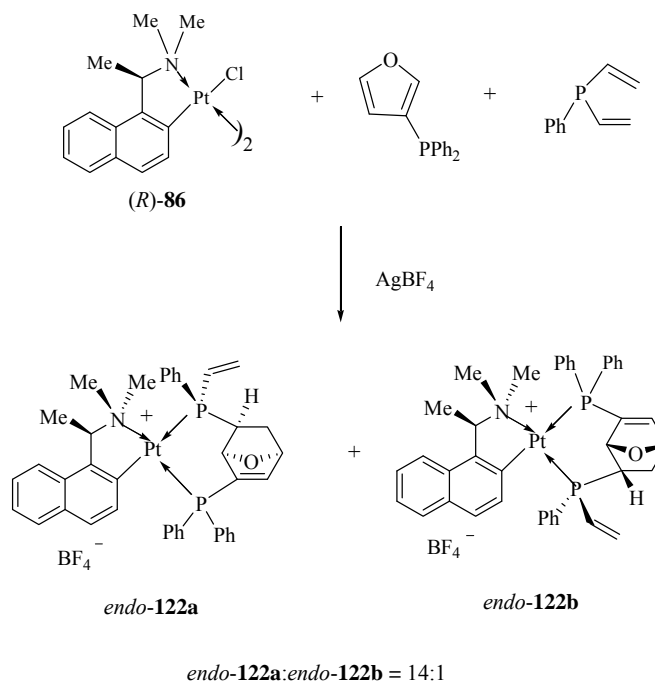
*endo*-**118b** generated from the original cycloaddition reaction are regioisomers.

In a further check, *endo*-**120** was recoordinated to (*S*)-**117** thus generating two regioisomers *endo*-**121a** and *endo*-**121b** in the ratio of 10:1. These two recomplexation products exhibit different  $^{31}\text{P}\{^1\text{H}\}$  NMR spectra to those recorded for the cycloadducts generated directly from the asymmetric cycloaddition reaction thus reaffirming that the liberated ligand is stereochemically pure.



Scheme 2.9

### 2-2.3 Intramolecular Endo-Diels-Alder Reaction between 3-Diphenylphosphino- ofuran and Phenyldivinylphosphine



Scheme 2.10

In order to further explore the reactions of vinylphosphines towards 3-diphenylphosphinofuran, a further reaction was carried out involving phenyldivinylphosphine and 3-diphenylphosphinofuran (Scheme 2.10). The reaction was monitored using  $^{31}\text{P}\{^1\text{H}\}$  NMR spectroscopy and was found to be completed in 7 d at 60 °C. Prior to the purification, the  $^{31}\text{P}\{^1\text{H}\}$  NMR spectrum of the crude reaction mixture in  $\text{CDCl}_3$  exhibited four pairs of doublets indicative of the formation of four stereochemically distinct products in the ratio 14:1:10:7. The major isomer *endo-122a* was successfully crystallized from dichloromethane-diethyl ether as pale yellow prisms in 18% isolated yield,  $[\alpha]_{\text{D}} -57^\circ$  ( $c$  0.5,  $\text{CH}_2\text{Cl}_2$ ). The  $^{31}\text{P}\{^1\text{H}\}$  NMR spectrum of the reaction mixture in  $\text{CDCl}_3$  exhibited one pair of doublets at  $\delta$  18.9 ( $J_{\text{PP}} = 4.5$  Hz,  $J_{\text{PtP}} = 1730$  Hz) and  $-4.6$  ( $J_{\text{PP}} = 14.5$  Hz,  $J_{\text{PtP}} = 3676$  Hz). The isolated product was

subsequently identified to be the complex *endo*-**122a** by crystallographic studies.

### 2-2.3.1 X-ray Structural Analysis of *endo*-**122a**

The molecular structure and absolute stereochemistry of complex *endo*-**122a** were established by X-ray diffraction studies (Figure 2.5). Interestingly, *endo*-**122a** crystallized as a pair of crystallographically independent molecules in the unit cell. However, the two molecules have the same absolute stereochemistry and molecular connectivity and differ only slightly in their bond angles. For clarity, only one molecule (molecule 1) is depicted in Figure 2.5. The analysis showed that the 5-membered (*R<sub>C</sub>*)-metallated naphthylamine PtCN ring adopts the  $\delta$  conformation. The major isomer isolated from the cycloaddition reaction was found to be an *endo*-cycloadduct. The chiral ligand coordinates as a bidentate chelate via its phosphorus donor atoms to the platinum, with the ethenylphenylphosphino group being substituted at the *endo* position at C(23). The geometry at platinum is distorted square planar with angles at platinum in the ranges of 79.1(2)-94.0(1) and 170.0(1)-173.5(1)°. The absolute configurations of the four newly generated stereogenic centers at P(1), C(23), C(25), and C(28) are *S*, *S*, *S*, and *R*, respectively. The Pt-P(1) distance [2.357(1) Å] is clearly longer than the Pt-P(2) bond [2.233(1) Å]. The bond lengths of the both C(15)-C(16) and C(26)-C(27) [1.299(8) and 1.325(7) Å] are consistent of a double bond. Selected bond lengths and angles are given in Table 2.5 (molecule 1) and Table 2.6 (molecule 2).

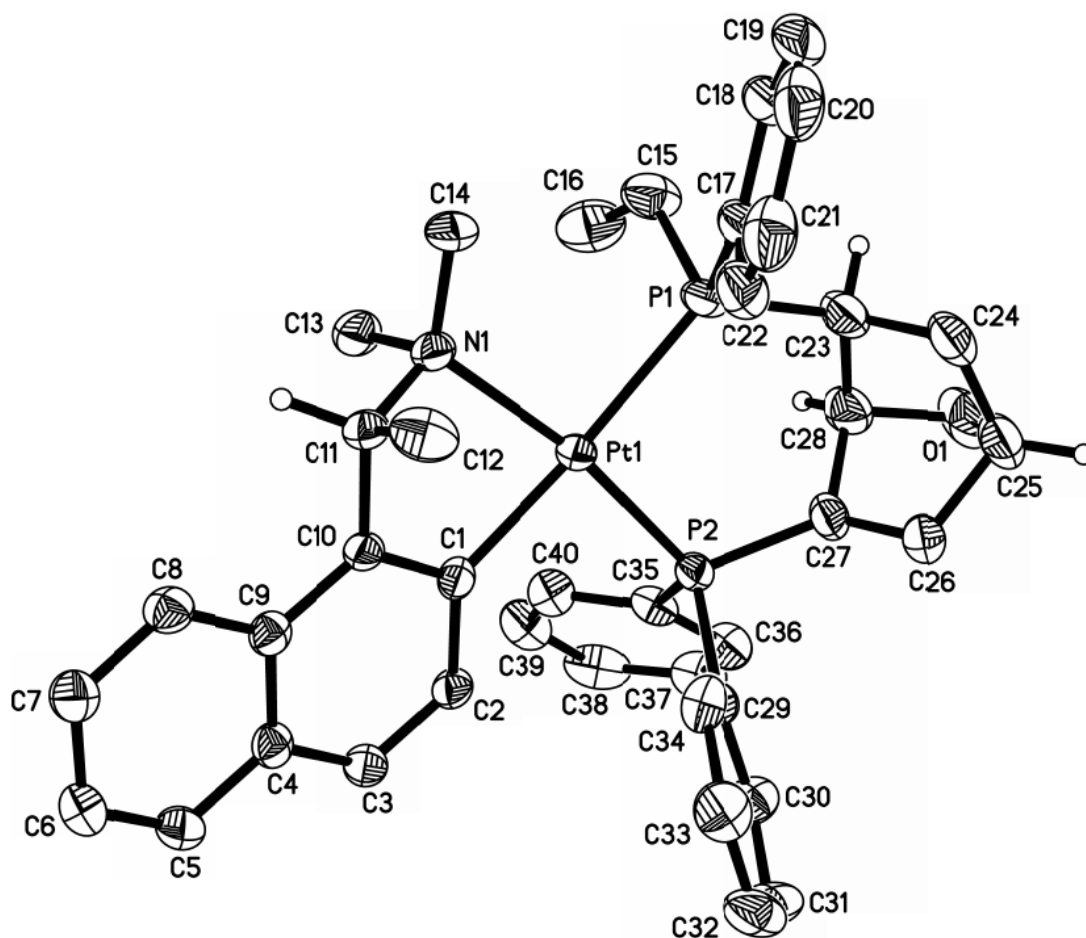
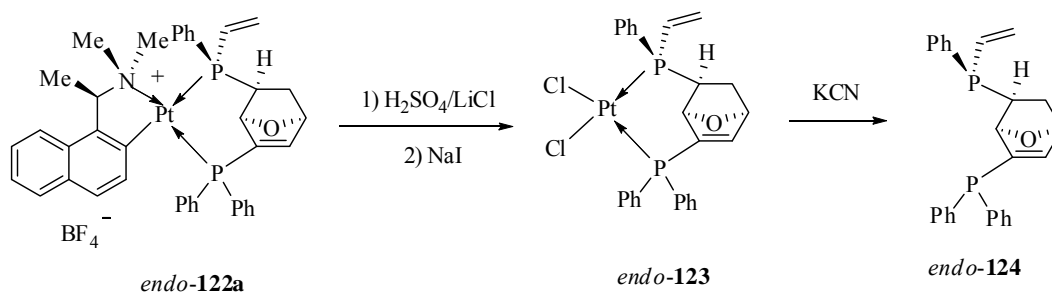


Figure 2.5 Molecular structure and absolute stereochemistry of *endo*-122a

### 2-2.3.2 Preparation of the Dichloro Complex *endo*-123

The complex *endo*-122a was treated with concentrated sulfuric acid to chemoselectively remove the naphthylamine auxiliary (Scheme 2.11). Upon addition of excess lithium chloride into the acidic solution, the dichloro complex *endo*-122 that precipitated from solution was recrystallized from dichloromethane-diethyl ether as pale yellow prisms in 91% yield,  $[\alpha]_D -19.6^\circ$  ( $c$  0.5,  $\text{CH}_2\text{Cl}_2$ ). The  $^{31}\text{P}\{^1\text{H}\}$  NMR spectrum of *endo*-123 in  $\text{CDCl}_3$  exhibited a pair of doublets at  $\delta$  14.1 ( $J_{\text{PP}} = 14.7$ ,  $J_{\text{PtP}} = 3573$  Hz) and  $-15.1$  ( $J_{\text{PP}} = 14.7$ ,  $J_{\text{PtP}} = 3412$  Hz). Both non-equivalent phosphorus

donors in complex *endo-123* are coordinated at the position *trans* to the chloro ligand as indicated by their similar Pt-P couplings. The structure of *endo-123* is further confirmed by X-ray structural analysis.



Scheme 2.11

Table 2.5 Selected bond lengths (Å) and angles (deg) for *endo-122a* (Molecule 1)

Pt(1)–C(1)	2.047(4)	N(1)–Pt(1)–P(2)	170.0(1)
Pt(1)–N(1)	2.168(4)	C(1)–Pt(1)–P(1)	173.5(1)
Pt(1)–P(2)	2.233(1)	N(1)–Pt(1)–P(1)	95.4(1)
Pt(1)–P(1)	2.357(1)	P(2)–Pt(1)–P(1)	94.0(1)
P(1)–C(23)	1.865(5)	C(23)–P(1)–Pt(1)	122.7(2)
P(2)–C(27)	1.783(4)	C(27)–P(2)–Pt(1)	112.6(2)
C(15)–C(16)	1.299(8)	C(16)–C(15)–P(1)	121.8(4)
C(23)–C(24)	1.536(8)	C(24)–C(23)–C(28)	101.3(4)
C(23)–C(28)	1.546(7)	C(28)–C(23)–P(1)	113.8(3)
C(24)–C(25)	1.551(8)	C(23)–C(24)–C(25)	101.5(4)
C(25)–O(1)	1.447(8)	C(26)–C(25)–C(24)	103.7(4)
C(25)–C(26)	1.529(7)	C(27)–C(26)–C(25)	104.6(5)
C(26)–C(27)	1.325(7)	C(26)–C(27)–C(28)	106.8(4)
C(27)–C(28)	1.533(7)	C(28)–C(27)–P(2)	122.5(4)
C(28)–O(1)	1.456(7)	C(27)–C(28)–C(23)	105.5(4)
C(1)–Pt(1)–N(1)	79.1(2)	C(25)–O(1)–C(28)	95.7(4)
C(1)–Pt(1)–P(2)	91.7(1)		

**Table 2.6 Selected bond lengths (Å) and angles (deg) for *endo*-122a (Molecule 2)**

Pt(2)–C(41)	2.071(4)	N(2)–Pt(2)–P(4)	170.3(1)
Pt(2)–N(2)	2.153(3)	C(41)–Pt(2)–P(3)	173.5(1)
Pt(2)–P(4)	2.234(1)	N(2)–Pt(2)–P(3)	95.2(1)
Pt(2)–P(3)	2.371(1)	P(4)–Pt(2)–P(3)	93.7(1)
P(3)–C(63)	1.857(5)	C(63)–P(3)–Pt(2)	123.2(2)
P(4)–C(67)	1.793(4)	C(67)–P(4)–Pt(2)	112.0(1)
C(55)–C(56)	1.332(8)	C(56)–C(55)–P(3)	122.6(4)
C(63)–C(68)	1.552(6)	C(68)–C(63)–C(64)	100.1(4)
C(63)–C(64)	1.567(7)	C(68)–C(63)–P(3)	114.4(3)
C(64)–C(65)	1.537(7)	C(65)–C(64)–C(63)	101.4(4)
C(65)–O(2)	1.443(6)	C(66)–C(65)–C(64)	105.3(4)
C(65)–C(66)	1.511(6)	C(67)–C(66)–C(65)	105.9(4)
C(66)–C(67)	1.323(6)	C(66)–C(67)–C(68)	105.5(4)
C(67)–C(68)	1.524(6)	C(68)–C(67)–P(4)	122.6(3)
C(68)–O(2)	1.441(6)	C(67)–C(68)–C(63)	106.3(3)
C(41)–Pt(2)–N(2)	78.5(1)	C(68)–O(2)–C(65)	96.1(3)
C(41)–Pt(2)–P(4)	92.7(1)		

### 2-2.3.3 X-ray Structural Analysis of *endo*-123

The molecular structure and the absolute configuration of the recrystallised *endo*-123 were established by single crystal X-ray crystallographic analysis (Figure 2.6). The absolute configurations of the stereogenic centers and the oxa-norbornene skeleton were found to be retained even after reaction under acidic conditions. Selected bond parameters are given in Table 2.7.

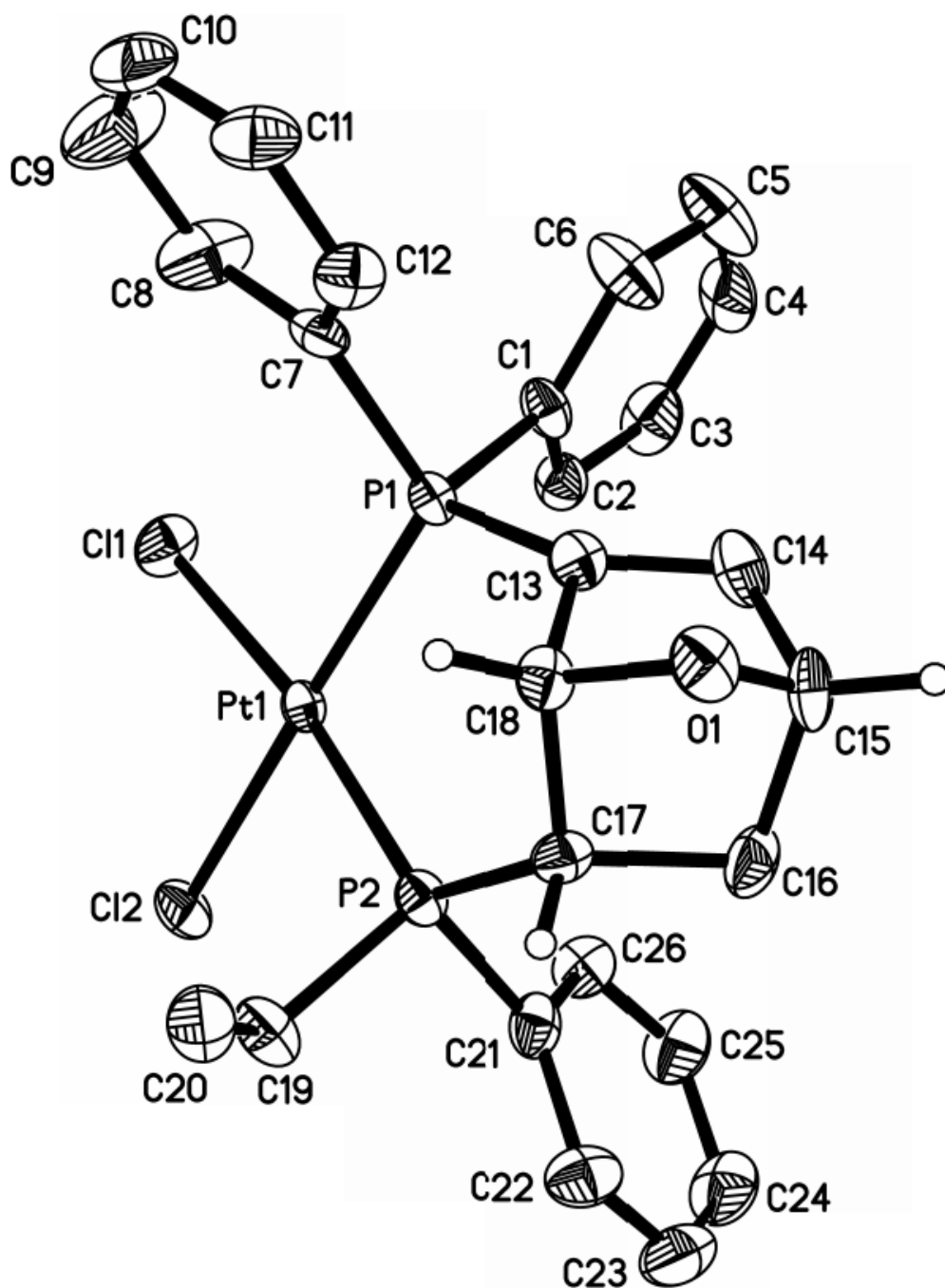


Figure 2.6 Molecular structure and absolute stereochemistry of *endo*-123

**Table 2.7 Selected bond lengths (Å) and angles (deg) for *endo*-123**

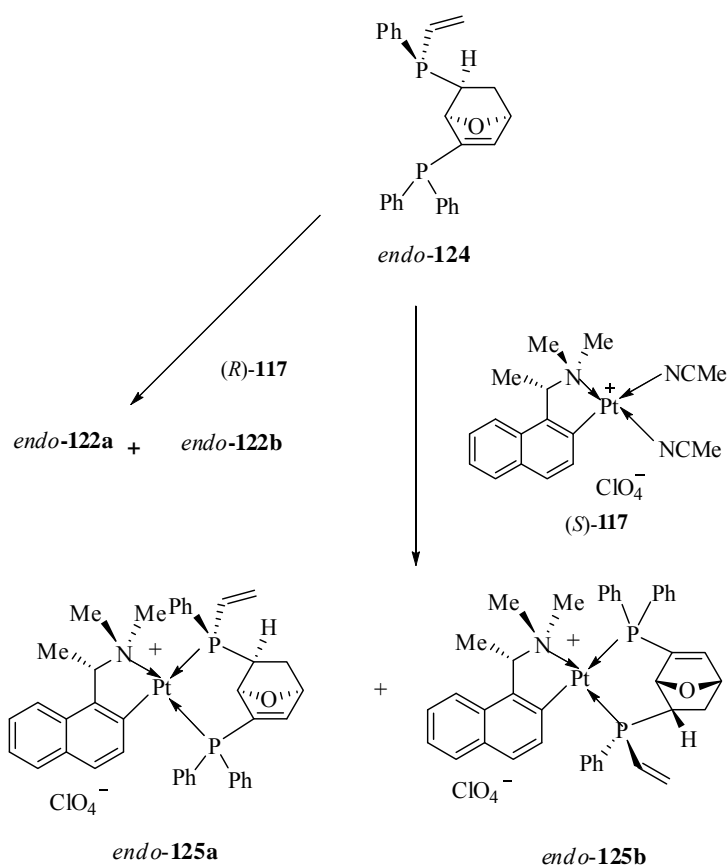
Pt(1)–P(1)	2.242(1)	P(1)–Pt(1)–Cl(1)	90.1 (1)
Pt(1)–P(2)	2.249(1)	P(2)–Pt(1)–Cl(1)	172.1(1)
Pt(1)–Cl(1)	2.345(1)	P(1)–Pt(1)–Cl(2)	175.2(1)
Pt(1)–Cl(2)	2.371(1)	P(2)–Pt(1)–Cl(2)	84.6(1)
P(1)–C(13)	1.778(4)	Cl(1)–Pt(1)–Cl(2)	87.8(1)
P(1)–C(1)	1.813(4)	C(13)–P(1)–Pt(1)	109.9(2)
P(2)–C(17)	1.846(4)	C(17)–P(2)–Pt(1)	122.0(2)
C(13)–C(14)	1.343(6)	C(14)–C(13)–C(18)	103.9(4)
C(13)–C(18)	1.542(6)	C(18)–C(13)–P(1)	124.8(3)
C(14)–C(15)	1.487(7)	C(13)–C(14)–C(15)	106.5(4)
C(15)–O(1)	1.432(6)	C(14)–C(15)–C(16)	105.5(4)
C(15)–C(16)	1.559(7)	C(15)–C(16)–C(17)	99.8(4)
C(16)–C(17)	1.566(6)	C(18)–C(17)–C(16)	101.3(4)
C(17)–C(18)	1.556(6)	C(18)–C(17)–P(2)	115.4(3)
C(18)–O(1)	1.436(5)	C(13)–C(18)–C(17)	105.7(3)
C(19)–C(20)	1.318(7)	C(20)–C(19)–P(2)	125.0(4)
P(1)–Pt(1)–P(2)	97.6 (1)	C(15)–O(1)–C(18)	96.4(3)

#### 2-2.3.4 Liberation and the Optical Purity of *endo*-124

As illustrated is Scheme 2.11, treatment of complex *endo*-123 with saturated aqueous potassium cyanide in dichloromethane gave the optically pure ligand *endo*-124 from the dichloro-platinum(II) complex as an air stable white solid in 95% yield upon removal of solvent,  $[\alpha]_D +15.1^\circ$  ( $c$  1.5,  $\text{CH}_2\text{Cl}_2$ ). The  $^{31}\text{P}\{^1\text{H}\}$  NMR spectrum of the free ligand in  $\text{CDCl}_3$  exhibited two doublets at  $\delta$  -16.8 ( $J_{\text{PP}} = 81$  Hz) and -21.3 ( $J_{\text{P}, \text{P}'} = 81$  Hz).

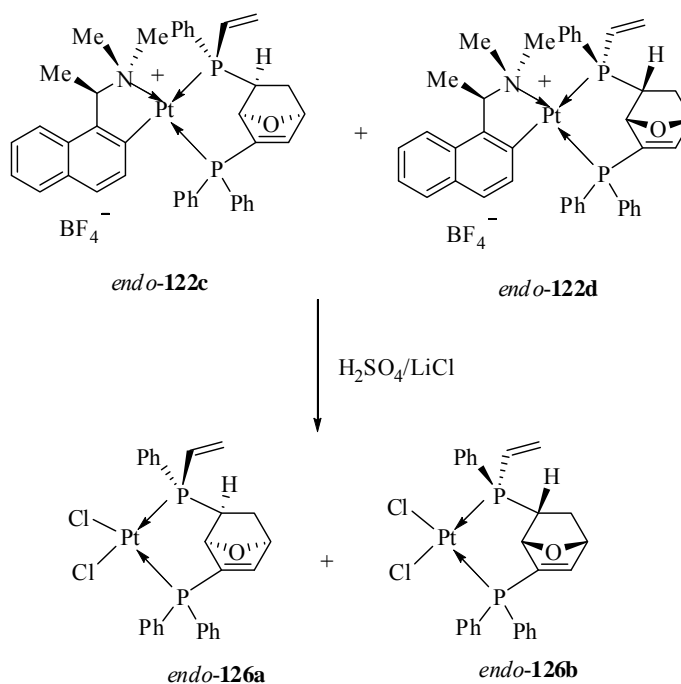
Furthermore, in order to determine the enantiomeric purity of *endo*-124, the liberated ligand was re-coordinated to the equally accessible (*R*)-117 (Scheme 2.12). This re-coordination process generated two regioisomers in the ratio of 5:1. These two recomplexation products exhibit identical  $^{31}\text{P}\{^1\text{H}\}$  NMR spectra to those recorded for

the product generated from the original cycloaddition reaction, so the product *endo-122a* and *endo-122b* generated from the original cycloaddition reaction are regioisomers. As a further check, *endo-124* was recoordinated to (*S*)-**117** generated two regioisomers *endo-125a* and *endo-125b* in the ratio of 5:1. These two recomplexation products exhibit different  $^{31}\text{P}\{^1\text{H}\}$  NMR spectra to those recorded for the cycloadducts generated directly from the asymmetric cycloaddition reaction thus reaffirming that the liberated diphosphine was stereochemically pure.



Scheme 2.12

### 2-2.3.5 Preparation of the Dichloro Complex *endo-126a,b*



Scheme 2.13

To isolate the other cycloadducts  $\delta$  20.2 ( $J_{\text{PP}} = 14.7$  Hz,  $J_{\text{PtP}} = 1735$  Hz),  $-4.9$  ( $J_{\text{PP}} = 14.7$  Hz,  $J_{\text{PtP}} = 3660$  Hz) and 21.7 ( $J_{\text{PP}} = 15.7$  Hz,  $J_{\text{PtP}} = 1728$  Hz) and  $-6.1$  ( $J_{\text{PP}} = 15.7$  Hz,  $J_{\text{PtP}} = 3656$  Hz) in their enantiomerically pure forms, the chiral naphthylamine auxiliary in the diastereomeric mixture was removed chemoselectively by stirring a dichloromethane solution of the diastereomeric complexes with concentrated sulfuric acid at room temperature (Scheme 2.13). Upon addition of excess lithium chloride into the acidic solution, the dichloro complexes precipitated from solution. The  $^{31}\text{P}\{^1\text{H}\}$  NMR spectrum of *endo-126a,b* in  $\text{CDCl}_3$  exhibited a pair of doublets at  $\delta$  15.4 ( $J_{\text{PP}} = 14.9$ ,  $J_{\text{PtP}} = 3581$  Hz) and  $-13.4$  ( $J_{\text{PP}} = 14.9$ ,  $J_{\text{PtP}} = 3388$  Hz).

### 2-2.3.6 X-ray Structural Analysis of *endo-126a,b*

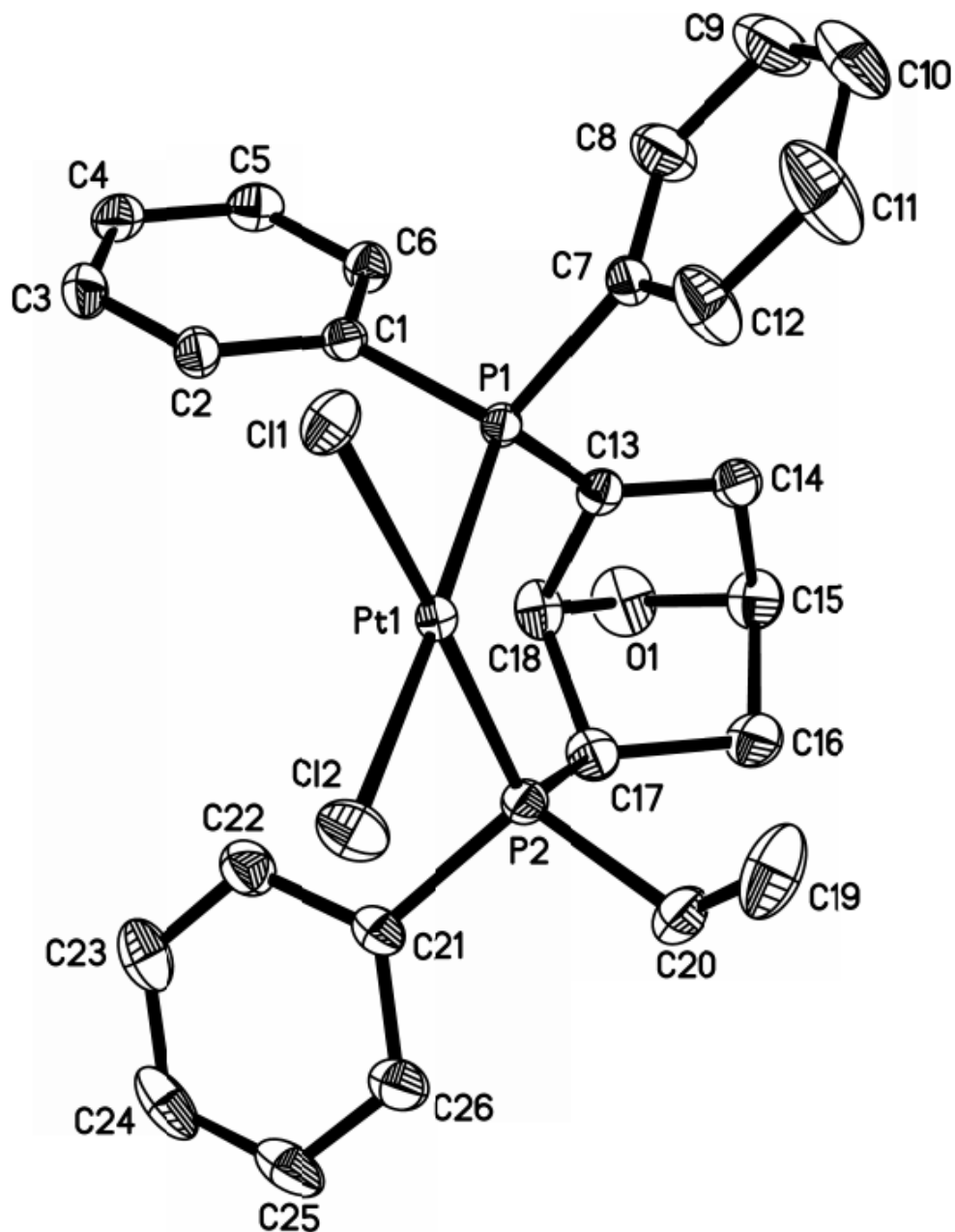


Figure 2.7 Molecular structure and absolute stereochemistry of *endo*-126a,b

The molecular structure of *endo*-126a,b was established by a single crystal X-ray structural determination (Figure 2.7). The single crystal X-ray diffraction analysis of *endo*-126a,b, however, reveals the presence of both enantiomers in the unit cell. The geometry at platinum is distorted square planar with angles at platinum

in the ranges of 85.6(1)-86.7(1) and 175.7(1)-176.7(1)°. The distances of the two Pt-Cl bonds are similar (2.360(1) and 2.357(1) Å), and so are the two Pt-P bonds (2.231(1) and 2.243(1) Å).

**Table 2.8 Selected bond lengths (Å) and angles (deg) for *endo*-126a,b**

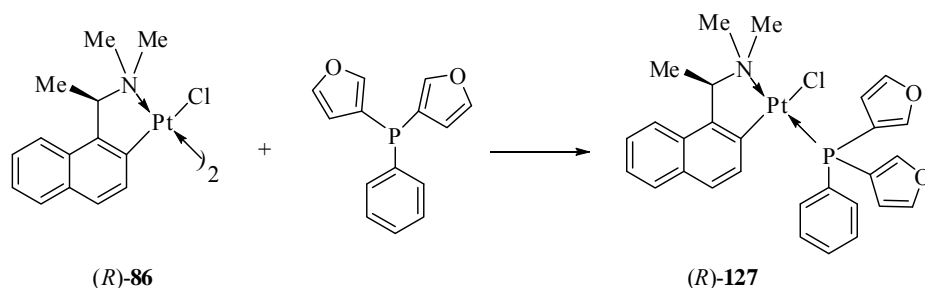
Pt(1)–P(1)	2.231(1)	P(1)–Pt(1)–Cl(1)	86.7(1)
Pt(1)–P(2)	2.243(1)	P(2)–Pt(1)–Cl(1)	175.7(1)
Pt(1)–Cl(2)	2.357(1)	P(1)–Pt(1)–Cl(2)	176.7(1)
Pt(1)–Cl(1)	2.360(1)	P(2)–Pt(1)–Cl(2)	85.6(1)
P(1)–C(13)	1.776(2)	Cl(1)–Pt(1)–Cl(2)	90.0(1)
P(1)–C(1)	1.821(2)	C(13)–P(1)–Pt(1)	111.5(1)
P(2)–C(17)	1.857(2)	C(17)–P(2)–Pt(1)	120.8(1)
C(13)–C(14)	1.336(3)	C(14)–C(13)–C(18)	105.5(2)
C(13)–C(18)	1.524(3)	C(18)–C(13)–P(1)	120.4(2)
C(14)–C(15)	1.512(3)	C(13)–C(14)–C(15)	105.0(2)
C(15)–O(1)	1.441(3)	C(14)–C(15)–C(16)	104.3(2)
C(15)–C(16)	1.561(3)	C(15)–C(16)–C(17)	100.9(2)
C(16)–C(17)	1.552(3)	C(18)–C(17)–C(16)	100.52(17)
C(17)–C(18)	1.551(3)	C(18)–C(17)–P(2)	114.95(15)
C(18)–O(1)	1.436(3)	C(13)–C(18)–C(17)	106.45(16)
C(19)–C(20)	1.302(3)	C(19)–C(20)–P(2)	123.2(2)
P(1)–Pt(1)–P(2)	97.47(2)	C(15)–O(1)–C(18)	95.76(15)

## 2.2.4 Intramolecular Endo-Diels-Alder Reaction Between Di-(3-furyl)phenylphosphine and Diphenylvinylphosphine

### 2.2.4.1 Preparation of Chloro Complex (*R*)-127

The ligand di-(3-furyl)phenylphosphine in dichloromethane was added to a solution containing the dimeric complex (*R*)-86 to yield the chloro complex (*R*)-127 in 85% yield (Scheme 2.14)

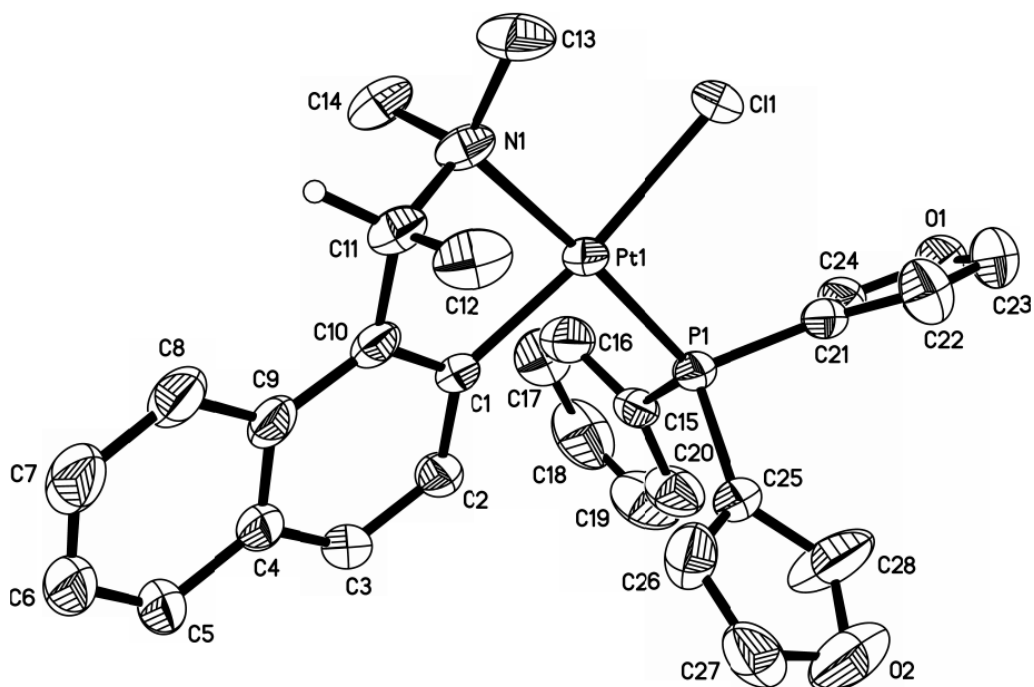
The  $^{31}\text{P}\{^1\text{H}\}$  NMR spectrum of the complex (*R*)-**127** showed a singlet at  $\delta$  21.0 ( $J_{\text{PtP}} = 4210$  Hz). The reaction mixture was concentrated and layered with *n*-hexanes to yield pale yellow prisms of (*R*)-**127**.



Scheme 2.14

### 2.2.4.2 Single Crystal X-ray Diffraction Studies on (*R*)-**127**

The single crystal X-ray diffraction analysis data showed that the ligand bis-(3-furyl)phenylphosphine had coordinated *trans* to the  $\text{NMe}_2$  group of the metal template (Figure 2.8). Selected bond lengths and bond angles are given in Table 2.9.

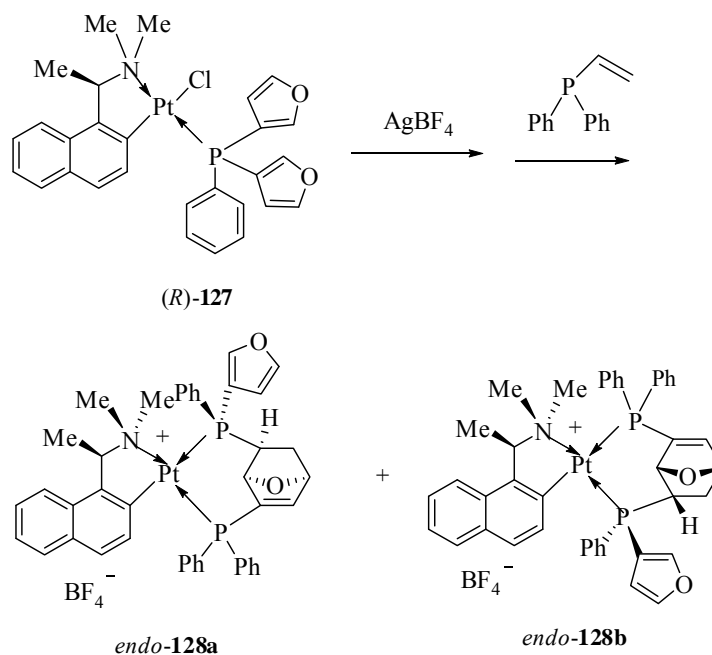
Figure 2.8 Molecular structure and absolute stereochemistry of (*R*)-**127**

**Table 2.9 Selected bond lengths (Å) and angles (deg) for *endo*-127**

Pt(1)–C(1)	2.017(3)	C(28)–O(2)	1.391(7)
Pt(1)–N(1)	2.136(3)	C(1)–Pt(1)–N(1)	80.61(14)
Pt(1)–P(1)	2.212 (1)	C(1)–Pt(1)–P(1)	95.67(11)
Pt(1)–Cl(1)	2.383 (1)	N(1)–Pt(1)–P(1)	176.18(10)
P(1)–C(15)	1.817(5)	C(1)–Pt(1)–Cl(1)	172.61(11)
P(1)–C(21)	1.824(4)	N(1)–Pt(1)–Cl(1)	92.07(10)
C(23)–O(1)	1.336(7)	P(1)–Pt(1)–Cl(1)	91.66(4)
C(24)–O(1)	1.371(5)	C(23)–O(1)–C(24)	106.1(4)
C(27)–O(2)	1.406(8)	C(28)–O(2)–C(27)	105.2(4)

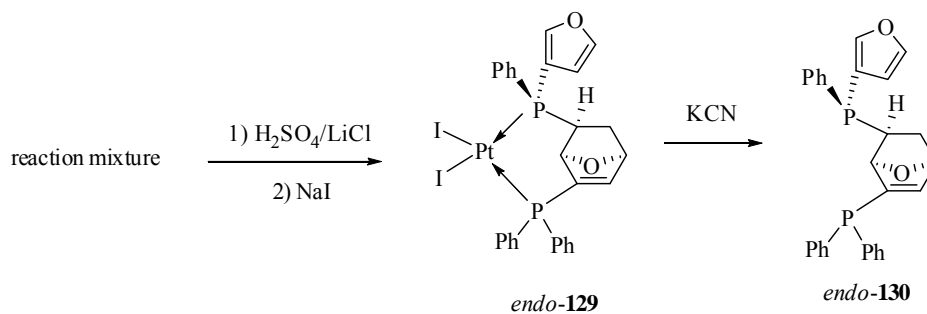
### 2.2.4.3 Asymmetric Diels-Alder Reaction involving (*R*)-127 and Diphenylvinylphosphine

The complex (*R*)-127 was treated with aqueous silver tetrafluoroborate to convert the Cl group to the more labile BF<sub>4</sub> entity (Scheme 2.15) and then was allowed to react with diphenylvinylphosphine. The reaction was monitored using <sup>31</sup>P{<sup>1</sup>H} NMR spectroscopy and was found to be complete in 7 d at 60 °C. Prior to purification, the <sup>31</sup>P{<sup>1</sup>H} NMR spectrum of the crude reaction mixture in CDCl<sub>3</sub> exhibited four pairs of doublets indicative of the formation of four stereochemically distinct products in the ratio 1:1:10:10. The doublets of two major diastereomers (Scheme 2.15) were observed at  $\delta$  27.0 ( $J_{PP}=14.5$  Hz,  $J_{PtP}=1706$  Hz) and -26.2 ( $J_{PP}=14.5$  Hz,  $J_{PtP}=3640$  Hz) and 26.9 ( $J_{PP}=14.8$  Hz,  $J_{PtP}=1706$  Hz) and -27.9 ( $J_{PP}=14.8$  Hz,  $J_{PtP}=3624$  Hz).

**Scheme 2.15**

Unfortunately, efforts to separate the isomers directly *via* column chromatography or fractional crystallization were unsuccessful. Hence, treatment of the tetrafluoroborate salt with concentrated sulfuric acid at room temperature removed the naphthylamine auxiliary chemoselectively. Upon addition of excess lithium chloride into the acidic solution, the dichloro complex precipitated from solution as a pale yellow solid. Upon treatment of the dichloro complex with sodium iodide (Scheme 2.16),<sup>163</sup> the  $^{31}\text{P}\{^1\text{H}\}$  NMR spectrum of the diiodo complexes in  $\text{CDCl}_3$  exhibited three pairs of doublets in the ratio 1:1 and at  $\delta$  18.9 ( $J_{\text{PP}} = 9.7$ ,  $J_{\text{PtP}} = 3389$  Hz) and -41.8 ( $J_{\text{PP}} = 9.7$ ,  $J_{\text{PtP}} = 3165$  Hz) and 18.4 ( $J_{\text{PP}} = 10.9$ ,  $J_{\text{PtP}} = 3352$  Hz) and -38.4 ( $J_{\text{PP}} = 10.9$ ,  $J_{\text{PtP}} = 3198$  Hz). The less soluble isomer was isolated via fractional crystallization from dichloromethane-diethyl ether as yellow prisms in 35% yield,  $[\alpha]_{\text{D}} +25^\circ$  ( $c$  0.7,  $\text{CH}_2\text{Cl}_2$ ). The  $^{31}\text{P}\{^1\text{H}\}$  NMR spectrum of the diiodo complex in

$\text{CDCl}_3$  exhibited only two doublets at  $\delta$  18.9 ( $J_{\text{PP}} = 9.7$   $J_{\text{PtP}} = 3389$  Hz) and -41.8 ( $J_{\text{PP}} = 9.7$ ,  $J_{\text{PtP}} = 3165$  Hz). The product was confirmed to be complex *endo*-**129** by X-ray crystallographic analysis.



#### 2-2.4.4 X-ray Structural Analysis of *endo*-**129**

The molecular structure and the absolute stereochemistry of *endo*-**129** were determined by X-ray structure analysis (Figure 2.9). The crystallographic study reveals that the cycloaddition reaction between the coordinated bis-(3-furyl)phenylphosphine and diphenylvinylphosphine has resulted in the formation of the *endo* phosphine. The chiral ligand coordinates as a bidentate chelate via its phosphorus donor atoms to the platinum, with the diphenylphosphino group substituted at the *endo* position at C(13). The geometry at platinum is distorted square planar with angles at platinum in the ranges of 86.2(1)–87.2(1) and 175.5(1)–175.6(1)°. The absolute configurations of the four newly generated stereogenic centers at P(2), C(13), C(15), and C(18) are *S*, *S*, *S*, and *R*, respectively. The five-membered furan ring is disordered in the molecule. Selected bond lengths and angles are given in Table 2.10.

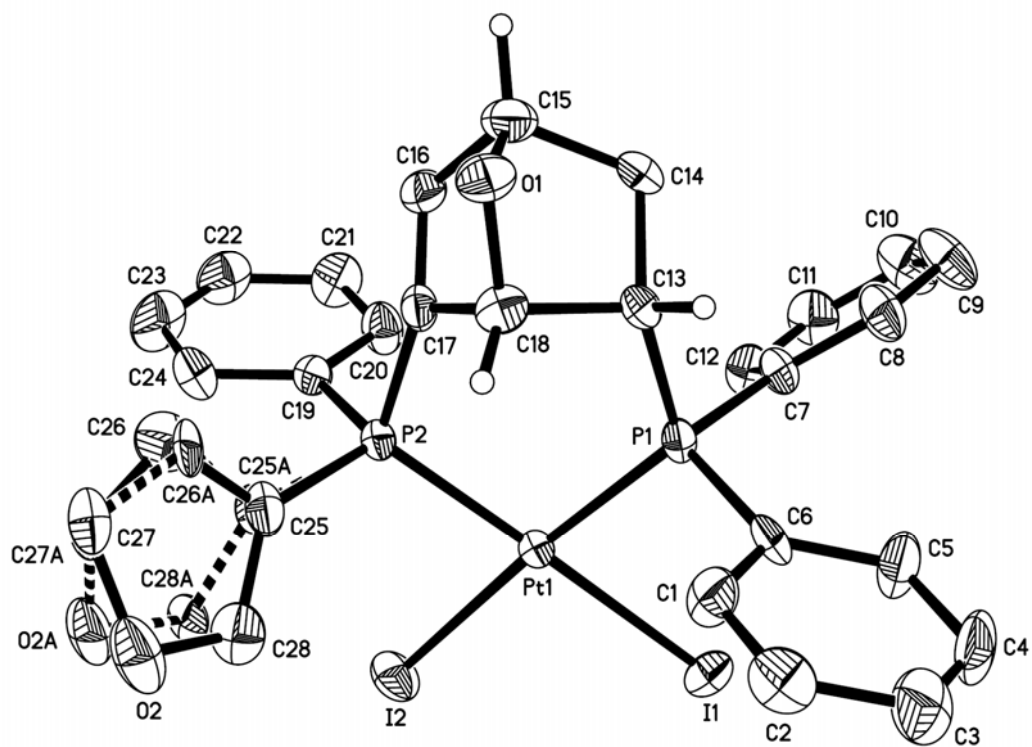
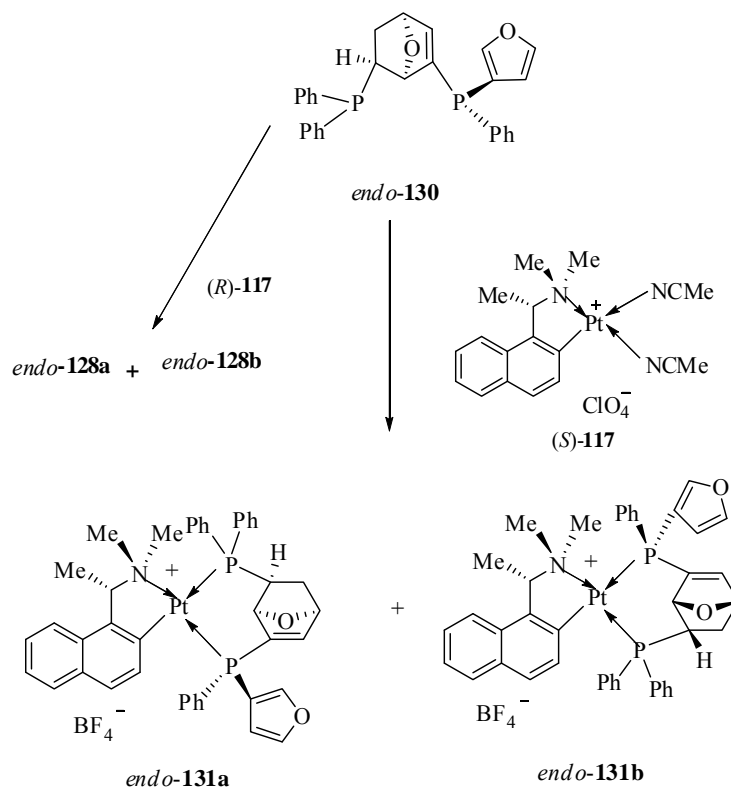


Figure 2.9 Molecular structure and absolute stereochemistry of *endo*-129

Table 2.10 Selected bond lengths (Å) and angles (deg) for *endo-129*

Pt(1)–P(2)	2.236(2)	P(2)–Pt(1)–I(1)	175.6(1)
Pt(1)–P(1)	2.270(2)	P(1)–Pt(1)–I(1)	86.2(1)
Pt(1)–I(2)	2.657(1)	I(2)–Pt(1)–I(1)	89.4(1)
Pt(1)–I(1)	2.658(1)	C(14)–C(13)–C(18)	98.7(6)
C(13)–C(14)	1.550(10)	C(18)–C(13)–P(1)	115.1(5)
C(13)–C(18)	1.573(10)	C(13)–C(14)–C(15)	102.4(6)
C(13)–P(1)	1.845(7)	C(16)–C(15)–C(14)	105.0(6)
C(14)–C(15)	1.552(11)	C(17)–C(16)–C(15)	104.1(6)
C(15)–O(1)	1.427(9)	C(16)–C(17)–C(18)	105.5(6)
C(15)–C(16)	1.510(11)	C(18)–C(17)–P(2)	123.8(5)
C(16)–C(17)	1.349(10)	C(17)–C(18)–C(13)	105.9(5)
C(17)–C(18)	1.522(10)	C(18)–O(1)–C(15)	96.4(5)
C(17)–P(2)	1.778(7)	C(13)–P(1)–Pt(1)	121.5(2)
C(18)–O(1)	1.422(9)	C(17)–P(2)–Pt(1)	110.9(2)
C(25)–P(2)	1.778(10)	C(28)–C(25)–C(26)	103.9(10)
C(25A)–P(2)	1.789(12)	C(28)–C(25)–P(2)	130.1(10)
C(25)–C(28)	1.356(16)	C(26)–C(25)–P(2)	125.9(11)
C(25A)–C(28A)	1.370(17)	C(27)–C(26)–C(25)	108.4(12)
C(25)–C(26)	1.449(15)	C(26)–C(27)–O(2)	109.1(11)
C(25A)–C(26A)	1.459(17)	C(28)–O(2)–C(27)	106.2(10)
C(26)–C(27)	1.298(14)	O(2)–C(28)–C(25)	112.2(11)
C(26A)–C(27A)	1.289(17)	C(28A)–C(25A)–C(26A)	103.0(11)
C(27)–O(2)	1.415(18)	C(28A)–C(25A)–P(2)	134.7(12)
C(27A)–O(2A)	1.40(2)	C(26A)–C(25A)–P(2)	122.3(12)
O(2)–C(28)	1.318(13)	C(27A)–C(26A)–C(25A)	109.7(14)
O(2A)–C(28A)	1.327(14)	C(26A)–C(27A)–O(2A)	108.5(14)
P(2)–Pt(1)–P(1)	97.2(1)	C(28A)–O(2A)–C(27A)	107.6(12)
P(2)–Pt(1)–I(2)	87.2 (1)	O(2A)–C(28A)–C(25A)	111.2(13)
P(1)–Pt(1)–I(2)	175.5(1)		

2-2.4.5 Liberation and the Optical Purity of *endo*-130

Scheme 2.17

The optically active ligand *endo*-130 can be chemoselectively liberated from the complex *endo*-129 by treatment of the diiodo complex with aqueous potassium cyanide at room temperature (Scheme 2.16). The liberated *endo*-130 was obtained as an air stable white solid in 87% yield,  $[\alpha] -30^\circ$  ( $c$  0.6,  $\text{CH}_2\text{Cl}_2$ ). The  $^{31}\text{P}\{^1\text{H}\}$  NMR spectrum of the free ligand in  $\text{CDCl}_3$  exhibited two doublets at  $\delta -13.0$  ( $J_{\text{PP}} = 78$  Hz) and  $-48.0$  ( $J_{\text{PP}} = 78$  Hz).

In order to determine the enantiomeric purity of *endo*-130, the liberated ligand was re-coordinated to the equally accessible (R)-117 (Scheme 2.17). This re-coordination process generated two regioisomers in the ratio of 7:1. These two

recomplexation products exhibit identical  $^{31}\text{P}\{^1\text{H}\}$  NMR spectra to those recorded for the product generated from the original cycloaddition reaction, so the products *endo-128a* and *endo-128b* generated from the original cycloaddition reaction are regioisomers. As a further check, *endo-130* was recoordinates to (*S*)-**117** generated two regioisomers *endo-131a* and *endo-131b* in the ratio of 8:1. These two recomplexation products exhibit different  $^{31}\text{P}\{^1\text{H}\}$  NMR spectra to those recorded for the two cycloadducts generated directly from the asymmetric cycloaddition reaction thus reaffirming that the liberated ligand is stereochemically pure.

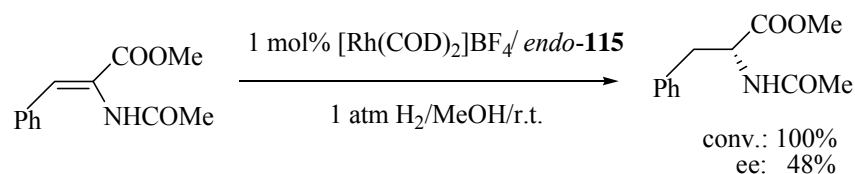
### 2.3 Conclusion

In the presence of complex (*R*)-**86** as the chiral template, 3-diphenylphosphinofuran and bis-(3-furyl)phenylphosphine function as the dienes with diphenylvinylphosphine, diphenyl[(*E*)-2-(ethoxycarbonyl)vinyl]phosphine and divinylphenylphosphine to form *endo* cycloaddition adducts. The Diels-Alder reactions between 3-diphenylphosphinofuran and diphenylvinylphosphine or diphenyl[(*E*)-2-(ethoxycarbonyl)vinyl]phosphine achieved high stereoselectivities. However, in the reactions (3-diphenylvinylfuran and divinylphenylphosphine, and bis-(3-furyl)phenylphosphine and diphenylvinylphosphine) the stereocontrol at the phosphorus stereogenic center is inefficient. The low selectivity may be due to the free rotation around the Pt-P bond of a monodentate phosphine which gives rise to equal opportunity for each olefin (furan) to undergo cycloaddition reaction.<sup>162b</sup>

In order to investigate the behavior of the optically pure diphosphine ligands

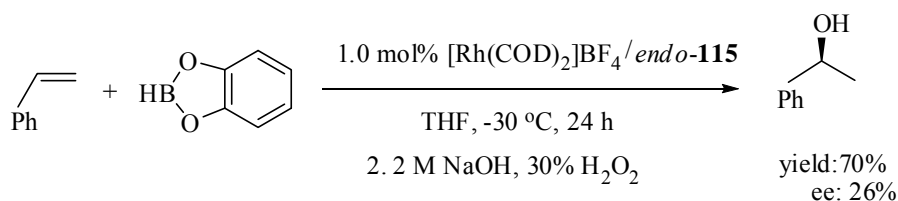
in asymmetric catalysis, *endo-115* has been used as a test ligand in asymmetric rhodium catalyzed hydrogenation and hydroboration.

The enantioselective hydrogenation of unsaturated enamides to amino acid derivatives was extensively studied using Rh catalysts.<sup>3b</sup> The hydrogenation of methyl 2-acetamidocinnamate was carried out in MeOH at room temperature under ambient H<sub>2</sub> pressure in the presence of 1 mol% catalyst formed in situ from [Rh(COD)<sub>2</sub>]BF<sub>4</sub> and *endo-115* (Rh/L = 1:1) for 12 h, leading to N-acetylphenylalanine in 100% yield and 48% enantiomeric excess (Scheme 2.18).



**Scheme 2.18**

The asymmetric hydroboration of styrene with catecholborane using chiral BINAP gave high enantioselectivity.<sup>3c</sup> We have used the chiral ligand *endo-115* in the Rh-catalyzed asymmetric hydroboration of styrene and found 99% regioselectivity of hydroboration leading to the branched alcohol after oxidation (30% H<sub>2</sub>O<sub>2</sub>, 2 M NaOH) in 70% yield and 26% enantiomeric excess (Scheme 2.19).



**Scheme 2.19**

In summary, the novel chiral ligand *endo-115* could be used for asymmetric Rh-catalyzed hydrogenation of methyl 2-acetamidocinnamate leading to

phenylalanine derivative in moderate enantioselectivity with full conversion. Remarkably, this reaction was carried out under ambient H<sub>2</sub> pressure at room temperature. The application of the same catalyst in the hydroboration of styrene has furnished good result in terms of regioselectivity and yield, but the enantioselectivity was not high. Further applications in new asymmetric catalysis of these new chiral ligands are currently underway in our laboratories.

## 2.4 Experimental Section

All air-sensitive manipulations were carried out using Schlenk and cannula techniques under a positive pressure of argon. All NMR spectra were recorded at 25 °C on Bruker ACF 300, 400 and 500 MHz spectrometers. Optical rotations were measured on the specified solution in a 0.1-dm cell at 25 °C with a Perkin-Elmer model 341 polarimeter. Elemental analyses were performed by the Elemental Analysis Laboratory of the Division of Chemistry and Biological Chemistry at Nanyang Technological University. All melting points were measured using the SRS Optimelt Automated Melting Point System, SRS MPA100.

The compounds diphenylvinylphosphine,<sup>164</sup> diphenyl[(*E*)-2-(ethoxycarbonyl)viny]phosphine,<sup>165</sup> divinylphenylphosphine,<sup>166</sup> bis( $\mu$ -chloro)bis[(*R/S*)-1-[1-(dimethylamino)ethyl]-2-naphthalenyl-*C,N*]diplatinum (II),<sup>167</sup> bis(acetonitrile)[1-[1-(dimethylamino)ethyl]-2-naphthalenyl-*C,N*]diplatinum (II) perchlorate<sup>167</sup> were prepared as previous reported. Solvents were distilled, dried and degassed by standard procedures

where necessary. Column chromatography was performed using silica gel 60 (0.040-0.063mm, Merck). Enantioselectivities were determined by High performance liquid chromatography (HPLC) analysis employing a Daicel Chirapak AD-H or AS-H column.

### **Preparation of 3-Ddiphenylphosphinofuran,**

To a solution of 3-bromofuran (1 g, 6.8 mmol) in tetrahydrofuran(15 mL) was dropped n-BuLi (1.6 M in THF, 4.25 mL, 6.8 mmol) in tetrahydrofuan over 10 min at -78 °C. After the reaction mixture was stirred for 30 min, Ph<sub>2</sub>PCl (1.3 mL) in solution in 20 mL of tetrahydrofuran was slowly added at -78 °C. This mixture was slowly raised to room temperature, and the solution was stirred for 3 h. The solvent was removed under reduced pressure and a saturated ammonium chloride solution (10.00 g in 50 mL of water) was added slowly into the reaction mixture. The product was then extracted with diethyl ether. The organic layer was separated and dried over magnesium sulfate. The solvent was removed and the residue (brownish oil) was distilled (b.p. 132–134 °C, 0.6 mmHg) to give the product as a colourless viscous oil: 1.51 g (87.9% yield); the product was chromatographed on a silica column with dichloromethane-hexane as eluent yielding a colorless oil: 0.86 g (50% yield). <sup>1</sup>H NMR (CDCl<sub>3</sub>): δ 6.33 (s, 1H, OC=CH), 7.33–7.42 (m, 11H, aromatics and Ph<sub>2</sub>PC=CH), 7.52 (s, 1H, OCH). <sup>31</sup>P{<sup>1</sup>H} NMR (CDCl<sub>3</sub>): δ -31.1 (s).

### **Preparation of Di-(3-furyl)phenylphosphine**

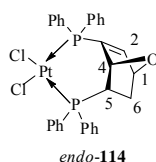
To a solution of 3-bromofuran (2 g, 13.6 mmol) in tetrahydrofuran(15 mL) was added dropwise n-BuLi (1.6 M in THF, 8.5 mL, 13.6 mmol) in tetrahydrofuan

over 10 min at  $-78\text{ }^{\circ}\text{C}$ . After the reaction mixture was stirred for 30 min,  $\text{Ph}_2\text{PCl}$  (1.3 mL) in solution in 40 mL of tetrahydrofuran was slowly added at  $-78\text{ }^{\circ}\text{C}$ . This mixture was slowly raised to room temperature, and the solution was stirred for 3 h. The solvent was removed under reduced pressure and a saturated ammonium chloride solution (10.00 g in 50 mL of water) was added slowly into the reaction mixture. The product was then extracted with diethyl ether. The organic layer was separated and dried over magnesium sulfate. The solvent was removed and the residue (brownish oil) was distilled (b.p.  $120\text{--}122\text{ }^{\circ}\text{C}$ , 0.6 mmHg) to give the product as a colourless viscous oil: 1.40 g (85% yield); the product was chromatographed on a silica column with dichloromethane-hexane as eluent yielding a colorless oil: 0.824 g (45% yield).  $^1\text{H}$  NMR ( $\text{CDCl}_3$ ):  $\delta$  6.40 (s, 2H,  $\text{OC}=\text{CH}$ ), 7.28–7.46 (m, 7H, aromatics and  $\text{Ph}_2\text{PC}=\text{CH}$ ), 7.52 (s, 2H,  $\text{OCH}$ ).  $^{31}\text{P}\{^1\text{H}\}$  NMR ( $\text{CDCl}_3$ ):  $\delta$  -57.3 (s).

**[*SP*-4-3- $\{$ (1*S*,4*R*,5*S*)-dichloro-[3,5-bis(diphenylphosphino)-7-oxabicyclo[2.2.1]hept-2-ene-*P*<sup>3</sup>, *P*<sup>5</sup>}]platinum (II), *endo*-114.**

A solution of silver tetrafluoroborate (0.138 g, 0.71 mmol) in water (1 mL) was added to a mixture containing the platinum template (*R*)-**86** (0.255 g, 0.29 mmol), diphenylvinylphosphine (0.126 g, 0.59 mmol), and 3-diphenylphosphinofuran (0.15 g, 0.59 mmol) in dichloromethane (20 mL). The solution was stirred vigorously at room temperature for 1 h. The solution was filtered (to remove silver chloride), washed with water, and then dried ( $\text{MgSO}_4$ ). Then the dichloromethane was removed and the reaction mixture dissolved in 1,2-dichloroethane. It was further stirred at  $60\text{ }^{\circ}\text{C}$  for 7 d. The cationic complex was treated with concentrated sulfuric acid (70%, 3 mL) for 0.5

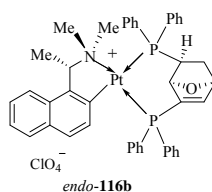
h, and the acidic solution was poured onto ice (ca. 4 g). Lithium chloride (0.6 g) was then added, and the mixture was stirred for 1 h. Addition of dichloromethane (20 mL) gave a clear yellow organic layer, which was subsequently separated, and the aqueous layer was extracted with dichloromethane. The combined organic layer was washed with water and then dried over anhydrous  $\text{MgSO}_4$ . Subsequently fractional crystallization from dichloromethane-diethylether gave complex *endo*-**114** as white prisms: mp 285-286 °C (decomp);  $[\alpha]_D^{+34.7^\circ}$  ( $c = 4$ ,  $\text{CH}_2\text{Cl}_2$ ); 0.303 g (70% yield). Anal. Calcd for  $\text{C}_{30}\text{H}_{26}\text{Cl}_2\text{OP}_2\text{Pt}$ : C, 49.3; H, 3.6. Found C, 49.2; H, 3.6.  $^{31}\text{P}\{^1\text{H}\}$  NMR ( $\text{CDCl}_3$ ):  $\delta$  21.2 (d, 1 P,  $J_{\text{PP}} = 14.7$  Hz,  $J_{\text{PtP}} = 3577$  Hz,  $P$ ), -15.1 (d, 1 P,  $J_{\text{PP}} = 14.7$  Hz,  $J_{\text{PtP}} = 3411$  Hz,  $P$ );  $^1\text{H}$  NMR ( $\text{CDCl}_3$ ):  $\delta$  1.08-1.15 (m, 1H,  $H_5$ ), 2.25-2.37 (m, 1H,  $H_6$ ), 3.43-3.67 (m, 1H,  $H_4$ ), 4.98 (d, 1H,  $^3J_{\text{HH}} = 3.9$  Hz,  $H_I$ ), 5.10 (d, 1H,  $^3J_{\text{HH}} = 3.9$  Hz,  $H_3$ ), 6.56 (dd, 1H,  $^3J_{\text{PH}} = 15.3$  Hz,  $^3J_{\text{HH}} = 7.0$  Hz,  $H_2$ ), 7.37-8.35 (m, 20H, aromatics).



**(1*S*,4*R*,5*S*)-3,5-bis(diphenylphosphino)-7-oxabicyclo[2.2.1]-hept-2-ene, *endo*-115 and {(*R*)-1-[1-(dimethylamino)ethyl]-2-naphthyl- $\text{C}^2$ , N}\{(1*S*,4*R*,5*S*)-[3,5-bis(diphenylphosphino)-7-oxabicyclo[2.2.1]-hept-2-ene- $P^3$ ,  $P^5$ }\}platinum (II)perchlorate, *endo*-116b.**

A solution of *endo*-**114** (0.2 g, 0.27 mmol) in dichloromethane (15 mL) was stirred vigorously with a saturated aqueous solution of potassium cyanide (0.2 g) for half an hour. The resulting colorless organic layer was separated, washed with water,

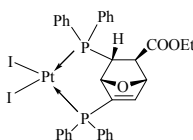
and dried (MgSO<sub>4</sub>). Upon the removal of solvent, a white solid *endo*-**115** was obtained:  $[\alpha]_{\text{D}} -37.6^{\circ}$  (*c* 1.7, CH<sub>2</sub>Cl<sub>2</sub>); 0.102 g (80% yield). <sup>31</sup>P{<sup>1</sup>H} NMR (CDCl<sub>3</sub>):  $\delta$  -12.5 (d, 1P, <sup>3</sup>J<sub>PP</sub> = 77 Hz, *P*), -20.8 (d, 1P, <sup>3</sup>J<sub>PP</sub> = 77 Hz, *P*) ppm. *Endo*-**115** (0.07 g, 0.27 mmol) was added to a solution of (*S*)-**117** (0.073 g, 0.27 mmol) in dichloromethane (15 mL) and stirred vigorously for 1 hour. Recrystallization of the crude product from dichloromethane-diethyl ether gave complex *endo*-**116b** as pale yellow crystals: mp 210–212 °C (decomp);  $[\alpha]_{\text{D}} -35^{\circ}$  (*c* 1.0, CH<sub>2</sub>Cl<sub>2</sub>); 0.122 g (85% yield). Anal. Calcd for C<sub>44</sub>H<sub>42</sub>ClNO<sub>5</sub>P<sub>2</sub>Pt: C, 55.2; H, 4.4; N, 1.5. Found: C, 54.7; H, 4.2; N, 1.4. <sup>31</sup>P{<sup>1</sup>H} NMR (CDCl<sub>3</sub>):  $\delta$  27.6 (d, 1 P, *J*<sub>P,P</sub> = 14.5 Hz, *J*<sub>Pt,P</sub> = 1710 Hz, *P*<sup>5</sup>), -6.2 (d, 1 P, *J*<sub>P,P</sub> = 14.5 Hz, *J*<sub>Pt,P</sub> = 3677 Hz, *P*<sup>3</sup>); <sup>1</sup>H NMR (CDCl<sub>3</sub>):  $\delta$  1.18-1.23 (m, 1H, *H*<sub>5</sub>), 1.42 (d, 3H, <sup>3</sup>*J*<sub>H,H</sub> = 6.2 Hz, CH*Me*), 2.18-2.24 (m, 1H, *H*<sub>6</sub>), 2.55 (s, 3H, CH*Me*), 2.91 (s, 3H, CH*Me*), 3.37-3.43 (m, 1H, *H*<sub>4</sub>), 4.69 (qn, 1H, <sup>3</sup>*J*<sub>H,H</sub> = <sup>4</sup>*J*<sub>P,H</sub> = 6.1 Hz, CH*Me*), 4.94 (d, 1H, <sup>3</sup>*J*<sub>H,H</sub> = 3.9 Hz, *H*<sub>1</sub>), 5.03 (d, 1H, <sup>3</sup>*J*<sub>H,H</sub> = 3.5 Hz, *H*<sub>3</sub>), 6.48 (d, 1H, <sup>3</sup>*J*<sub>H,H</sub> = 9.1 Hz, *H*<sub>2</sub>), 6.98-8.14 (m, 26H, aromatics).



**[*SP*-4-3-{(1*R*,4*S*,5*R*,6*R*)-diiodo-[3,5-bis(diphenylphosphino)-6-(ethoxycarbonyl)-7-oxabicyclo[2.2.1]-hept-2-ene-*P*<sup>3</sup>, *P*<sup>5</sup>}]platinum (II), *endo*-**119****

A solution of silver tetrafluoroborate (0.234 g, 1.20 mmol) in water (1 mL) was added to a mixture containing the platinum template (*R*)-**86** (0.429 g, 0.5 mmol), diphenyl[(*E*)-2-(ethoxycarbonyl)vinyl]phosphine (0.284 g, 1.00 mmol), and 3-diphenylphosphinofuran (0.252 g, 1.00 mmol) in dichloromethane (30 mL). The

solution was stirred vigorously at room temperature for 1 h. The solution was filtered (to remove silver chloride), washed with water, and then dried ( $\text{MgSO}_4$ ). Dichloromethane was removed and the reaction mixture dissolved in 1,2-dichloroethane. It was further stirred at room temperature for 20 d. The cationic complex was treated with concentrated sulfuric acid (70%, 10 mL) for 0.5 h, and the acidic solution was poured onto ice (ca. 10 g). Lithium chloride (0.8 g) was then added, and the mixture was stirred for 1 h. Addition of dichloromethane (30 mL) gave a clear yellow organic layer, which was subsequently separated, and the aqueous layer was extracted with dichloromethane. The combined organic layer was washed with water and mixed with NaI (0.10 g) in acetone (1 mL) and stirred vigorously for 2h. The solvents were removed, and the residue was extracted with  $\text{CH}_2\text{Cl}_2$  and then dried over anhydrous  $\text{MgSO}_4$ . Subsequently fractional crystallization from dichloromethane-diethylether gave complex *endo*-**119** as yellow prisms: mp 233-235 °C (decomp);  $[\alpha]_{436} +12.7^\circ$  ( $c$  0.6,  $\text{CH}_2\text{Cl}_2$ ); 0.709 g (72% yield). Anal. Calcd for  $\text{C}_{33}\text{H}_{30}\text{I}_2\text{O}_3\text{P}_2\text{Pt}$ : C, 40.2; H, 3.1. Found: C, 40.6.2; H, 3.6.  $^{31}\text{P}\{^1\text{H}\}$  NMR ( $\text{CDCl}_3$ ):  $\delta$  20.5 (d, 1 P,  $J_{\text{PP}} = 8.9$ ,  $J_{\text{PtP}} = 3396$  Hz, P), -17.9 (d, 1 P,  $J_{\text{PP}} = 8.9$ ,  $J_{\text{PtP}} = 3181$  Hz, P);  $^1\text{H}$  NMR ( $\text{CDCl}_3$ ):  $\delta$  1.10 (t, 3H,  $^3J_{\text{HH}} = 7.1$  Hz,  $\text{CH}_3$ ), 2.24 (dd, 1H,  $^3J_{\text{PH}} = 10.6$  Hz,  $^3J_{\text{HH}} = 5.1$  Hz,  $\text{H}_5$ ), 3.95 (qn, 2H,  $\text{CH}_2$ ), 4.11-4.14 (m, 1H,  $\text{H}_4$ ), 5.05 (d, 1H,  $^3J_{\text{HH}} = 4$  Hz,  $\text{H}_3$ ), 6.60 (dd, 1H,  $^3J_{\text{PH}} = 15.5$  Hz,  $^3J_{\text{HH}} = 7.3$  Hz,  $\text{H}_2$ ), 7.96-8.32 (m, 20H, aromatics).

*endo*-**119**

**(1*R*,4*S*,5*R*,6*R*)-3,5-bis(diphenylphosphino)-6-(ethoxycarbonyl)-7-oxabicyclo[2.2.1**

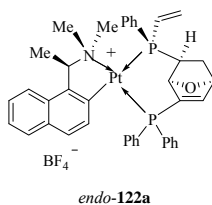
**]-hept-2-ene, endo-120**

A solution of *endo-119* (0.25 g, 0.25 mmol) in dichloromethane (15 mL) was stirred vigorously with a saturated aqueous solution of potassium cyanide (0.2 g) for half an hour. The resulting colorless organic layer was separated, washed with water, and dried (MgSO<sub>4</sub>). Upon the removal of solvent, a white solid *endo-119* was obtained:  $[\alpha]_{365}^{20} +18^\circ$  (*c* 0.8, CH<sub>2</sub>Cl<sub>2</sub>); 0.123 g (90% yield). <sup>31</sup>P{<sup>1</sup>H} NMR (CDCl<sub>3</sub>):  $\delta$  -12.3 (d, 1P,  $J_{PP} = 81$  Hz, *P*), -21.4 (d, 1P,  $J_{PP} = 81$ Hz, *P*).

**{(R)-1-[1-(dime-thylamino)ethyl]-2-naphthyl-C<sup>2</sup>, N}{(1S,4R,5S)-[3-(diphenylphosphino)-5-(S)-(ethenylphenylphosphino)-7-oxabicyclo[2.2.1]-hept-2-ene-P<sup>3</sup>, P<sup>5</sup>}platinum (II)perchlorate, endo-122a:**

A solution of silver tetrafluoroborate (0.233 g, 1.20 mmol) in water (1 mL) was added to a mixture containing the platinum template (*R*)-**86** (0.428 g, 0.5 mmol), divinylphenylphosphine (0.162 g, 1.00 mmol), and 3-diphenylphosphinofuran (0.252 g, 1.00 mmol) in dichloromethane (40 mL). The solution was stirred vigorously at room temperature for 1 h. The solution was filtered (to remove silver chloride), washed with water, and then dried (MgSO<sub>4</sub>). Dichloromethane was removed and the reaction mixture dissolved in 1,2-dichloroethane. It was further stirred at 60 °C for 7 d. The crude product was chromatographed on a silica column with acetone-dichloromethane as eluent. Subsequent fractional crystallization from dichloromethane-diethyl ether gave complex *endo-122a* as pale yellow crystals: mp 236-237 °C (decomp);  $[\alpha]_{\text{D}}^{20} -57^\circ$  (*c* 0.5, CH<sub>2</sub>Cl<sub>2</sub>); 0.161 g (18% yield). Anal. Calcd for C<sub>40</sub>H<sub>40</sub>BF<sub>4</sub>NOP<sub>2</sub>Pt: C, 53.7; H, 4.5; N, 1.6. Found: C, 53.4; H, 4.2; N, 1.4. <sup>31</sup>P{<sup>1</sup>H}

NMR (CDCl<sub>3</sub>):  $\delta$  18.9 (d, 1 P,  $J_{PP} = 14.5$  Hz,  $J_{PtP} = 1730$  Hz,  $P^5$ ), -4.6 (d, 1 P,  $J_{PP} = 14.5$  Hz,  $J_{PtP} = 3676$  Hz,  $P^3$ ); <sup>1</sup>H NMR (CDCl<sub>3</sub>):  $\delta$  1.70 (m, 1H,  $H_{6endo}$ ), 1.81 (d, 3H,  $^3J_{HH} = 6.2$  Hz, CHMe), 2.11 (m, 1H,  $H_{6exo}$ ), 2.56 (s, 3H, NMe), 2.82 (d, 3H,  $^4J_{PH} = 1.5$  Hz, NMe), 3.15 (m, 1H,  $H_5$ ), 4.73 (qn, 1H,  $^3J_{HH} = 6.1$  Hz, CHMe), 4.77 (m, 1H,  $H_1$ ), 5.02 (d, 1H,  $^3J_{HH} = 3.8$  Hz,  $H_4$ ), 6.41 (t, 1H,  $^3J_{PH} = ^3J_{HH} = 19.2$  Hz, PCH=HH'), 6.45 (dd, 1H,  $^3J_{PH} = 30.7$  Hz,  $^3J_{HH} = 3.7$  Hz, PCH=HH'), 6.54 (s, 1H,  $H_2$ ), 6.95 (m, 1H, PCH=H<sub>2</sub>), 7.01-8.28 (m, 21H, aromatics).



**[*SP-4-3*-(1*S*,4*R*,5*S*)-Dichloro[3-(diphenylphosphino)-5-(*S*)-(ethenylphenylphosphino)-7-oxabicyclo[2.2.1]-hept-2-ene- $P^3$ ,  $P^5$ ]]platinum(II), *endo-123*.**

The naphthylamine auxiliary in *endo-122a* (0.1 g, 0.11 mmol) was removed chemoselectively by addition of concentrated sulfuric acid (70%, 10 mL). The reaction mixture was stirred vigorously for 0.5 h at room temperature, and the acidic solution was poured onto ice (ca. 10 g). Lithium chloride (0.8 g) was then added, and the mixture was stirred for 1 h. Addition of dichloromethane (30 mL) gave a clear yellow organic layer, which was subsequently separated, and the aqueous layer was extracted with dichloromethane. The combined organic layer was washed with water and then dried over anhydrous MgSO<sub>4</sub>. Subsequently, fractional crystallization from dichloromethane-diethylether gave complex *endo-123* as white prisms: mp 268-270 °C (decomp);  $[\alpha]_D -19.6^\circ$  (*c* 0.5, CH<sub>2</sub>Cl<sub>2</sub>); 0.069 g (91% yield). Anal. Calcd for C<sub>26</sub>H<sub>24</sub>Cl<sub>2</sub>OP<sub>2</sub>Pt: C, 45.9; H, 3.6. Found: C, 46.2; H, 3.4. <sup>31</sup>P{<sup>1</sup>H} NMR (CDCl<sub>3</sub>):  $\delta$

14.1 (d, 1 P,  $J_{PP} = 14.7$  Hz,  $J_{PtP} = 3573$  Hz,  $P$ ), -15.1 (d, 1 P,  $J_{PP} = 14.7$  Hz,  $J_{PtP} = 3412$  Hz,  $P$ );  $^1\text{H}$  NMR ( $\text{CDCl}_3$ ):  $\delta$  1.70 (m, 1H,  $H_{6endo}$ ), 2.11 (m, 1H,  $H_{6exo}$ ), 3.20 (m, 1H,  $H_5$ ), 5.01 (m, 2H,  $H_1, H_4$ ), 6.09 (dd, 1H,  $^3J_{PH} = 42.1$  Hz,  $^3J_{HH} = 12.1$  Hz,  $\text{PCH}=\text{HH}'$ ), 6.18 (t, 1H,  $^3J_{PH} = ^3J_{HH} = 19.4$  Hz,  $\text{PCH}=\text{HH}'$ ), 6.31 (d, 1H,  $H_2$ ), 6.87 (dt, 1H,  $^2J_{PH} = ^3J_{HH} = 18.8$  Hz,  $^3J_{HH} = 12.1$  Hz,  $\text{PCH}=\text{H}_2$ ), 7.43-8.29 (m, 15H, *aromatics*).

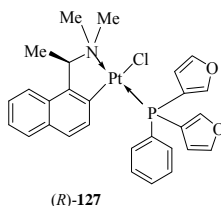
**(1*S*,4*R*,5*S*)-3-(diphenylphosphino)-5-(*S*)-(ethenylphenylphosphino)-7-oxabicyclo[2.2.1]-hept-2-ene, *endo*-124.**

A solution of *endo*-**123** (0.05 g, 0.073 mmol) in dichloromethane (10 mL) was stirred vigorously with a saturated aqueous solution of potassium cyanide (0.1 g) for half an hour. The resulting colorless organic layer was separated, washed with water, and dried ( $\text{MgSO}_4$ ). Upon the removal of solvent, a white solid *endo*-**124** was obtained:  $[\alpha]_{\text{D}} +15.1^\circ$  ( $c$  1.5,  $\text{CH}_2\text{Cl}_2$ ); 0.029g (95% yield).  $^{31}\text{P}\{^1\text{H}\}$  NMR ( $\text{CDCl}_3$ ):  $\delta$  -16.8 (d, 1P,  $J_{PP} = 81$  Hz,  $P$ ), -21.3 (d, 1P,  $J_{PP} = 81$  Hz,  $P$ ).

**Chloro[(*R*)-1-[1-(dimethylamino)ethyl]-2-naphthyl-C,N][di-(3-fural)phenylphosphine]platinum(II), (*R*)-127**

A solution of di-(3-furyl)phenylphosphine (0.29 g, 1.2 mmol) in dichloromethane (20 mL) was added dropwise with stirring to a solution of complex (*R*)-**86** (0.513 g, 0.6 mmol) in dichloromethane. The reaction was allowed to stir for 2 h after which solvent was removed under reduced pressure to give the crude product as pale yellow solid. The crude product was purified via silica gel column chromatography using acetone-dichloromethane as eluent. The pure product was crystallized from dichloromethane-*n*-hexanes as pale yellow prisms: mp 256-257 °C

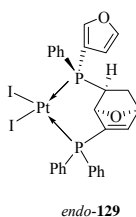
(decomp);  $[\alpha]_{-25^\circ}$  (*c* 0.6, CH<sub>2</sub>Cl<sub>2</sub>); 0.68 g (85% yield). Anal. Calcd for C<sub>28</sub>H<sub>27</sub>ClONPPt: C, 50.1; H, 4.1, N, 2.1. Found: C, 50.6; H, 4.3, N, 1.9. <sup>31</sup>P{<sup>1</sup>H} NMR (CDCl<sub>3</sub>):  $\delta$  21.0 (s, 1 P,  $J_{\text{PtP}} = 4210$  Hz); <sup>1</sup>H NMR (CDCl<sub>3</sub>):  $\delta$  1.97 (d, 3H,  $^3J_{\text{HH}} = 6.4$  Hz, CHMe), 2.83 (s, 3H, NMe), 3.16 (d, 3H,  $^4J_{\text{PH}} = 3.0$  Hz, NMe), 4.60 (qn, 1H,  $^3J_{\text{HH}} = 6.4$  Hz, CHMe), 6.55-7.85 (m, 17H, aromatics).



**[SP-4-3-{(1*S*,4*R*,5*S*)-diiodo-[3-(*S*)-(furylphenylphosphino)-5-(diphenylphosphino)-7-oxabicyclo[2.2.1]-hept-2-ene-*P*<sup>3</sup>, *P*<sup>5</sup>]}]platinum (II), *endo*-129**

A solution of silver tetrafluoroborate (0.234 g, 1.20 mmol) in water (1 mL) was added to a mixture containing (R)-127 (0.429 g, 0.5 mmol) and diphenylvinylphosphine (0.284 g, 1.00 mmol) in dichloromethane (30 mL). The solution was stirred vigorously at room temperature for 1 h. The solution was filtered (to remove silver chloride), washed with water, and then dried (MgSO<sub>4</sub>). Dichloromethane was removed and the reaction mixture dissolved in 1,2-dichloroethane. It was further stirred at 60 °C for 7 d. The cationic complex was treated with concentrated sulfuric acid (70%, 10 mL) for 0.5 h, and the acidic solution was poured onto ice (ca. 10 g). Lithium chloride (0.8 g) was then added, and the mixture was stirred for 1 h. Addition of dichloromethane (30 mL) gave a clear yellow organic layer, which was subsequently separated, and the aqueous layer was extracted with dichloromethane. The combined organic layer was washed with water and mixed with NaI (0.10 g) in acetone (1 mL) and stirred vigorously for 2 h. The solvents were

removed, and the residue was extracted with  $\text{CH}_2\text{Cl}_2$  and then dried over anhydrous  $\text{MgSO}_4$ . Subsequently, fractional crystallization from dichloromethane-diethylether gave complex *endo-129* as yellow prisms: mp 242-244 °C (decomp);  $[\alpha] +25^\circ$  ( $c$  0.7,  $\text{CH}_2\text{Cl}_2$ ); 0.310 g (35% yield). Anal. Calcd for  $\text{C}_{28}\text{H}_{24}\text{I}_2\text{OP}_2\text{Pt}$ : C, 37.9; H, 2.7. Found: C, 37.4; H, 3.1.  $^{31}\text{P}\{^1\text{H}\}$  NMR ( $\text{CDCl}_3$ ):  $\delta$  18.9 (d, 1 P,  $J_{\text{PP}} = 9.7$ ,  $J_{\text{PtP}} = 3389$  Hz, P), -41.8 (d, 1 P,  $J_{\text{PP}} = 9.7$ ,  $J_{\text{PtP}} = 3165$  Hz, P);  $^1\text{H}$  NMR ( $\text{CDCl}_3$ ):  $\delta$  0.99-1.05 (m, 1H,  $H_5$ ), 2.35-2.41 (m, 1H,  $H_6$ ), 3.54-3.67 (m, 1H,  $H_4$ ), 4.96 (d, 1H,  $^3J_{\text{HH}} = 4$  Hz,  $H_3$ ), 5.35-4.96 (d, 1H,  $^3J_{\text{HH}} = 3.8$  Hz,  $H_1$ ), 6.29 (dd, 1H,  $^3J_{\text{PH}} = 15.5$  Hz,  $^3J_{\text{HH}} = 7.2$  Hz,  $H_2$ ), 7.00-8.48 (m, 18H, aromatics).



**(1*S*,4*R*,5*S*)-3-(*S*)-(furylphenylphosphino)-5-(diphenylphosphino)-7-oxabicyclo[2.2.1]-hept-2-ene, *endo-130***

A solution of *endo-129* (0.1 g, 0.11 mmol) in dichloromethane (10 mL) was stirred vigorously with a saturated aqueous solution of potassium cyanide (0.2 g) for half an hour. The resulting colorless organic layer was separated, washed with water, and dried ( $\text{MgSO}_4$ ). Upon the removal of solvent, a white solid *endo-130* was obtained:  $[\alpha] -30^\circ$  ( $c$  0.6,  $\text{CH}_2\text{Cl}_2$ ); 0.043 g (87% yield).  $^{31}\text{P}\{^1\text{H}\}$  NMR ( $\text{CDCl}_3$ ):  $\delta$  -13.0 (d, 1P,  $J_{\text{PP}} = 78$  Hz, P), -48.0 (d, 1P,  $J_{\text{PP}} = 78$  Hz, P).

**Procedure for the hydrogenation with *endo-115***

A solution of  $[\text{Rh}(\text{COD})_2]\text{BF}_4$  (4.0 mg, 0.01 mmol) and *endo-115* (4.7 mg,

0.01 mmol) in MeOH (5 mL) was stirred under argon at room temperature for 10 min to generate the catalyst. This catalyst solution was added into the solution of methyl 2-acetamidocinnamate (0.205 g, 1 mmol) in MeOH (5 mL) and the reaction mixture was left stirring at room temperature under ambient H<sub>2</sub> pressure for 12 h. After releasing H<sub>2</sub>, the reaction mixture was passed through a short silica gel column and concentrated under reduced pressure to give hydrogenation product in quantitative yield (48% ee): HPLC (Chiralcel OJ, <sup>i</sup>PrOH/Hex (10/90), 1.0 mL/min)  $t_R = 11.12$  min (major isomer),  $t_S = 16.37$  min.

#### **Procedure for the hydroboration with *endo*-115**

A mixture of [Rh(COD)<sub>2</sub>]BF<sub>4</sub> (8.1 mg, 0.02 mmol) and *endo*-115 (9.3 mg, 0.02 mmol) in dry THF (5 mL) was stirred under argon at room temperature for 10 min. Styrene (2 mmol) was added to the resulting orange solution at -30 °C. Catecholborane (2.4 mmol, 0.26 mL) was added at -30 °C, and the mixture was stirred at -30 °C for 24 h and then quenched with 5 mL of ethanol. The mixture was added 5 mL of 2 M NaOH and 0.5 mL of 30% H<sub>2</sub>O<sub>2</sub>, and it was stirred at room temperature for 3 h. Extraction with Et<sub>2</sub>O followed by chromatography on a silica gel column with hexane/diethyl ether (v/v, 10:1) as eluent gave 171 mg (70%) of (*R*)-1-phenylethanol, 99% secondary isomer, 24% ee: HPLC (Chiralcel ADH, <sup>i</sup>PrOH/Hex (15/85), 1.0 mL/min)  $t_R = 19.57$  min,  $t_S = 25.00$  min (major isomer).

## Chapter 3

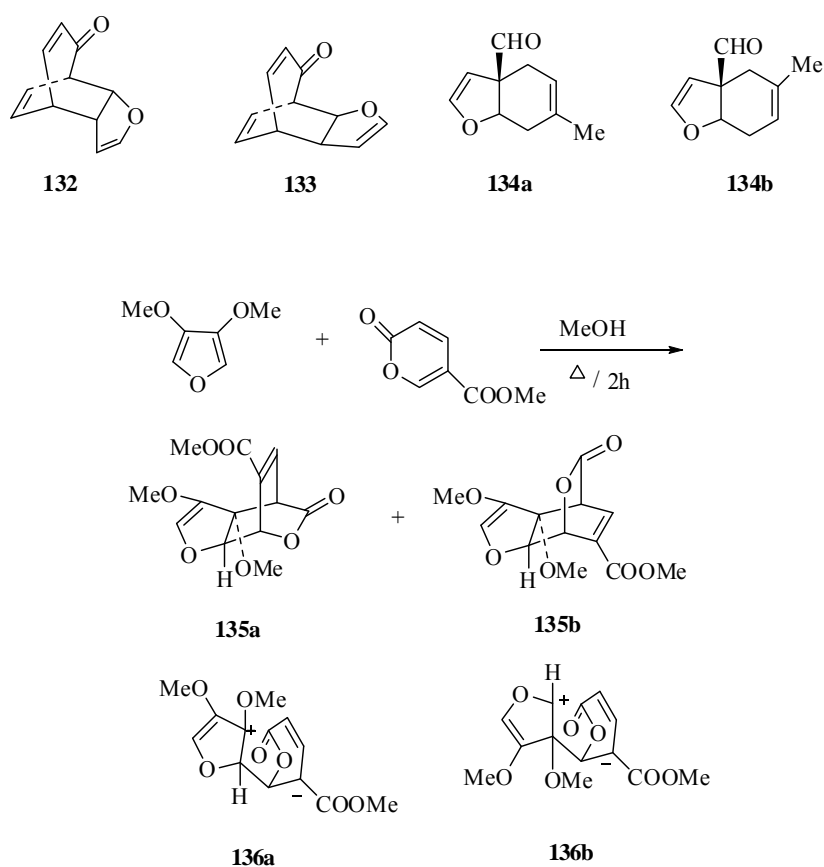
# 3-Diphenylphosphinofuran as Dienophile in Asymmetric Diels-Alder Reaction

### 3.1 Introduction

Despite their aromaticity, many furan derivatives react with ethylenic and acetylenic dienophiles to form bicycle compounds with one oxygen bridge.<sup>168</sup> In contrast, furans in general do not efficiently participate as dienophiles in Diels-Alder reactions.<sup>169-173</sup>

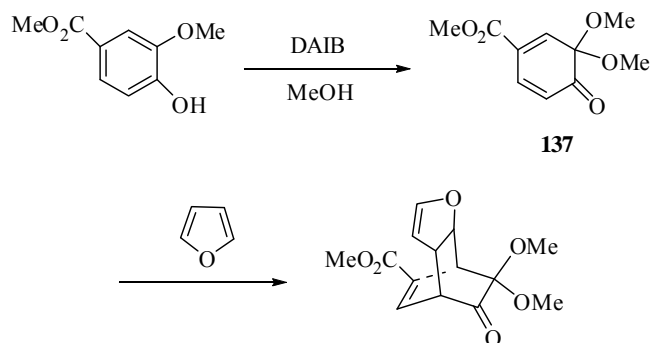
Until now, there are three different ways to activate furan as the dienophile in Diels-Alder reactions. (a) High pressure. Takeshita found that under high pressure, furan can be forced to participate in  $[4\pi + 2\pi]$  cycloadditions as the  $2\pi$  component. Thus, treatment of furan, 2-methoxyfuran, or 3,4-dimethoxyfuran with tropone at 3 kbar and 130 °C produced a 1:1 mixture of cycloadducts **132** in 6% yield and **133** in 5% yields.<sup>170a</sup> (b) High temperature. Heating a 12:1 mixture of isoprene and 3-furaldehyde at 195 °C for 72 h afforded a ca 1:1 mixture (74%) of aldehydes **134a** and **134b**. The formation of 1:1 adducts in respectable yields showed that  $\beta$ -acylfurans could function as normal dienophiles.<sup>171a</sup> (c) Reactive dienes. In 1969, Tedder and coworkers have reported the cycloaddition of furan as a dienophile with tetrachloro-*o*-benzoquinone which often reacts as a conjugated diene rather than a dienophile in boiling benzene to give a single product in 62% yield.<sup>169</sup> Later, a highly electron-rich 3,4-dialkoxyfuran underwent Diels-Alder addition with alkyl coumalates

by refluxing in methanol for 2 h to give two products **135a** and **135b** in combined yield of 52% (Scheme 3.1). This type of cycloaddition is probably not a concerted Diels-Alder reaction but rather the addition of the electron-rich olefin to the pyrone to generate a zwitterions **136a** and **136b** which closes to give the bridged lactone in preference to the cyclobutane.<sup>171b</sup>



**Scheme 3.1**

In 1998, it has been reported furan can function efficiently as a dienophile towards to highly reactive diene masked *o*-benzoquinones (MOBs) **137** which was generated in situ by oxidation of 2-methoxyphenol with (diacetoxy)iodobenzene (DAIB) in methanol at 50 °C to obtain a single stereoisomer in 80% (Scheme 3.2).<sup>173a</sup>



Scheme 3.2

The 3,4-dimethyl-1-phenyl-phosphole (DMPP) ligand is one of the most versatile phosphine ligands in coordination chemistry. The *P*-substituted phospholes are not planar and the geometry of the phosphorus in the phospholes is pyramidal (Figure 3.1).<sup>174</sup> Hence, there is a significant overlap between the  $\sigma$ -orbital of P-R exocyclic bond and the  $\pi$ -dienic system. The character of such phospholes is that their electronic delocalization is weak, therefore no aromatic chemistry of phospholes has been discovered.<sup>174,175</sup> So it is inert to dienophiles due to its apparent cyclic delocalization within the five-membered ring. This was proven experimentally where no coupling reaction was observed when DMPP was left to react with diphenylvinylphosphine at 60 °C in a sealed glass tube over a period of one month.<sup>176</sup> On the contrary, the DMPP ligand could be activated toward Diels-Alder reaction upon metal complexation. The possible reasoning for the observation was that the coordination of the phosphole to the metal centre helps to polarize the 5-membered ring, hence increasing the electron density on the  $\alpha$ -carbon while decreasing that on the  $\beta$ -carbon,<sup>176a</sup> then DMPP shows high reactivity towards various dienophiles. The group of Mathey and Nelson discovered that transition metals such as Cr(0),<sup>177</sup>

Mo(0),<sup>178</sup> W(0),<sup>179</sup> Rh(0),<sup>180</sup> Ir(0),<sup>181</sup> Ru(0),<sup>182</sup> Pd(II),<sup>183</sup> Pt(II)<sup>184</sup> and Ni(II)<sup>185</sup> activate DMPP effectively, and the double bonds of the dienophiles that are coordinated on the metals are also polarized in a reverse order to DMPP. Coordination of the reactants to the transition metals provides further stereochemical control over the transition state that only the *syn-exo* diastereomerism is adopted. The dimerization reaction of DMPP also can be promoted by transition metals such as Cr(0), Mo(0), W(0) under UV irradiation with moderate yields.<sup>178</sup>

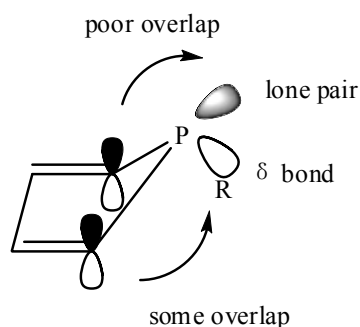


**Figure 3.1 The pyramidal structure of phospholes**

Our group have reported a series of asymmetric Diels-Alder reactions between the cyclic diene 3,4-dimethyl-1-phenylphosphole and various dienophiles in the presence of an organopalladium complex containing the enantiomerically pure form of N, N-dimethyl-1-(1-naphthylethyl)amine in which it is an efficient reaction promoter and stereochemical controller for the activation of DMPP in these asymmetric synthesis.<sup>32</sup> On the other hand, the analogous cycloplatinum complex was used to activate the dimerization of DMPP in which DMPP can be act as cyclic diene as well as a dienophile to obtain an optically pure *P*-chiral diphosphine.<sup>160</sup>

Recently, we have discovered that 3-diphenylphosphinofuran reacted chemoselectively as the dienophile in the Diels-Alder reaction when it is treated with DMPP. This reaction will be described in detail in this chapter.

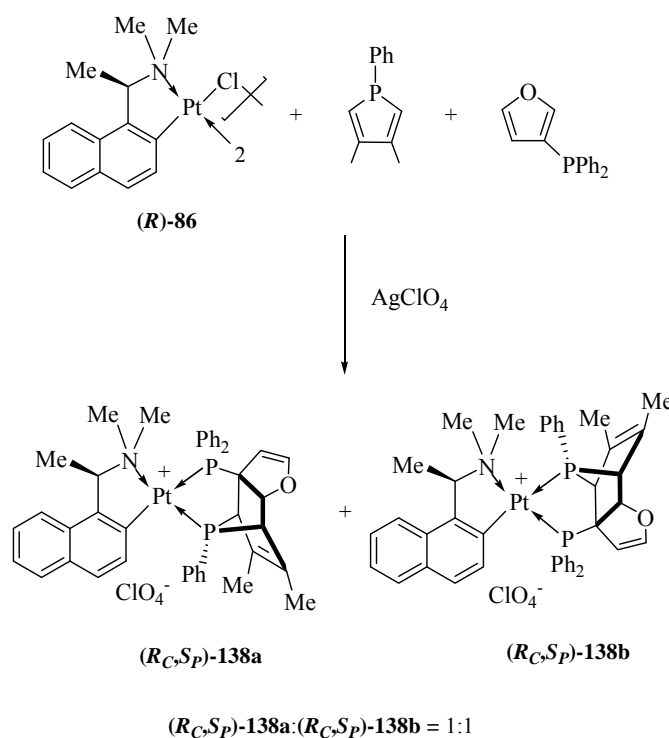
## 3.2 Results and Discussion

### 3.2.1 Asymmetric Diels-Alder Reaction Involving 3-Diphenylphosphinofuran and 1-phenyl-3, 4-dimethylphosphole

Without a metal template, no reaction was observed between 3-diphenylphosphinofuran and 3, 4-dimethyl-1-phenylphosphole (DMPP), even upon prolonged heating. However, with the use of chiral platinum complex (*R*)-**86** (after chloro ligands were abstracted with silver perchlorate<sup>157-158</sup>) as the reaction promoter, the corresponding asymmetric Diels-Alder reaction was completed in 14 days at 40 °C (Scheme 3.3).

Prior to purification, the <sup>31</sup>P{<sup>1</sup>H} NMR spectrum of the crude reaction mixture in CDCl<sub>3</sub> exhibited two pairs of doublets indicative of the formation of only two stereo/regio-chemically distinct products in the ratio 1:1. The doublets of one product (*R<sub>C</sub>,S<sub>P</sub>*)-**138a** were observed at δ 89.4 (*J<sub>PP</sub>*=13.3 Hz, *J<sub>PtP</sub>* = 3256 Hz) and 35.3 (*J<sub>PP</sub>*=13.3Hz, *J<sub>PtP</sub>*=1612 Hz) and the doublets of the other product (*R<sub>C</sub>,S<sub>P</sub>*)-**138b** were recorded at δ 111.1 (*J<sub>PP</sub>* = 13.3 Hz, *J<sub>PtP</sub>*=1536 Hz) and 30.1 (*J<sub>PP</sub>* = 13.3 Hz, *J<sub>PtP</sub>* = 3560 Hz). The <sup>31</sup>P{<sup>1</sup>H} NMR signals in the low field region at δ 89.4 and 111.1 are typical for bridgehead phosphorus adopting the *exo-syn* stereochemistry.<sup>186</sup> According to the

spectroscopic information, both products were generated from the reaction in which DMPP was reacted as cyclic diene. Therefore, a pair of diastereomeric phospho-norbornene complexes were obtained *via* the intramolecular [4+2] cycloaddition reaction mechanism.



**Scheme 3.3**

The two products could be separated into their stereoisomerically pure forms by fractional recrystallization from dichloromethane–diethyl ether. (R<sub>C</sub>,S<sub>P</sub>)-138b was obtained as pale yellow prisms in 35% yield,  $[\alpha]_{\text{D}} -5.8^{\circ}$  (*c* 0.5, CH<sub>2</sub>Cl<sub>2</sub>). Due to the unique *trans*–electronic influences which originate from the organoplatinum unit, the larger platinum-phosphorus coupling constants observed for the doublet signal at  $\delta$  30.1 is diagnostic of the PPh<sub>2</sub> group coordinated *trans* to the  $\sigma$ -donating nitrogen atom.<sup>133,157,185</sup> On the other hand, the doublet at  $\delta$  111.1, which show the smaller

platinum-phosphorus coupling constant, is unambiguously assigned to the PPh<sub>2</sub> group that is coordinated *trans* to the strong  $\pi$ -accepting aromatic carbon atom. The structure of this crystalline product was confirmed by X-ray crystallography. The crystallization of the more soluble isomer was less efficient, and it was isolated in 30% yield as pale yellow microprisms, with  $[\alpha]_D^{+32}$  ( $c$  0.7, CH<sub>2</sub>Cl<sub>2</sub>).

### 3.2.2 X-ray Structural Analysis of (*R<sub>C</sub>,S<sub>P</sub>*)-138b

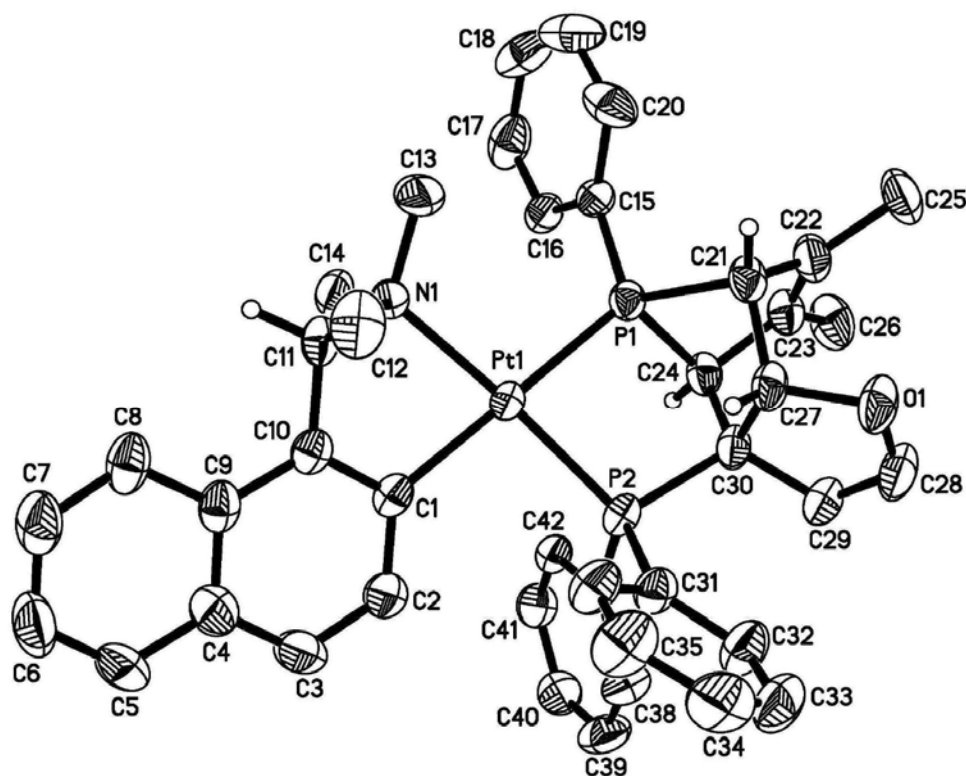


Figure 3.2: Molecular structure and absolute configuration of (*R<sub>C</sub>,S<sub>P</sub>*)-138b

The molecular structure and the absolute stereochemistry of (*R<sub>C</sub>,S<sub>P</sub>*)-138b were determined by X-ray structure analysis (Figure 3.2). The crystallographic study

revealed that absolute configurations at P(1), C(11), C(21), C(24), C(27) and C(30) in the complex were *S*, *R*, *R*, *S*, *S*, and *R* respectively.

**Table 3.1 Selected bond lengths (Å) and (deg) angles for (*R<sub>C</sub>*,*S<sub>P</sub>*)-138b**

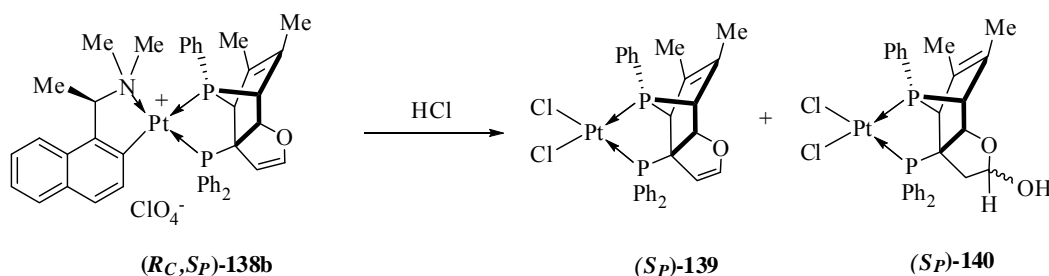
Pt(1)–C(1)	2.056(4)	C(28)–O(1)	1.379(6)
Pt(1)–N(1)	2.141(3)	C(1)–Pt(1)–N(1)	79.2(1)
Pt(1)–P(2)	2.241(1)	C(1)–Pt(1)–P(2)	96.2(1)
Pt(1)–P(1)	2.315(1)	N(1)–Pt(1)–P(2)	174.6(1)
P(1)–C(24)	1.847(4)	C(1)–Pt(1)–P(1)	174.2(1)
P(2)–C(31)	1.820(4)	N(1)–Pt(1)–P(1)	101.2(1)
C(21)–C(27)	1.545(6)	P(2)–Pt(1)–P(1)	83.7(1)
C(24)–C(30)	1.576(6)	C(24)–P(1)–Pt(1)	106.9(1)
C(27)–O(1)	1.456(5)	C(21)–P(1)–Pt(1)	121.5(2)
C(27)–C(30)	1.574(6)	C(30)–P(2)–Pt(1)	105.1(1)
C(28)–C(29)	1.312(6)	C(28)–O(1)–C(27)	106.4(3)

The geometry at the platinum centre is slightly distorted square planar with angles in the range of 79.2(1)–101.2(1)° and 174.2(1)–174.6(1)°. The bond angle at the bridgehead phosphorus, C(21)–P(1)–C(24)[80.7(2)°], is indicative of the elevated levels of strain at the bridge.<sup>187</sup> This bridgehead angle was similar to that observed for the cycloadduct obtained from the asymmetric dimerization of DMPP promoted by the same template.<sup>160</sup> It is important to note that the structural investigations reaffirmed that furan functions as a dienophile whereas DMPP functions as the cyclic diene in the cyclo addition reaction. In agreement with the marked differences in the two Pt–P coupling constants observed in the <sup>31</sup>P NMR spectrum, the Pt(1)–P(1) distances (2.315(1)Å) are clearly longer than the Pt(1)–P(2) bonds (2.241(1)Å). These spectroscopic and structural data are consistent with the unique *trans*-electronic

influences which originate from the organoplatinum unit.<sup>157,160,167</sup> Selected bond lengths and angles are given in Table 3.1.

### 3.2.3 Preparation of Dichloro Complexes for (*S<sub>P</sub>*)-139 and (*S<sub>P</sub>*)-140

The chiral naphthylamine auxiliary in complex (*R<sub>C</sub>,S<sub>P</sub>*)-138b was subsequently removed chemoselectively by treatment with concentrated hydrochloric acid at room temperature (Scheme 3.4). Interestingly when the reaction was stirred for 4h, the <sup>31</sup>P{<sup>1</sup>H} NMR spectrum of the reaction mixture in CDCl<sub>3</sub> exhibited three pairs of doublets in the ratio of 5:4:1, thus indicating that three new complexes have been formed. This is in stark contrast to the usual facile auxiliary cleavage we have observed in our studies.<sup>174</sup>



**Scheme 3.4**

The major product (*S<sub>P</sub>*)-139 was subsequently isolated by crystallization from dichloromethane-diethyl ether as white prisms in 36% yield, [ $\alpha$ ]<sub>D</sub> -60° (*c* 0.5, CH<sub>2</sub>Cl<sub>2</sub>). The <sup>31</sup>P{<sup>1</sup>H} NMR spectrum of the neutral dichloro complex in CD<sub>2</sub>Cl<sub>2</sub> exhibited two doublets at  $\delta$  88.3 ( $J_{PP}$  = 16.9 Hz,  $J_{PtP}$  = 3225 Hz) and 21.1 ( $J_{PP}$  = 16.9 Hz,  $J_{PtP}$  = 3411 Hz). In the absence of the asymmetric naphthylamine auxiliary, two

Pt-P coupling constants are similar in magnitude. The molecular structure and absolute stereochemistry of (*S<sub>P</sub>*)-**139** was established by X-ray crystallography (Figure 3.3). The other two dichloro complexes were recrystallized from CDCl<sub>3</sub> in the ratio of 4:1 as white prisms. The <sup>31</sup>P{<sup>1</sup>H} NMR spectrum of the crystallized product in CDCl<sub>3</sub> showed two pairs of doublets at δ 23.2 (*J*<sub>PP</sub> = 18.0, *J*<sub>Pt,P</sub> = 3408 Hz) and 96.2 (*J*<sub>PP</sub> = 18.3, *J*<sub>Pt,P</sub> = 3147 Hz) and δ 22.7 (*J*<sub>PP</sub> = 18.0, *J*<sub>Pt,P</sub> = 3426 Hz) and 99.2 (*J*<sub>PP</sub> = 18.0, *J*<sub>Pt,P</sub> = 3141 Hz).

### 3.2.4 X-ray Structural Analysis of (*S<sub>P</sub>*)-139

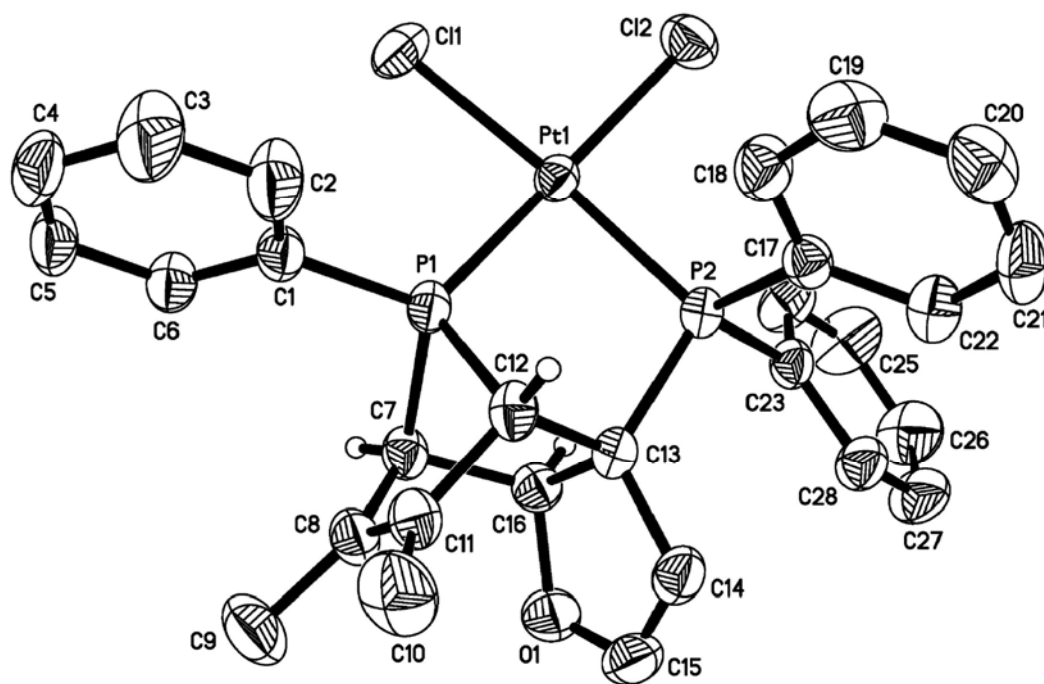


Figure 3.3: Molecular structure and absolute configuration of (*S<sub>P</sub>*)-139

The molecular structure and the absolute configuration of the recrystallised (*S<sub>P</sub>*)-**139** were established by single crystal X-ray crystallographic analysis (Figure 3.3). The absolute configurations of the stereogenic centers were found to be retained even after reaction under acidic conditions. Selected bond lengths and angles are given in Table 3.2.

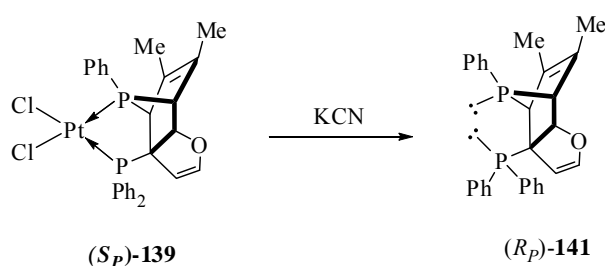
**Table 3.2 Selected bond lengths (Å) and (deg) angles for (*S<sub>P</sub>*)-**139****

Pt(1)–P(1)	2.209(1)	P(1)–Pt(1)–Cl(1)	91.2(1)
Pt(1)–P(2)	2.252(1)	P(2)–Pt(1)–Cl(1)	175.8(1)
Pt(1)–Cl(1)	2.354(1)	P(1)–Pt(1)–Cl(2)	176.4(1)
Pt(1)–Cl(2)	2.369(1)	P(2)–Pt(1)–Cl(2)	94.7(1)
P(2)–C(13)	1.869(2)	Cl(1)–Pt(1)–Cl(2)	89.6(1)
C(13)–C(16)	1.574(3)	C(12)–P(1)–Pt(1)	109.5(1)
P(1)–Pt(1)–P(2)	84.65 (2)	C(13)–P(2)–Pt(1)	103.8(1)

### 3.2.5 Liberation and the Optical Purity of (*R<sub>P</sub>*)-**141**

The optically active ligand (*R<sub>P</sub>*)-**141** can be stereospecifically liberated from the complex (*S<sub>P</sub>*)-**139** by treatment of the dichloro complex with aqueous potassium cyanide at room temperature (Scheme 3.5). The liberated (*R<sub>P</sub>*)-**141** was obtained as a colourless oil in 88% yield,  $[\alpha]_{\text{D}} -18.6^{\circ}$  (*c* 1.2, CH<sub>2</sub>Cl<sub>2</sub>). The <sup>31</sup>P{<sup>1</sup>H} NMR spectrum of the free ligand in CDCl<sub>3</sub> exhibited two doublets at  $\delta$  58.1 (*J<sub>PP</sub>* = 7.6 Hz) and 106.6 (*J<sub>PP</sub>* = 7.6 Hz). The low field resonance signal confirms the retention of the *exo-syn* stereochemistry.<sup>133</sup> It is noteworthy the apparent inversion of configuration that occurs at the tertiary phosphorus stereogenic center when the ligand is liberated from the metal is merely a consequence of the Cahn-Ingold-Prelog (CIP) sequence rule.<sup>188</sup>

Owing to the susceptibility of the non-coordinated bridgehead phosphorus to oxidation, the liberated (*R<sub>P</sub>*)-**141** cannot be stored in its pure form. Hence the liberated ligand was re-complexed to selected metal ions to form stable metal complexes. Furthermore, in order to determine the enantiomeric purity of (*R<sub>P</sub>*)-**141** and to establish the identity of the other isomer, the liberated ligand was re-coordinated to the equally accessible (*R*)-**86**, and the resulting chloride counterion was replaced with a perchlorate anion by treatment with AgClO<sub>4</sub>. This re-coordination process generated two regioisomers in the ratio of 5:1. These two recomplexation products exhibit identical <sup>31</sup>P{<sup>1</sup>H} NMR spectra to those recorded for the product generated from the original cycloaddition reaction, so (*R<sub>C,S<sub>P</sub></sub>*)-**138a** is the regioisomer of (*R<sub>C,S<sub>P</sub></sub>*)-**138b**. As a further check, (*R<sub>P</sub>*)-**141** was re-coordinated to (*S*)-**86**. No resonance signal could be detected at δ 111.1 and 30.1, thus reaffirming that the liberated (*R<sub>P</sub>*)-**141** is enantiomerically pure.



Scheme 3.5

### 3.2.6 X-ray Structural Analysis of (*S<sub>P</sub>*)-**140**

The X-ray crystallographic analysis of a single crystal showed that only one of the diastereomers was present in the unit cell of the selected single crystal. However,

as indicated by NMR spectroscopy this was not representative of the crop of crystals which were a mixture of diastereomers (*S<sub>P</sub>*)-**140a** and (*S<sub>P</sub>*)-**140b**. The structural analysis of (*S<sub>P</sub>*)-**140a** (Figure 3.4) reveals that the enol ether moiety underwent hydrolysis in hydrochloric acid with the introduction of a hydroxyl group. The crystallographic study revealed that absolute configurations at P(1), C(7), C(8), C(13), C(14) and C(16) in the complex were *S*, *R*, *S*, *S*, *R* and *R*, respectively. The geometry at the platinum centre is slightly distorted square planar with angles in the range of 84.6(1)–89.7(1)° and 175.2(1)–176.5(1)°. Selected bond lengths and angles are given in Table 3.3.

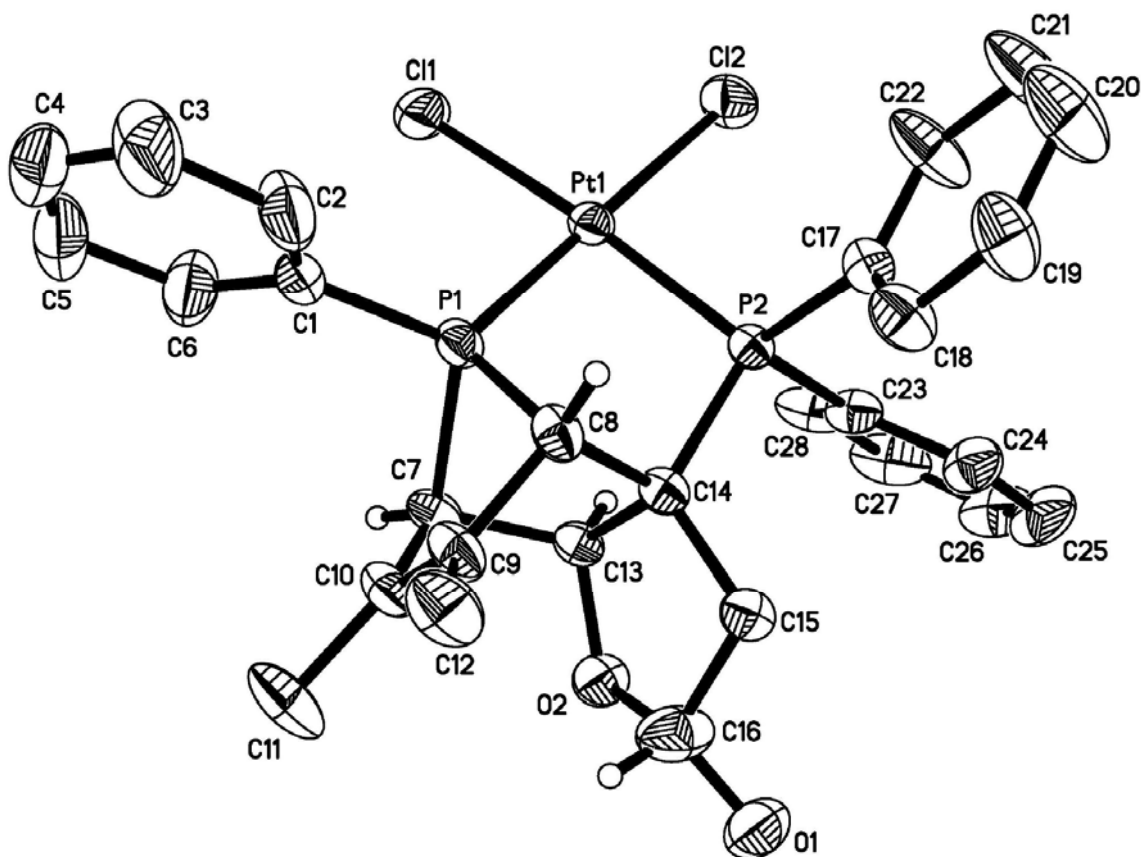


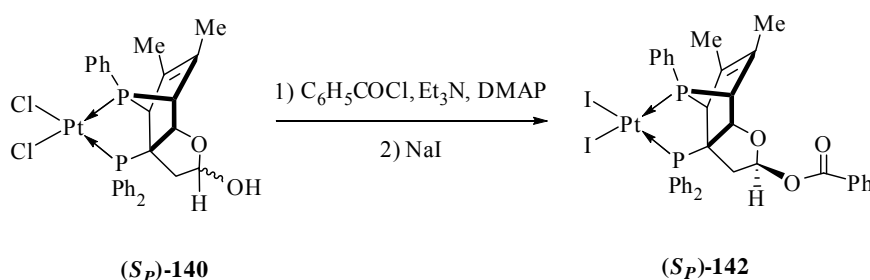
**Figure 3.4:** Molecular structure and absolute configuration of (*S<sub>P</sub>*)-**140a**

**Table 3.3 Selected bond lengths (Å) and (deg) angles for (*S<sub>P</sub>*)-140a**

Pt(1)–P(1)	2.216(2)	P(2)–Pt(1)–Cl(1)	175.2(1)
Pt(1)–P(2)	2.228(1)	P(1)–Pt(1)–Cl(2)	176.5(1)
Pt(1)–Cl(1)	2.360(1)	P(2)–Pt(1)–Cl(2)	93.3(1)
Pt(1)–Cl(2)	2.362(1)	Cl(1)–Pt(1)–Cl(2)	89.7(1)
O(1)–C(16)	1.310(9)	C(8)–P(1)–C(7)	82.6(2)
C(15)–C(16)	1.544(9)	C(8)–P(1)–Pt(1)	109.8(2)
P(1)–Pt(1)–P(2)	84.6(1)	C(14)–P(2)–Pt(1)	103.7(2)
P(1)–Pt(1)–Cl(1)	92.7(1)	O(2)–C(16)–C(15)	107.8(5)

### 3.2.7 Preparation of the Diiodo complex (*S<sub>P</sub>*)-142

After benzylation<sup>189</sup> of (*S<sub>P</sub>*)-140, and subsequent treatment of the dichloro complex with sodium iodide (Scheme 3.6),<sup>163</sup> the <sup>31</sup>P{<sup>1</sup>H} NMR spectrum of the diiodo complex in CDCl<sub>3</sub> exhibited only two doublets at δ 21.1 (*J*<sub>PP</sub> = 18.2, *J*<sub>PtP</sub> = 3400 Hz) and 97.4 (*J*<sub>PP</sub> = 18.2, *J*<sub>PtP</sub> = 3130 Hz). The complex was obtained as yellow crystals in 72% yield, [ $\alpha$ ]<sub>D</sub> –34° (*c* 0.5, CH<sub>2</sub>Cl<sub>2</sub>). This crystallized product was subsequently confirmed by X-ray crystallography.

**Scheme 3.6**

### 3.2.8 X-ray Structural Analysis of (*S<sub>P</sub>*)-142

The molecular structure and the absolute stereochemistry of (*S<sub>P</sub>*)-142 were determined by X-ray structure analysis (Figure 3.5). The absolute configuration at

P(1), C(7), C(8), C(13), C(14) and C(16) in the complex were *S*, *R*, *S*, *S*, *R* and *S*, respectively. Selected bond lengths and angles are given in Table 3.4.

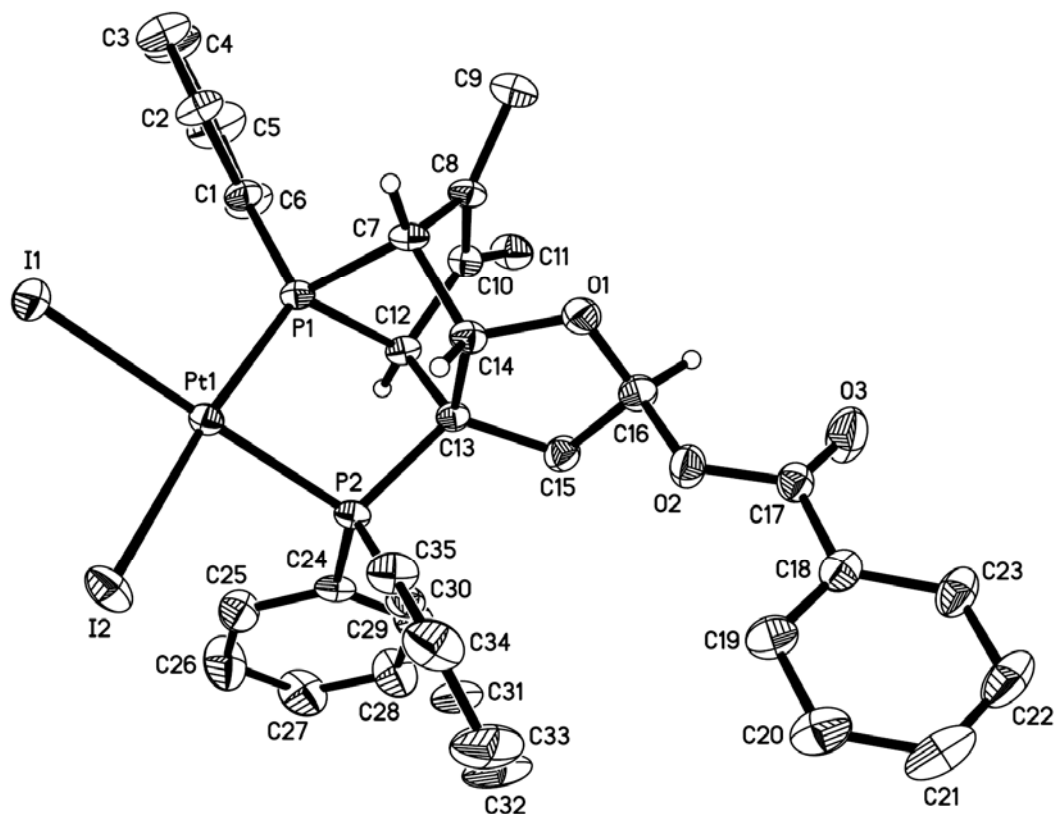


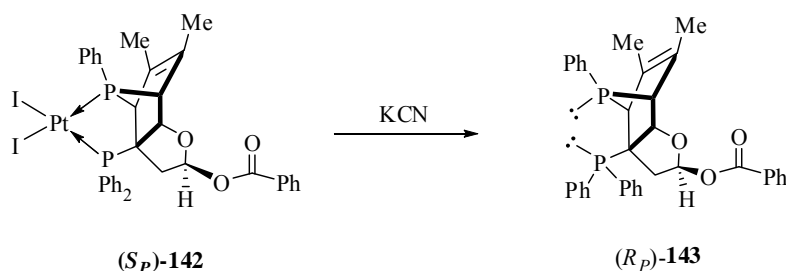
Figure 3.5: Molecular structure and absolute configuration of (*S<sub>P</sub>*)-142

Table 3.4 Selected bond lengths (Å) and (deg) angles for (*S<sub>P</sub>*)-142

Pt(1)–P(1)	2.220(1)	P(1)–Pt(1)–I(1)	94.5(1)
Pt(1)–P(2)	2.249(1)	P(2)–Pt(1)–I(1)	177.2(1)
Pt(1)–I(1)	2.633(1)	P(1)–Pt(1)–I(2)	174.1(1)
Pt(1)–I(2)	2.653(1)	P(2)–Pt(1)–I(2)	91.1(1)
C(15)–C(16)	1.534(6)	I(1)–Pt(1)–I(2)	91.1(1)
C(16)–O(1)	1.394(5)	O(1)–C(16)–C(15)	108.6(3)
C(16)–O(2)	1.438(5)	O(2)–C(16)–C(15)	108.2(3)
P(1)–Pt(1)–P(2)	83.3(1)	C(17)–O(2)–C(16)	117.7(3)

### 3.2.9 Liberation and the Optical Purity of (*R<sub>P</sub>*)-143

The optically pure free diphosphine ligand (*R<sub>P</sub>*)-143 was obtained by ligand displacement of (*S<sub>P</sub>*)-142 with aqueous cyanide (Scheme 3.7), as a white solid in quantitative yield,  $[\alpha]_D +67^\circ(c\ 1.0, CH_2Cl_2)$ . The  $^{31}P\{^1H\}$  NMR spectrum of the free ligand (*R<sub>P</sub>*)-143 in  $CDCl_3$  exhibited two doublets at  $\delta\ 58.12$  ( $^3J_{PP} = 7.6\text{Hz}$ ) and  $106.65$  ( $^3J_{PP} = 7.6\text{Hz}$ ). The low field  $^{31}P\{^1H\}$  NMR resonance indicated that the *exo-syn* stereochemistry remains. It is to be noted that the apparent inversion of configuration that takes place at the phosphorus stereogenic centre during the liberation process is merely a consequence of the Cahn-Ingold-Prelog (CIP) rules.<sup>188</sup>



**Scheme 3.7**

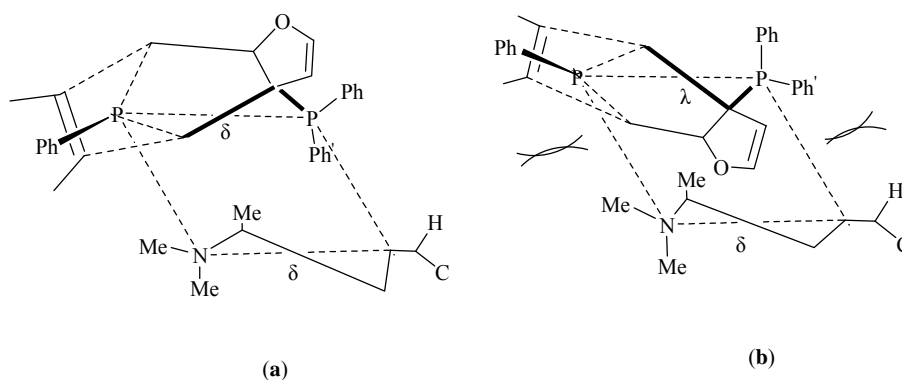
### 3.2.10 The Role of the Platinum Template

The central metal ion in transition metal promoted organometallic reactions can regulate the electronic environment of organic substrates within its coordination sphere. The outer layer orbitals of platinum(II) are easier polarized than those of palladium(II). Therefore its *d* orbitals can accept, donate and redistribute electrons to fit into the electronic requirement of the incoming ligands. Through the possible direct  $d\pi\text{-}d\pi\text{-}d\pi$  overlap of molecular orbitals, the metal center gives a pathway for

electronic movement between DMPP and 3-diphenylphosphinofuran. This special feature provides the most favorable electronic environment for the reaction. As for palladium(II), its outer layer orbitals are relatively harder polarized. Therefore, the incoming ligands could take mostly the specific directions to the metal centre and lead to unstable formation in some instances.<sup>175</sup> There was NMR spectroscopic evidence that that the Diels-Alder reaction between DMPP and 3-diphenylphosphinofuran possibly occurred on palladium complex (*R*)-**7**, but the product complex decomposed rapidly.

The organoplatinum complex also provided the stereochemical control for the cycloaddition reaction. A correlation between the X-ray crystallography data of the cycloaddition product and a Dreiding model study indicated that in the (*R<sub>C</sub>,S<sub>P</sub>*)-**138b**, the absolute configuration at P is *S* and the P-C-C-P linkage may be viewed as part of the rigid five-membered P-Pd-P chelate ring which adopts the rigid  $\delta$  conformation, hence, P-Ph occupied a pseudoequatorial position above the CNPP square plane and P-Ph' is in an axial position below the plane. The bridgehead substituent, P-Ph, projects toward the space below the plane. Model studies indicate that there is no major steric repulsion between the two chelated metals. Figure b, on the other hand, shows the structure of the unfavored diastereomer that was not formed in the Diels-Alder reaction. In this unfavored complex, the absolute configuration at P is *R* and the P-C-C-P ring adopts the  $\lambda$  conformation. Accordingly, P-Ph occupies the axial position above the square plane and P-Ph' is equatorially disposed below it. In contrast to its counterpart in (*R<sub>C</sub>,S<sub>P</sub>*)-**138b**, P-Ph in this unfavored diastereomer projects to the

space above the plane. Model studies also indicate that two major interchelate repulsions within the isomer (b): one exists between the sterically protruding H naphthyl proton and the equatorial P-Ph' group; another severe steric constraint is observed between the proximal N-Me(eq) steric group and P-Ph. These interchelate repulsive forces are the discriminating factors that hinder the formation of this unfavored diastereomer in the Diels-Alder reaction.



### 3.3 Conclusion

In conclusion, the chiral organoplatinum template promoted asymmetric [4+2] Diels-Alder reaction between DMPP and 3-diphenylphosphinofuran proceeded smoothly with furan acting exclusively as dienophile and DMPP as diene. Two regioisomeric *P*-chiral phosphines with furan fused polycyclic rings carrying phosphorus and three carbon chiral centers were obtained from the reaction with high yield and stereoselectively under mild conditions during which two non-benzenoid aromatic systems lost their aromaticity in a single thermal cycloaddition.

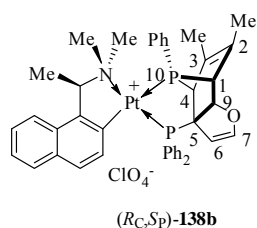
### 3.4 Experimental Section

3,4-dimethyl-1-phenylphosphole<sup>190</sup> was prepared according to the method reported in literature.

**Synthesis of [SP-4-3-{(R)-1-[1-(dimethylamino)ethyl]-2-naphthyl-C,N}]{(1S,4R,6S,10S)-[5-(diphenylphosphino)-6-oxa-2,3-dimethyl-5-ethylene-10-phenyl-10-phosphabicyclo [2.2.1]-hept-2-ene-*P*<sup>5</sup>,*P*<sup>10</sup>]}]platinum (II) perchlorate [(*R*<sub>C</sub>,*S*<sub>P</sub>)-138b] and [SP-4-4-{(R)-1-[1-(dimethylamino)ethyl]-2-naphthyl-C,N}]{(1S,4R,6S,10S)-[5-(diphenylphosphino)-6-oxa-2,3-dimethyl-5-ethylene-10-phenyl-10-phosphabicyclo [2.2.1]-hept-2-ene-*P*<sup>5</sup>,*P*<sup>10</sup>]}]platinum (II) perchlorate [(*R*<sub>C</sub>,*S*<sub>P</sub>)-138a]**

A solution of silver perchlorate (0.83 g, 4 mmol) in water (2 mL) was added to a mixture containing the platinum template (*R*)-**86** (0.86 g, 1 mmol), 3, 4-dimethyl-1-phenylphosphole (0.38 g, 2mmol), and 3-diphenylphosphinofuran (0.5 g, 2mmol) in dichloromethane (75 mL). The solution was stirred vigorously at room temperature for 1 h. The solution was filtered (to remove silver chloride), washed with water, and then dried (MgSO<sub>4</sub>). The dried reaction mixture was further stirred at 40 °C for 14 d. The crude product was chromatographed on a silica column with acetone-dichloromethane as eluent. Subsequent fractional crystallization from dichloromethane-diethyl ether gave complex (*R*<sub>C</sub>,*S*<sub>P</sub>)-**138b** as pale yellow crystals: mp 206-207 °C (decomp); [ $\alpha$ ]<sub>D</sub> -5.8° (*c* 0.5, CH<sub>2</sub>Cl<sub>2</sub>); 0.65 g (35% yield). Anal. Calcd for C<sub>42</sub>H<sub>42</sub>ClNO<sub>5</sub>P<sub>2</sub>Pt: C, 49.3; H, 4.3; N, 1.3. Found: C, 48.9; H, 4.2; N, 1.4. <sup>31</sup>P{<sup>1</sup>H} NMR (CDCl<sub>3</sub>):  $\delta$  30.1 (d, 1 P, *J*<sub>PP</sub> = 3.3 Hz, *J*<sub>PtP</sub> = 3560 Hz, *P*<sup>5</sup>), 111.1(d, 1 P, *J*<sub>PP</sub> = 13.3 Hz, *J*<sub>PtP</sub> = 1536 Hz,

$P^{I0}$ ),  $^1\text{H}$  NMR ( $\text{CDCl}_3$ ):  $\delta$  1.38 (s, 3H,  $\text{C}=\text{CMe}$ ), 1.78 (s, 3H,  $\text{C}=\text{CMe}$ ), 2.62 (d, 3H,  $^3J_{\text{HH}}=6$  Hz,  $\text{CHMe}$ ), 2.85 (s, 1H,  $H_4$ ), 4.37 (d, 1H,  $^3J_{\text{HH}}=5$  Hz,  $H_1$ ), 4.85 (qn, 1H,  $^3J_{\text{HH}}=^4J_{\text{PH}}=6.1$  Hz,  $\text{CHMe}$ ), 5.60 (dd, 1H,  $^3J_{\text{PH}}=21.9$  Hz,  $^3J_{\text{HH}}=5$  Hz,  $H_6$ ), 6.34-6.36 (m, 1H,  $H_8$ ), 6.86-6.90 (m, 1H,  $H_9$ ), 7.07-8.44 (m, 21H, aromatics). After isolation of the less soluble isomer, the more soluble isomer ( $R_C, S_P$ )-**138a** subsequently crystallized from the concentrated mother liquor as pale yellow microplates: mp 208–209 °C (dec);  $[\alpha]_{\text{D}}=+32$  ( $c=0.7$ ,  $\text{CH}_2\text{Cl}_2$ ); 0.631 g (30% yield). Anal. Calcd for  $\text{C}_{42}\text{H}_{42}\text{ClNO}_5\text{P}_2\text{Pt}$ .  $1.5\text{CH}_2\text{Cl}_2$ : C, 49.3; H, 4.3; N, 1.3. Found: C, 48.9; H, 4.8; N, 1.5.  $^{31}\text{P}\{^1\text{H}\}$  NMR ( $\text{CDCl}_3$ ,  $\delta$ ): 35.3 (d, 1 P,  $J_{\text{PP}}=14.3$  Hz,  $J_{\text{PtP}}=1612$  Hz,  $P^5$ ), 89.4 (d, 1 P,  $J_{\text{PP}}=14.3$  Hz,  $J_{\text{PtP}}=3256$  Hz,  $P^{I0}$ ).  $^1\text{H}$  NMR ( $\text{CDCl}_3$ ,  $\delta$ ): 1.42 (s, 3H,  $\text{C}=\text{CMe}$ ), 1.83 (s, 3H,  $\text{C}=\text{CMe}$ ), 2.65 (d, 3H,  $^3J_{\text{HH}}=6$  Hz,  $\text{CHMe}$ ), 2.91 (s, 1H,  $H_4$ ), 4.39 (d, 1H,  $^3J_{\text{HH}}=5$  Hz,  $H_1$ ), 4.85 (qn, 1H,  $^3J_{\text{HH}}=^4J_{\text{PH}}=6.1$  Hz,  $\text{CHMe}$ ), 5.62 (dd, 1H,  $^3J_{\text{PH}}=21.5$  Hz,  $^3J_{\text{HH}}=5.2$  Hz,  $H_9$ ), 6.37-6.40 (m, 1H,  $H_7$ ), 6.96-6.92 (m, 1H,  $H_6$ ), 7.10-8.42 (m, 21H, aromatics).

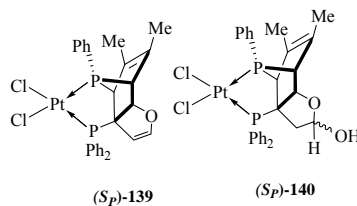


**Dichloro-[[ $(1S,4R,6S,10S)$ ]-[5-(diphenylphosphino)-6-oxa-2,3-dimethyl-5-ethylene-10-phenyl-10-phosphabicyclo [2.2.1]-hept-2-ene- $P^5$ ,  $P^{I0}$ ]]platinum (II), ( $S_P$ )-**139** dichloro-[5-(diphenylphosphino)-6-oxa-8-hydroxy-2, 3-dimethyl-10-phenyl-10-phosphabicyclo [2.2.1]-hept-2-ene- $P^5$ ,  $P^{I0}$ ]]platinum(II) [( $S_P$ )-**140**]**

The naphthylamine auxiliary in ( $R_C, S_P$ )-**138b** was removed chemoselectively by adding concentrated hydrochloric acid (12 mL) to a solution of the complex (0.40 g)

in dichloromethane (20 mL). The reaction mixture was stirred vigorously for 4 h at room temperature. The reaction mixture was then washed with water ( $4 \times 10$  mL), and dried ( $\text{MgSO}_4$ ). Subsequently fractional crystallization from dichloromethane-diethylether gave complex ( $S_p$ )-**139** as white prisms: mp 255-256 °C (decomp);  $[\alpha]_D -60^\circ$  ( $c$  0.5,  $\text{CH}_2\text{Cl}_2$ ); 0.11 g (36% yield). Anal. Calcd for  $\text{C}_{28}\text{H}_{26}\text{Cl}_2\text{OP}_2\text{Pt}$ : C, 47.6; H, 3.7. Found: C, 47.3; H, 3.6.  $^{31}\text{P}\{^1\text{H}\}$  NMR ( $\text{CDCl}_3$ ):  $\delta$  21.1 (d, 1 P,  $J_{\text{PP}} = 16.9$  Hz,  $J_{\text{PtP}} = 3411$  Hz,  $P^5$ ), 88.3(d, 1 P,  $J_{\text{PP}} = 16.9$  Hz,  $J_{\text{PtP}} = 3225$  Hz,  $P^{10}$ );  $^1\text{H}$  NMR ( $\text{CDCl}_3$ ):  $\delta$  1.56 (s, 3H, C=CMe), 1.73 (s, 3H, C=CMe), 3.23 (s, 1H,  $H_4$ ), 4.03 (d, 1H,  $^3J_{\text{HH}} = 5$  Hz,  $H_1$ ), 5.25 (s, 1H,  $H_8$ ), 5.76 (dd, 1H,  $^3J_{\text{PH}} = 22.0$  Hz,  $^3J_{\text{HH}} = 5$  Hz,  $H_6$ ), 6.36 (m, 1H,  $H_9$ ), 7.49-8.24 (m, 15H, aromatics).

A diastereomer mixture of hemiacetal ( $S_p$ )-**140** were subsequently isolated from the concentrated mother liquor as white prisms: 0.145 g (47% yield). Anal. Calcd for  $\text{C}_{28}\text{H}_{28}\text{Cl}_2\text{O}_2\text{P}_2\text{Pt}$ : C, 45.3; H, 3.8. Found: C, 44.9; H, 4.1.  $^{31}\text{P}\{^1\text{H}\}$  NMR ( $\text{CDCl}_3$ ):  $\delta$  23.2 (d, 1 P,  $J_{\text{PP}} = 18.3$  Hz,  $J_{\text{PtP}} = 3408$  Hz,  $P^5$ ), 96.2(d, 1 P,  $J_{\text{PP}} = 18.3$  Hz,  $J_{\text{PtP}} = 3147$  Hz,  $P^{10}$ );  $\delta$  22.7(d, 1 P,  $J_{\text{PP}} = 18.0$  Hz,  $J_{\text{PtP}} = 3426$  Hz,  $P^5$ ), 99.2(d, 1 P,  $J_{\text{PP}} = 18.0$  Hz,  $J_{\text{PtP}} = 3141$  Hz,  $P^{10}$ );  $^1\text{H}$  NMR ( $\text{CDCl}_3$ ):  $\delta$  1.69 (s, 3H, C=CMe), 1.76 (s, 3H, C=CMe), 2.48 (s, 1H,  $H_{9,10}$ ), 2.89 (m, 1H,  $H_{9,10}$ ), 3.17 (s, 1H,  $H_4$ ), 3.23 (s, 1H,  $H_4$ ), 3.84 (s, 1H,  $H_1$ ), 4.66 (m, 1H,  $H_8$ ), 5.42 (m, 1H,  $H_8$ ), 5.50(dd, 1H,  $^3J_{\text{PH}} = 18$  Hz,  $^3J_{\text{HH}} = 5$  Hz,  $H_6$ ), 5.75 (dd, 1H,  $^3J_{\text{HH}} = 16.5$  Hz,  $^4J_{\text{PH}} = 4$  Hz,  $H_6$ ), 7.47-8.23 (m, 15H, aromatics).



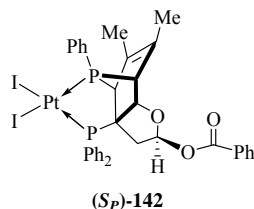
**(1*S*, 4*R*, 6*S*, 10*S*)-[5-(diphenylphosphino)-6-oxa-2, 3-dimethyl -5-ethylene-10-phenyl-10-phosphabicyclo [2.2.1]-hept-2-ene [(*R*<sub>P</sub>)-141]**

A solution of (*S*<sub>P</sub>)-**139** (0.1 g) in dichloromethane (20 mL) was stirred vigorously with a saturated aqueous solution of potassium cyanide (0.5 g) for 1 min. The resulting colorless organic layer was separated, washed with water, and dried (MgSO<sub>4</sub>). Upon the removal of solvent, a white solid (*R*<sub>P</sub>)-**141** was obtained: [α]<sub>D</sub> –18.6° (*c* 1.2, CH<sub>2</sub>Cl<sub>2</sub>); 0.055 g (88% yield). <sup>31</sup>P{<sup>1</sup>H} NMR (CDCl<sub>3</sub>): δ 9.9 (d, 1P, *J*<sub>PP</sub> = 121.2 Hz, *P*), 94.6 (d, 1P, *J*<sub>PP</sub> = 21.2 Hz, *P*).

**Diiodo-[(1*S*,4*R*,6*S*,8*S*,10*S*)-[5-(diphenylphosphino)-6-oxa-8-benzoyloxy-2,3-dimethyl-10-Phenyl-10-phosphabicyclo [2.2.1]-hept-2-ene-*P*<sup>5</sup>, *P*<sup>10</sup>]} platinum (II) [*S*<sub>P</sub>)-142]**

Hemiacetal (*S*<sub>P</sub>)-**140a** (0.05 g, 0.07 mmol), triethylamine (0.008 g, 0.077 mmol), and DMAP (0.68 mg, 0.006 mmol) were dissolved in dichloromethane (5 mL). The solution was cooled to 0 °C and benzoyl chloride (0.011 g, 0.077 mmol) was added in three portions. After 10 h, the reaction was quenched with 1 N NaOH, the layers were separated, and the organic layer was washed with 2N HCl followed by water. The combined organic fractions were mixed with NaI (0.10 g) in acetone (1 mL) and stirred vigorously for 2 h. The solvents were removed, and the residue was extracted with CH<sub>2</sub>Cl<sub>2</sub> and then dried over anhydrous MgSO<sub>4</sub>. Removal of the solvent gave

(*S<sub>P</sub>*)-**142** as a yellow solid, which was then recrystallized from dichloromethane-diethyl ether forming yellow prisms: mp 217-219 °C (decomp); [ $\alpha$ ]<sub>D</sub> -34° (*c* 0.5, CH<sub>2</sub>Cl<sub>2</sub>); 0.05 g (72% yield). Anal. Calcd for C<sub>35</sub>H<sub>32</sub>I<sub>2</sub>O<sub>3</sub>P<sub>2</sub>Pt: C, 41.6; H, 3.2. Found: C, 41.9; H, 2.9. <sup>31</sup>P{<sup>1</sup>H} NMR (CDCl<sub>3</sub>):  $\delta$  21.1(d, 1 P,  $J_{PP}$  = 18.2 Hz,  $J_{PtP}$  = 3400 Hz,  $P^5$ ), 97.4 (d, 1 P,  $J_{PP}$  = 18.2 Hz,  $J_{PtP}$  = 3130 Hz,  $P^{10}$ ); <sup>1</sup>H NMR (CDCl<sub>3</sub>):  $\delta$  1.76 (s, 3H, C = *CMe*), 1.81 (s, 3H, C = *CMe*), 2.77-2.83 (m, 1H, H<sub>exo</sub>), 2.89-2.95 (m, 1H, H<sub>endo</sub>), 3.22 (s, 1H, H<sub>4</sub>), 3.87 (d, 1H, <sup>3</sup> $J_{HH}$  = 5 Hz, H<sub>7</sub>), 5.89 (dd, 1H, <sup>3</sup> $J_{PH}$  = 15.9 Hz, <sup>3</sup> $J_{HH}$  = 5 Hz, H<sub>6</sub>), 6.34-6.35 (m, 1H, H<sub>8</sub>), 7.11-8.23 (m, 20H, aromatics).



**(1*S*,4*R*,6*S*,8*S*,10*S*)-[5-(diphenylphosphino)-6-oxa-8-benzoyloxy-2,3-dimethyl-10-phenyl-10-phosphabicyclo [2.2.1]-hept-2-ene] [(*R<sub>P</sub>*)-**143**]**

Diphosphine ligand (*R<sub>P</sub>*)-**143** was similarly obtained from the reaction of (*S<sub>P</sub>*)-**142** (0.05 g) and saturated aqueous KCN (1 g), as a white solid: [ $\alpha$ ]<sub>D</sub> +67° (*c* 1.0, CH<sub>2</sub>Cl<sub>2</sub>); 0.024 g (86% yield). <sup>31</sup>P{<sup>1</sup>H} NMR (CDCl<sub>3</sub>):  $\delta$  17.5 (d, 1P,  $J_{PP}$  = 141.6 Hz, *P*), 112.1 (d, 1P,  $J_{PP}$  = 41.6 Hz, *P*).

# Chapter 4

## Asymmetric Hydrophosphination Reaction

### 4.1 Introduction

Pyridylphosphines are an important class of functionalized phosphines containing both P- and N-donor centres.<sup>191</sup> Recently, chiral 2-pyridylphosphines have received considerable attention. This type of unsymmetrical chiral ligand possesses a combination of hard (N) and soft donor (P) atoms, and therefore have different features associated with each donor atom that provide unique reactivity to their metal complexes in catalytic asymmetric processes. Hence, they have been used very successfully in asymmetric catalytic reactions.<sup>192</sup> However synthesis of these P–N ligands often involves tedious organic manipulations and the methodologies are limited to compounds that are not base sensitive or those including aryl halide/ triflate groups. Until now, no efficient synthesis of enantiomerically pure keto- and ester-substituted C-chiral 2-pyridylphosphines have been reported.

The asymmetric addition reaction of the P–H moiety to carbon-carbon multiple bonds is generally considered a straightforward and efficient reaction pathway in organophosphorus chemistry.<sup>193</sup> In general, metal complexes offer superior reaction rates, selectivity and stereocontrol in hydrophosphination reactions than other reaction promoters such as strong bases,<sup>194</sup> acids<sup>195</sup> and free radicals.<sup>196</sup> Moreover, many functional groups can be incorporated into substrates without special protection as relatively mild conditions are usually required in these metal-activated

addition reactions.

Our group recently has reported the use of organopalladium complex containing (*R*)- or (*S*)-(1-(dimethylamino)ethyl)naphthalene as the chiral auxiliary to promote the asymmetric hydrophosphination of vinylic phosphines to generate chiral diphosphines in high enantioselectivity under mild conditions.<sup>134,135</sup> In order to extend this protocol to the hydrophosphination of other functionalized olefinic systems, we hereby prepared the keto- and ester- functionalized chiral pyridylphosphine ligands via the asymmetric hydrophosphination reaction promoted by the chiral cyclopalladated-amine template.

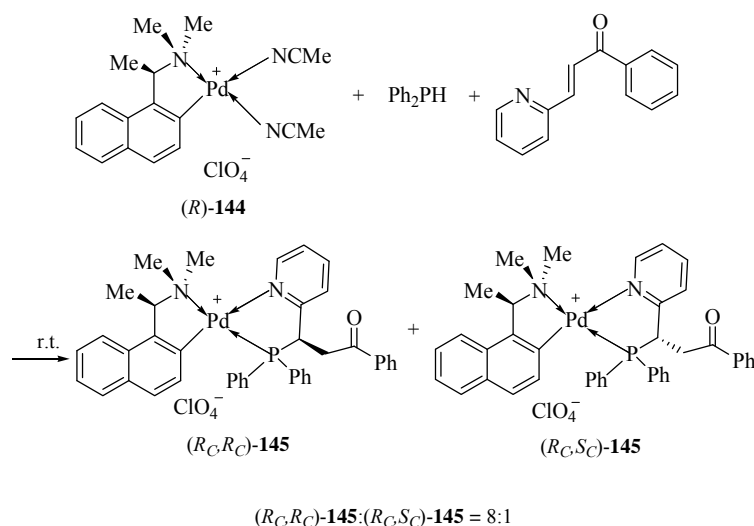
## 4.2 Results and Discussion

### 4.2.1 Hydrophosphination of (*E*)-1-phenyl-3-pyridin-2-yl-2-propenone

In the absence of a metal ion, diphenylphosphine shows no reactivity with (*E*)-1-phenyl-3-pyridin-2-yl-2-propenone. However, as illustrated in Scheme 4.11, in the presence of chiral complex (*R*)-**144**, the reaction proceeded smoothly at room temperature.

The reaction was found to be completed in 4 days. Before purification, the <sup>31</sup>P{<sup>1</sup>H} NMR spectrum of the reaction mixture in CDCl<sub>3</sub> exhibited two sharp singlets at  $\delta$  60.2 and 54.0 in the ratio of 1:8; thus indicating that only two diastereomeric complexes have been formed. While the addition of the secondary phosphine to vinylic phosphines resulted in *cis-trans* regioisomers of the products,<sup>134</sup> the addition

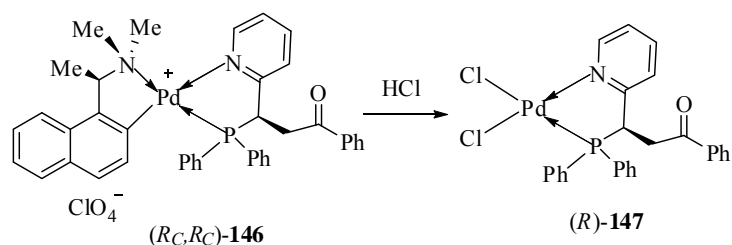
of diphenylphosphine in this case is 100% regioselective, wherein the P atom occupies the coordination site trans to NMe<sub>2</sub>. The high regioselectivity observed in the present case is in agreement with what has been observed for other P–N heterobidentate ligands.<sup>42</sup> The diastereomeric products were subsequently separated by column chromatography. The major diastereomer (*R<sub>C</sub>, R<sub>C</sub>*)-**145** was obtained as a pale yellow solid in 70% isolated yield. The <sup>31</sup>P{<sup>1</sup>H} NMR spectrum of (*R<sub>C</sub>, R<sub>C</sub>*)-**145** in CDCl<sub>3</sub> exhibited a singlet at δ 54.0.



**Scheme 4.11**

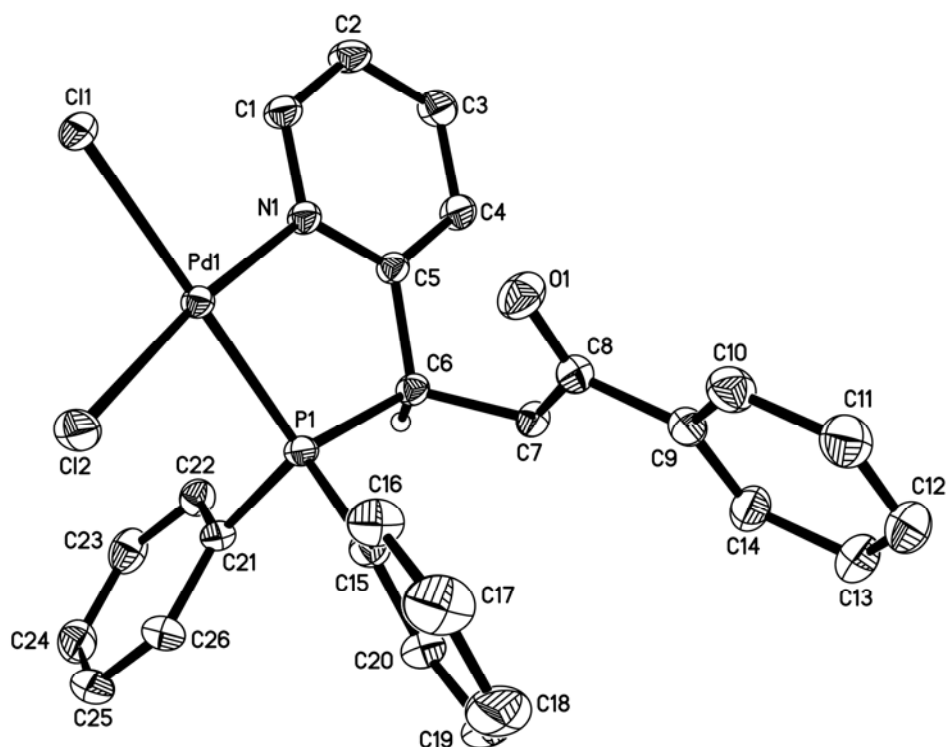
Although it is stable in the solid state and in solution, (*R<sub>C</sub>, R<sub>C</sub>*)-**145** is highly soluble in most organic solvent systems and could not be induced to crystallize. Upon subsequent treatment of the perchlorate salt with concentrated hydrochloric acid, the resultant dichloro complex (*R*)-**146** was obtained as yellow prisms in 85% isolated yield (Scheme 4.12), [ $\alpha$ ]<sub>D</sub> –54° (*c* 0.7, CH<sub>2</sub>Cl<sub>2</sub>). The <sup>31</sup>P{<sup>1</sup>H} NMR spectrum of (*R*)-**146** in CD<sub>2</sub>Cl<sub>2</sub> exhibited a sharp singlet at δ 52.4. The chelating properties and the

absolute configuration of the coordinated pyridine-substituted phosphine ligand in complex *(R)*-**146** were studied by X-ray crystallography.



**Scheme 4.12**

#### 4.2.1.1 Single Crystal X-ray Structural Analysis of *(R)*-**146**

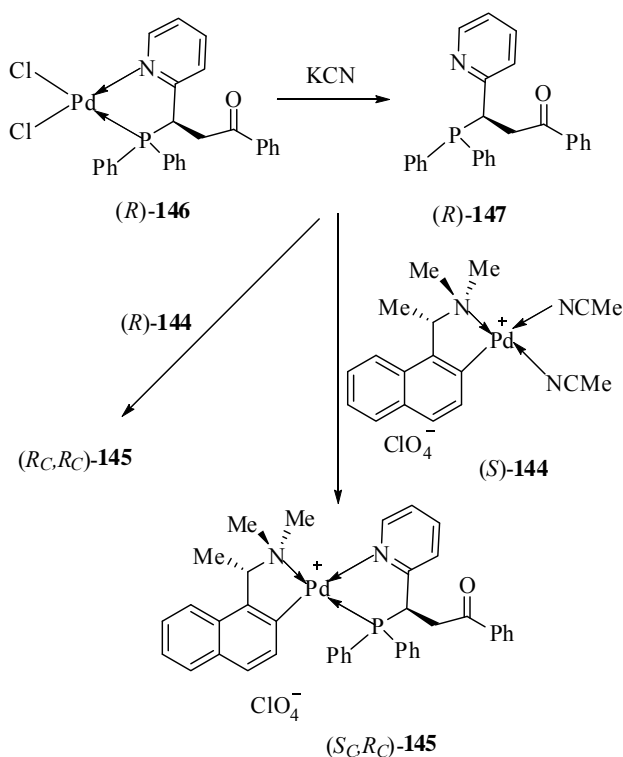


**Figure 4.1** Molecular structure and absolute configuration of *(R)*-**146**

The molecular structure and the absolute stereochemistry of (*R*)-**146** were determined by X-ray structure analysis (Figure 4.1). The structure analysis established that the newly formed stereogenic center at C(6) adopted the *R* absolute configuration. The geometry at the Pd center is distorted square planar with angles of 84.5(4)-95.1(4)° and 172.4(4)-179.4(1)°. Both the Pd-P and Pd-N bond lengths, 2.184(4) and 2.055(1) Å are typical, but the two Pd-Cl distances 2.304(4) and 2.387(4) Å differ significantly, with the bond *trans* to the phosphorus being noticeably longer than normal.<sup>197</sup> This reflects the stronger electronic *trans* effect of the phosphorus relative to the aromatic nitrogen donor. The C(6)-C(7) bond distance [1.536(2) Å] showed marked lengthening, which is clearly attributed to the intrachelate repulsive interactions between the COPh moiety and the phenyl groups on the phosphorus. The CH<sub>2</sub>COPh substituent at C(6) of the five-membered Pd-N chelate is in the preferred equatorial disposition.<sup>198</sup> Selected bond parameters are given in Table 4.1.

**Table 4.1 Selected bond lengths (Å) and (deg) angles for (*R*)-**146****

Pd(1)–N(1)	2.055(1)	Pd(1)–P(1)	2.184(4)
Pd(1)–Cl(2)	2.304(4)	Pd(1)–Cl(1)	2.387(4)
C(1)–N(1)	1.345(2)	C(5)–N(1)	1.357(2)
C(6)–P(1)	1.859(2)	C(8)–O(1)	1.220(2)
C(6)–C(7)	1.536(2)	C(5)–C(6)	1.516(2)
N(1)–Pd(1)–P(1)	84.5(4)	N(1)–Pd(1)–Cl(2)	172.4(4)
P(1)–Pd(1)–Cl(2)	88.0 (1)	N(1)–Pd(1)–Cl(1)	95.1(4)
P(1)–Pd(1)–Cl(1)	179.4 (1)	N(1)–C(5)–C(6)	119.3(1)
Cl(2)–Pd(1)–Cl(1)	92.3(1)	C(5)–C(6)–C(7)	113.8(1)
C(4)–C(5)–C(6)	119.8(1)	C(7)–C(6)–P(1)	114.0(1)
C(5)–C(6)–P(1)	109.3(9)	C(1)–N(1)–C(5)	118.5(1)
C(8)–C(7)–C(6)	114.3(1)	C(6)–P(1)–Pd(1)	104.7(5)
C(5)–N(1)–Pd(1)	121.5(1)		

4.2.1.2 Liberation and the Optical Purity of (*R*)-147

Scheme 4.13

The liberation of the free P–N ligand (*R*)-147 was achieved by the treatment of the dichloro complex with aqueous potassium cyanide (Scheme 4.13). Thus, the (2-pyridyl)phosphine was obtained as a white solid in 81% yield,  $[\alpha]_{\text{D}} +58^{\circ}$  ( $c$  2.0,  $\text{CH}_2\text{Cl}_2$ ). The  $^{31}\text{P}$  NMR spectrum of (*R*)-147 in  $\text{CDCl}_3$  exhibited a sharp singlet at  $\delta$  0.5. Because of the potential air sensitivity of the noncoordinated phosphorus atoms, the liberated (*R*)-147 was not stored in its pure form but was re-coordinated again to (*R*)-144. The recoordination process is also a means of verifying the optical purity of the released ligand to establish the identity of the minor isomers that were generated in the original hydrophosphination reaction.<sup>199,134</sup> The recoordination procedure was

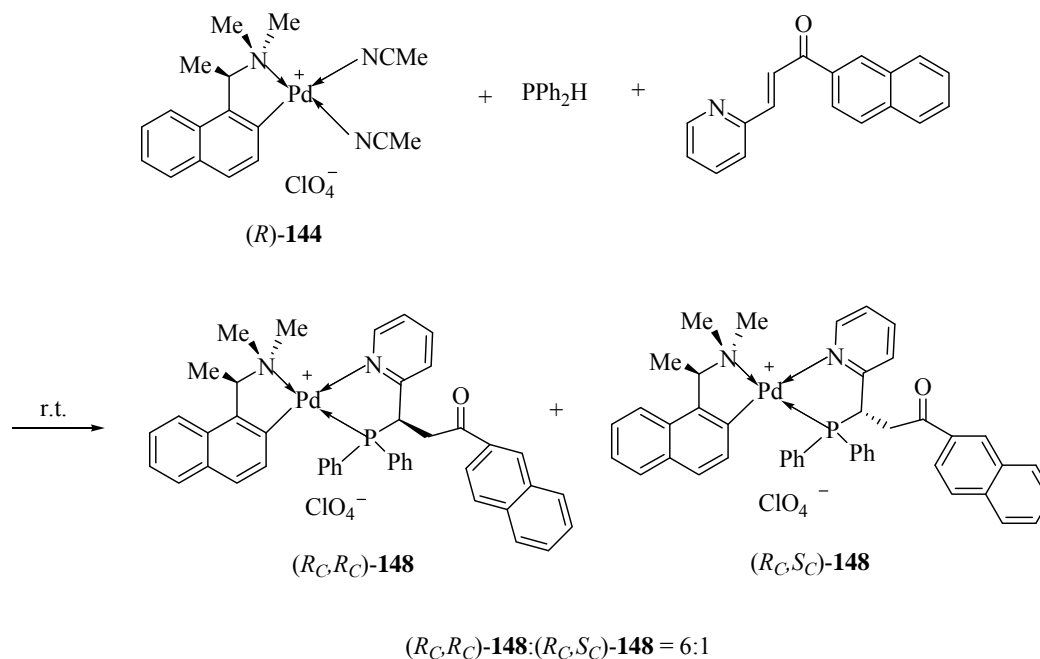
monitored by  $^{31}\text{P}\{^1\text{H}\}$  NMR spectroscopy. In  $\text{CDCl}_3$ , the  $^{31}\text{P}\{^1\text{H}\}$  NMR spectrum of the crude recoordination product showed only one singlet at  $\delta$  54.0, thus confirming that the liberated (*R*)-**147** is optically pure.

In order to establish the identity of the minor product that was formed from hydrophosphination reaction, (*R*)-**147** was reordinated regiospecifically to (*S<sub>C</sub>*)-**144** to generate the diastereomeric complex (*S<sub>C</sub>*, *R<sub>C</sub>*)-**145**. The  $^{31}\text{P}\{^1\text{H}\}$  NMR spectrum of the crude product in  $\text{CDCl}_3$  showed one singlet at  $\delta$  60.2. The phosphorus resonances for complex (*S<sub>C</sub>*, *R<sub>C</sub>*)-**145**, which is the enantiomer of (*R<sub>C</sub>*, *S<sub>C</sub>*)-**145**, was identical with those observed from the minor product generated from the hydrophosphination reaction. Hence, it could be confirmed that complex (*R<sub>C</sub>*, *S<sub>C</sub>*)-**145** was the minor product of the original hydrophosphination reaction. No  $^{31}\text{P}\{^1\text{H}\}$  NMR signals could be detected for the major diastereomer, thus reaffirming that liberated (*R*)-**147** was enantiomerically pure.

#### 4.2.2 Hydrophosphination of (*E*)-1-naphthyl-3-pyridin-2-yl-2-propenone

Complex (*R*)-**144** in dichloromethane (40mL) was treated with (*E*)-1-naphthyl-3-pyridin-2-yl-2-propenone and  $\text{Ph}_2\text{PH}$  at room temperature for 6 days (Scheme 4.14). The  $^{31}\text{P}\{^1\text{H}\}$  NMR spectrum of the reaction mixture in  $\text{CDCl}_3$  exhibited two sharp singlets at  $\delta$  60.4 and 54.2 in the ratio of 1:6; thus indicating that two diastereomeric complexes have been formed. After purification by column chromatography, the major diastereomer (*R<sub>C</sub>*, *R<sub>C</sub>*)-**148** was subsequently crystallized

as yellow prisms from dichloromethane-diethyl ether in 51.4% isolated yield,  $[\alpha]_{\text{D}}^{-175^{\circ}}$  ( $c$  0.6,  $\text{CH}_2\text{Cl}_2$ ).



**Scheme 4.14**

#### 4.2.2.1 Single Crystal X-ray Structural Analysis of (R<sub>C</sub>, R<sub>C</sub>)-148

The molecular structure and the absolute stereochemistry of (R<sub>C</sub>, R<sub>C</sub>)-148 were determined by X-ray structure analysis (Figure 4.2). The structure analysis established that the newly formed stereogenic center at C(20) adopted the *R* absolute configuration. The geometry at the Pd center is distorted square planar with angles of 80.6(3)–98.8(2)° and 170.8(2)–177.0(3)°. The C(20)–P(1), C(19)–C(20), C(20)–C(21), and C(21)–C(22) distance [1.853(8), 1.519(10), 1.510(12), and 1.529(11) Å] are elongated noticeably by the intrachelate interactions. Selected bond parameters are given in Table 4.2.

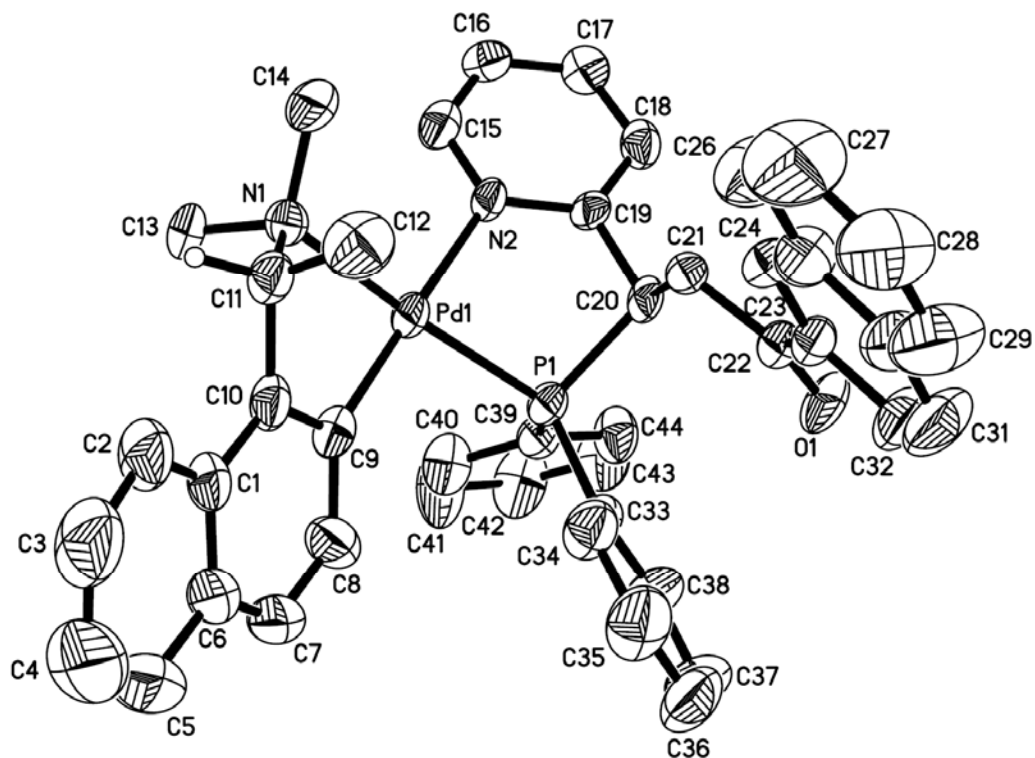


Figure 4.2 Molecular structure and absolute configuration of ( $R_C$ ,  $R_C$ )-148

Table 4.2 Selected bond lengths (Å) and (deg) angles for ( $R_C$ ,  $R_C$ )-148

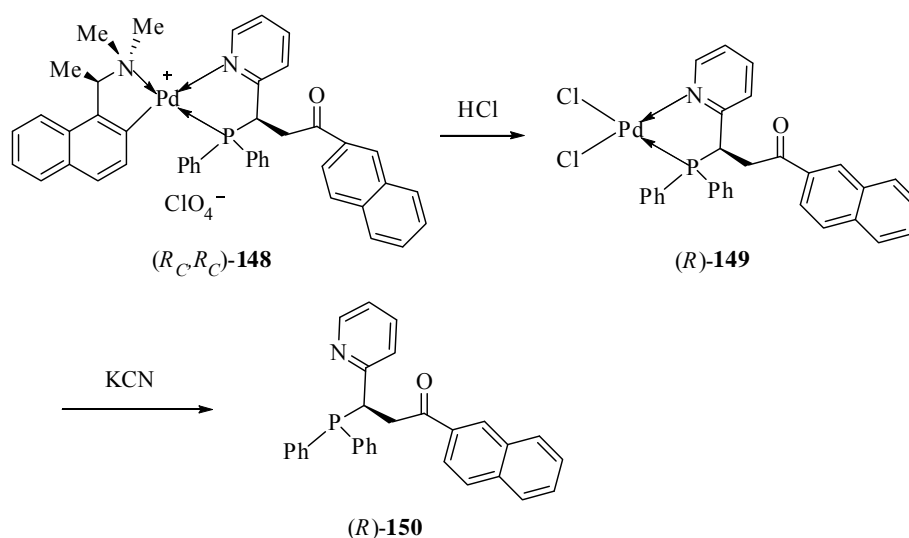
Pd(1)–C(9)	1.970(9)	N(2)–Pd(1)–N(1)	101.4(2)
Pd(1)–N(2)	2.149(6)	C(9)–Pd(1)–P(1)	98.8(2)
Pd(1)–N(1)	2.156(6)	N(2)–Pd(1)–P(1)	79.6(2)
Pd(1)–P(1)	2.234(2)	N(1)–Pd(1)–P(1)	170.8(2)
C(15)–N(2)	1.335(9)	N(2)–C(19)–C(20)	116.3(7)
C(19)–N(2)	1.357(9)	C(21)–C(20)–C(19)	111.6(6)
C(19)–C(20)	1.519(10)	C(21)–C(20)–P(1)	112.4(6)
C(20)–C(21)	1.510(12)	C(19)–C(20)–P(1)	104.7(5)
C(20)–P(1)	1.853(8)	C(20)–C(21)–C(22)	116.6(6)
C(21)–C(22)	1.529(11)	O(1)–C(22)–C(23)	120.6(7)
C(22)–O(1)	1.218(9)	O(1)–C(22)–C(21)	119.7(8)
C(22)–C(23)	1.479(12)	C(23)–C(22)–C(21)	119.7(7)
C(9)–Pd(1)–N(2)	177.0(3)	C(19)–N(2)–Pd(1)	118.5(5)
C(9)–Pd(1)–N(1)	80.6(3)	C(20)–P(1)–Pd(1)	98.3(2)

#### 4.2.2.2 Liberation and the Optical Purity of (*R*)-150

Upon subsequent treatment of the perchlorate salt with concentrated hydrochloric acid, the resultant dichloro complex (*R*)-149 was obtained as yellow prisms in 91.5% isolated yield,  $[\alpha]_D -111^\circ$  ( $c$  0.7,  $\text{CH}_2\text{Cl}_2$ ) (Scheme 4.15). The  $^{31}\text{P}\{^1\text{H}\}$  NMR spectrum of (*R*)-149 in  $\text{CD}_2\text{Cl}_2$  exhibited a sharp singlet at  $\delta$  51.8.

The optically active ligand (*R*)-150 can be stereospecifically liberated from the complex (*R*)-149 by treatment of the dichloro complex with aqueous potassium cyanide at room temperature. The liberated (*R*)-150 was obtained as an air sensitive white solid in 89% yield,  $[\alpha]_D +80^\circ$  ( $c$  0.7,  $\text{CH}_2\text{Cl}_2$ ). The  $^{31}\text{P}\{^1\text{H}\}$  NMR spectrum of the free ligand in  $\text{CDCl}_3$  exhibited one singlet at  $\delta$  -0.2.

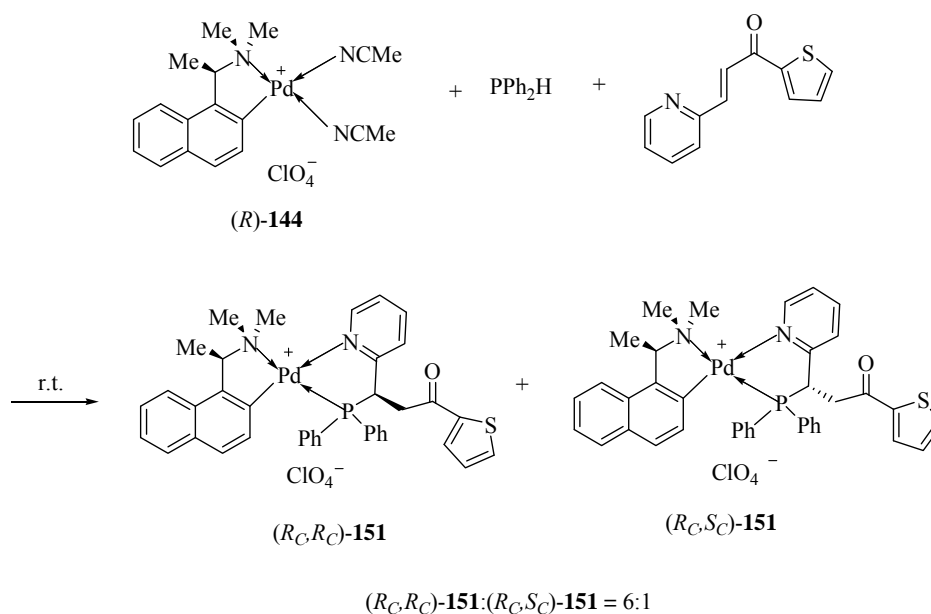
The enantiomeric ligand was confirmed to be optically pure by the methods described in Chapter 4.2.1.2.



Scheme 4.15

### 4.2.3 Hydrophosphination of (*E*)-1-thiophenyl-3-pyridin-2-yl-2-propenone

(*R*)-**144** in dichloromethane (40mL) was treated with (*E*)-1-thiophenyl-3-pyridin-2-yl-2-propenone and Ph<sub>2</sub>PH at room temperature for 6 days (Scheme 4.16). The <sup>31</sup>P{<sup>1</sup>H} NMR spectrum of the reaction mixture in CDCl<sub>3</sub> exhibited two sharp singlets at δ 60.2 and 53.8 in the ratio of 1:6; thus indicating that only two diastereomeric complexes have been formed. The diastereomeric products were subsequently separated by silica gel column chromatography. The major diastereomer (*R<sub>C</sub>, R<sub>C</sub>*)-**151** was obtained as pale yellow prisms in 64.3 % isolated yield. The <sup>31</sup>P{<sup>1</sup>H} NMR spectrum of (*R<sub>C</sub>, R<sub>C</sub>*)-**151** in CDCl<sub>3</sub> exhibited a singlet at δ 53.8.



Scheme 4.16

#### 4.2.3.1 Single Crystal X-ray Structural Analysis of (*R<sub>C</sub>, R<sub>C</sub>*)-**151**

The molecular structure and the absolute stereochemistry of (*R<sub>C</sub>, R<sub>C</sub>*)-**151** were

determined by X-ray structure analysis (Figure 4.3). The structure analysis established that the newly formed stereogenic center at C(20) adopted the *R* absolute configuration. The geometry at the Pd center is distorted square planar with angles of  $80.7(2)$ – $99.1(1)^\circ$  and  $171.28(1)$ – $177.7(2)^\circ$ . The C(20)–P(1), C(19)–C(20), C(20)–C(21), and C(21)–C(22) distance [ $1.859(4)$ ,  $1.507(6)$ ,  $1.533(6)$ , and  $1.517(6)$  Å] are elongated noticeably by the intrachelate interactions. One of two phenyl rings in the phosphorus atom is disordered in the molecule. Selected bond parameters are given in Table 4.3.

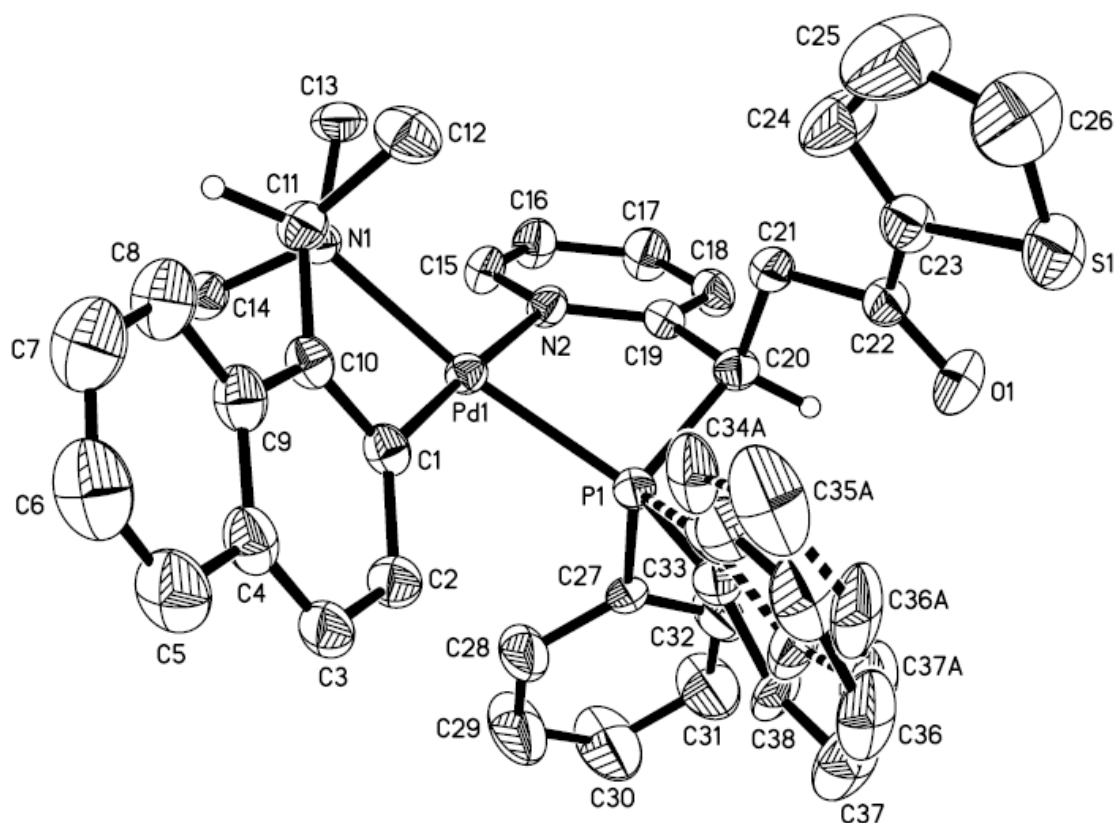


**Figure 4.3** Molecular structure and absolute configuration of (*R<sub>C</sub>*, *R<sub>C</sub>*)-151

**Table 4.3 Selected bond lengths (Å) and (deg) angles for (*R<sub>C</sub>*, *R<sub>C</sub>*)-151**

Pd(1)-C(1)	2.001(4)	C(33A)-P(1)	1.839(9)
Pd(1)-N(1)	2.141(4)	C(34A)-C(35A)	1.380(12)
Pd(1)-N(2)	2.144(4)	C(35A)-C(36A)	1.360(13)
Pd(1)-P(1)	2.230(1)	C(36A)-C(37A)	1.381(13)
C(13)-N(1)	1.481(5)	C(37A)-C(38A)	1.385(13)
C(15)-N(2)	1.354(6)	C(1)-Pd(1)-N(1)	80.69(16)
C(19)-C(20)	1.507(6)	C(1)-Pd(1)-N(2)	177.7(2)
C(20)-C(21)	1.533(6)	N(1)-Pd(1)-N(2)	101.60(13)
C(20)-P(1)	1.859(4)	C(1)-Pd(1)-P(1)	99.02(14)
C(21)-C(22)	1.517(6)	N(1)-Pd(1)-P(1)	171.21(10)
C(22)-O(1)	1.193(6)	N(2)-Pd(1)-P(1)	78.80(10)
C(22)-C(23)	1.472(7)	O(1)-C(22)-C(23)	121.0(4)
C(23)-C(24)	1.314(8)	C(23)-C(22)-C(21)	116.0(4)
C(23)-S(1)	1.727(5)	C(34)-C(33)-P(1)	116.2(7)
C(24)-C(25)	1.410(9)	C(33)-C(34)-C(35)	118.9(9)
C(26)-S(1)	1.683(8)	C(36)-C(35)-C(34)	120.1(9)
C(33)-C(34)	1.371(11)	C(35)-C(36)-C(37)	119.7(9)
C(33)-C(38)	1.380(11)	C(38)-C(37)-C(36)	121.1(9)
C(33)-P(1)	1.821(7)	C(37)-C(38)-C(33)	117.9(9)
C(34)-C(35)	1.388(11)	C(36A)-C(35A)-C(34A)	117.3(13)
C(35)-C(36)	1.361(12)	C(35A)-C(36A)-C(37A)	123.2(12)
C(36)-C(37)	1.392(12)	C(20)-P(1)-Pd(1)	97.92(14)
C(37)-C(38)	1.367(10)	C(37A)-C(38A)-C(33A)	121.4(13)
C(33A)-C(34A)	1.400(13)	C(26)-S(1)-C(23)	91.1(3)
C(33A)-C(38A)	1.401(12)	C(34A)-C(33A)-P(1)	122.3(9)

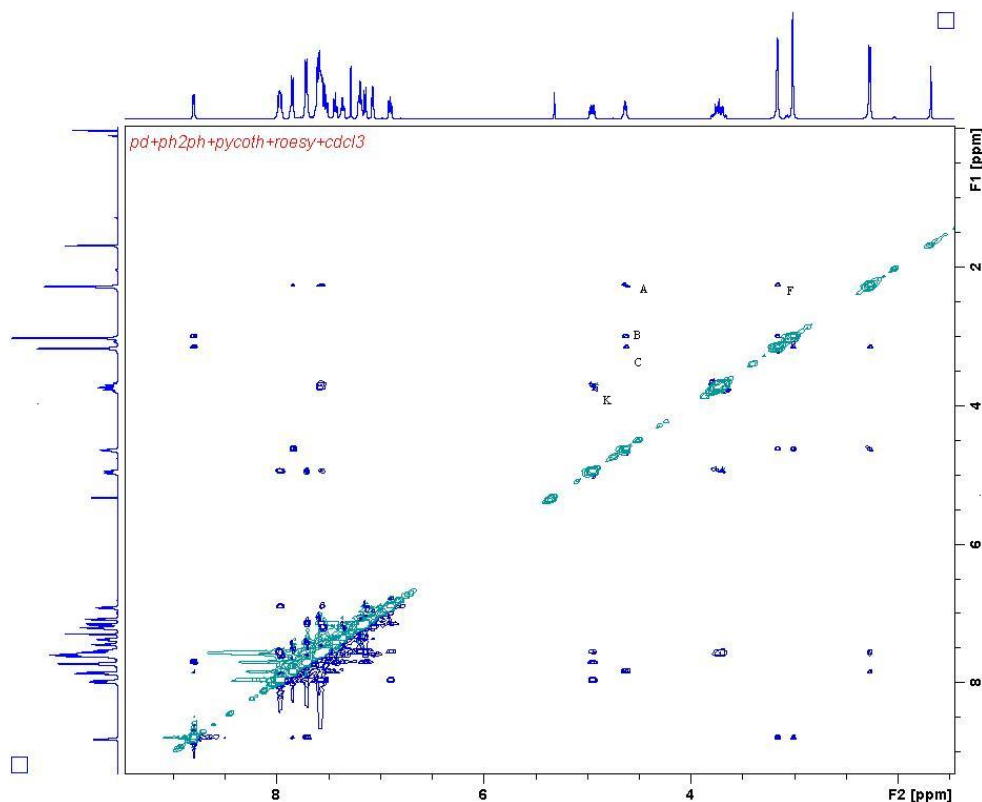
#### 4.2.3.2 Two Dimensional <sup>1</sup>H-<sup>1</sup>H ROESY NMR of (*R<sub>C</sub>*, *R<sub>C</sub>*)-151

In order to confirm the structure of *R<sub>C</sub>*, *R<sub>C</sub>*-151 in solution state, a 500 MHz solution 2D <sup>1</sup>H-<sup>1</sup>H ROESY NMR study was carried out in CDCl<sub>3</sub>.

Similar to the 2D <sup>1</sup>H-<sup>1</sup>H ROESY NMR analysis of the other analogous organometallic complexes<sup>133</sup> comprising the 5-membered *ortho*-metalated dimethyl[(*S/R*)-1-(1-naphthyl)ethyl]amine auxiliary, the 5-membered organo-palladium(II) complex moiety of (*R<sub>C</sub>*, *R<sub>C</sub>*)-151 is locked in a stable

conformation defined by a set of characteristic NOE patterns: NOE signals (A-C) are observed due to the interactions of H(11) with Me(12)-Me(14), the very strong interaction between this proton and H(8) of the aromatic ring (D) indicates the close proximity of these protons with each other while the weaker signal (E) shows that the methyl group on the stereogenic carbon Me(12) exclusively adopts the axial position locking the 5-membered organometallic ring in a stable  $\delta$  conformation (Figure 3.3). There is no signal showing any interaction between this methyl group and the axially oriented Me(14) on nitrogen, only its interaction with the equatorial methyl group Me(13) of nitrogen was observed (F). The strong signal corresponding to G represents the interaction of the pyridine ring H15 with *ortho* protons of the axial Ph group on phosphine. The signal (H) shows H16 also interacts with the *o*-H, which establishes that H16 and the Ph group are located on the same side below the square plane. On the other hand, the signal (I) shows a strong interaction between H17 and H18 with the equatorial Ph group on phosphine which means that they are located on the other side of the square plane. Therefore, C(16) has an *R* absolute configuration.

**Figure 4.17. 2D-ROESY NMR of  $R_C, R_C$ -151. Selected NOE Interactions: A:  $H_{11}$ - $M_{12}$ , B:  $H_{11}$ - $M_{14}$ , C:  $H_{11}$ - $M_{13}$ , D:  $H_{11}$ - $H_8$ , E:  $M_{12}$ - $H_8$ , F:  $M_{12}$ - $M_{13}$ , G:  $H_{15}$ - $o$ -PhP(ax), H:  $H_{16}$ - $o$ -PhP(ax), I:  $H_{17}, H_{18}$ - $o$ -PhP(eq), J:  $H_{16}$ - $H_{19}$ , K:  $H_{16}$ - $H_{17}, H_{18}$ .**

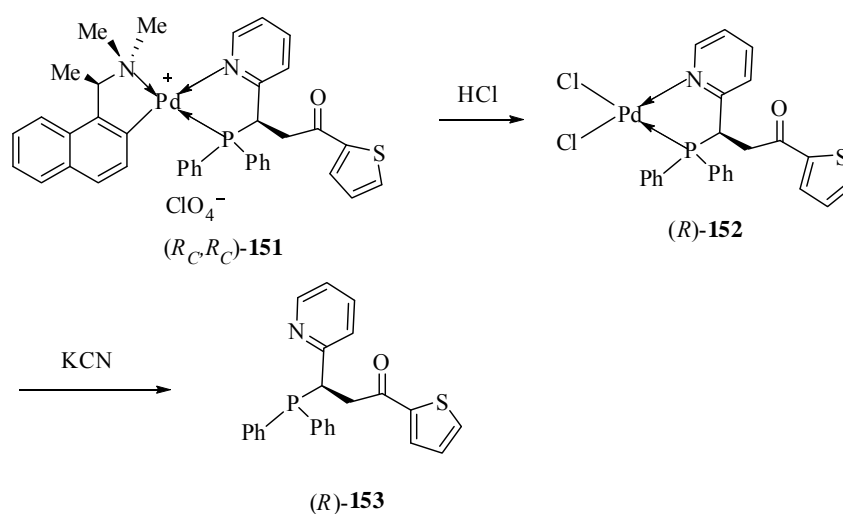


#### 4.2.3.3 Liberation and the Optical Purity of (*R*)-153

Upon subsequent treatment of the perchlorate salt with concentrated hydrochloric acid, the resultant dichloro complex (*R*)-152 was obtained as yellow prisms in 90% isolated yield,  $[\alpha]_D -345^\circ$  ( $c$  0.6,  $CH_2Cl_2$ ). The  $^{31}P\{^1H\}$  NMR spectrum of (*R*)-152 in  $CDCl_3$  exhibited a sharp singlet at  $\delta$  51.2. The optically active ligand (*R*)-153 can be stereospecifically liberated from the complex (*R*)-152 by treatment of the dichloro complex with aqueous potassium cyanide at room temperature (Scheme

4.17). The liberated (*R*)-**153** was obtained as an air sensitive white solid in 85% yield,  $[\alpha]_D^{25} +217^\circ$  (*c* 0.7,  $\text{CH}_2\text{Cl}_2$ ). The  $^{31}\text{P}\{^1\text{H}\}$  NMR spectrum of the free ligand in  $\text{CDCl}_3$  exhibited one singlet at  $\delta$  -0.3.

The enantiomeric ligand was confirmed to be optically pure by the methods described in Chapter 4.2.1.2.

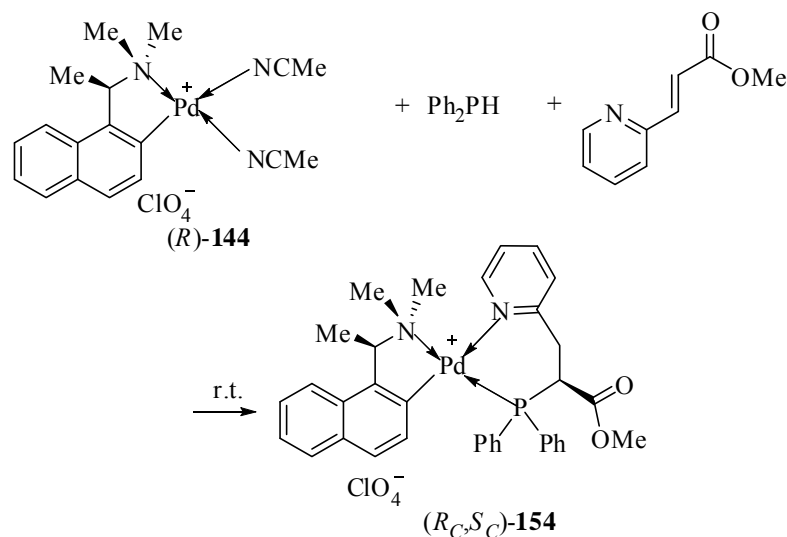


**Scheme 4.17**

#### 4.2.4 Hydrophosphination of (*E*)-1-methyl-3-pyridin-2-yl-2-propenoate

In principle, the hydrophosphination reaction between (*E*)-1-methyl-3-pyridin-2-yl-2-propenoate and  $\text{Ph}_2\text{PH}$  may generate similar five-membered P–N chelate products as that obtained from the reaction involving (*E*)-1-phenyl-3-pyridin-2-yl-2-propenone. Interestingly after 7 days at room temperature the crude product mixture only exhibited a new sharp singlet at  $\delta$  46.4 in the  $^{31}\text{P}\{^1\text{H}\}$  NMR spectrum, indicating the formation of only one diastereomer (Scheme 4.18). After purification by column chromatography, the product ( $R_C$ ,

*S<sub>C</sub>*-**154** was subsequently crystallized as pale yellow prisms from chloroform,  $[\alpha]_{\text{D}} -91^{\circ}$  (*c* 1.5, CH<sub>2</sub>Cl<sub>2</sub>).



#### 4.2.4.1 Single Crystal X-ray Structural Analysis of (*R<sub>C</sub>*, *S<sub>C</sub>*)-**154**

The X-ray crystallographic analysis of the complex reaffirms that an enantiomerically pure product has been formed in which the six-membered P-N chelate coordinated to palladium as a bidentate chelate with a twist-boat conformation (Figure 4.4). Furthermore, the structure analysis unambiguously established that the newly formed stereogenic center at C(21) adopts the *S* configuration. The P and N donor atoms of the new heterobidentate are bonded regiospecifically to the Pd atom, with the softer P donor taking up the position *trans* to the NMe<sub>2</sub> group. Selected bond lengths and angles are listed in Table 4.4. The angles formed by the P-N chelate and the naphthylamine template at the Pd metal center were in the range of 80.5(7)-

95.6(7)° and 172.1(5)-173.3(9)°. The C(21)-P(1) and C(20)-C(21) distance [1.883(2) and 1.539(3) Å] are elongated noticeably by the intrachelate interactions.

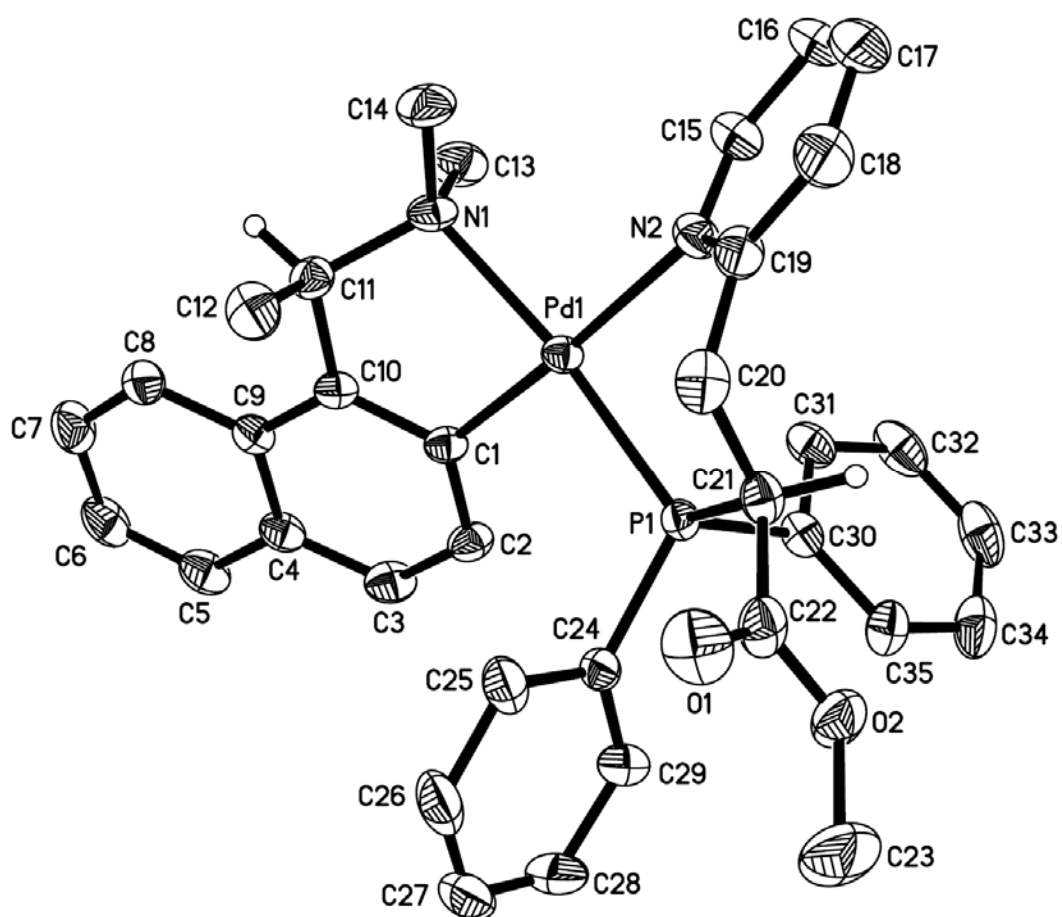
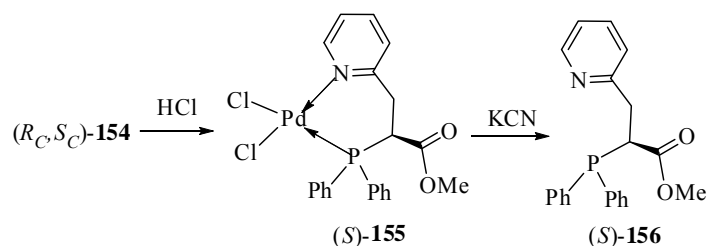


Figure 4.4 Molecular structure and absolute configuration of (R<sub>C</sub>, S<sub>C</sub>)-154

**Table 4.4 Selected bond lengths (Å) and (deg) angles for (*R<sub>C</sub>, S<sub>C</sub>*)-154**

Pd(1)–C(1)	2.006(2)	Pd(1)–N(1)	2.136(2)
Pd(1)–N(2)	2.136(2)	Pd(1)–P(1)	2.239(5)
C(15)–N(2)	1.339(3)	C(19)–N(2)	1.349(3)
C(19)–C(20)	1.492(3)	C(20)–C(21)	1.539(3)
C(21)–P(1)	1.883(2)	C(22)–O(1)	1.203(3)
C(22)–O(2)	1.334(3)	C(30)–P(1)	1.810(2)
C(1)–Pd(1)–N(1)	80.5(7)	C(1)–Pd(1)–N(2)	173.3(9)
N(1)–Pd(1)–N(2)	95.6(7)	C(1)–Pd(1)–P(1)	95.6(6)
N(1)–Pd(1)–P(1)	172.1(5)	N(2)–Pd(1)–P(1)	88.9(5)
N(2)–C(19)–C(20)	117.6(2)	C(19)–C(20)–C(21)	111.5(2)
C(22)–C(21)–C(20)	110.3(2)	C(22)–C(21)–P(1)	111.9(1)
C(20)–C(21)–P(1)	112.4(1)	C(15)–N(2)–C(19)	118.9(2)
C(19)–N(2)–Pd(1)	122.9(2)	C(21)–P(1)–Pd(1)	107.6(6)

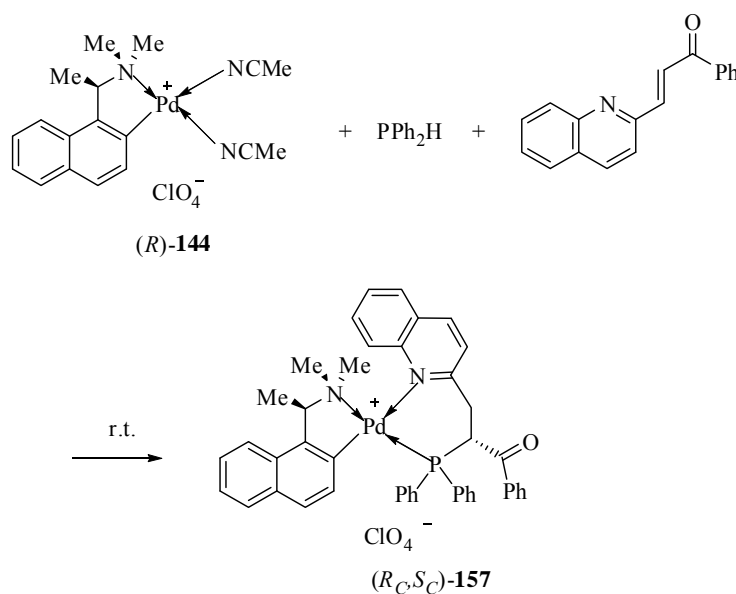
**4.2.4.2 Liberation and the Optical Purity of (*S<sub>C</sub>*)-156****Scheme 4.19**

The treatment of complex (*R<sub>C</sub>, S<sub>C</sub>*)-154 with concentrated hydrochloric acid generated (*S<sub>C</sub>*)-155 (Scheme 4.19). The dichloro complex was subsequently crystallized from dichloromethane-diethyl ether as yellow prisms in 86% yield,  $[\alpha]_D^{25} -85^\circ$  (*c* 0.4, CH<sub>2</sub>Cl<sub>2</sub>). The <sup>31</sup>P{<sup>1</sup>H} NMR spectrum of this neutral dichloro complex in CD<sub>2</sub>Cl<sub>2</sub> exhibited one singlet at  $\delta$  37.0. Further treatment of (*S<sub>C</sub>*)-155 with aqueous cyanide liberated the optically pure (*S<sub>C</sub>*)-156 as a white solid in quantitative yield,

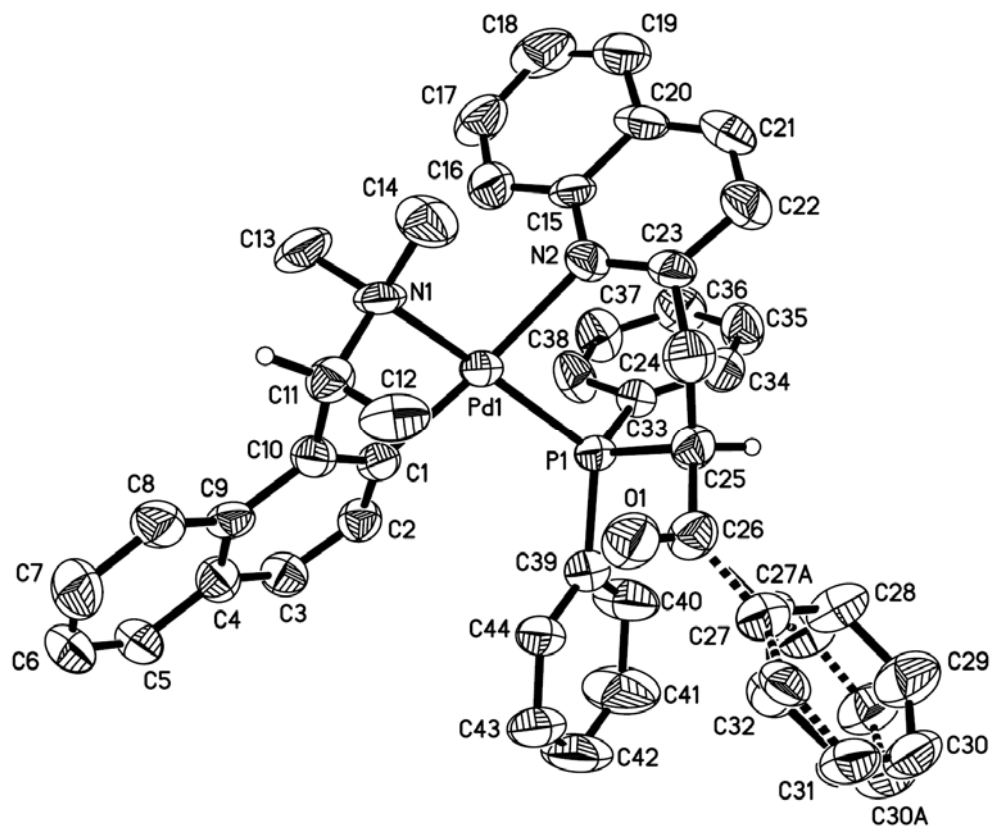
$[\alpha]_D -27^\circ$  ( $c$  0.4,  $\text{CH}_2\text{Cl}_2$ ). The  $^{31}\text{P}\{^1\text{H}\}$  NMR spectrum of (*S<sub>C</sub>*)-**156** in  $\text{CDCl}_3$  exhibited one singlet at  $\delta$  0.5. The recoordination of the free ligand to (*R*)- and (*S*)-**144** confirmed that (*S<sub>C</sub>*)-**156** is optically pure.

#### 4.2.5 Hydrophosphination of (*E*)-1-phenyl-3-quinolin-2-yl-2-propenone

(*R*)-**144** in dichloromethane (40mL) was treated with (*E*)-1-phenyl-3-quinolin-2-yl-2-propenone and  $\text{PPh}_2\text{H}$  at room temperature for 4 days (Scheme 4.20). The  $^{31}\text{P}$  NMR spectrum of the reaction mixture in  $\text{CDCl}_3$  exhibited one sharp singlet at  $\delta$  42.3; thus indicating that only one diastereomeric complex has been formed. After purification by column chromatography, (*R<sub>C</sub>*, *S<sub>C</sub>*)-**157** was subsequently crystallized as yellow prisms from dichloromethane-diethyl ether in 70% isolated yield,  $[\alpha]_D -30^\circ$  ( $c$  1.5,  $\text{CH}_2\text{Cl}_2$ ).



**Scheme 4.20**

4.2.5.1 Single Crystal X-ray Structural Analysis of ( $R_C, S_C$ )-157

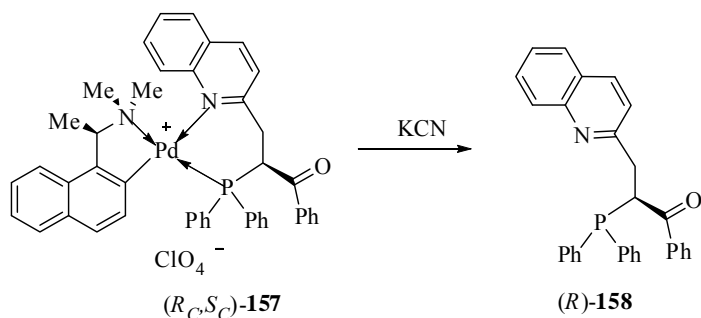
**Figure 4.5** Molecular structure and absolute configuration of ( $R_C, S_C$ )-157

The X-ray crystallographic analysis of the complex reaffirms that an enantiomerically pure product has been formed in which the six-membered P-N chelate coordinated to palladium as a bidentate chelate (Figure 4.5) with a twist-boat conformation with the C(Ph) group at C(25) occupying the sterically favorable equatorial position. The newly formed stereogenic center at C(21) adopts the  $S$  configuration. The P and N donor atoms of the new heterobidentate are bonded regioselectively to the Pd atom, with the softer P donor taking up the position *trans*

to the NMe<sub>2</sub> group. Selected bond lengths and angles are listed in Table 4.5. In this molecule, the quinoline proton H(16) is far away from the two NMe groups to achieve the least steric repulsion state. The phenyl groups on P(1) and the naphthylene proton H(2) adopt a staggered orientation to relieve the interchelate steric interactions. The angles formed by the P–N chelate and the naphthylamine template at the Pd metal center were in the range of 79.7(2)–99.9(2)° and 165.1(2)–175.2(2)°. The C(25)–P(1), C(24)–C(25) and C(25)–C(26) distance [1.864(6), 1.532(8) and 1.525(8) Å] are elongated noticeably by the interchelate interactions. There is orientational disorder in the arrangement of phenyl ring at the C(26).

#### 4.2.5.2 Liberation and the Optical Purity of (*S<sub>C</sub>*)-158

The liberation of free P–N ligand (*S<sub>C</sub>*)-158 was achieved by the treatment of the palladium template (*S<sub>C</sub>*,*R<sub>C</sub>*)-157 with aqueous potassium cyanide (Scheme 4.21). Thus, the quinolinylphosphine was obtained as a white solid in 75%, [ $\alpha$ ]<sub>D</sub>–150° (*c* 0.4, CH<sub>2</sub>Cl<sub>2</sub>). The <sup>31</sup>P{<sup>1</sup>H} NMR spectrum of (*S<sub>C</sub>*)-158 in CDCl<sub>3</sub> exhibited a sharp singlet at  $\delta$  0.5. The recoordination of the free ligand to (*R*)- and (*S*)-144 confirmed that (*S<sub>C</sub>*)-158 is optically pure.



Scheme 4.21

**Table 4.5 Selected bond lengths (Å) and (deg) angles for (*R<sub>C</sub>*, *S<sub>C</sub>*)-157**

C(27)–C(28)	1.386(13)	C(31)–C(32)–C(27)	120.4(11)
C(27)–C(32)	1.407(11)	C(28A)–C(27A)–C(32A)	117.9(14)
C(27)–C(26)	1.486(10)	C(28A)–C(27A)–C(26)	122.1(13)
C(28)–C(29)	1.397(12)	C(32A)–C(27A)–C(26)	120.0(13)
C(29)–C(30)	1.343(13)	C(27A)–C(28A)–C(29A)	121.8(16)
C(30)–C(31)	1.364(13)	C(30A)–C(29A)–C(28A)	118.3(17)
C(31)–C(32)	1.365(10)	C(29A)–C(30A)–C(31A)	121.1(18)
C(27A)–C(28A)	1.382(17)	C(30A)–C(31A)–C(32A)	121.6(19)
C(27A)–C(32A)	1.402(16)	C(31A)–C(32A)–C(27A)	119.0(17)
C(27A)–C(26)	1.485(14)	C(1)–Pd(1)–N(1)	79.7 (2)
C(28A)–C(29A)	1.391(16)	C(1)–Pd(1)–N(2)	175.2 (2)
C(29A)–C(30A)	1.345(17)	N(1)–Pd(1)–N(2)	99.9 (2)
C(30A)–C(31A)	1.36(2)	C(1)–Pd(1)–P(1)	100.0(2)
C(31A)–C(32A)	1.363(15)	N(1)–Pd(1)–P(1)	165.1(2)
Pd(1)–C(1)	1.987(5)	N(2)–Pd(1)–P(1)	81.6 (1)
Pd(1)–N(1)	2.129(5)	N(2)–C(23)–C(24)	116.8(5)
Pd(1)–N(2)	2.173(4)	C(22)–C(23)–C(24)	120.6(6)
Pd(1)–P(1)	2.246(2)	C(23)–C(24)–C(25)	114.3(5)
C(23)–N(2)	1.328(7)	C(26)–C(25)–C(24)	108.4(5)
C(23)–C(24)	1.492(8)	C(26)–C(25)–P(1)	110.3(4)
C(24)–C(25)	1.532(8)	C(24)–C(25)–P(1)	112.3(4)
C(25)–C(26)	1.525(8)	O(1)–C(26)–C(27A)	117.7(10)
C(25)–P(1)	1.864(6)	O(1)–C(26)–C(27)	120.6(7)
C(26)–O(1)	1.227(7)	C(27A)–C(26)–C(27)	4(2)
C(28)–C(27)–C(32)	117.9(9)	O(1)–C(26)–C(25)	118.6(5)
C(28)–C(27)–C(26)	124.1(9)	C(27A)–C(26)–C(25)	123.7(10)
C(32)–C(27)–C(26)	117.8(9)	C(27)–C(26)–C(25)	120.7(7)
C(27)–C(28)–C(29)	120.4(9)	C(23)–N(2)–C(15)	119.5(5)
C(30)–C(29)–C(28)	119.5(11)	C(23)–N(2)–Pd(1)	120.2(4)
C(29)–C(30)–C(31)	121.7(10)	C(15)–N(2)–Pd(1)	119.9(4)
C(30)–C(31)–C(32)	120.1(12)	C(25)–P(1)–Pd(1)	102.8(2)

#### 4.2.6 Mechanistic Considerations

From a mechanistic standpoint,<sup>200</sup> the simultaneous coordination of diphenylphosphine and pyridine on the chiral palladium template polarized the P-H and vinylic C=C bonds concurrently. An intermediate involving the deprotonated

form of the highly reactive coordinated phosphido ligand could thus be generated. This nucleophilic phosphido moiety subsequently undergoes addition to the activated alkene. A correlation between the X-ray crystallography data of the hydrophosphination product and a Dreiding model study confirmed that the formation of the P-Pd-N six-membered ring would markedly relieve the interchelate repulsive interactions than a five-membered ring. Therefore, the formation of the six-membered ring between (*E*)-1-methyl-3-pyridin-2-yl-2-propenoate and Ph<sub>2</sub>PH must be due to the predominant steric factors. The X-ray crystallographic analysis of (*R<sub>C</sub>*, *S<sub>C</sub>*)-**154** revealed that the COOMe group at C(21) occupies the sterically favorable equatorial position in the twist boat conformation (Figure 4.6).<sup>198</sup> The H<sub>6</sub> of the pyridine ring is far away from the two NMe groups and there should not be any significant steric repulsions. In addition, less steric repulsion exists between the naphthylene proton H<sub>γ</sub> and the quasi-axial phenyl group on P.<sup>129,201</sup> However, model studies show that in (*R<sub>C</sub>*, *R<sub>C</sub>*), the COOMe group occupies the sterically unfavorable axial position. Although the H<sub>6</sub> of the pyridine ring is far away from to the two NMe groups, there is still significant steric repulsion between the naphthylene proton H<sub>γ</sub> and the quasi-quasi phenyl group on P. We believe that these interchelate repulsive forces are the discriminating factors that hinder the formation of the unfavored diastereomer.

The formation of the five-membered ring between (*E*)-1-phenyl-3-pyridin-2-yl-2-propenone and Ph<sub>2</sub>PH is because there are more severe interchelate steric constrains within phenyl groups of Ph<sub>2</sub>P and CPh in the six-membered ring. The model studies clearly indicate that in the major isomer (*R<sub>C</sub>*,

*R<sub>C</sub>*-**145**, the CPh group at C(6) of the five-membered P-Pd-N chelate occupies the sterically favorable equatorial position (Figure 4.7). In this molecule, however, the H<sub>6</sub> of the pyridine ring is unfavorably oriented towards the NMe group which is in the equatorial position. In the minor isomer (*R<sub>C</sub>, S<sub>C</sub>*)-**145**, the CPh group occupies the sterically unfavorable axial position. In addition, the H<sub>6</sub> of the pyridine ring intrudes into the space between the two methyl groups on N to achieve the least steric repulsion state.

As to the hydrophosphination reactions between quinoline complexes and diphenylphosphine, the quinoline ring is a more bulky group than the pyridine ring, so P-Pd-N six-membered ring is the best choice to relieve the interchelate repulsive interactions. The X-ray crystallographic analysis of (*R<sub>C</sub>, S<sub>C</sub>*)-**157** revealed that the CPh group at C(25) occupies the sterically favorable equatorial position in the twist boat conformation.

In conclusion, the efficient synthesis of keto- and ester- functionalized C-chiral (2-pyridyl)phosphines and (2-quinoliny)phosphines via chiral organopalladium template promoted asymmetric hydrophosphination has been demonstrated. The hydrophosphination reactions proceed with high regio- and stereoselectivities under mild conditions.

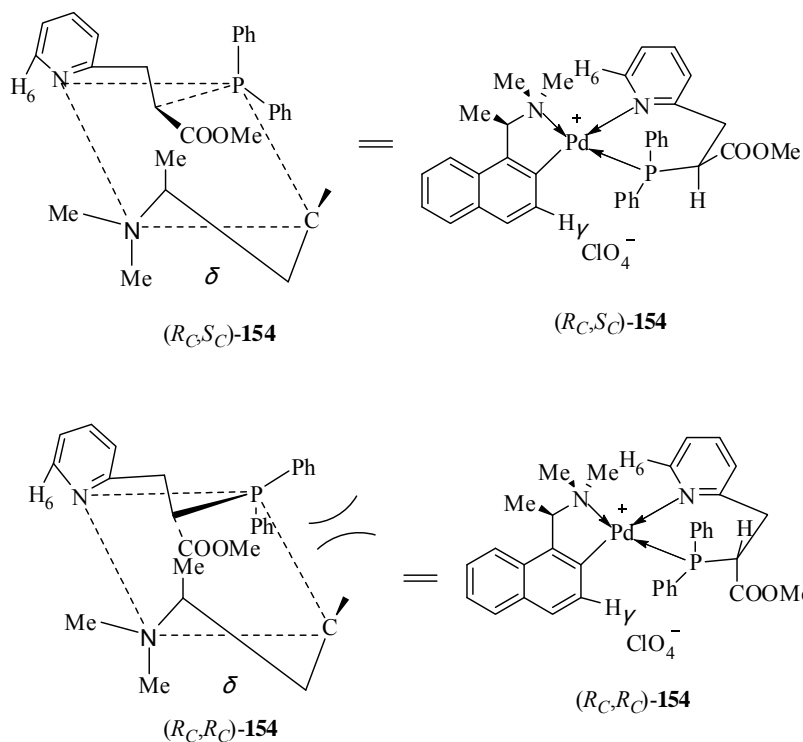


Figure 4.6. Interchelate interactions in  $(R_C, S_C)$ -154 and  $(R_C, R_C)$ -154

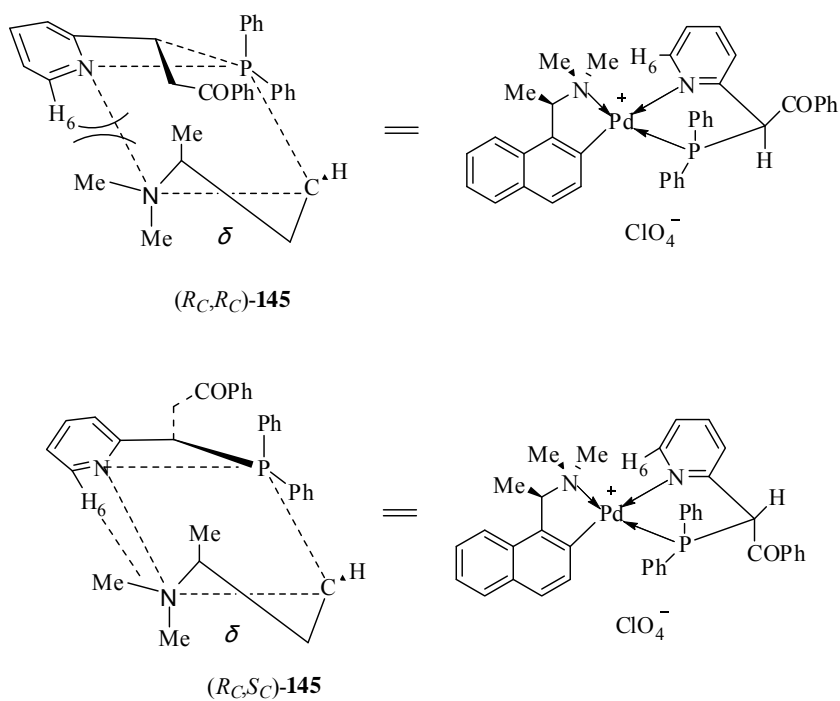


Figure 4.7 Interchelate interactions in  $(R_C, R_C)$ -145 and  $(R_C, S_C)$ -145

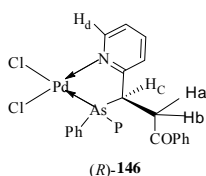
### 4.3 Experimental Section

Both enantiomerically pure forms of the complexes (*R*)-**144**, (*S*)-**144**,<sup>202</sup> (*E*)-1-phenyl-3-pyridin-2-yl-2-propenone, (*E*)-1-thiophenyl-3-pyridin-2-yl-2-propenone, (*E*)-1-phenyl-3-quinolin-2-yl-2-propenone, (*E*)-1-naphthyl-3-pyridin-2-yl-2-propenone<sup>203</sup> and (*E*)-1-methyl-3-pyridin-2-yl-2-propenoate,<sup>204</sup> were prepared as previously reported.

**Dichloro-[(*R*)-1-phenyl-3-(diphenylphosphino)-3-pyridin-2-yl-pentan-1-one-N<sup>1</sup>, P<sup>2</sup>]palladium (II), [(*R*)-**146**].**

The bis(acetonitrile) Pd complex (*R*)-**144** (1.50 g, 3.09 mmol) in dichloromethane (50 mL) was treated with (*E*)-1-phenyl-3-pyridin-2-yl-2-propenone (0.99 g, 4.80 mmol) and Ph<sub>2</sub>PH (0.57 g, 3.09 mmol) at room temperature for 4 days. Removal of solvent under reduced pressure gave the crude product as a yellow solid. The crude product mixture was then purified through a column with dichloromethane-acetone as the eluent and then crystallized from dichloromethane-diethyl ether to give the complex (*R*<sub>C</sub>, *R*<sub>C</sub>)-**145** as pale yellow solid (1.727 g, 70% yield) that could not be crystallized from any of the solvents attempted: <sup>31</sup>P{<sup>1</sup>H} NMR (CDCl<sub>3</sub>): δ 54.0 (s). The cationic complex (0.50 g, 0.62 mmol) in dichloromethane (20 mL) was treated with concentrated hydrochloric acid (12 mL) for 1 h at room temperature. The reaction mixture was then washed with water (4 × 10 mL), and dried (MgSO<sub>4</sub>). Subsequently fractional recrystallization from dichloromethane-diethyl ether gave complex (*R*)-**146** as yellow prisms: 0.304 g (85%

yield); mp 243-244 °C (decomp.);  $[\alpha]_D -54^\circ$  ( $c$  0.7,  $\text{CH}_2\text{Cl}_2$ ). Anal. Calcd for  $\text{C}_{26}\text{H}_{22}\text{Cl}_2\text{NOPPd}$ : C, 54.5; H, 3.9; N, 2.5. Found: C, 54.1; H, 3.6; N, 2.6.  $^{31}\text{P}\{^1\text{H}\}$  NMR ( $\text{CD}_2\text{Cl}_2$ ):  $\delta$  52.4 (s);  $^1\text{H}$  NMR ( $\text{CD}_2\text{Cl}_2$ ):  $\delta$  3.57-3.81(m, 2H,  $\text{CH}_2$ ), 5.12(dt, 1H,  $^2J_{\text{PH}} = 14.8$  Hz,  $^3J_{\text{HH}} = 6.5$  Hz,  $\text{CH}$ ), 7.33-8.08 (m, 18H, aromatics), 9.76(d, 1H,  $^3J_{\text{HH}} = 5.9$  Hz,  $H_d$ ).



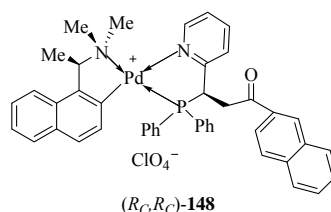
**(*R*)-1-phenyl-3-(diphenylphosphino)-3-pyridin-2-yl-pentan-1-one, [(*R*)-147].**

A solution of (*R*)-**146** (0.25 g, 0.44 mmol) in dichloromethane (20 mL) was stirred vigorously with a saturated aqueous solution of potassium cyanide (1 g) for 5 min. The resulting colorless organic layer was separated, washed with water, and dried ( $\text{MgSO}_4$ ). Upon the removal of solvent, a white solid (*R*)-**147** was obtained: yield 0.155 g (90%);  $[\alpha]_D +58^\circ$  ( $c$  2.0,  $\text{CH}_2\text{Cl}_2$ ).  $^{31}\text{P}\{^1\text{H}\}$  NMR ( $\text{CDCl}_3$ ):  $\delta$  0.5 (s).

**{(*R*)-1-[1-(Dimethylamino)ethyl]naphthyl- $\text{C}^2\text{N}$ }-[(*R*)-1-naphthyl-3-(diphenylphosphino)-3-pyridin-2-yl-pentan-1-one- $\text{N}^1, \text{P}^2$ ]palladium (II) perchlorate, [(*R\_C*, *R\_C*)-148].**

The bis(acetonitrile) Pd complex (*R*)-**144** (1.2 g, 2.5 mmol) in dichloromethane (40mL) was treated with (*E*)-1-naphthyl-3-pyridin-2-yl-2-propenone (0.704 g, 2.75 mmol) and  $\text{Ph}_2\text{PH}$  (0.459 g, 2.5 mmol) at room temperature for 6 days. Removal of solvent under reduced pressure gave the crude product as a yellow solid. The crude product mixture was then purified through a silica gel column with dichloromethane-acetone as the eluent and then crystallized from

dichloromethane-diethyl ether to give the complex ( $R_C$ ,  $R_C$ )-**148** as pale yellow crystals: mp 198-199 °C (decomp.);  $[\alpha]_D^{25}$  -175° ( $c$  0.6, CH<sub>2</sub>Cl<sub>2</sub>); 1.078 g (51.4% yield). Anal. Calcd for C<sub>44</sub>H<sub>40</sub>ClN<sub>2</sub>O<sub>5</sub>PPd: C, 62.2; H, 4.8; N, 3.3. Found: C, 62.5; H, 4.3; N, 3.6. <sup>31</sup>P{<sup>1</sup>H} NMR (CDCl<sub>3</sub>):  $\delta$  53.5 (s); <sup>1</sup>H NMR (CDCl<sub>3</sub>):  $\delta$  2.28 (d, 3H, <sup>3</sup>J<sub>HH</sub> = 6.4 Hz, CHMe), 3.01 (s, 3H, NMe), 3.18 (s, 3H, NMe), 4.64 (qn, 1H, <sup>3</sup>J<sub>HH</sub> = <sup>4</sup>J<sub>PH</sub> = 6.3 Hz, CHMe), 3.94-3.99 (m, 1H, <sup>3</sup>J<sub>HH</sub> = 6.1 Hz, <sup>2</sup>J<sub>HH</sub> = 18.1 Hz, H<sub>a</sub>), 4.07-4.14 (m, 1H, <sup>3</sup>J<sub>HH</sub> = 6.5 Hz, <sup>2</sup>J<sub>HH</sub> = 18.1 Hz, H<sub>b</sub>), 5.09 (t, 1H, <sup>3</sup>J<sub>HH</sub> = 6.2 Hz, H<sub>c</sub>), 6.89-8.33 (m, 26H, aromatics ), 8.82(d, 1H, <sup>3</sup>J<sub>HH</sub> = 5.5 Hz, H<sub>d</sub>).



**Dichloro-[( $R$ )-1-naphthyl-3-(diphenylphosphino)-3-pyridin-2-yl-pentan-1-one-N<sup>1</sup>,P<sup>2</sup>]palladium (II), [( $R$ )-**149**].**

The naphthylamine auxiliary in ( $R_C$ ,  $S_C$ )-**148** was removed chemoselectively by adding concentrated hydrochloric acid (15 mL) to a solution of the complex ( $R_C$ ,  $S_C$ )-**148** (0.45 g, 0.66 mmol) in dichloromethane (30 mL). The reaction mixture was stirred vigorously for 1 h at room temperature. The reaction mixture was then washed with water (4 × 10 mL), and dried (MgSO<sub>4</sub>). Subsequent fractional crystallization from dichloromethane-diethyl ether gave complex ( $R$ )-**149** as yellow prisms: mp 235-236 °C (decomp);  $[\alpha]_D^{25}$  -111° ( $c$  0.6, CH<sub>2</sub>Cl<sub>2</sub>); 0.268 g (91.5% yield). Anal. Calcd for C<sub>30</sub>H<sub>24</sub>Cl<sub>2</sub>NOPPd: C, 57.9; H, 3.9; N, 2.6. Found C 57.5, H 3.5, N 2.9. <sup>31</sup>P{<sup>1</sup>H} NMR (CD<sub>2</sub>Cl<sub>2</sub>):  $\delta$  51.8 (s); <sup>1</sup>H NMR (CDCl<sub>3</sub>):  $\delta$  3.72-3.87 (m, 2H, CH<sub>2</sub>), 5.11(dt, 1H,

$^2J_{P,H} = 14.6$  Hz,  $^3J_{H,H} = 6.6$  Hz, CH), 7.31-8.24 (m, 20H, aromatics), 9.84(d, 1H,  $^3J_{HH} = 6.0$  Hz,  $H_d$ ).

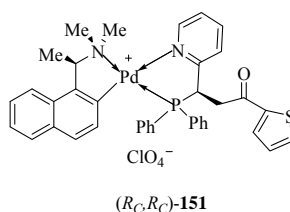
**(R)-1-naphthyl-3-(diphenylphosphino)-3-pyridin-2-yl-pentan-1-one, [(R)-150].**

A solution of (R)-**149** (0.1 g, 0.53mmol) in dichloromethane (20 mL) was stirred vigorously with a saturated aqueous solution of potassium cyanide (0.5 g) for 5 min. The resulting colorless organic layer was separated, washed with water, and dried ( $MgSO_4$ ). Upon the removal of solvent, a white solid (R)-**150** was obtained:  $[\alpha]_D^{+80} (c 0.7, CH_2Cl_2)$ ; 0.06 g (89% yield).  $^{31}P\{^1H\}$  NMR ( $CDCl_3$ ):  $\delta$  -0.2 (s).

**Dichloro-[(R)-1-thiophenyl-3-(diphenylphosphino)-3-pyridin-2-yl-pentan-1-one- $N^1, P^2$ ]palladium (II), [(R)-152].**

The bis(acetonitrile) Pd complex (R)-**144** (1.00 g, 2.06 mmol) in dichloromethane (40 mL) was treated with (*E*)-1-thiophenyl-3-pyridin-2-yl-2-propenone (0.49 g, 2.3 mmol) and  $Ph_2PH$  (0.38 g, 2.06 mmol) at room temperature for 6 days. Removal of solvent under reduced pressure gave the crude product as a yellow solid. The crude product mixture was then purified through a silica gel column with dichloromethane-acetone as the eluent and then crystallized from dichloromethane-diethylether to give the complex ( $R_C, R_C$ )-**151** as pale yellow crystals (1.065 g, 64.3% yield):  $^{31}P\{^1H\}$  NMR ( $CDCl_3$ ):  $\delta$  53.8 (s). The cationic complex (0.50 g, 0.62mmol) in dichloromethane (30 mL) was treated with concentrated hydrochloric acid (12 mL) for 1 h at room temperature. The reaction mixture was then washed with water ( $4 \times 10$  mL), and dried ( $MgSO_4$ ). Subsequent fractional recrystallization from dichloromethane-diethylether gave complex (R)-**152**

as yellow prisms: mp 253-254 °C (decomp.);  $[\alpha]_{\text{D}}^{-345}$  ( $c$  0.6,  $\text{CH}_2\text{Cl}_2$ ); 0.323 g (90% yield). Anal. Calcd for  $\text{C}_{24}\text{H}_{20}\text{Cl}_2\text{NOPPdS}$ : C, 49.8; H, 3.5; N, 2.4. Found: C, 54.1; H, 3.6; N, 2.6.  $^{31}\text{P}\{^1\text{H}\}$  NMR ( $\text{CDCl}_3$ ):  $\delta$  51.2 (s);  $^1\text{H}$  NMR ( $\text{CDCl}_3$ ):  $\delta$  3.45-3.54(m, 2H,  $\text{CH}_2$ ), 5.00(dt, 1H,  $^2J_{\text{PH}} = 14.8$  Hz,  $^3J_{\text{HH}} = 6.6$  Hz,  $\text{CH}$ ), 7.07-8.01 (m, 17H, aromatics), 9.81(d, 1H,  $^3J_{\text{HH}} = 6.0$  Hz,  $H_d$ ).



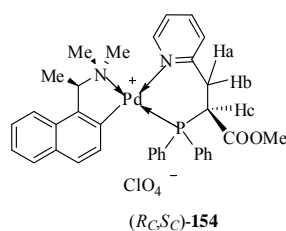
**(*R*)-1-thiophenyl-3-(diphenylphosphino)-3-pyridin-2-yl-pentan-1-one,**  
**[(*R*)-153].**

A solution of (*R*)-152 (0.2 g, 0.346 mmol) in dichloromethane (20 mL) was stirred vigorously with a saturated aqueous solution of potassium cyanide (1 g) for 5 min. The resulting colorless organic layer was separated, washed with water, and dried ( $\text{MgSO}_4$ ). Upon the removal of solvent, a white solid (*R*)-153 was obtained:  $[\alpha]_{\text{D}}^{+217}$  ( $c$  0.7,  $\text{CH}_2\text{Cl}_2$ ); 0.118 g (85% yield).  $^{31}\text{P}\{^1\text{H}\}$  NMR ( $\text{CDCl}_3$ ):  $\delta$  -0.3 (s).

**{(*R*)-1-[1-(Dimethylamino)ethyl]naphthyl- $\text{C}^2\text{N}$ }-[(*S*)-methyl-2-(diphenylphosphino)-3-pyridin-2-yl-propanoate- $\text{N}^1,\text{P}^2$ ]palladium (II) perchlorate, [(*R*<sub>C</sub>, *S*<sub>C</sub>)-154].**

The bis(acetonitrile) Pd complex (*R*)-144 (0.60 g, 1.23 mmol) in dichloromethane (40 mL) was treated with (*E*)-1-methyl-3-pyridin-2-yl-2-propenoate (0.302 g, 1.90 mmol) and  $\text{Ph}_2\text{PH}$  (0.23 g, 1.23 mmol) at room temperature for 7 days. Removal of solvent under reduced pressure gave the crude product as a yellow solid.

The crude product mixture was then purified through a column with dichloromethane-acetone as the eluent and then crystallized from chloroform to give the complex ( $R_C$ ,  $S_C$ )-**154** as pale yellow crystals: yield 0.772 g (83%); mp 193-194 °C (decomp.);  $[\alpha]_D -91^\circ$  ( $c$  1.5,  $\text{CH}_2\text{Cl}_2$ ). Anal. Calcd for  $\text{C}_{35}\text{H}_{36}\text{ClN}_2\text{O}_6\text{PPd}$ : C, 51.2; H, 4.4; N, 3.4. Found: C, 51.5; H, 4.3; N, 3.6.  $^{31}\text{P}\{^1\text{H}\}$  NMR ( $\text{CD}_2\text{Cl}_2$ ):  $\delta$  46.4 (s);  $^1\text{H}$  NMR ( $\text{CD}_2\text{Cl}_2$ ):  $\delta$  2.22 (d, 3H,  $^3J_{\text{HH}} = 6.4$  Hz,  $\text{CHMe}$ ), 2.53 (d, 3H,  $^4J_{\text{PH}} = 3.5$  Hz,  $\text{NMe}$ ), 2.90 (d, 3H,  $^4J_{\text{PH}} = 1.7$  Hz,  $\text{NMe}$ ), 3.14 (s, 3H,  $\text{COOMe}$ ), 3.54 (dt, 1H,  $^3J_{\text{HH}} = ^3J_{\text{PH}} = 13.1$  Hz,  $^2J_{\text{HH}} = 2.4$  Hz,  $H_a$ ), 3.74 (dddd, 1H,  $^3J_{\text{PH}} = 35.7$  Hz,  $^3J_{\text{HH}} = 14.3$  Hz,  $^2J_{\text{HH}} = 2.4$  Hz,  $H_b$ ), 4.20 (dd, 1H,  $^2J_{\text{PH}} = 27.8$  Hz,  $^3J_{\text{HH}} = 14.3$  Hz,  $H_c$ ), 4.54 (qn, 1H,  $^3J_{\text{HH}} = ^4J_{\text{PH}} = 6.3$  Hz,  $\text{CHMe}$ ), 6.51-8.40 (m, 19H, aromatics), 8.74 (d, 1H,  $^3J_{\text{HH}} = 5.3$  Hz,  $H_d$ ).



**Dichloro [(*S*)-methyl-2-(diphenylphosphino)-3-pyridin-2-yl-propanoate- $\text{N}^1$ ,  $\text{P}^2$ ]palladium (II), [( $S_C$ )-**155**].**

The naphthylamine auxiliary in ( $R_C$ ,  $S_C$ )-**154** was removed chemoselectively by adding concentrated hydrochloric acid (15 mL) to a solution of the complex ( $R_C$ ,  $S_C$ )-**154** (0.50 g, 0.66 mmol) in dichloromethane (30 mL). The reaction mixture was stirred vigorously for 1 h at room temperature. The reaction mixture was then washed with water ( $4 \times 10$  mL), and dried ( $\text{MgSO}_4$ ). Subsequent fractional crystallization from dichloromethane-diethyl ether gave complex ( $S_C$ )-**155** as yellow prisms: 0.301 g

(86% yield); mp 219-220 °C (decomp);  $[\alpha]_{\text{D}}^{-85^{\circ}}$  (*c* 0.4, CH<sub>2</sub>Cl<sub>2</sub>). Anal. Calcd for C<sub>21</sub>H<sub>20</sub>Cl<sub>2</sub>NO<sub>2</sub>PPd: C, 47.9; H, 3.8; N, 2.7. Found: C, 47.9; H, 3.5; N, 3.0. <sup>31</sup>P{<sup>1</sup>H} NMR (CD<sub>2</sub>Cl<sub>2</sub>):  $\delta$  37.0 (s); <sup>1</sup>H NMR (CD<sub>2</sub>Cl<sub>2</sub>):  $\delta$  3.21(s, 3H, COOCH<sub>3</sub>), 3.37(dt, 1H, <sup>3</sup>J<sub>HH</sub> = <sup>3</sup>J<sub>PH</sub> = 12.3 Hz, <sup>2</sup>J<sub>HH</sub> = 1.9 Hz, H<sub>a</sub>), 3.66 (dddd, 1H, <sup>3</sup>J<sub>PH</sub> = 33.6 Hz, <sup>3</sup>J<sub>HH</sub> = 14.6Hz, <sup>2</sup>J<sub>HH</sub> = 1.9 Hz, H<sub>b</sub>), 3.98-4.13(m, 1H, H<sub>c</sub>), 7.34-8.33(m, 13H, aromatics ), 9.37(d, 1H, <sup>3</sup>J<sub>HH</sub> = 5.7 Hz, H<sub>d</sub>).

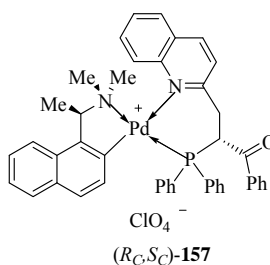
**(S)-methyl-2-(diphenylphosphino)-3-pyridin-2-yl-propanoate, [(S<sub>C</sub>)-156].**

A solution of (S<sub>C</sub>)-**155** (0.28 g, 0.53mmol) in dichloromethane (20 mL) was stirred vigorously with a saturated aqueous solution of potassium cyanide (0.5 g) for 5 min. The resulting colorless organic layer was separated, washed with water, and dried (MgSO<sub>4</sub>). Upon the removal of solvent, a white solid (S<sub>C</sub>)-**156** was obtained: 0.155 g (90% yield);  $[\alpha]_{\text{D}}^{-27^{\circ}}$  (*c* 0.3, CH<sub>2</sub>Cl<sub>2</sub>). <sup>31</sup>P{<sup>1</sup>H} NMR (CDCl<sub>3</sub>):  $\delta$  0.5 (s).

**{(R)-1-[1-(Dimethylamino)ethyl]naphthyl-C<sup>2</sup>N}-[(S)-1-phenyl-2-(diphenylphosphino)-3-quinolin-2-yl-pentan-1-one-N<sup>1</sup>,P<sup>2</sup>]-palladium (II) Perchlorate, [(R<sub>C</sub>, S<sub>C</sub>)-157].**

The bis(acetonitrile) Pd complex (R)-**144** (1.3 g, 2.673 mmol) in dichloromethane (40 mL) was treated with (E)-1-phenyl-3-quinolin-2-yl-2-propenone (0.762 g, 2.937 mmol) and Ph<sub>2</sub>PH (0.498 g, 2.673 mmol) at room temperature for 4 days. Removal of solvent under reduced pressure gave the crude product as a yellow solide. The crude product mixture was then purified through a silica gel column with dichloromethane-acetone as the eluent and then crystallized from acetone-diethyl ether to give the complex (R<sub>C</sub>, S<sub>C</sub>)-**157** as pale yellow crystals: mp 234-235 °C

(decomp);  $[\alpha]_D -30^\circ$  ( $c$  1.5,  $\text{CH}_2\text{Cl}_2$ ); 1.703 g (75% yield). Anal. Calcd for  $\text{C}_{44}\text{H}_{40}\text{ClN}_2\text{O}_5\text{PPd}$ : C, 62.2; H, 4.8; N, 3.3. Found: C, 62.6; H, 4.4; N, 3.6.  $^{31}\text{P}\{^1\text{H}\}$  NMR ( $\text{CD}_2\text{Cl}_2$ ):  $\delta$  42.3 (s);  $^1\text{H}$  NMR ( $\text{CD}_2\text{Cl}_2$ ):  $\delta$  2.33 (d, 3H,  $^4J_{\text{PH}} = 3.2$  Hz, *NMe*), 2.54 (d, 3H,  $^3J_{\text{HH}} = 6.4$  Hz, *CHMe*), 2.75 (d, 3H,  $^4J_{\text{PH}} = 1.5$  Hz, *NMe*), 4.05 (dddd, 1H,  $^3J_{\text{PH}} = 35.2$  Hz,  $^3J_{\text{HH}} = 13.5$  Hz,  $^2J_{\text{HH}} = 4.1$  Hz, *H<sub>a</sub>*), 4.49 (qn, 1H,  $^3J_{\text{HH}} = ^4J_{\text{PH}} = 6.3$  Hz, *CHMe*), 4.73-4.82 (m, 1H, *H<sub>c</sub>*), 5.54 (dt, 1H,  $^2J_{\text{PH}} = ^3J_{\text{HH}} = 12.0$  Hz,  $^2J_{\text{HH}} = 4.1$  Hz, *H<sub>b</sub>*), 6.78-8.71 (m, 27H, aromatics).



**(*S*)-1-phenyl-2-(diphenylphosphino)-3-quinolin-2-yl-pentan-1-one [(*S<sub>C</sub>*)-158]**

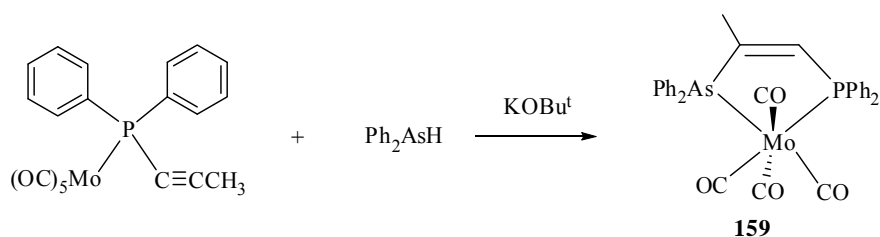
A solution of (*S<sub>C</sub>*)-157 (0.50 g, 0.59mmol) in dichloromethane (20 mL) was stirred vigorously with a saturated aqueous solution of potassium cyanide (1 g) for 5 min. The resulting colorless organic layer was separated, washed with water. The solution was dried over magnesium sulfate then filtered. Upon the removal of solvent, a white solid (*S<sub>C</sub>*)-158 was obtained:  $[\alpha]_D -150^\circ$  ( $c$  0.4,  $\text{CH}_2\text{Cl}_2$ ); 0.197 g (75% yield).  $^{31}\text{P}\{^1\text{H}\}$  NMR ( $\text{CDCl}_3$ ):  $\delta$  0.5 (s).

## Chapter 5

### Asymmetric Hydroarsination Reaction

#### 5.1 Introduction

The number of reports on the addition of As-H moiety to C=C or C≡C bonds is only a few. King's group reported the addition of As-H bond to the carbon-carbon double bonds of vinylphosphines in the presence of base catalyst potassium *tert*-butoxide to give the As-P ligand in 77% yield at room temperature.<sup>205</sup> However the reaction between diphenylarsine and vinyl isocyanide only give 31% yield in boiling benzene.<sup>206</sup> The intermolecular hydroarsination of phosphinoalkyne Mo complex and diphenylarsine can be achieved under base catalysis to give **159** in 46% yield (Scheme 5.1).<sup>207</sup>



**Scheme 5.1**

Although several chiral arsine compounds have been used in asymmetric catalytic reactions,<sup>208</sup> these earlier studies have not involved optically active pyridylarsines which would provide a variety of applications in asymmetric catalysis as shown by their phosphorus analogues.<sup>191</sup> However, most available arsination

protocols are limited to compounds that are not base and reducible agent sensitive<sup>122a</sup> and devoid of functionalities. The only straightforward method for synthesis of functionalized arsines has been recently reported,<sup>122b</sup> Pd-catalyzed arsination of aryl triflates using triphenylarsine as the arsinating agent. However via that methodology, heteroatom-substituted pyridyl triflates did not react at all. Until now, no synthesis of enantiomerically pure keto- and ester- substituted C-chiral pyridylarsines have been reported.

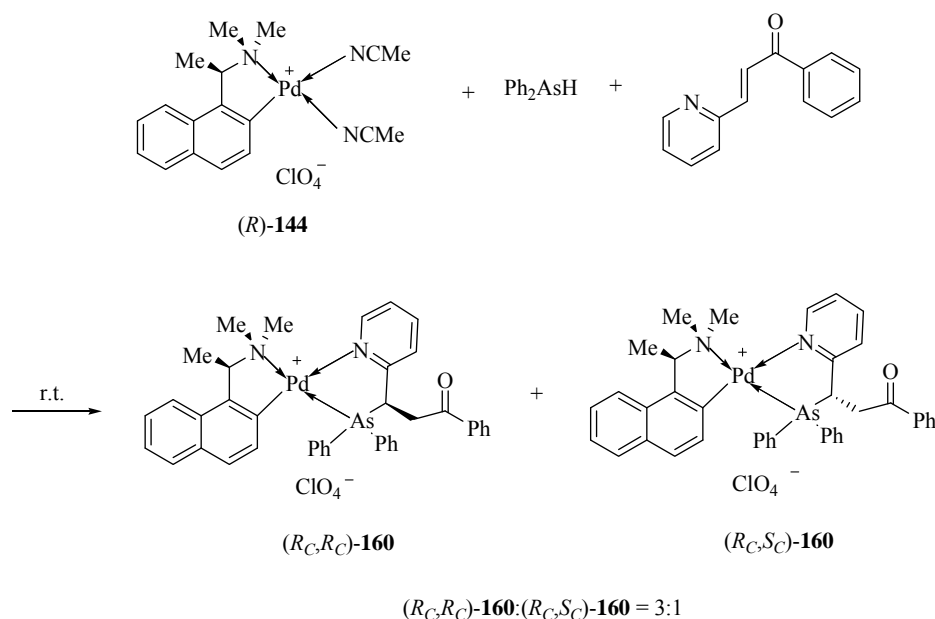
Recently our group reported the first use of an organopalladium complex containing (*S*)-(1-(dimethylamino)ethyl)naphthalene as the chiral auxiliary to promote the asymmetric hydroarsination between vinylphosphine and diphenylarsine to generate chiral an As-P ligand in high enantioselectivity under mild conditions (see 1.3.5). In order to extend this protocol to the hydroarsination of functionalized olefinic systems, we hereby prepared the keto- and ester- functionalized chiral pyridylarsine ligands *via* the asymmetric hydroarsination reaction promoted by the chiral cyclopalladated-amine template.

## 5.2 Results and Discussion

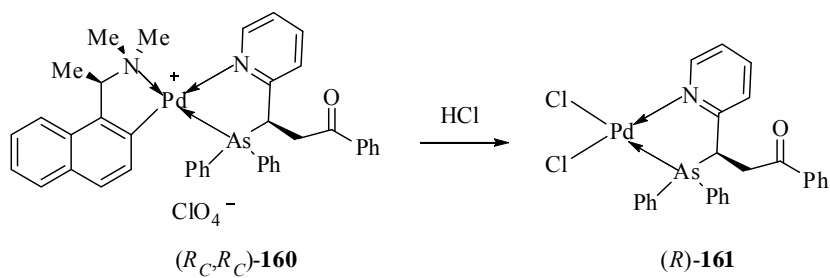
### 5.2.1 Hydroarsination of (*E*)-1-phenyl-3-pyridin-2-yl-2-propenone

In the absence of a metal ion, diphenylarsine shows no reactivity with (*E*)-1-phenyl-3-pyridin-2-yl-2-propenone. However, as illustrated in Scheme 5.2, in the presence of chiral complex (*R*)-**144**, the reaction is completed in 12 days at room

temperature to give a 3:1 diastereomeric mixture of ( $R_C$ ,  $R_C$ )-**160** and ( $R_C$ ,  $S_C$ )-**160**. While the addition of the secondary phosphine to vinylic phosphines resulted in *cis-trans* regioisomers of the products,<sup>134</sup> the addition of diphenylarsine to vinylic pyridines is 100% regioselective, wherein the As atom occupies the coordination site *trans* to NMe<sub>2</sub>. The high regioselectivity observed in the present case is in agreement with what has been observed for similar N-P heterobidentate ligands.<sup>209</sup> The diastereomeric products were subsequently separated by column chromatography. The major diastereomer ( $R_C$ ,  $R_C$ )-**160** was obtained as a pale yellow solid in 30% isolated yield. Although it is stable in the solid state and in solution, it is highly soluble in most organic solvents and could not be induced to crystallize. Upon subsequent treatment of the perchlorate salt with concentrated hydrochloric acid, the resultant neutral dichloro complex ( $R$ )-**168** was obtained as yellow prisms in 87% isolated yield, [ $\alpha$ ]<sub>D</sub> -122° (*c* 0.6, CH<sub>2</sub>Cl<sub>2</sub>) (Scheme 5.3).



Scheme 5.2



Scheme 5.3

### 5.2.1.1 Single Crystal X-ray Structural Analysis of (R)-161

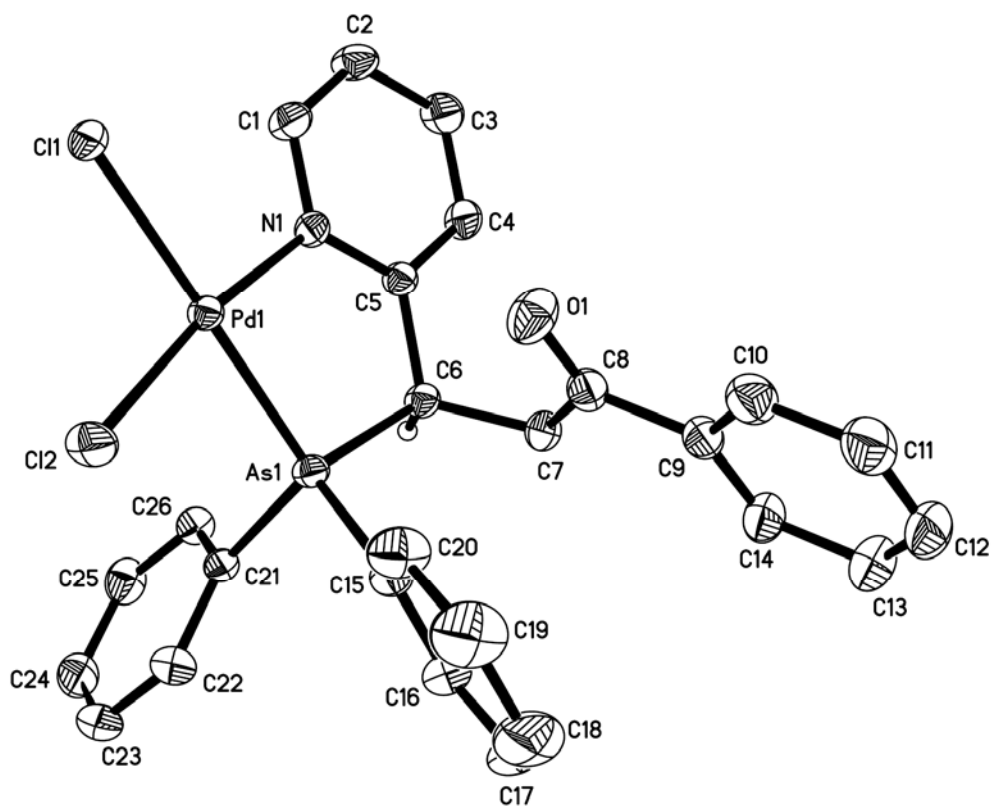


Figure 5.1 Molecular structure and absolute configuration of (R)-161

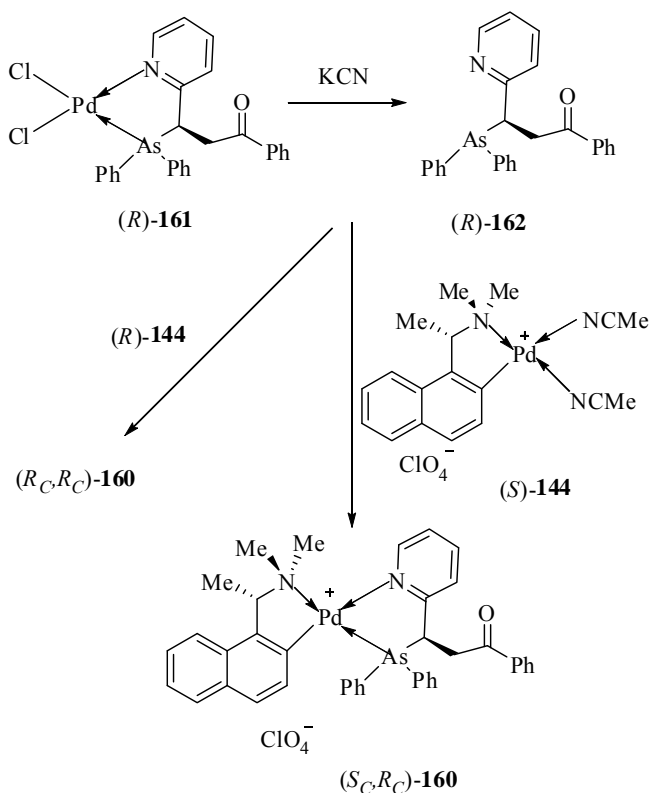
**Table 5.1 Selected bond lengths (Å) and (deg) angles for (*R*)-161**

Pd(1)–N(1)	2.071(2)	Pd(1)–As(1)	2.279(1)
Pd(1)–Cl(2)	2.305 (1)	Pd(1)–Cl(1)	2.376 (1)
C(1)–N(1)	1.341(4)	C(5)–N(1)	1.368(3)
C(6)–As(1)	1.971(3)	C(8)–O(1)	1.216(4)
C(6)–C(7)	1.536(4)	C(5)–C(6)	1.510(4)
N(1)–Pd(1)–As(1)	84.3 (1)	N(1)–Pd(1)–Cl(2)	171.0 (1)
As(1)–Pd(1)–Cl(2)	86.7 (1)	N(1)–Pd(1)–Cl(1)	96.1 (1)
As(1)–Pd(1)–Cl(1)	179.4(1)	N(1)–C(5)–C(6)	120.8(2)
C(4)–C(5)–C(6)	118.7(2)	C(5)–C(6)–C(7)	114.4(2)
C(5)–C(6)–As(1)	108.6 (2)	C(7)–C(6)–As(1)	112.7 (2)
C(8)–C(7)–C(6)	113.8(2)	C(1)–N(1)–C(5)	118.1(2)
C(5)–N(1)–Pd(1)	118.6(2)	C(6)–As(1)–Pd(1)	102.3 (1)

The chelating properties and the absolute configuration of the coordinated pyridine-substituted arsine ligand in complex (*R*)-**161** were studied by X-ray crystallography (Figure 5.1). Selected bond distances and angles of the complex are given in Table 5.1. The structure analysis established that the newly formed stereogenic center at C(6) adopted the *R* absolute configuration. The geometry at the Pd center is distorted square planner with angles of 84.3(1)–92.8(1) and 171.0(1)–179.3(1)°. Both the Pd–As and Pd–N bond lengths, 2.278(1) and 2.071(2) Å, are typical, but the two Pd–Cl distances 2.305(1) and 2.376(1) Å differ significantly, with the bond *trans* to the As being noticeably larger than the bond *trans* to the NMe<sub>2</sub>. This reflects the stronger electronic *trans* effect of the As relative to the aromatic nitrogen donor. The C(6)–C(7) bond distance [1.536(4) Å] showed marked lengthening, which is clearly attributed to the intrachelate repulsive interactions between the CPh moiety at C(7) and the phenyl groups on the As donor atom. The

CH<sub>2</sub>COPh substituent of the five-membered Pd–N chelate is in the preferred equatorial disposition.<sup>198</sup> The bond length of Pd–As in (*R*)-**161** (2.278(1) Å) is longer than that of the corresponding Pd–P (2.184(4)Å),<sup>209</sup> which is in agreement with the 0.10–0.11 Å difference in the covalent bond radii of As (1.21 Å) and P (1.10 Å).<sup>210</sup>

### 5.2.1.2 Liberation and the Optical Purity of (*R*)-**162**



**Scheme 5.4**

The liberation of the free As–N ligand (*R*)-**162** was achieved by the treatment of the dichloro complex with aqueous potassium cyanide (Scheme 5.4). Thus the pyridylarsine was obtained as a white solid in 75% yield,  $[\alpha]_{\text{D}} +78^{\circ}$  ( $c$  0.4, CH<sub>2</sub>Cl<sub>2</sub>).

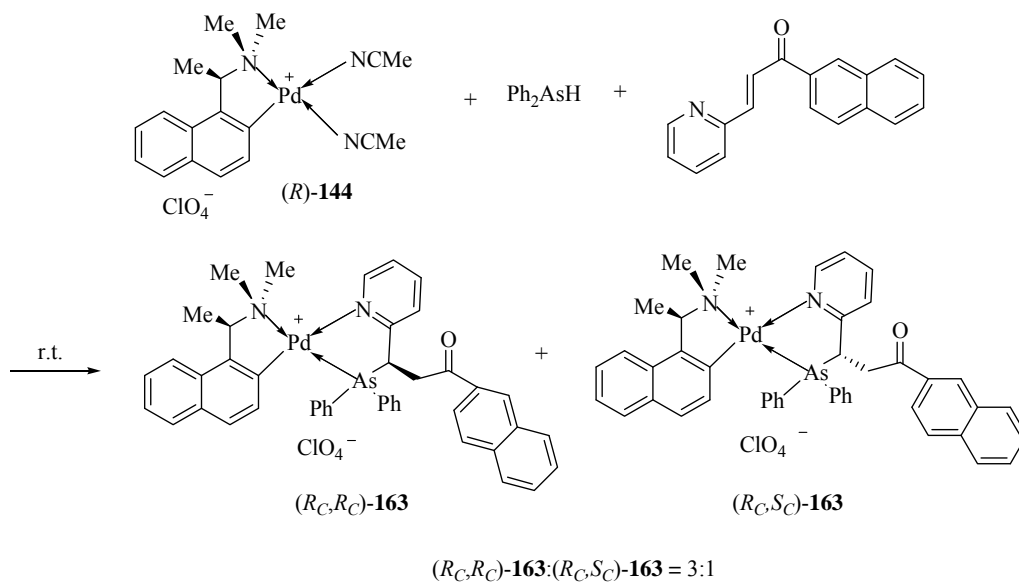
Because of the air sensitivity of the noncoordinated As atom, liberated (*R*)-**162** was not stored in its pure form but was reassociated again to (*R*)-**144**. The reassociation process is also a means of verifying the optical purity of the released ligand and to establish the identity of the minor isomers that were generated in the original hydroarsination reaction.<sup>199,134</sup> The reassociation procedure was monitored by <sup>1</sup>H NMR spectroscopy. In CDCl<sub>3</sub>, the <sup>1</sup>H NMR spectrum of the reassociation product showed only one product, thus confirming that the liberated (*R*)-**162** is optically pure.

In order to establish the identity of the minor product that was formed from hydroarsination reaction, (*R*)-**162** was reassociated regioselectively to (*S<sub>C</sub>*)-**144** to generate the diastereomeric complex (*S<sub>C</sub>*, *R<sub>C</sub>*)-**160** (Scheme 5.4). The <sup>1</sup>H NMR spectrum of the complex (*S<sub>C</sub>*, *R<sub>C</sub>*)-**160** was identical with those observed from the minor product generated from the hydroarsination reaction. Hence, it could be confirmed that complex (*R<sub>C</sub>*, *S<sub>C</sub>*)-**160** is the minor product in the original hydroarsination reaction. No <sup>1</sup>H NMR signals could be detected for the major diastereomer thus reaffirming that liberated (*R*)-**162** is enantiomerically pure.

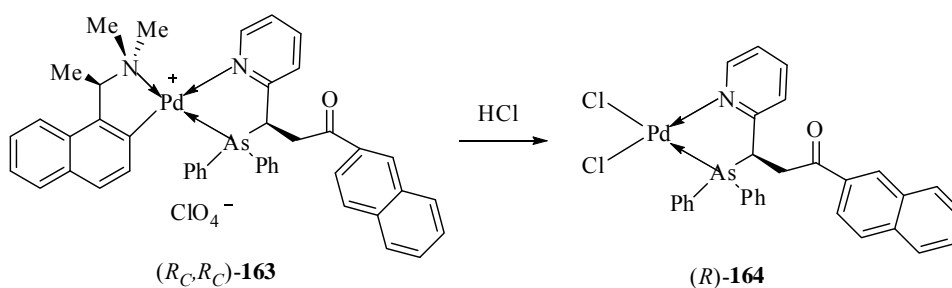
### 5.2.2 Hydroarsination of (*E*)-1-naphthyl-3-pyridin-2-yl-2-propenone

A solution of (*R*)-**144** in dichloromethane (40 mL) was treated with (*E*)-1-naphthyl-3-pyridin-2-yl-2-propenone and Ph<sub>2</sub>AsH at room temperature for 15 days to give a 3:1 diastereomeric mixture of (*R<sub>C</sub>*, *R<sub>C</sub>*)-**163** and (*R<sub>C</sub>*, *S<sub>C</sub>*)-**163** (Scheme 5.5). The major diastereomer (*R<sub>C</sub>*, *R<sub>C</sub>*)-**163** was obtained as a pale yellow solid in 28%

isolated yield. Although it is stable in the solid and in solution, it is highly soluble in most organic solvents and could not be induced to crystallize. Two products were subsequently separated by silica gel column chromatography. Treatment of the perchlorate salt with concentrated hydrochloric acid, the resultant dichloro complex (*R*)-**164** is thus obtained from dichloromethane-diethyl ether as yellow prisms in 92% isolated yield,  $[\alpha]_{\text{D}} -76.5^{\circ}$  ( $c$  0.7,  $\text{CH}_2\text{Cl}_2$ ) (Scheme 5.6).



Scheme 5.5



Scheme 5.6

### 5.2.2.1 Single Crystal X-ray Structural Analysis of (*R*)-164

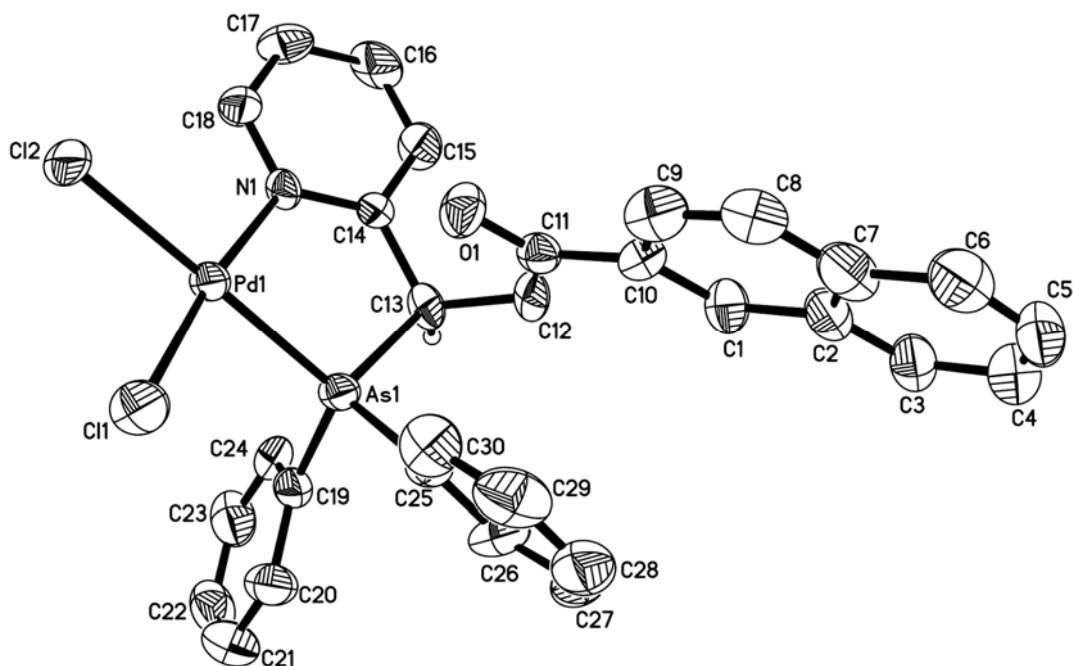


**Figure 5.2** Molecular structure and absolute configuration of (*R*)-164

The chelating properties and the absolute configuration of the coordinated pyridine-substituted arsine ligand in complex (*R*)-164 were studied by X-ray crystallography (Figure 5.2). Selected bond distances and angles of the complex are given in Table 5.2. The structure analysis establishes that the newly formed stereogenic center at C(13) adopts the *R* configuration. The geometry at the Pd center is distorted square planer with angles of 84.3(1)–96.0(2)° and 172.4(2)–178.9(1)°. Both the Pd–As and Pd–N bond lengths, 2.292(1) and 2.086(6) Å, are typical, but the two Pd–Cl distances 2.280(2) and 2.366(2) Å differ significantly, with the bond *trans* to the As being noticeably longer than normal. This reflects the stronger electronic

*trans* effect of the As relative to the aromatic nitrogen donor. The C(12)–C(13) bond distance [1.535(10) Å] is marked lengthening, which is clearly attributed to the intrachelate repulsive interactions between the naphthylene moiety and the phenyl groups on the As donor atom. The CH<sub>2</sub>CONAP substituent at C(13) of the five-membered Pd–N chelate is in the preferred equatorial disposition.<sup>200</sup>

**Table 5.2 Selected bond lengths (Å) and (deg) angles for (*R*)-164**

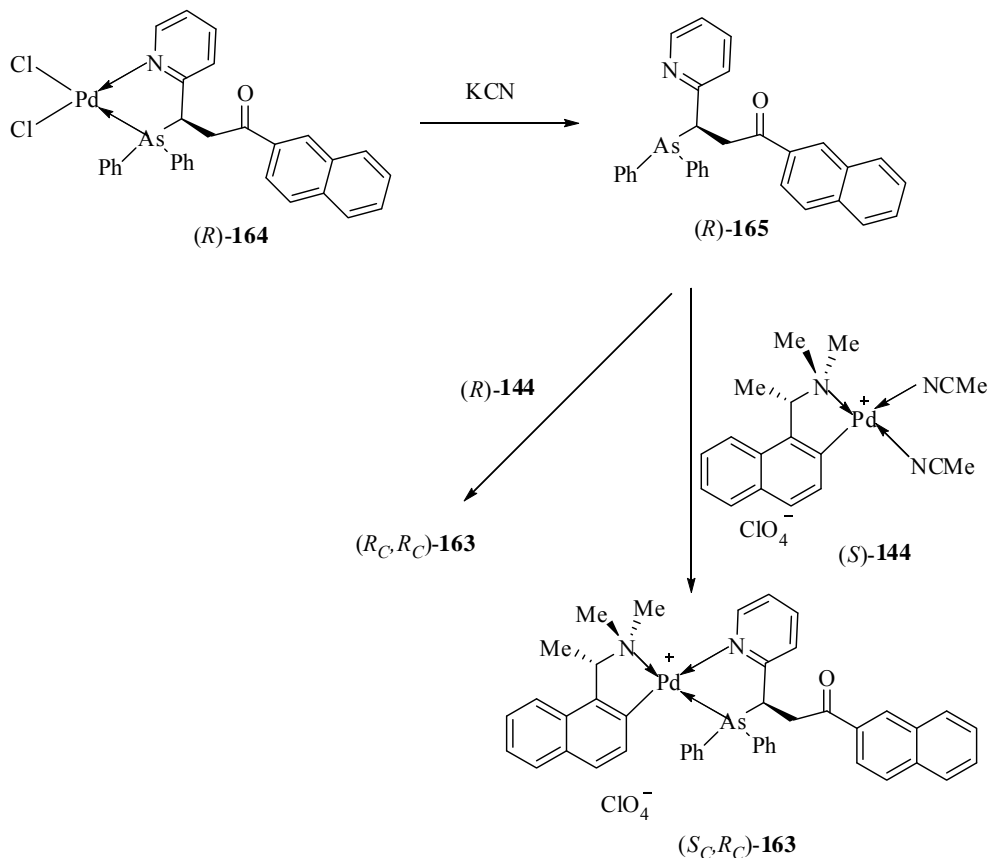
Pd(1)–N(1)	2.086(6)	Cl(1)–Pd(1)–As(1)	88.1(1)
Pd(1)–Cl(1)	2.280(2)	N(1)–Pd(1)–Cl(2)	96.0(2)
Pd(1)–As(1)	2.292 (1)	Cl(1)–Pd(1)–Cl(2)	91.6 (1)
Pd(1)–Cl(2)	2.366(2)	As(1)–Pd(1)–Cl(2)	178.9 (1)
As(1)–C(13)	1.973(7)	C(13)–As(1)–Pd(1)	101.7(2)
C(10)–C(11)	1.484(10)	O(1)–C(11)–C(10)	120.8(7)
C(11)–O(1)	1.215(9)	O(1)–C(11)–C(12)	120.1(7)
C(11)–C(12)	1.504(10)	C(10)–C(11)–C(12)	119.1(6)
C(12)–C(13)	1.535(10)	C(11)–C(12)–C(13)	114.2(6)
C(13)–C(14)	1.511(10)	C(14)–C(13)–C(12)	113.1(6)
C(14)–N(1)	1.364(8)	C(14)–C(13)–As(1)	108.3(4)
C(18)–N(1)	1.331(9)	C(12)–C(13)–As(1)	111.3(5)
N(1)–Pd(1)–Cl(1)	172.4(2)	N(1)–C(14)–C(13)	122.0(6)
N(1)–Pd(1)–As(1)	84.3 (2)	C(14)–N(1)–Pd(1)	121.9(5)

### 5.2.2.2 Liberation and the Optical Purity of (*R*)-165

The liberation of free (*R*)-**165** was achieved by the treatment of the dichloro complex with aqueous potassium cyanide (Scheme 5.7). Thus the pyridylarsine was obtained as a white solid in 85%, [ $\alpha$ ]<sub>D</sub> +174° (CH<sub>2</sub>Cl<sub>2</sub>).

The enantiomeric ligand was confirmed to be optically pure (Scheme 5.7) by

the methods described in Chapter 5.2.1.3.

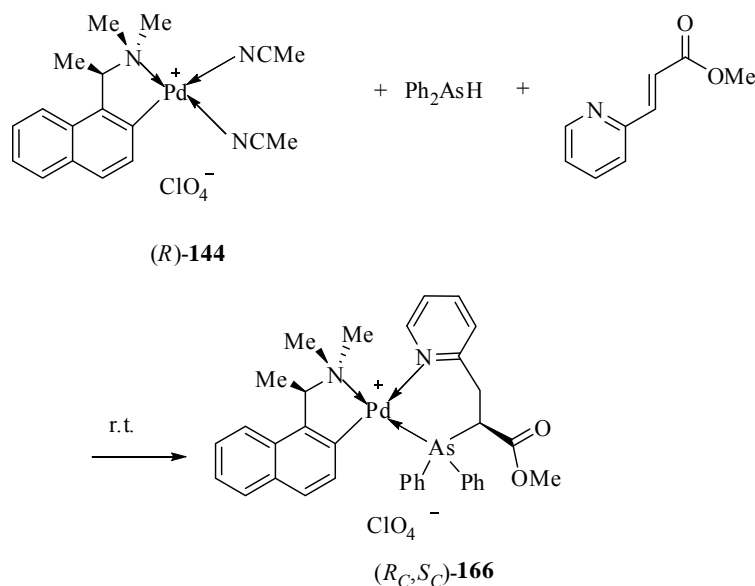


**Scheme 5.7**

### 5.2.3 Hydroarsination of (*E*)-1-Methyl-3-pyridin-2-yl-2-propenoate

In principle, the hydroarsination reaction between (*E*)-1-methyl-3-pyridin-2-yl-2-propenoate and Ph<sub>2</sub>AsH should generate similar five-membered As–N chelate products as that obtained from the reaction involving (*E*)-1-phenyl-3-pyridinyl-2-yl-2-propenone. Interestingly, after 14 days at room temperature the chelating As–N complex (*R<sub>C</sub>*, *S<sub>C</sub>*)-**166** was generated as the sole product in the hydroarsination reaction (Scheme 5.8). After purification by column

chromatography, the product ( $R_C, S_C$ )-**166** was subsequently crystallized from dichloromethane–diethyl ether as pale yellow prisms in 51% yield,  $[\alpha]_D -77^\circ$  ( $c$  0.6,  $\text{CH}_2\text{Cl}_2$ ).



**Scheme 5.8**

### 5.2.3.1 Single Crystal X-ray Structural Analysis of ( $R_C, S_C$ )-**166**

The X-ray crystallographic analysis of the complex ( $R_C, S_C$ )-**166** confirmed that an enantiomerically pure product has been formed in which the six-membered As–N ligand coordinated to palladium as a bidentate chelate (Figure 5.3) with a twist-boat conformation. Furthermore, the structure analysis unambiguously established that the newly formed stereogenic center at C(21) adopts the  $S$  configuration. The As and N donor atoms of the new heterobidentate ligand are bonded regiospecifically to the Pd atom, with the softer As donor expectedly taking up the position *trans* to the  $\text{NMe}_2$

group. Selected bond lengths and angles are listed in Table 5.3. The angles formed by the As–N chelate and the naphthylamine template at the Pd metal center were in the range of 81.0(2)–97.8(2) and 169.6 (1)–171.6(2)°. The C(21)–As(1) and C(20)–C(21) distances [2.002(5) and 1.533(7) Å] are elongated noticeably by the intrachelate interactions. The bond length of Pd–As in (*R<sub>C</sub>*, *S<sub>C</sub>*)-**166** (2.345 (1) Å) is also longer than that of the corresponding Pd–P (2.239 (1)Å).<sup>211</sup>

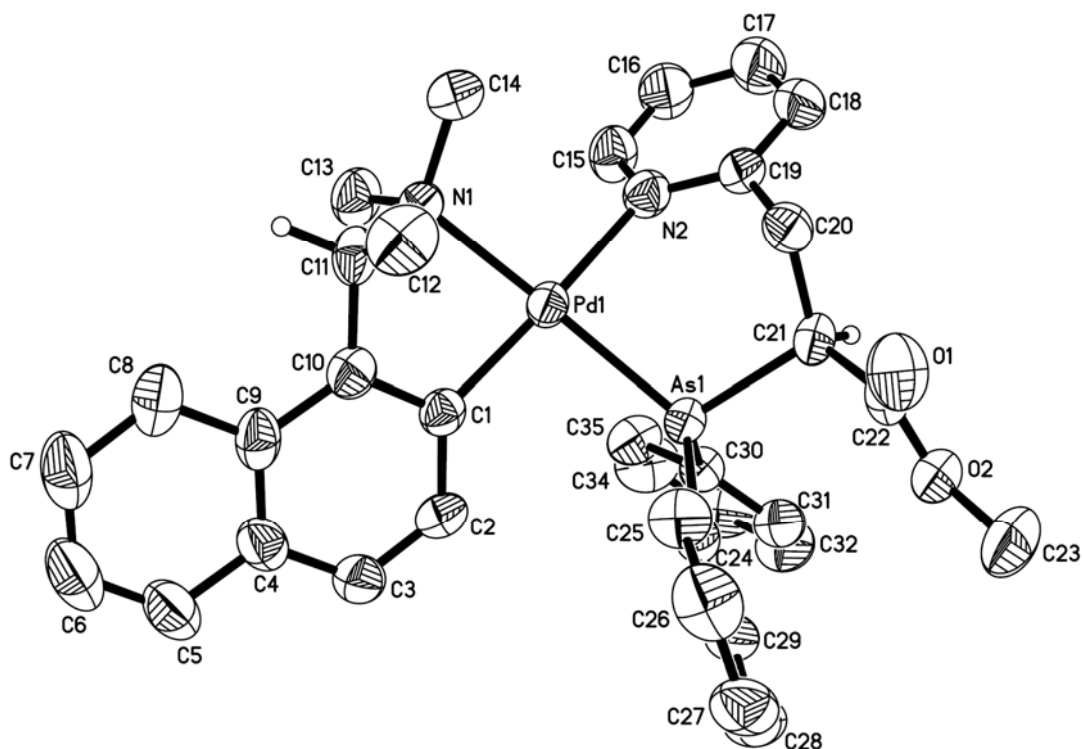
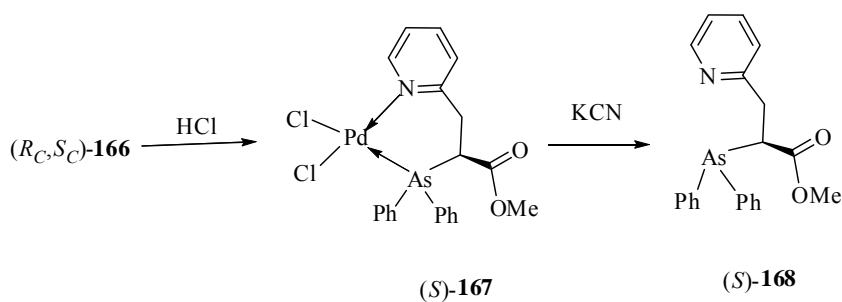


Figure 5.3 Molecular structure and absolute configuration of (*R<sub>C</sub>*, *S<sub>C</sub>*)-**166**

**Table 5.3 Selected bond lengths (Å) and (deg) angles for (*R<sub>C</sub>*, *S<sub>C</sub>*)-166**

Pd(1)–C(1)	1.994(5)	Pd(1)–N(1)	2.123(4)
Pd(1)–N(2)	2.168(4)	Pd(1)–As(1)	2.345 (1)
C(15)–N(2)	1.348(6)	C(19)–N(2)	1.346(6)
C(19)–C(20)	1.505(7)	C(20)–C(21)	1.533(7)
C(21)–As(1)	2.002(5)	C(22)–O(1)	1.195(6)
C(22)–O(2)	1.334(7)	C(30)–As(1)	1.938(4)
C(1)–Pd(1)–N(1)	81.0(2)	C(1)–Pd(1)–N(2)	171.6(2)
N(1)–Pd(1)–N(2)	95.6(1)	C(1)–Pd(1)–As(1)	95.57(6)
N(1)–Pd(1)–As(1)	97.7 (2)	N(2)–Pd(1)–As(1)	169.6 (2)
N(2)–C(19)–C(20)	117.1(4)	C(19)–C(20)–C(21)	111.0(4)
C(22)–C(21)–C(20)	110.9(4)	C(22)–C(21)–As(1)	110.6(3)
C(20)–C(21)–As(1)	110.0(3)	C(15)–N(2)–C(19)	118.9(2)
C(19)–N(2)–Pd(1)	118.5(4)	C(21)–As(1)–Pd(1)	106.4 (1)

**5.2.3.2 Liberation and the Optical Purity of (*S*)-168****Scheme 5.9**

The treatment of complex (*R<sub>C</sub>*, *S<sub>C</sub>*)-166 with concentrated hydrochloric acid generated (*S*)-167 (Scheme 5.9). The dichloro complex was subsequently crystallized from dichloromethane–diethyl ether as yellow prisms in 91% yield,  $[\alpha]_D -113^\circ$  (*c* 0.6, CH<sub>2</sub>Cl<sub>2</sub>). Further treatment of (*S*)-167 with aqueous cyanide liberated the optically

pure (*S*)-**168** as pale yellow solid in 80% yield,  $[\alpha]_D -102^\circ$  ( $c$  1.0,  $\text{CH}_2\text{Cl}_2$ ). The recoordination of the free ligand to (*R*)- and (*S*)-**144** employing the same protocol used for (*R*)-**161** confirmed that (*S*)-**168** is optically pure.

From a mechanistic standpoint, we believe that the mechanism involved in the asymmetric hydroarsination is similar to that of the hydrophosphination reaction.<sup>200</sup>

### 5.3 Conclusion

The chiral organopalladium template promoted asymmetric hydroarsination of pyridine and quinoline complexes has been demonstrated. The reaction showed regioselectivity in the case of (*E*)-1-phenyl-3-pyridin-2-yl-2-propenone and (*E*)-1-naphthyl-3-pyridin-2-yl-2-propenone with the hydroarsination products being formed in the ratio 3:1 as five-membered As-N bidentate chelates on the chiral naphthylamine palladium template. While using the same chiral metal template, the corresponding hydrophosphination reaction with (*E*)-1-methyl-3-pyridin-2-yl-2-propenoate only gave one product as a six-membered As-N bidentate chelate.

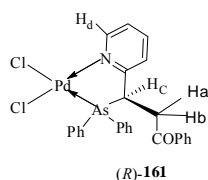
### 5.4 Experimental Section

Diphenylarsine<sup>211</sup> was prepared according to the literature methods.

**Dichloro-[(*R*)-1-phenyl-3-(diphenylarsino)-3-pyridin-2-yl-propanone- $N^1,As^2$ ]-palladium (II), [(*R*)-**161**].**

The bis(acetonitrile) Pd complex (*R*)-**144** (1 g, 2.05 mmol) in dichloromethane

(40 mL) was treated with (*E*)-1-phenyl-3-pyridin-2-yl-2-propenone (0.473 g, 2.26 mmol) and Ph<sub>2</sub>AsH (0.473 g, 2.05 mmol) at room temperature for 12 days. Removal of solvent under reduced pressure gave the crude product as a yellow solid. The crude product mixture was then purified through a silica gel column with dichloromethane–acetone as the eluent and then crystallized from dichloromethane–diethylether to give the complex (*R<sub>C</sub>*, *R<sub>C</sub>*)-**160** as a pale yellow glass (0.52 g, 30% yield) that could not be crystallized from any of the solvents attempted. The cationic complex (0.50 g, 0.593mmol) in dichloromethane (30 mL) was treated with concentrated hydrochloric acid (12 mL) for 1 h at room temperature. The reaction mixture was then washed with water (4 × 10 mL), and dried (MgSO<sub>4</sub>). Subsequent fractional recrystallization from dichloromethane–diethylether gave complex (*R*)-**161** as yellow prisms: mp 207–208 °C (decomp). [ $\alpha$ ]<sub>D</sub> -122° (*c* 0.6, CH<sub>2</sub>Cl<sub>2</sub>); 0.318 g (87% yield). Anal. Calcd for C<sub>26</sub>H<sub>22</sub>Cl<sub>2</sub>NOAsPd: C, 50.6; H, 3.6; N, 2.3. Found: C, 50.6; H, 4.0; N, 2.0. <sup>1</sup>H NMR (CD<sub>2</sub>Cl<sub>2</sub>):  $\delta$  3.57 (dd, <sup>2</sup>*J*<sub>HH</sub> = 18.6 Hz, <sup>3</sup>*J*<sub>HH</sub> = 5.6 Hz, 1 H, CH<sub>a</sub>H<sub>b</sub>), 3.87 (dd, <sup>2</sup>*J*<sub>HH</sub> = 18.6 Hz, <sup>3</sup>*J*<sub>HH</sub> = 8.0 Hz, 1H, CH<sub>a</sub>H<sub>b</sub>), 5.14 (dd, <sup>3</sup>*J*<sub>HH</sub> = 5.6 Hz, <sup>3</sup>*J*<sub>HH</sub> = 8.0 Hz, 1H, H<sub>c</sub>), 7.30–8.02 (m, 18 H, aromatics), 9.81(d, <sup>3</sup>*J*<sub>HH</sub> = 5.9 Hz, 1H, H<sub>d</sub>).



**(*R*)-1-phenyl-3-(diphenylarsino)-3-pyridin-2-yl-propanone, [(*R*)-**162**].**

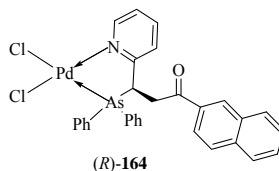
A solution of (*R*)-**161** (0.0617 g, 0.1mmol) in dichloromethane (15 mL) was

stirred vigorously with a saturated aqueous solution of potassium cyanide (0.2 g) for 5 min. The resulting colorless organic layer was separated, washed with water, and dried (MgSO<sub>4</sub>). Upon the removal of solvent, a white solid (*R*)-**162** was obtained:  $[\alpha]_D^{+77.8^\circ}$  (*c* 0.4, CH<sub>2</sub>Cl<sub>2</sub>); 0.033 g (75% yield). <sup>1</sup>H NMR (CD<sub>2</sub>Cl<sub>2</sub>):  $\delta$  3.23 (d, 1H, <sup>2</sup>*J*<sub>HH</sub> = 16Hz, CH<sub>a</sub>H<sub>b</sub>), 4.30-4.41 (m, 2H, H<sub>c</sub> + CH<sub>a</sub>H<sub>b</sub>), 6.84-7.88 (m, 18H, aromatics), 8.48(d, 1H, <sup>3</sup>*J*<sub>HH</sub> = 4.6 Hz, H<sub>d</sub>).

**Dichloro-[(*R*)-1-naphthyl-3-(diphenylarsino)-3-pyridin-2-yl-pentan-1-one-*N*<sup>I</sup>, As<sup>2</sup>]-palladium (II), [(*R*)-**164**].**

The bis(acetonitrile) Pd complex (*R*)-**144** (1.2 g, 2.468 mmol) in dichloromethane (40 mL) was treated with (*E*)-1-naphthyl-3-pyridin-2-yl-2-propenone (0.692 g, 2.668 mmol) and Ph<sub>2</sub>AsH (0.568 g, 2.468 mmol) at room temperature for 15 days. Removal of solvent under reduced pressure gave the crude product as a yellow solid. The crude product mixture was then purified through a silica gel column with dichloromethane-acetone as the eluent and then crystallized from dichloromethane-diethylether to give the complex (*R*<sub>C</sub>, *R*<sub>C</sub>)-**163** as a pale yellow glass (0.617 g, 28% yield) that could not be crystallized from any of the solvents attempted. The cationic complex (0.40 g, 0.448mmol) in dichloromethane (30 mL) was treated with concentrated hydrochloric acid (10 mL) for 1 h at room temperature. The reaction mixture was then washed with water (4 × 10 mL), and dried (MgSO<sub>4</sub>). Subsequent fractional recrystallization from dichloromethane-diethylether gave complex (*R*)-**164** as yellow prisms: mp 199-200 °C (decomp.);  $[\alpha]_D^{-76.5^\circ}$  (*c* 0.7, CH<sub>2</sub>Cl<sub>2</sub>); 0.275 g (92% yield). Anal. Calcd for C<sub>30</sub>H<sub>24</sub>Cl<sub>2</sub>NOAsPd: C, 54.0; H, 3.6; N,

2.1. Found: C, 54.1; H, 3.6; N, 2.5.  $^1\text{H NMR}$  ( $\text{CDCl}_3$ ):  $\delta$  3.69 (dd, 1H,  $^2J_{\text{HH}} = 18.3\text{Hz}$ ,  $^3J_{\text{HH}} = 6.4\text{Hz}$ ,  $\text{CH}_a\text{H}_b$ ), 3.91 (dd, 1H,  $^2J_{\text{HH}} = 18.3\text{Hz}$ ,  $^3J_{\text{HH}} = 7.2\text{Hz}$ ,  $\text{CH}_a\text{H}_b$ ), 5.11 (t, 1H,  $^3J_{\text{HH}} = 6.87\text{Hz}$ ,  $H_c$ ), 7.20-8.16 (m, 20H, aromatics), 9.87 (d, 1H,  $^3J_{\text{HH}} = 5.9\text{ Hz}$ ,  $H_d$ ).



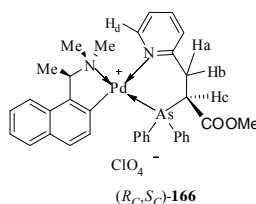
**(*R*)-1-Naphthyl-3-(diphenylarsino)-3-pyridin-2-yl-pentan-1-one, [(*R*)-165].**

A solution of (*R*)-**164** (0.12 g, 0.18 mmol) in dichloromethane (10 mL) was stirred vigorously with a saturated aqueous solution of potassium cyanide (0.4 g) for 5 min. The resulting colorless organic layer was separated, washed with water, and dried ( $\text{MgSO}_4$ ). Upon the removal of solvent, a white solid (*R*)-**165** was obtained:  $[\alpha]_{\text{D}}^{+174}$  ( $c$  0.5,  $\text{CH}_2\text{Cl}_2$ ); 0.075 g (85% yield).  $^1\text{H NMR}$  ( $\text{CD}_2\text{Cl}_2$ ):  $\delta$  3.34 (d, 3H,  $^3J_{\text{HH}} = 15.0\text{Hz}$ ,  $\text{CH}_a\text{H}_b$ ), 4.40-4.50 (m, 2H,  $H_c + \text{CH}_a\text{H}_b$ ), 6.82-8.47 (m, 21H, aromatics).

**{(*R*)-1-[1-(Dimethylamino)ethyl]naphthyl- $C^2,N$ }-[(*S*)-methyl-2-(diphenylarsino)-3-pyridin-2-yl-propanoate- $N^1,As^2$ ]-palladium (II) perchlorate, [( $R_C, S_C$ )-166].**

The bis(acetonitrile) Pd complex (*R*)-**144** (1.1 g, 2.3 mmol) in dichloromethane (40 mL) was treated with (*E*)-1-methyl-3-pyridin-2-yl-2-propenoate (0.411 g, 2.53 mmol) and  $\text{Ph}_2\text{AsH}$  (0.529 g, 2.3 mmol) at room temperature for 14 days. Removal of solvent under reduced pressure gave the crude product as a yellow solid. The crude product mixture was then purified through a silica gel column with dichloromethane–acetone as the eluent and then crystallized from dichloromethane–diethylether to give the complex ( $R_C, S_C$ )-**166** as pale yellow crystals: mp 204–205 °C (decomp).  $[\alpha]_{\text{D}}^{-77}$  ( $c$  0.6,  $\text{CH}_2\text{Cl}_2$ ); 0.92 g (51% yield). Anal. Calcd

for  $C_{35}H_{36}ClN_2O_6AsPd$ : C, 52.7; H, 4.6; N, 3.5. Found: C, 52.3; H, 4.5; N, 3.1.  $^1H$  NMR ( $CD_2Cl_2$ ):  $\delta$  2.23 (d,  $^3J_{HH} = 6.4$  Hz, 3 H, CHMe), 2.60 (s, 3 H, NMe), 3.00 (s, 3 H, NMe), 3.09 (s, 3 H, COOMe), 3.49 (dd,  $^3J_{HH} = 13.0$  Hz,  $^2J_{HH} = 2.3$  Hz, 1 H,  $H_a$ ), 3.82 (dd,  $^2J_{HH} = 14.3$  Hz,  $^3J_{HH} = 2.3$  Hz, 1 H,  $H_b$ ), 4.13 (m, 1 H,  $H_c$ ), 4.56 (qn,  $^3J_{HH} = 6.3$  Hz, 1 H, CHMe), 6.63–8.08 (m, 19 H, aromatics), 8.80 (d,  $^3J_{HH} = 5.3$  Hz, 1 H,  $H_d$ ).

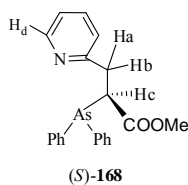


**Dichloro [(*S*)-methyl-2-(diphenylarsino)-3-pyridin-2-yl-propanoate- $N^1,As^2$ ]-palladium (II), [(*S*)-166].**

The naphthylamine auxiliary in  $(R_C, S_C)$ -166 was removed chemoselectively by adding concentrated hydrochloric acid (15 mL) to a solution of the complex  $(R_C, S_C)$ -166 (0.3705 g, 0.46 mmol) in dichloromethane (20 mL). The reaction mixture was stirred vigorously for 1 h at room temperature. The reaction mixture was then washed with water ( $4 \times 10$  mL), and dried ( $MgSO_4$ ). Subsequent fractional crystallization from dichloromethane–diethylether gave complex (*S*)-167 as yellow prisms: mp 233–234 °C (decomp);  $[\alpha]_D -113^\circ$  ( $c$  0.6,  $CH_2Cl_2$ ); 0.2 g (91% yield). Anal. Calcd for  $C_{21}H_{20}Cl_2NO_2AsPd$ : C, 44.2; H, 3.5; N, 2.5. Found: C, 44.3; H, 3.9; N, 2.1.  $^1H$  NMR ( $CD_2Cl_2$ ):  $\delta$  3.18 (s, 3 H,  $COOCH_3$ ), 3.35 (dd,  $^2J_{HH} = 12.3$  Hz,  $^3J_{HH} = 2$  Hz, 1 H,  $H_a$ ), 3.78 (dd,  $^2J_{HH} = 14.5$  Hz,  $^3J_{HH} = 2$  Hz, 1 H,  $H_b$ ), 4.04 (dd,  $^3J_{HH} = 14.5$  Hz,  $^3J_{HH} = 12.3$  Hz, 1 H,  $H_c$ ), 7.34–8.14 (m, 14H, aromatics), 9.34 (d,  $^3J_{HH} = 5.3$  Hz, 1H,  $H_d$ ).

**(*S*)-methyl-2-(diphenylarsino)-3-pyridin-2-yl-propanoate, [(*S*)-168].**

A solution of (*S*)-**167** (0.057 g, 0.1mmol) in dichloromethane (15 mL) was stirred vigorously with a saturated aqueous solution of potassium cyanide (0.2 g) for 5 min. The resulting colorless organic layer was separated, washed with water, and dried ( $\text{MgSO}_4$ ). Upon the removal of solvent, a white solid (*S*)-**168** was obtained:  $[\alpha]_D -102^\circ$  ( $c$  1.0,  $\text{CH}_2\text{Cl}_2$ ); 0.031 g (80% yield).  $^1\text{H NMR}$  ( $\text{CD}_2\text{Cl}_2$ ):  $\delta$  3.13 (dd,  $^3J_{\text{HH}} = 14.8$  Hz,  $^2J_{\text{HH}} = 4.7$  Hz, 1 H,  $H_a$ ), 3.22(s, 3 H,  $\text{COOCH}_3$ ), 3.47 (dd,  $^3J_{\text{HH}} = 14.8$  Hz,  $^3J_{\text{HH}} = 10.9$  Hz, 1 H,  $H_c$ ), 3.93(dd,  $^3J_{\text{HH}} = 10.9$  Hz,  $^2J_{\text{HH}} = 4.7$  Hz, 1 H,  $H_b$ ), 7.07–7.63(m, 14H, aromatics ), 8.49(d,  $^3J_{\text{HH}} = 4.5$  Hz, 1 H,  $H_d$ ).



# Chapter 6

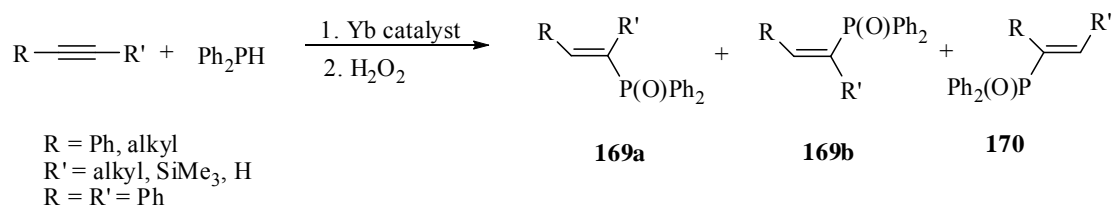
## Asymmetric Hydrophosphination Reaction of Phosphinoalkynes

### 6.1 Introduction

In many organoalkynyl complexes, the carbon-carbon triple bonds are chemically reactive and are able to undergo various addition reactions, such as hydrogenation, acid-catalyzed hydration, hydroboration, and other hydrometallation reactions.<sup>212</sup> Addition of P-H bonds to carbon-carbon unsaturated compounds of alkynes also can proceed by thermal,<sup>213</sup> acidic,<sup>195a,214</sup> basic,<sup>215</sup> or free radical<sup>216</sup> pathways. The metal-catalyzed hydrophosphination of alkynes has been less explored than the corresponding reaction involving alkene derivatives, only a few examples of intramolecular processes with organolanthanide complexes have been reported, together with some palladium-, rhodium-, and nickel-catalyzed intermolecular reactions.<sup>213d</sup>

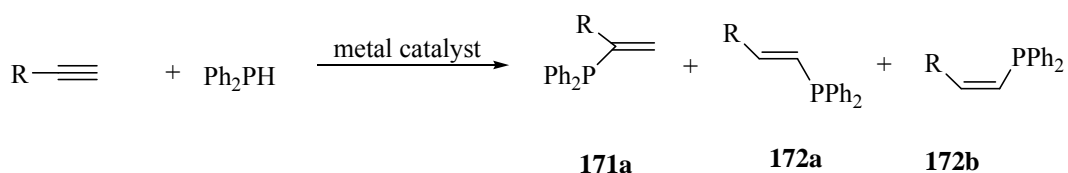
The ytterbium-imine complex  $(Yb(\eta^2\text{-Ph}_2\text{CNPh})(\text{hmpa})_3)$  can catalyze the intermolecular hydrophosphination of alkynes with diphenylphosphine to give alkenylphosphine oxides after treatment with  $\text{H}_2\text{O}_2$  (Scheme 6.1).<sup>217</sup> Aromatic alkynes gave exclusively the products **169a** and **169b** where a  $\text{Ph}_2\text{P(O)}$  group was added to the opposite side of the aryl group, with *E*-adducts **169a** being formed predominantly. With aliphatic alkynes, a mixture of the products, **169** and **170** are produced with

Z-adduct **169b** predominant.



**Scheme 6.1**

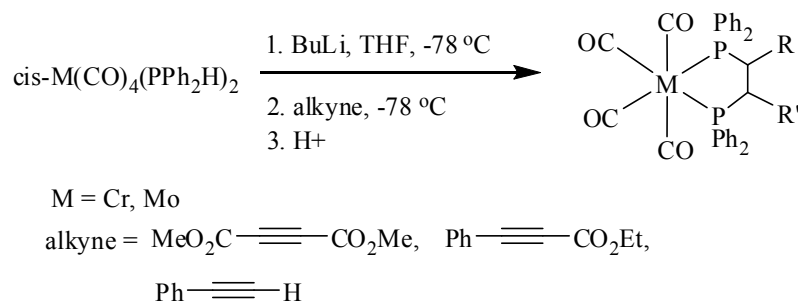
In 2001, Beletskaya reported palladium and nickel complexes catalyze the hydrophosphination of aliphatic and aromatic alkynes in high yields (Scheme 6.2).<sup>218</sup> The regio- and stereoselectivities of the reaction depends on the nature of the catalyst, alkyne and solvent. Pd(0), Ni(0) and Ni(acac)<sub>2</sub> complexes generated anti-Markovnikov vinylphosphines **172** as the major products, while Pd(II) or Ni(II), complexes favoured Markovnikov adducts **171** as the major products.



**Scheme 6.2**

Stoichiometric transition metal complexes were used to promote the P-H addition to alkynes. Diphenylphosphine chromium, molybdenum and manganese complexes were first deprotonated with strong base to generate the phosphido

complex, which subsequently underwent Michael addition to alkynes, followed by protonation with acid to give the products in low to moderate yields (Scheme 6.3).<sup>219</sup>



**Scheme 6.3**

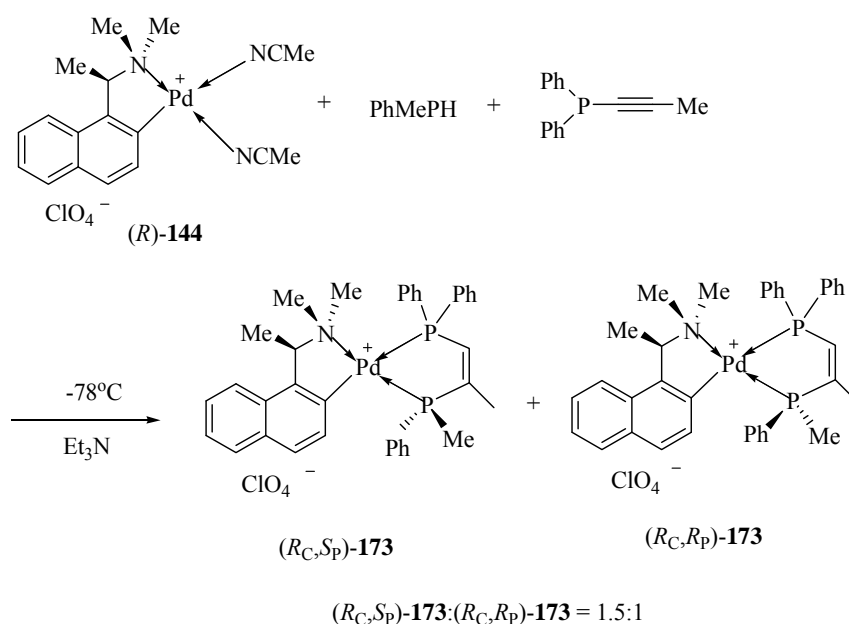
In this chapter, we would like to extend the scope of the chiral cyclometalated-amine template promoted asymmetric hydrophosphination to those between ethynylphosphines and methylphenylphosphine to form a *P*-chiral diphosphine.

## 6.2 Results and Discussion

### 6.2.1 Hydrophosphination of Diphenyl(phenylethynyl)phosphine

In the presence of chiral palladium complex (*R*)-**144** and a trace amount of  $\text{Et}_3\text{N}$ , the reaction between diphenyl(phenylethynyl)phosphine and methylphenylphosphine proceeded smoothly at  $-78\text{ }^\circ\text{C}$  for 1 h to generate two stereochemically distinct products (Scheme 6.4). Prior to purification, the  $^{31}\text{P}\{^1\text{H}\}$  NMR spectrum in  $\text{CDCl}_3$  exhibited two pairs of doublets in the ratio of 1:1.5. The

doublets of major diastereomer ( $R_C, S_P$ )-**173** were observed at  $\delta$  52.9, 38.2 ( $J_{PP} = 16.1$  Hz) and the doublets of the other isomer ( $R_C, R_P$ )-**173** were recorded at  $\delta$  51.5, 37.5 ( $J_{PP} = 16.0$  Hz). After purification by column chromatography, the major isomer ( $R_C, S_P$ )-**173** was subsequently crystallized as colorless crystals from dichloromethane-diethyl ether in 35% yield,  $[\alpha]_D +36.7^\circ$  ( $c$  0.9,  $\text{CH}_2\text{Cl}_2$ ).



**Scheme 6.4**

### 6.2.1.1 Single Crystal X-ray Structural Analysis of ( $R_C, S_P$ )-**173**

The molecular structure and the absolute stereochemistry of the major product ( $R_C, S_P$ )-**173** were determined by single crystal X-ray diffraction analysis (Figure 6.1). As expected, the five-membered diphosphine chelates were formed and the absolute stereochemistries at the newly generated P(2) was *S*. The geometry at the Pd centre is distorted square planar with angles of 84.2(1)-103.5(1) $^\circ$  and 167.9(1)-174.3(1) $^\circ$ . In this molecule, the phenyl group on P(1) and the neighboring N-Me groups on the

organometallic ring are in an unfavorable pseudoeclipsed orientation. In addition, the naphthylene proton H(2) is protruding toward the quasi-axial phenyl group on P(2). A serious tetrahedral distortion of  $10.3^\circ$  is observed in the square planar geometry at palladium. This geometrical adjustment is crucial in providing partial relief to the unfavorable interchelate steric repulsions. Selected bond lengths and angles are given in Table 6.1.

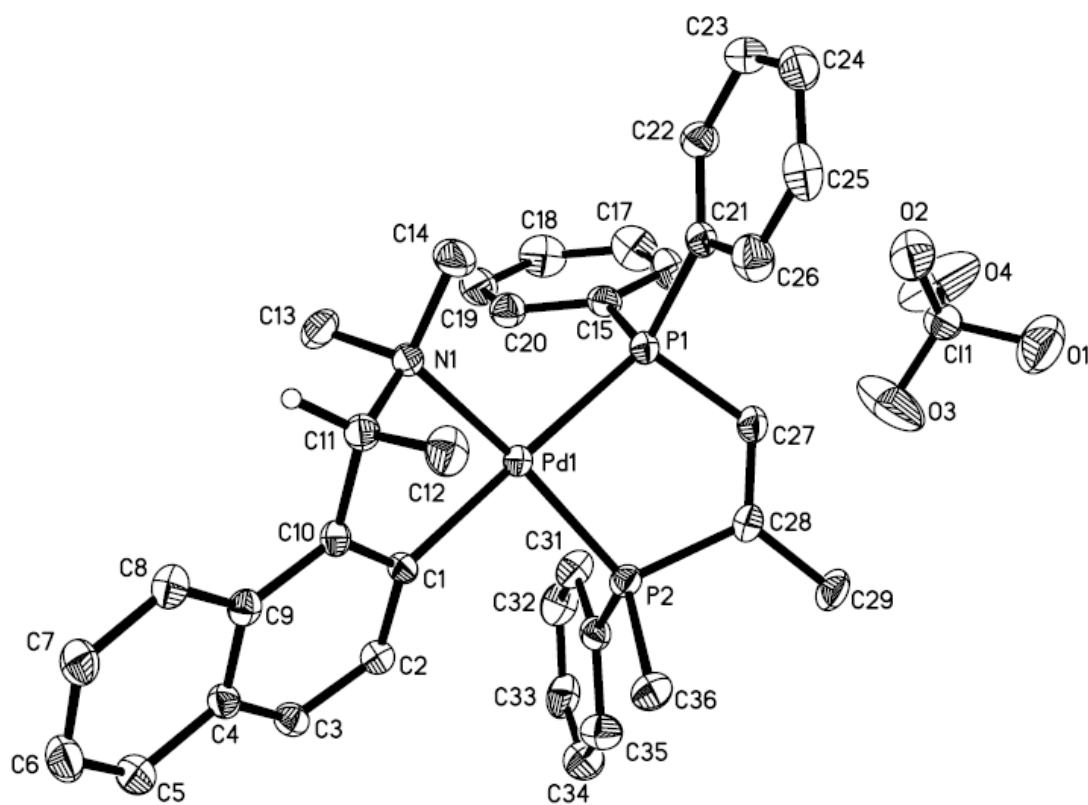


Figure 6.1 Molecular structure and absolute configuration of ( $R_C$ ,  $S_P$ )-173

**Table 6.1 Selected bond lengths (Å) and (deg) angles for (*R<sub>C</sub>*, *S<sub>P</sub>*)-173**

Pd(1)-C(1)	2.046(4)	N(1)-Pd(1)-P(2)	167.9(1)
Pd(1)-N(1)	2.157(3)	C(1)-Pd(1)-P(1)	174.3(1)
Pd(1)-P(2)	2.241(1)	N(1)-Pd(1)-P(1)	103.5(1)
Pd(1)-P(1)	2.349 (1)	P(2)-Pd(1)-P(1)	84.2 (1)
C(27)-C(28)	1.311(6)	C(28)-C(27)-P(1)	120.6(3)
C(27)-P(1)	1.810(4)	C(27)-C(28)-C(29)	123.7(4)
C(28)-C(29)	1.506(5)	C(27)-C(28)-P(2)	117.4(3)
C(28)-P(2)	1.832(4)	C(29)-C(28)-P(2)	118.7(3)
C(1)-Pd(1)-N(1)	80.1(1)	C(27)-P(1)-Pd(1)	106.3(2)
C(1)-Pd(1)-P(2)	93.1(1)	C(28)-P(2)-Pd(1)	109.6(1)

### 6.2.1.2 Preparation of the Dichloro Complex (*S<sub>P</sub>*)-174

Upon subsequent treatment of the perchlorate salt with concentrated hydrochloric acid, the resultant dichloro complex (*S<sub>P</sub>*)-**174** was obtained as colorless crystals in 88.2% isolated yield,  $[\alpha]_D +44^\circ$  (*c* 0.5, CH<sub>2</sub>Cl<sub>2</sub>) (Scheme 6.5). The <sup>31</sup>P{<sup>1</sup>H} NMR spectrum of (*S<sub>P</sub>*)-**174** in CD<sub>2</sub>Cl<sub>2</sub> exhibited two doublets at  $\delta$  68.7, 58.3 ( $J_{PP} = 14.6$ ). The structure of (*S<sub>P</sub>*)-**174** is further confirmed by X-ray structural analysis.

### 6.2.1.3 X-ray Structural Analysis of (*S<sub>P</sub>*)-174

The molecular structure and the absolute configuration of the recrystallised (*S<sub>P</sub>*)-**174** were established by single crystal X-ray crystallographic analysis (Figure 6.2). The absolute configurations of the stereogenic centers were found to be retained even after reaction under acidic conditions. Selected bond parameters are given in Table 6.2.

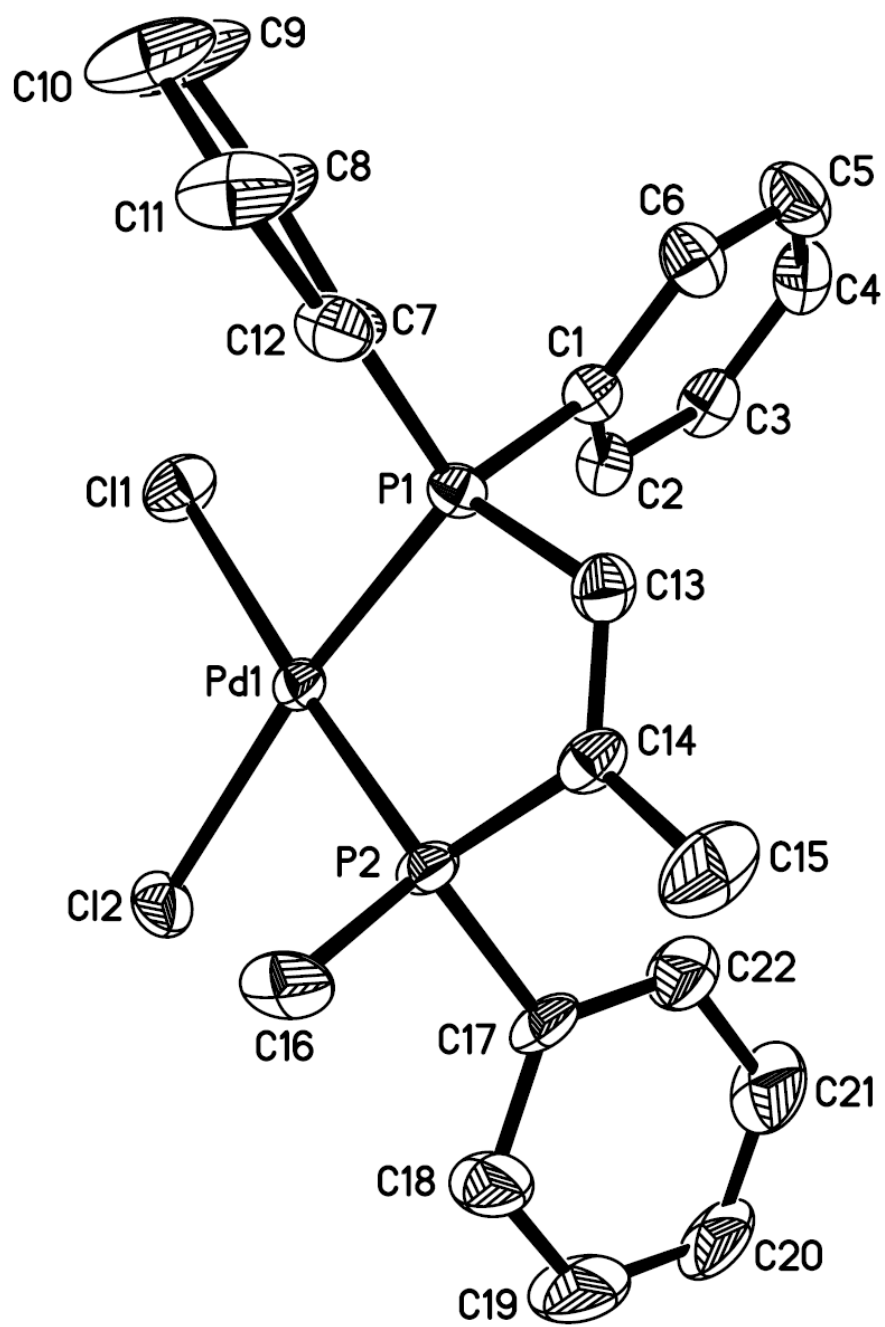


Figure 6.2 Molecular structure and absolute configuration of (S<sub>P</sub>)-174

**Table 6.2 Selected bond lengths (Å) and (deg) angles for (*S<sub>P</sub>*)-174**

Pd(1)-P(2)	2.208(2)	P(2)-Pd(1)-Cl(2)	87.3(1)
Pd(1)-P(1)	2.220(2)	P(1)-Pd(1)-Cl(2)	172.7(1)
Pd(1)-Cl(2)	2.365(2)	P(2)-Pd(1)-Cl(1)	176.2(1)
Pd(1)-Cl(1)	2.370(2)	P(1)-Pd(1)-Cl(1)	90.5(1)
C(13)-C(14)	1.340(9)	Cl(2)-Pd(1)-Cl(1)	96.4(1)
C(13)-P(1)	1.805(6)	C(14)-C(13)-P(1)	118.8(5)
C(13)-H(13)	0.950	C(13)-C(14)-C(15)	124.1(7)
C(14)-C(15)	1.499(9)	C(13)-C(14)-P(2)	116.1(5)
C(14)-P(2)	1.819(7)	C(13)-P(1)-Pd(1)	109.1(2)
C(16)-P(2)	1.808(6)	C(16)-P(2)-C(14)	104.6(4)
P(2)-Pd(1)-P(1)	85.7(1)	C(14)-P(2)-Pd(1)	110.2(2)

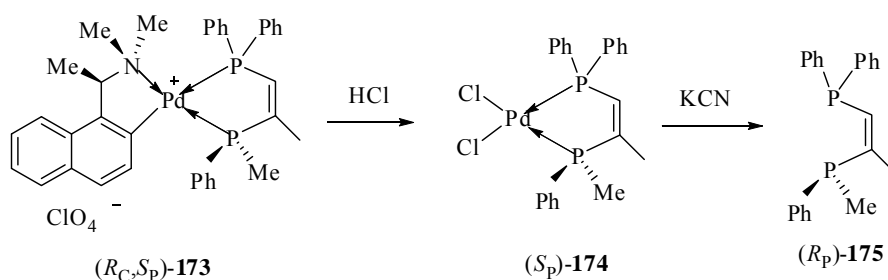
#### 6.2.1.4 Liberation and the Optical Purity of (*R<sub>P</sub>*)-175

It is noteworthy that the optically active diphosphine ligand with chirality residing on the P atom (*R<sub>P</sub>*)-175 can be stereospecifically cleaved from the complex (*S<sub>P</sub>*)-174 by treatment of the dichloro complex with aqueous potassium cyanide at room temperature for 1 h.

The liberated (*R<sub>P</sub>*)-175 was obtained as an air stable white solid in 87% yield,  $[\alpha]_D +80^\circ$  (*c* 0.7, CH<sub>2</sub>Cl<sub>2</sub>). The <sup>31</sup>P{<sup>1</sup>H} NMR spectrum showed resonances at  $\delta$  -26.0 and -33.5 (<sup>3</sup>*J*<sub>PP</sub> = 160 Hz). To establish the identities of the minor products generated in the hydrophosphination reaction, (*R<sub>P</sub>*)-175 was re-complexed to the bis(acetonitrile) complex (*R*)-144. The re-complexation of the related ligand (*R<sub>P</sub>*)-175 to the bis(acetonitrile) complex (*R*)-144 was monitored by <sup>31</sup>P{<sup>1</sup>H} NMR spectroscopy and gave signals at  $\delta$  52.9, 38.2 (*J*<sub>PP</sub> = 16.1 Hz) and 51.2, 40.6 (*J*<sub>PP</sub> = 16.3 Hz). The resonance signals at  $\delta$  52.9, 38.2 (*J*<sub>PP</sub> = 16.1 Hz) are identical to those observed for the

major product ( $R_C, S_P$ )-**173** in the original hydrophosphination reaction. The signals at  $\delta$  51.2 and 40.6 ( $J_{PP} = 16.3$  Hz) were not seen in the original reaction mixture and so the two products in the original reaction are not the regioisomers.

The re-complexation reaction with ( $S$ )-**144** gave signals at  $\delta$  51.5, 37.5 ( $J_{PP} = 16.0$  Hz) and 50.9, 39.7 ( $J_{PP} = 15.5$  Hz). The resonance signals at  $\delta$  51.5, 37.5 ( $J_{PP} = 16.0$  Hz) are identical to those observed for the minor product ( $R_C, R_P$ )-**173** in the original hydrophosphination reaction. So the minor product ( $R_C, R_P$ )-**173** is the diastereomeric complex of the major product ( $R_C, S_P$ )-**173**.

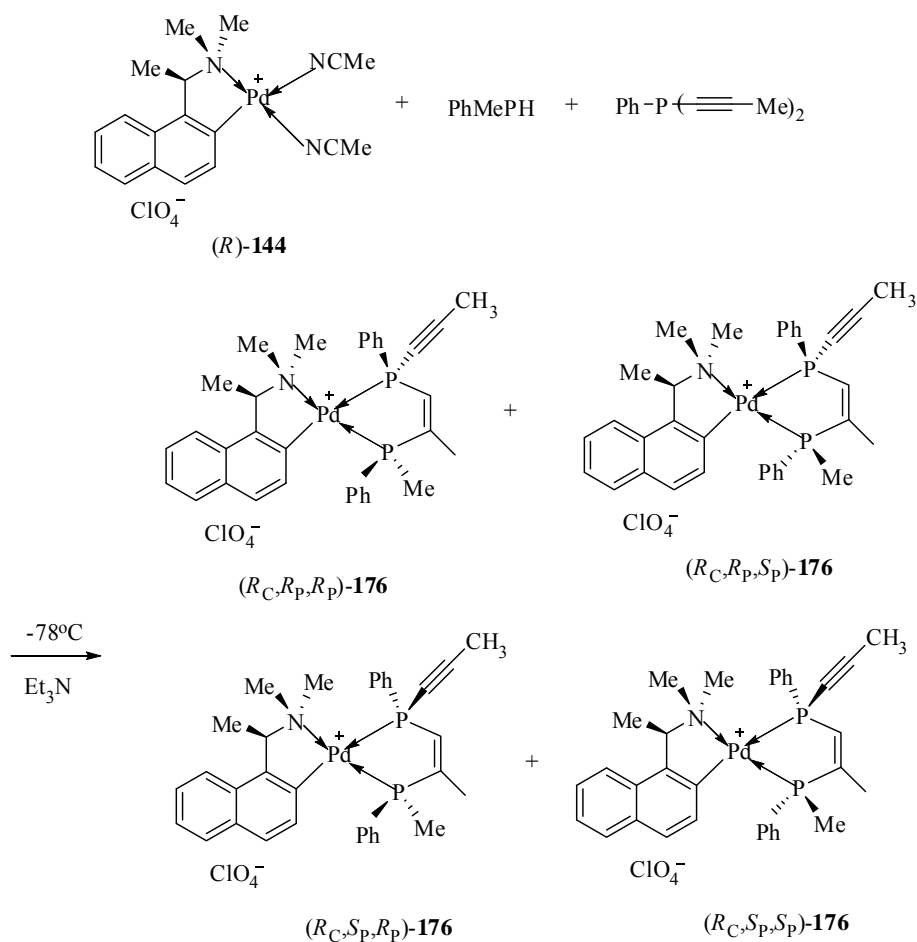


**Scheme 6.5**

### 6.2.2 Hydrophosphination of Di(phenylethynyl)phenylphosphine

In the presence of chiral palladium complex ( $R$ )-**144** and a trace amount of  $\text{Et}_3\text{N}$ , the reaction between di(phenylethynyl)phenylphosphine and methylphenylphosphine proceeded at  $-78^\circ\text{C}$  for 2 h to generate four stereochemically distinct products. Prior to purification, the  $^{31}\text{P}\{^1\text{H}\}$  NMR spectrum in  $\text{CDCl}_3$  exhibited four pairs of doublets in the ratio of 1:3:4:1.1 (Scheme 6.6). The doublets of these diastereomers were observed at  $\delta$  54.1, 13.2 ( $J_{PP} = 14.8$  Hz), and 53.8, 13.0 ( $J_{PP} = 16.1$  Hz), and 52.4, 12.4 ( $J_{PP} = 14.8$  Hz), and 50.9, 13.5 ( $J_{PP} = 16.1$  Hz). After

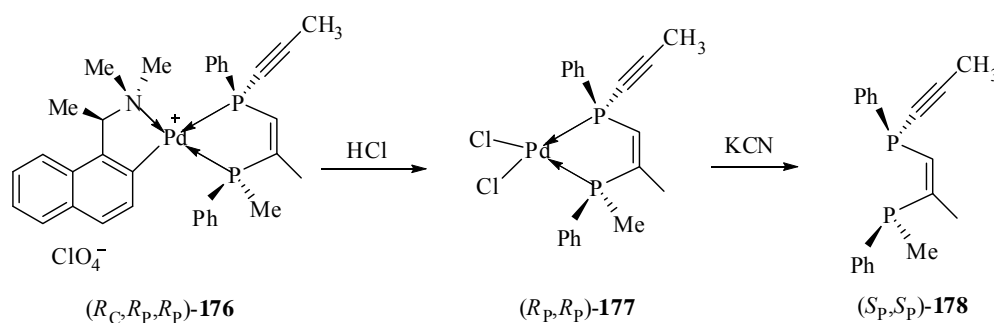
purification by column chromatography, the major product ( $R_P, R_P, R_P$ )-**176** ( $\delta$  52.4, 12.4 ( $J_{PP} = 14.8$  Hz)) could be obtained as the predominant species in a diastereomerically enriched mixture, with only a small amount of the other isomeric product  $\delta$  50.9, 13.5 ( $J_{PP} = 16.1$  Hz) (<10%).



Scheme 6.6

Subsequent treatment of this mixture with concentrated hydrochloric acid effected the chemoselective removal of the chiral naphthylamine auxiliary. Upon recrystallization of the crude product from dichloromethane-diethyl ether, the optically pure dichloro complex ( $R_P, R_P$ )-**177** was obtained as colorless crystals in

25.4% yield,  $[\alpha]_{436} +47.5^\circ$  ( $c$  0.4,  $\text{CH}_2\text{Cl}_2$ ). The  $^{31}\text{P}\{^1\text{H}\}$  NMR spectrum of this neutral dichloro complex in  $\text{CDCl}_3$  exhibited two doublets at  $\delta$  70.6, 29.7 ( $J_{\text{PP}} = 14.6$  Hz). The chelating properties and the absolute configuration of the coordinated diphosphine ligand in complex  $(R_{\text{P}}, R_{\text{P}})$ -**177** were studied by X-ray crystallography.



**Scheme 6.7**

### 6.2.2.1 Single Crystal X-ray Structural Analysis of $(R_{\text{P}}, R_{\text{P}})$ -**177**

The molecular structure and the absolute configuration of  $(R_{\text{P}}, R_{\text{P}})$ -**177** were established by single crystal X-ray crystallographic analysis. The absolute configurations at P(1), and P(2) in the complex were *R* and *R*. The geometry at the palladium centre is distorted square planar with angles at palladium in the range of  $85.4(1)$ - $95.4(1)^\circ$  and  $173.8(1)$ - $176.2(1)^\circ$ .

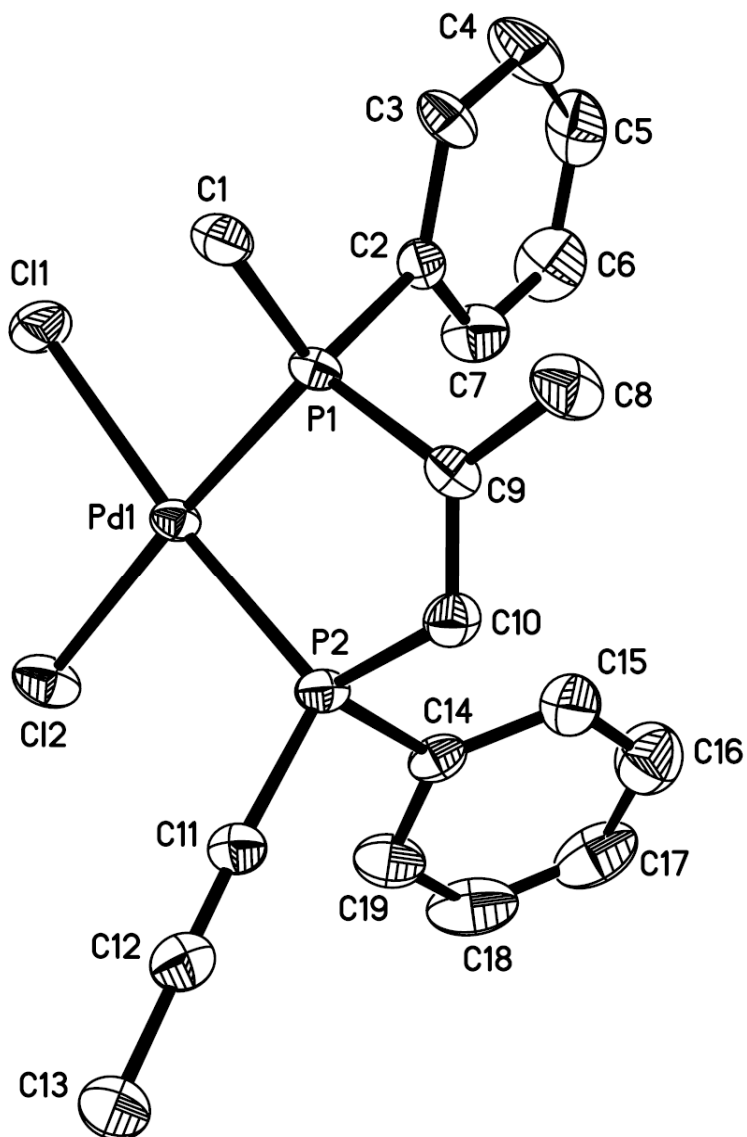


Figure 6.3 Molecular structure and absolute configuration of ( $R_p$ ,  $R_p$ )-177

**Table 6.3 Selected bond lengths (Å) and (deg) angles for (*R<sub>P</sub>*, *R<sub>P</sub>*)-177**

C(1)-P(1)	1.805(4)	C(12)-C(11)-P(2)	177.3(5)
C(8)-C(9)	1.504(5)	C(11)-C(12)-C(13)	178.8(7)
C(9)-C(10)	1.333(6)	C(1)-P(1)-C(9)	105.1(2)
C(9)-P(1)	1.814(4)	C(1)-P(1)-C(2)	108.0(2)
C(10)-P(2)	1.812(4)	C(1)-P(1)-Pd(1)	116.5 (2)
C(11)-C(12)	1.176(7)	C(9)-P(1)-Pd(1)	109.6(2)
C(11)-P(2)	1.753(5)	C(11)-P(2)-C(10)	106.9(2)
C(12)-C(13)	1.462(8)	C(11)-P(2)-Pd(1)	115.5(2)
Cl(1)-Pd(1)	2.356(1)	C(10)-P(2)-Pd(1)	109.2(2)
Cl(2)-Pd(1)	2.355(1)	P(2)-Pd(1)-P(1)	85.4 (1)
P(1)-Pd(1)	2.215(1)	P(2)-Pd(1)-Cl(2)	90.8(1)
P(2)-Pd(1)	2.212(1)	P(1)-Pd(1)-Cl(2)	176.2 (1)
C(10)-C(9)-C(8)	123.8(4)	P(2)-Pd(1)-Cl(1)	173.8(1)
C(10)-C(9)-P(1)	116.9(3)	P(1)-Pd(1)-Cl(1)	88.4(1)
C(9)-C(10)-P(2)	117.9(3)	Cl(2)-Pd(1)-Cl(1)	95.4 (1)

**6.2.2.2 Liberation and the Optical Purity of (*S<sub>P</sub>*, *S<sub>P</sub>*)-178**

The optically active diphosphine ligand (*S<sub>P</sub>*, *S<sub>P</sub>*)-**178** can be stereospecifically cleaved from the complex (*R<sub>P</sub>*, *R<sub>P</sub>*)-**177** by treatment of the dichloro complex with aqueous potassium cyanide at room temperature for 1 h (Scheme 6.7). The liberated (*S<sub>P</sub>*, *S<sub>P</sub>*)-**178** was obtained as an air stable white solid in 80% yield,  $[\alpha]_{\text{D}} +27^{\circ}$  (*c* 0.5, CH<sub>2</sub>Cl<sub>2</sub>). The <sup>31</sup>P{<sup>1</sup>H} NMR spectrum showed resonances at  $\delta$  -25.5 and -32.0 (<sup>3</sup>*J*<sub>PP</sub> = 164 Hz).

In order to confirm the optical purity of the liberated diphosphine ligand (*S<sub>P</sub>*, *S<sub>P</sub>*)-**185** and to established the identity of the other isomers that were generated in the original hydrophosphination reaction, (*S<sub>P</sub>*, *S<sub>P</sub>*)-**178** re-complexed to the bis(acetonitrile) complex (*R*)-**144** to give only a pair of regioisomeric complexes. The resonance signals at  $\delta$  52.4, 12.4 (*J*<sub>PP</sub> = 14.8 Hz) are identical to those observed for the major

product ( $R_P, R_P, R_P$ )-**176** in the original hydrophosphination reaction. Reoordination of ( $S_P, S_P$ )-**178** with ( $S$ )-**144** to gave signals at  $\delta$  49.5, 15.0 ( $J_{PP} = 15.7$  Hz) and 50.9, 13.5 ( $J_{PP} = 16.1$ Hz). The resonance signals at  $\delta$  50.9, 13.5 ( $J_{PP} = 16.1$  Hz) are identical to those observed for the minor product ( $R_C, S_P, S_P$ )-**176** in the original hydrophosphination reaction. So ( $R_C, S_P, S_P$ )-**176** is the diastereomeric complex of the major product ( $R_P, R_P, R_P$ )-**176**.

### 6.3 Conclisitons

In summary, we have demonstrated that transition metal complex-promoted asymmetric hydrophosphination is a potential synthetic route for the preparation of *P*-chiral diphosphines. However the stereocontrol at the phosphorus center is not very efficient ( $S_P:R_P = 1:3$  or 1:1).

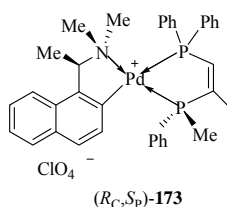
### 6.4 Experimental Section

Methylphenylphosphine,<sup>220</sup> diphenyl(phenylethynyl)phosphine and di(phenylethynyl)phenylphosphine<sup>221</sup> were prepared according to literature methods.

**{(R)-1-[1-(Dimethylamino)ethyl]naphthyl-C<sup>2</sup>N}-[(S)-1-methyl-(1-phenyl)phosphino-2-diphenylphosphinopropene-*P*<sup>1</sup>,*P*<sup>2</sup>]palladium (II) Perchlorate, [( $R_C, S_P$ )-**173**].**

To the bis(acetonitrile) Pd complex ( $R$ )-**144** (0.486 g, 1 mmol) in dichloromethane (40 mL), PhMePH (0.124 g, 1 mmol) and diphenyl(phenylethynyl)p-

hosphine (0.224 g, 1 mmol) were added at  $-78\text{ }^{\circ}\text{C}$ . Then a trace amount of  $\text{Et}_3\text{N}$  was added into the solution with stirring for 1 h. Removal of solvent under reduced pressure gave the crude product as a dark yellow solid. The crude product mixture was then purified through a silica gel column with dichloromethane-acetone as the eluent and then crystallized from dichloromethane-diethyl ether to give the complex ( $R_C$ ,  $S_P$ )-**173** as colorless crystals: mp  $216\text{-}217\text{ }^{\circ}\text{C}$  (decomp.);  $[\alpha]_D +36.7^{\circ}$  ( $c$  0.9,  $\text{CH}_2\text{Cl}_2$ ); 0.264 g (35% yield). Anal. Calcd for  $\text{C}_{36}\text{H}_{38}\text{ClNO}_4\text{P}_2\text{Pd}$ : C, 57.5; H, 5.1; N, 1.9. Found: C, 57.9; H, 4.8; N, 1.6.  $^{31}\text{P}\{^1\text{H}\}$  NMR ( $\text{CDCl}_3$ ):  $\delta$  52.9 (d, 1 P,  $J_{\text{PP}} = 16.1$ , P), 38.2 (d, 1 P,  $J_{\text{PP}} = 16.1$ , P);  $^1\text{H}$  NMR ( $\text{CDCl}_3$ ):  $\delta$  1.77 (d, 3H,  $^3J_{\text{HH}} = 6.1$  Hz,  $\text{CHMe}$ ), 2.14 (d, 3H,  $^3J_{\text{PH}} = 8.9$  Hz,  $\text{Me}$ ), 2.20 (d, 3H,  $^2J_{\text{PH}} = 10.3$  Hz,  $\text{PMe}$ ), 2.64 (s, 3H,  $\text{NMe}$ ), 2.81 (s, 3H,  $\text{NMe}$ ), 4.42 (qn, 1H,  $^3J_{\text{HH}} = ^4J_{\text{PH}} = 6.1$  Hz,  $\text{CHMe}$ ), 6.80-7.90 (m, 21H, aromatics+ $\text{CH}$ ).



**Dichloro-[(*S*)-1-methyl-(1-phenyl)phosphino-2-diphenylphosphinopropene- $P^1$ ,  $P^2$ ]palladium (II), [( $S_P$ )-**174**].**

The naphthylamine auxiliary in dichloromethane was removed chemoselectively by adding concentrated hydrochloric acid (15 mL) to a solution of the complex ( $R_C$ ,  $S_P$ )-**173** (0.100 g, 0.13mmol) in dichloromethane (15 mL). The reaction mixture was stirred vigorously for 1 h at room temperature. The reaction mixture was then washed with water ( $4 \times 10$  mL), and dried ( $\text{MgSO}_4$ ). Subsequent fractional crystallization from dichloromethane-diethyl ether gave complex ( $S_P$ )-**174**

as colorless prisms: mp 255-256 °C (decomp);  $[\alpha]_D +44^\circ$  ( $c$  0.5, CH<sub>2</sub>Cl<sub>2</sub>); 0.07 g (88.2% yield). Anal. Calcd for C<sub>30</sub>H<sub>24</sub>Cl<sub>2</sub>NOPPd: C, 50.3; H, 4.2. Found C 50.5, H 3.8. <sup>31</sup>P{<sup>1</sup>H} NMR (CD<sub>2</sub>Cl<sub>2</sub>):  $\delta$  68.7 (d, 1 P,  $J_{PP} = 14.6$ ,  $P$ ), 58.3 (d, 1 P,  $J_{PP} = 14.6$ ,  $P$ ); <sup>1</sup>H NMR (CDCl<sub>3</sub>):  $\delta$  2.15 (d, 3H,  $^3J_{PH} = 8.7$  Hz,  $Me$ ), 2.32 (d, 3H,  $^2J_{PH} = 10.3$  Hz,  $PMe$ ), 6.83 (dd, 1H,  $^2J_{PH} = 63.5$  Hz,  $^3J_{PH} = 13.0$  Hz,  $CH$ ), 7.54-7.96 (m, 15H, aromatics).

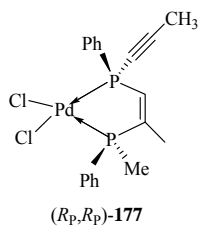
**[(*S*)-1-methyl-(1-phenyl)phosphino-2-diphenylphosphinopropene, (*R<sub>P</sub>*)-175].**

A solution of (*S<sub>P</sub>*)-**174** (0.02 g, 0.02 mmol) in dichloromethane (20 mL) was stirred vigorously with a saturated aqueous solution of potassium cyanide (0.5 g) for 5 min. The resulting colorless organic layer was separated, washed with water, and dried (MgSO<sub>4</sub>). Upon the removal of solvent, a white solid (*R<sub>P</sub>*)-**175** was obtained:  $[\alpha]_D +80^\circ$  ( $c$  0.7, CH<sub>2</sub>Cl<sub>2</sub>); 0.011 g (87% yield). <sup>31</sup>P{<sup>1</sup>H} NMR (CDCl<sub>3</sub>):  $\delta$  -26.0 (d, 1P,  $^3J_{PP} = 160$  Hz,  $P$ ), -33.5 (d, 1P,  $^3J_{PP} = 160$  Hz,  $P$ ).

**Dichloro-[(1*R*,2*R*)-1-methyl-(1-phenylphosphino)-2-phenyl-(methylethynyl)phosphinopropene -*P*<sup>1</sup>,*P*<sup>2</sup>]palladium (II), [(*R<sub>P</sub>*, *R<sub>P</sub>*)-177].**

To the bis(acetonitrile) Pd complex (*R*)-**144** (0.392 g, 0.81 mmol) in dichloromethane (40 mL), PhMePH (0.1 g, 0.81 mmol) and di(phenylethynyl)phenylphosphine (0.15 g, 0.81 mmol) were added at -78 °C. Then a trace amount of Et<sub>3</sub>N was added into the solution with stirring for 2 h. Removal of solvent under reduced pressure gave the crude product as a dark yellow solid. The crude product mixture was then purified through a silica gel column with dichloromethane-acetone as the eluent and the diastereomerically enriched portion

which contained predominantly the major product ( $R_C, R_P, R_P$ )-**176** was stirred vigorously with concentrated hydrochloric acid (12 mL) for 1 h at room temperature. The reaction mixture was then washed with water ( $4 \times 10$  mL), and dried ( $\text{MgSO}_4$ ). Subsequent fractional recrystallization from dichloromethane-diethylether gave complex ( $R_P, R_P$ )-**177** as colorless crystals: mp 288-289 °C (decomp.);  $[\alpha]_{436} +47.5^\circ$  ( $c$  0.4,  $\text{CH}_2\text{Cl}_2$ ); 0.1 g (25.4% yield). Anal. Calcd for  $\text{C}_{24}\text{H}_{20}\text{Cl}_2\text{NOPPdS}$ : C, 46.8; H, 4.1. Found: C, 46.5; H, 3.6.  $^{31}\text{P}\{^1\text{H}\}$  NMR ( $\text{CDCl}_3$ ):  $\delta$  70.6(d, 1 P,  $J_{\text{PP}} = 14.6$ ,  $P$ ), 29.7 (d, 1 P,  $J_{\text{PP}} = 14.6$ ,  $P$ );  $^1\text{H}$  NMR ( $\text{CDCl}_3$ ):  $\delta$  2.13 (d, 3H,  $^3J_{\text{PH}} = 8.8$  Hz,  $\text{PMe}$ ), 2.25 (d, 3H,  $^4J_{\text{PH}} = 4.4$  Hz,  $\equiv\text{Me}$ ), 2.33 (d, 3H,  $^3J_{\text{PH}} = 12.3$  Hz,  $\text{CH}_3$ ), 6.67 (dd, 1H,  $^2J_{\text{PH}} = 63.2$  Hz,  $^3J_{\text{PH}} = 13.5$  Hz,  $\text{CH}$ ), 7.92-7.98 (m, 10H, aromatics).



**(1R,2R)-1-methyl-(1-phenylphosphino)-2-phenyl-(methylethynyl)phosphinopropene, ( $S_P, S_P$ )-**178**].**

A solution of ( $R_P, R_P$ )-**177** (0.03 g, 0.06mmol) in dichloromethane (10 mL) was stirred vigorously with a saturated aqueous solution of potassium cyanide (0.5 g) for 1 h. The resulting colorless organic layer was separated, washed with water, and dried ( $\text{MgSO}_4$ ). Upon the removal of solvent, a white solid ( $S_P, S_P$ )-**178** was obtained:  $[\alpha]_{\text{D}} +27^\circ$  ( $c$  0.5,  $\text{CH}_2\text{Cl}_2$ ); 0.015 g (80% yield).  $^{31}\text{P}\{^1\text{H}\}$  NMR ( $\text{CDCl}_3$ ):  $\delta$  -25.5 (d, 1P,  $^3J_{\text{PP}} = 164$  Hz,  $P$ ), -32.0 (d, 1P,  $^3J_{\text{PP}} = 164$  Hz,  $P$ ).

## References

1. (a) Noyori, R. *Asymmetric Catalysis in Organic Synthesis*; Wiley: New York, **1994**. (b) Crépy, K. V. L.; Imamoto, T. *Adv. Synth. Catal.* **2003**, *345*(1-2), 79.
2. (a) Blaser, H.-U.; Pugin, B.; Spindler, F. In Cornils, B., Herrmann, W. A., Eds.; *Applied Homogeneous Catalysis with Organometallic Compounds*; VCH: Weinheim, **1996**; Vol. 3, p 1131. (b) Jacobsen, E. N.; Pfaltz, A.; Yamamoto, H., Eds. *Comprehensive Asymmetric Catalysis Supplement 1*; Springer-Verlag: Berlin, **2004**. (c) Williams, J. M. J. *Catalysis in Asymmetric Synthesis*, Sheffield: England, **1999**. (d) Blaser, H.-U.; Malan, C.; Pugin, B.; Spindler, F.; Steiner, H.; Studer, M. *Adv. Synth. Catal.* **2003**, *345*, 103. (e) Shimizu, H.; Nagasaki, I.; Saito, T. *Tetrahedron* **2005**, *61*, 5405.
3. (a) Ojima, I., Ed. *Catalytic Asymmetric Synthesis*, 2nd Ed.; Wiley-VCH: New York, **2000**. (b) Tang, W.; Zhang, X. *Chem. Rev.* **2003**, *103*, 3029. (c) Börner, A. *Phosphorus Ligands in Asymmetric Catalysis*; Wiley-VCH: Weinheim, **2008**.
4. Knowles, W. S.; Sabacky, M. *J. Chem. Soc., Chem. Commun.* **1968**, 1445.
5. Horner, L.; Siegel, H.; Büthe, H. *Angew. Chem. Int. Ed. Engl.* **1968**, *7*, 942.
6. (a) Kagan, H. B.; Sasaki, M. *The Chemistry of Organophosphorus Compounds*; Hartley, F. R., Ed.; John Wiley and Sons: Chichester, England, **1990**, Chapter 3, p.51. (b) Gilheany, D. G.; Mitchell, C. M. *The Chemistry of Organophosphorus Compounds*; Hartley, F. R., Ed.; John Wiley and Sons: Chichester, England, **1990**, Chapter 7, p.151. (c) Imamoto, T. *Handbook of Organophosphorus Chemistry*;

- Engel, R., Ed.; Marcel Dekker: New York, **1992**, Chapter 1, p.1. (d) Pietrusiewicz, K. M.; Zablocka, M. *Chem. Rev.* **1994**, *94*, 1375. (e) Ohff, M.; Holz, J.; Quirnbach, M.; Börner, A. *Synthesis* **1998**, 1391. (f) Quin, L. D.; Quin, G. S. *A Guide to Organophosphorus Chemistry*; Wiley-Interscience: New York, **2000**, Chapter 9, p.272. (g) Crépy, K. V. L.; Imamoto, T. *Top. Curr. Chem.* **2003**, *229*, 1.
7. Meisenheimer, J.; Lichtenstadt, L. *Chem. Ber.* **1911**, *44*, 456.
  8. Chen, C. H.; Berlin, K. D. *J. Org. Chem.* **1971**, *36*, 2791.
  9. Marsi, K. L.; Tuinstra, H. *J. Org. Chem.* **1975**, *40*, 1843.
  10. Balzer, W.-D. *Chem. Ber.* **1969**, *102*, 3546.
  11. Hart, F. A.; Mann, F. G. *J. Chem. Soc.* **1955**, 4107.
  12. Bodalski, R.; Janecki, R.; Galdecki, Z.; G/6wka, M. *Phosphorus, Sulfur* **1982**, *14*, 15.
  13. S. Otsuka, A. Nakamura, T. Kano, K. Tani, *J. Am. Chem. Soc.* **1971**, *93*, 4301.
  14. Tani, K.; Brown, L. D.; Ahmed, J.; Ibers, J. A.; Yokota, M.; Nakamura, A.; Otsuka, S. *J. Am. Chem. Soc.* **1977**, *99*, 7876.
  15. Wild, S. B. *Coord. Chem. Rev.* **1997**, *166*, 291 and refs therein.
  16. Horner, L.; Jordan, M. *Phosphorus, Sulfur* **1980**, *8*, 225.
  17. (a) Pirkle, W. H.; Pochapsky, T. C. *Adv. Chromatogr.* **1987**, *27*, 73; Pirkle, W. H.; Pochapsky, T. C. *Chem. Rev.* **1989**, *89*, 347. (b) Pescher, P.; Caude, M.; Rosaet, R.; Tambuté, A. *J. Chromatogr.* **1986**, *371*, 159. (c) Gasparrini, F.; Misiti, D.; Villani, C. *Chirality* **1992**, *4*, 447. (d) Klärner, F.-G.; Oebels, D.; Sheldricks, W. S. *Chem. Ber.* **1993**, *126*, 473.

18. Nudelman, A.; Cram, D. J. *J. Am. Chem. Soc.* **1968**, *90*, 3869.
19. Korpium, O.; Mislow, K.; *J. Am. Chem. Soc.* **1967**, *89*, 4784.
20. Korpium, O.; Lewis, R. A.; Chickos, J.; Mislow, K. *J. Am. Chem. Soc.* **1968**, *90*, 4842.
21. Vineyard, B. D.; Knowles, W. S.; Sabacky, M. J.; Bachman, G. L. Weinkauff, D.J. *J. Am. Chem. Soc.* **1977**, *99*, 5946.
22. Imamoto, T.; Hoshiki, T.; Onozawa, T.; Kusumoto, T. Sato, K. *J. Am. Chem. Soc.* **1990**, *112*, 5244.
23. (a) McKinstry, L.; Livinghouse, T. *Tetrahedron Lett.* **1994**, *35*, 9319. (b) Grabulosa, A.; Granell, J.; Muller, G. *Coord. Chem. Rev.* **2007**, *251*, 25.
24. (a) Jugé, S.; Stephan, M.; Laffitte, J. A.; Genet, J. P. *Tetrahedron Lett.* **1990**, *31*, 6357. (b) Jugé, S.; Stephan, M.; Merdès, R.; Genet, J. P.; Halut-Desportes, S. *J. Chem. Soc., Chem. Commun.* **1993**, 531. (c) Brown, J. M.; Carey, J. V.; Russell, M. J. H. *Tetrahedron* **1990**, *46*, 4877.
25. A. Muci, R.; Campos, K. R.; Evans, D. A. *J. Am. Chem. Soc.* **1995**, *117*, 9075.
26. Imamoto, T.; Watanabe, J.; Wada, Y.; Masuda, H.; Yamada, H.; Tsuruta, H.; Matsukawa, S.; Yamaguchi, K. *J. Am. Chem. Soc.* **1998**, *120*, 1635.
27. Gridnev, I. D.; Yamanoi, Y.; Higashi, N.; Tsuruta, H.; Yasutake, M.; Imamoto, T. *Adv. Synth. Catal.* **2001**, *343*, 118.
28. Nagata, K.; Matsukawa, S.; Imamoto, T. *J. Chem. Soc.* **2000**, *65*, 4185.
29. Muci, A. R.; Campos, K. R.; Evans, D. A. *J. Am. Chem. Soc.* **1995**, *117*, 9075.
30. Hoge, G. *J. Am. Chem. Soc.* **2003**, *125*, 10219.

31. Tang, W.; Zhang, X. *Angew. Chem., Int. Ed.* **2002**, *41*, 1612.
32. Leung, P.H. *Acc. Chem. Res.* **2004**, *37*, 169.
33. Loh, S.; Mok, K. F.; Leung, P. H.; White, A. J. P.; Williams, D. J. *Tetrahedron: Asymmetry* **1996**, *7*, 45.
34. Leung, P. H.; Loh, S.; Mok, K. F.; White, A. J. P.; Williams, D. J. *J. Chem. Soc., Chem. Commun.* **1996**, 591.
35. Leung, P. H.; He, G.; Lang, H.; Liu, A.; S. Loh; Selvaratnam, S.; Mok, K. F.; White, A. J. P.; Williams, D. J. *Tetrahedron* **2000**, *56*, 7.
36. Leung, P. H.; Loh, S. Vittal, J. J.; White, A. J. P.; Williams, D. J. *Chem. Commun.* **1997**, 1987.
37. Qin, Y.; Lang, H.; Vittal, J. J.; Tan, G.; Selvaratnam, S.; White, A. J. P.; Williams, D. J.; Leung, P.H. *Organometallics* **2003**, *22*, 3944.
38. Leung, P. H.; Qin, Y.; He, G.; Mok, K. F.; Vittal, J. J. *J. Chem. Soc., Dalton Trans.* **2001**, 309.
39. Leung, P. H.; Loh, S.; Mok, K. F.; White, A. J. P.; Williams, D. J. *J. Chem. Soc., Dalton Trans.* **1996**, 4443.
40. Siah, S. Y.; Leung, P. H.; Mok, K. F.; *J. Chem. Soc., Chem. Commun.* **1995**, 1747.
41. Leung, P. H.; Siah, S.Y.; White, A. J. P.; Williams, D. J. *J. Chem. Soc., Dalton Trans.* **1998**, 893.
42. He, G.; Loh, S.; Vittal, J. J.; Mok, K. F.; Leung, P.H. *Organometallics* **1998**, *17*, 3931.

43. Aw, B.; Leung, P.H.; White, A. J. P.; Williams, D. J. *Organometallics* **1996**, *15*, 3640.
44. Leung, P. H.; Lang, H.; White, A. H.; Williams, D. J. *Tetrahedron: Asymmetry* **1998**, *9*, 2961.
45. Song, Y.; Vittal, J. J.; Chan, S.; Leung, P. H. *Organometallics* **1999**, *18*, 650.
46. Chooi, S.Y. M.; Siah, S. Y.; Leung, P. H.; Mok, K. F. *Inorg. Chem.* **1993**, *32*, 4812.
47. Loh, S.; Vittal, J. J.; Leung, P. H.; *Tetrahedron: Asymmetry* **1998**, *9*, 423.
48. Leung, P. H.; Lang, H.; Zhang, X.; Selvaratnam, S.; Vittal, J. J. *Tetrahedron: Asymmetry* **2000**, *11*, 2661.
49. Li, Y.; Ng, K.; Selvaratnam, S.; Tan, G.; Vittal, J. J.; Leung, P. H. *Organometallics* **2003**, *22*, 834.
50. Li, Y.; Selvaratnam, S.; Vittal, J. J.; Leung, P.H. *Inorg. Chem.* **2003**, *42*, 3229.
51. Korff, C.; Helmchen, G. *Chem. Commun.* **2004**, 530.
52. Join, B.; Mimeau, D.; Delacroix, O.; Gaumont, A.-C. *Chem. Commun.* **2006**, 3249.
53. Fryzuk, M. D.; Bosnich, B. *J. Am. Chem. Soc.* **1977**, *99*, 6262.
54. (a) Brunner, H.; Pieronczyk, W. *Angew. Chem. Int. Ed. Engl.* **1979**, *18*, 620. (b) Brunner, H.; Pieronczyk, W.; Schönhammer, B.; Streng, K.; Bernal, I.; Korp, J. *Chem. Ber.* **1981**, *114*, 1137.
55. Zhu, G.; Cao, P. Jiang, Q.; Zhang, X. *J. Am. Chem. Soc.* **1997**, *119*, 1799.
56. (a) Xie, Y.; Lou, R.; Li, Z.; Mi, A.; Jiang, Y. *Tetrahedron: Asymmetry* **2000**, *11*,

1487. (b) Lou, R.; Mi, A.; Jiang, Y.; Qin, Y.; Li, Z.; Fu, F.; Chan, A. S. C. *Tetrahedron* **2000**, *56*, 5857.
57. (a) Burk, M. J.; Feaster, J. E.; Harlow, R. L. *Organometallics* **1990**, *9*, 2653. (b) Burk, M. J.; Harlow, R. L.; *Angew. Chem., Int. Ed. Engl.* **1990**, *29*, 1462.
58. (a) Nagel, U. *Angew. Chem., Int. Ed. Engl.* **1984**, *23*, 435. (b) Nagel, U.; Kinzel, E.; Andrade, J.; Prescher, G. *Chem. Ber.* **1986**, *119*, 3326. (c) Inoguchi, K.; Achiwa, K. *Chem. Pharm. Bull.* **1990**, *38*, 818.
59. (a) Helmchen, G.; Kudis, S.; Sennhenn, P.; Steinhagen, H. *Pure Appl. Chem.* **1997**, *69*, 513. (b) Pfaltz, A. *Acta Chem. Scand. B* **1996**, *50*, 189. (c) Williams, J. M. J. *Synlett* **1996**, 705. (b) Helmchen, G.; Pfaltz, A. *Acc. Chem. Res.* **2000**, *33*, 336.
60. (a) Dang, T. P.; Kagan, H. B. *Chem. Commun.* **1971**, 481. (b) Kagan, H. B.; Dang, T. P. *J. Am. Chem. Soc.* **1972**, *94*, 6429
61. Koch, G.; Liloyd-Jones, G. C.; Loiseleur, O.; Prétôt, R.; Pfaltz, A.; Schaffner, S.; Schnider, P.; von Matt, P. *Recl. Trav. Chim. Pays-Bas* **1995**, *114*, 206.
62. Burk, M. J. *J. Am. Chem. Soc.* **1991**, *113*, 8518.
63. Jacobsen, E.; Pfaltzer, A.; Yamamoto, H. *Comprehensive Asymmetric Catalysis*; Springer-Verlag: Berlin, **1999**.
64. Schmid, R.; Foricher, J.; Cereghetti, M.; Schönholzer, P. *Helv. Chim. Acta* **1991**, *74*, 870.
65. (a) Van den Berg, M.; Minnaard, A. J.; Schudde, E. P.; van Esch, J.; de Vries, A. H. M.; de Vries, J. G.; Feringa, B. L. *J. Am. Chem. Soc.* **2000**, *122*, 11539. (b)

- van den Berg, M.; Minnaard, A. J.; Haak, R. M.; Leeman, M.; Schudde, E. P.; Meetsma, A.; Feringa, B. L.; de Vries, A. H. M.; Maljaars, C. E. P.; Willans, C. E.; Hyett, D.; Boogers, J. A. F.; Henderickx, H. J. W.; de Vries, J. G. *Adv. Synth. Catal.* **2003**, *345*, 308.
66. (a) Benincori, T.; Brenna, E.; Sannicolò, F.; Trimarco, L.; Antognazza, P.; Cesarotti, E. *J. Chem. Soc., Chem. Commun.* **1995**, 685. (b) Benincori, T.; Brenna, E.; Sannicolò, F.; Trimarco, L.; Antognazza, P.; Cesarotti, E. Demartin, F.; Pilati, T. *J. Org. Chem.* **1996**, *61*, 6244.
67. (a) Saito, T.; Yokozawa, T.; Zhang, X.; Sayo, N. (Takasago International Corporation) U.S. Patent 5, 872, 273, **1999**. (b) Saito, T.; Yokozawa, T.; Ishizaki, T.; Mori, T.; Sayo, N.; Miura, T.; Kumobayashi, H. *Adv. Synth. Catal.* **2001**, *343*, 264.
68. (a) Miyashita, A.; Yasuda, A.; Takaya, H.; Toriumi, K.; Ito, T.; Souchi, T.; Noyori, R. *J. Am. Chem. Soc.* **1980**, *102*, 7932. (b) Miyashita, A.; Takaya, H.; Souchi, T.; Noyori, R. *Tetrahedron* **1984**, *40*, 1245.
69. Kumobayashi, H.; Miura, T.; Sayo, N.; Saito, T.; Zhang, X. *Synlett* **2001**, 1055.
70. (a) Sayo, N.; Zhang, X.; Ohmoto, T.; Yoshida, A.; Yokozawa, T. Eur. Patent 0 771 812, **1997**; Chem. Abstr.1997, 127, 50792. (b) Zhang, X.; Sayo, N. Eur. Patent 0 839 819, **1998**; Chem. Abstr. 1998, 129, 16234.
71. (a) Alcock, N. W.; Brown, J. M.; Hulmes, D. I. *Tetrahedron: Asymmetry* **1993**, *4*, 743. (b) Lim, C.W.; Tissot, O.; Mattison, A.; Hooper, M.W.; Brown, J. M.; Cowley, A. R.; Hulmes, D. I. Blacker, A. J. *Org. Proc. Dev.* **2003**, *7*, 379.

72. Hayashi, T.; Mise, T.; Kumada, M. *Tetrahedron Lett.* **1976**, 4351.
73. (a) Sawamura, M.; Hamashima, H.; Ito, Y. *Tetrahedron: Asymmetry* **1991**, 2, 593.  
(b) Sawamura, M.; Hamashima, H.; Sugawara, M.; Kuwano, R.; Ito, Y. *Organometallics* **1995**, 14, 4549.
74. Pye, P. J.; Rossen, K.; Reamer, R. A.; Tsou, N. N.; Volante, R. P.; Reider, P. J. *J. Am. Chem. Soc.* **1997**, 119, 6207.
75. M. Lotz, G. Kramer, P. Knochel, *Chem. Commun.* **2002**, 2546.
76. Togni, A.; Breutel, C.; Schnyder, A.; Spindler, F.; Landert, H.; Tijani, A. *J. Am. Chem. Soc.* **1994**, 116, 4062.
77. Dang, T. P.; Kagan, H. B. *J. Chem. Soc., Chem. Commun.* **1971**, 481. (b) Kagan, H. B.; Dang, T. P. *J. Am. Chem. Soc.* **1972**, 94, 6429.
78. (a) Noyori, R. *Chem. Soc. Rev.* **1989**, 18, 187. (b) Noyori, R.; Takaya, H. *Acc. Chem. Res.* **1990**, 23, 345. (c) Noyori, R. *Science* **1990**, 248, 1194. (d) Noyori, R. *CHEMTECH* **1992**, 360. (e) Noyori, R. *Tetrahedron* **1994**, 50, 4259.
79. Zhu, G.; Zhang, X. *Tetrahedron: Asymmetry* **1998**, 9, 2415.
80. Uozumi, Y.; Lee, S.-Y.; Hayashi, T. *Tetrahedron Lett.* **1992**, 33, 7185.
81. Kitayama, K.; Uozumi, Y.; Hayashi, T. *J. Chem. Soc., Chem. Commun.* **1995**, 1533.
82. Nishibayashi, Y.; Segawa, K.; Takada, H.; Ohe, K.; Uemura, S. *J. Chem. Soc., Chem. Commun.* **1996**, 847
83. Hayashi, T.; Yamamoto, A.; Hagihara, T.; Ito, Y., *Tetrahedron Lett.* **1986**, 27, 191.
84. Brown, J. M.; Hulmes, D. I.; Guiyr, P. J. *Tetrahedron* **1994**, 50, 4493.

85. Abbenhuis, H. C. L.; Burckhardt, U.; Gramlich, V.; Kollner, C.; Pregosin, P. S.; Salzman, R.; Togni, A. *Organometallics* **1995**, *14*, 759.
86. Trost, B. M.; Bunt, R. C. *J. Am. Chem. Soc.* **1994**, *116*, 4089.
87. Ozawa, F.; Kubo, A.; Matsumoto, Y.; Hayashi, T., *Organometallics* **1993**, *12*, 4188.
88. Ripa, L.; Hallberg, A. *J. Org. Chem.* **1997**, *62*, 595.
89. Schnyder, A.; Hintermann, L.; Togni, T. *Angew. Chem., Int. Ed. Engl.* **1995**, *34*, 931.
90. Schnyder, A.; Togni, A.; Wiesli, U. *Organometallics* **1997**, *16*, 255.
91. James, B. R.; Yong, C. G. *Chem. Commun.* **1983**, 1215.
92. (a) Taura, Y.; Tanaka, M.; Funakoshi, K.; Sakai, K.; *Tetrahedron Lett.* **1989**, *30*, 6349. (b) Wu, X. M.; Funakoshi, K.; Sakai, K. *Tetrahedron Lett.* **1992**, *33*, 6331. (c) Sakai, N.; Mano, S.; Nozaki, K.; Takaya, H. *J. Am. Chem. Soc.* **1993**, *115*, 7033.
93. (a) Nozaki, K.; Takaya, H.; Hiyama, T. *Top. Catal.* **1998**, *4*(3,4), 175. (b) Kockritz, A.; Sonnenschein, H.; Bischoff, S.; Theil, F.; Gloede, J. *Phosphorus, Sulfur Silicon Relat. Elem.* **1998**, *132*, 15. (c) Deerenberg, S.; Kamer, P. C. J.; Van Leeuwen, P. W. N. M. *Organometallics* **2000**, *19*, 2065. (d) Horiuchi, T.; Ohta, T.; Shirakawa, E.; Nozaki, K.; Takaya, H. *Tetrahedron* **1997**, *53*, 7795. (e) Horiuchi, T.; Ohta, T.; Shirakawa, E.; Nozaki, K.; Takaya, H. *J. Org. Chem.* **1997**, *62*, 4285. (f) Horiuchi, T.; Shirakawa, E.; Nozaki, K.; Takaya, H. *Organometallics* **1997**, *16*, 2981.

94. Consiglio, G.; Bottegni, C. *Helv. Chim. Acta.* **1973**, *56*, 460.
95. Kiso, Y.; Tamao, K.; Miyake, N.; Yamamoto, K.; Kumada, M. *Tetrahedron Lett.* **1974**, *3*.
96. Hayashi, M.; Takaoki, K.; Hashimoto, Y.; Saigo, K. *Enantiomer* **1997**, *2*, 293.
97. Wimmer, P.; Widhalm, M. *Monatsh. Chem.* **1996**, *127*, 669.
98. Hayashi, T.; Konishi, M.; Fukushima, M.; Kanehira, K.; Hioki, T.; Kumada, M. *J. Org. Chem.* **1983**, *48*, 2195.
99. (a) Lautens, M.; Lautens, J.C.; Smith, A. C. *J. Am. Chem. Soc.* **1990**, *112*, 5627.  
(b) Brunner, H.; Muschiol, M.; Prester, F. *Angew. Chem., Int. Ed. Engl.* **1990**, *29*, 625.
100. Sawamura, M.; Hamashima, H.; Ito, Y. *J. Am. Chem. Soc.* **1992**, *114*, 8295.
101. Buono, G.; Siv, C.; Peiffer, G.; Triantaphylide, C.; Deins, P.; Mortreux, A.; Peti, F. *J. Org. Chem.* **1985**, *50*, 1781.
102. (a) Demay, S.; Volant, F.; Knochel, P.; *Angew. Chem., Int. Ed. Engl.* **2001**, *40*, 1235. (b) Hayashi, T.; Matsumoto, Y.; Ito, Y.; *Tetrahedron: Asymmetry* **1991**, *2*, 601.
103. (a) Jensen, J. F.; Johannsen, M. *Org. Lett.* **2003**, *5*, 3025. (b) Pickett, T. E.; Roca, F. X.; Richards, C. J.; *J. Org. Chem.* **2003**, *68*, 2592.
104. (a) Stoop, R. M.; Bachmann, S.; Valentini, M.; Mezzetti, A. *Organometallics* **2000**, *19*, 4117. (b) Cross, R. J.; Newman, P. D.; Peacock, R. D.; Stirling, D. J. *Mol. Catal. A: Chem.* **1999**, *144*, 273.
105. (a) Norman, N. C. *Chemistry of Arsenic, Antimony and Bismuth*; Academic and

- Professional: London, **1998**. (b) Wild, S. B. In *The Chemistry of Organic Arsenic, Antimony, and Bismuth Compounds*; Patai, S. Ed.; John Wiley & Sons Ltd.: Chichester, **1994**. (c) Kwong, F. Y.; Lai, C. W.; Chan, K. S. *J. Am. Chem. Soc.* **2001**, *123*, 8864.
- 106.(a) Farina, V. K.; Krishnan, B. *J. Am. Chem. Soc.* **1991**, *113*, 9585. (b) Nicolaou, K. C.; Bulger, P. G.; Sarlah, D. *Angew. Chem., Int. Ed.* **2005**, *44*, 4442. (c) Lau, K. C.Y.; Chiu, P. *Tetrahedron Lett.* **2007**, *48*, 1813.
- 107.Baber, R. A.; Collard, S.; Hooper, M.; Orpen, A. G.; Pringle, P. G.; Wilkinson, M. J.; Wingad, R. L. *Dalton Trans.* **2005**, 1491.
- 108.van der Veen, L. A.; Keeven, P. K.; Kamer, P. C.; P. van Leeuwen, W. N. M. *Chem. Commun.* **2000**, 333.
- 109.(a) Johnson, C. R.; Braun, M. P. *J. Am. Chem. Soc.* **1993**, *115*, 11014. (b) Bedford, R. B.; Cazin, C. S. J.; Coles, S. J.; Gelbrich, T.; Hursthouse, M. B.; Scordia, V. J. M. *Dalton Trans.* **2003**, 3350.
- 110.Ceccarelli, S.; Piarulli, U.; Gennari, C. *J. Org. Chem.* **2000**, *65*, 6254.
- 111.Casares, J. A.; Espinet, P.; Salas, G. *Organometallics* **2008**, *27*, 3761.
- 112.Cao, P.; Li, C.-Y.; Kang, Y.-B.; Xie, Z.; Sun, X.-L.; Tang, Y. *J. Org. Chem.* **2007**, *72*, 6628.
- 113.Hennings, D. D.; Iwama, T.; Rawai, V. H. *Org. Lett.* **1999**, *1*, 1205.
- 114.Gustafsson, M.; Bergqvist, K.-E.; Frejd, T. *J. Chem. Soc., Perkin Trans. 1* **2001**, 1452.
- 115.(a) Ceccarelli, S.; Piarulli, U.; Gennari, C. *J. Org. Chem.* **2000**, *65*, 6254. (b) Cai,

- M.; Huang, Y.; Hu, R.; Song, C. *J. Mol. Catal. A* **2004**, *212*, 151.
- 116.(a) Aguiar, A. M.; Archibald, T. G. *J. Org. Chem.* **1967**, *32*, 2627. (b) Ellermann, J.; Dorn, K. *Chem. Ber.* **1967**, *100*, 1230. (c) Namyslo, J. C.; Kaufmann, D. E. *Synlett* **1999**, 114.
117. Wallow, T. I.; Goodson, F. E.; Novak, B. M. *Organometallics* **1996**, *15*, 3708.
- 118.(a) Rossi, R. A.; Pierini, A. B.; Peñeñory, A. B. *Chem. Rev.* **2003**, *103*, 71, and references therein. (b) Rossi, R. A.; Alonso, R. A.; Palacios, S. M. *J. Org. Chem.* **1981**, *46*, 2498. (c) Bornancini, E. R. N.; Alonso, R. A.; Rossi, R. A. *J. Organomet. Chem.* **1984**, *270*, 177.
- 119.(a) Fitzpatrick, M. G.; Hanton, L. R.; Henderson, W.; Kneebone, P. E.; Levy, E. G.; McCaffrey, L. J.; McMorran, D. A. *Inorg. Chim Acta* **1998**, *281*, 101. (b) Ketelaere, R. F.; Delbeke, F. T.; Van der Kelen, G. P. *J. Organomet. Chem.* **1971**, *28*, 217. (c) Bishop, J. J.; Davison, A.; Katcher, M. L.; Lichtenberg, D. W.; Merrill, R. E.; Smart, J. C. *J. Organomet. Chem.* **1971**, *27*, 241. (d) Heaney, H.; Heinekey, D. M.; Mann, F. G.; Millar, I. T. *J. Chem. Soc.* **1958**, 3838.
120. Kojima, A.; Boden, C. D. J.; Shibasaki, M. *Tetrahedron Lett.* **1997**, *38*, 3459.
121. Bonaterra, M.; Martin, S. E.; Rossi, R. A. *Org. Lett.* **2003**, *5*, 2731.
122. Kwong, F. Y.; Lai, C. W.; Tan, D. -M.; Lam, F. L.; Chan, A. S. C.; Chan, K. S. *Organometallics* **2005**, *24*, 4170.
- 123.(a) Downard, A. J.; Bond, A. M.; Clayton, A. J.; Hanton, L. R.; Mc-Morran, D. A. *Inorg. Chem.* **1996**, *35*, 7684. (b) Bricklebank, N.; Godfrey, S. M.; McAuliffe, C. A.; Pritchard, R. G.; *J. Chem. Soc., Dalton Trans.* **1996**, 157. (c) Doward, A. J.;

- (d) Hanton, L. R.; R. L. Paul, *J. Chem. Soc. Chem. Commn.* **1992**, 235. (d)
- Downard, A. J.; Hanton, L. R.; McMorran, D. A.; Paul, R.L. *Inorg. Chem.* **1993**, 32, 6028. (e) Coe, B. J.; Chevy, M.; Beddoes, R. L.; Hope, H.; White, P. S. *J. Chem. Soc., Dalton Trans.* **1996**, 3917.
124. Martin, J. W. L.; Stephens, F. S.; Weerasuria, K. D. V.; Wild, S. B., *J. Am. Chem. Soc.* **1988**, 110, 4346.
125. Calhoun, A. D.; Kobos, W. J.; Nile, T. A.; Smith, C. A.; *J. Organomet. Chem.*, **1979**, 170, 175.
126. Cho, Y.; Shibasaki, M. *Tetrahedron Lett.* **1998**, 39, 1773.
127. Allen, D. G.; Wild, S. B.; Wood, D. L., *Organometallics* **1986**, 5, 1009.
128. Tan, D.-M.; Chan, K.S. *Tetrahedron Lett.* **2005**, 46, 503.
129. Chooi, S.; Tan, M. K.; Leung, P. H.; Mork, K. F. *Inorg. Chem.* **1994**, 33, 3096.
130. Aw, B. H.; Selvaratnam, S.; Leung, P. H.; Rees, N. H.; McFarlane, W., *Tetrahedron: Asymmetry* **1996**, 7, 1753.
131. Yeo, W. C.; Tan, G. K.; Koh, L. L.; Leung, P. H. *Eur. J. Inorg. Chem.* **2005**, 4723.
132. Liu, X. M.; Mok, K. F.; Vittal, J. J.; Leung, P. H. *Organometallics* **2000**, 19, 3722.
133. Liu, X. M.; Mok, K. F.; Leung, P. H. *Organometallics* **2001**, 20, 3918.
134. Yeo, W. C.; Tee, S. Y.; Tan, H. B.; Tan, G. K.; Koh, L. L.; Leung, P. H. *Inorg. Chem.* **2004**, 43, 8102.
135. Pullarkat, S. A.; Ding, Y.; Li, Y.; Tan, G. K.; Leung, P. H. *Inorg. Chem.* **2006**, 45, 7455.

136. Tang, L.; Zhang, Y.; Luo, D.; Li, Y.; Mok, K. F.; Yeo, W. C.; Leung, P. H. *Tetrahedron Lett.* **2007**, *48*, 33.
137. Bungbong, M. L.; Tan, K. W.; Li, Y.; Selvaratnam, S. V.; Dongol, K. G.; Leung, P. H. *Inorg. Chem.* **2007**, *46*, 4733.
138. (a) Fringnelli, F.; Tatichi, A. *Dienes in the Diels-Alder Reaction*. Wiley, New York, **1990** and the references cited therein. (b) Carrnthey, W. *Cycloaddition Reactions in Organic Synthesis*. Pergamon, Oxford. **1990** and the references Cited therein.
139. Narisada, M.; Ohtani, M.; Watanabe, F.; Uchida, K.; Doteuchi, M.; Hanasaki, K.; Kakashi, H.; Otani, K.; Hara, S. *J. Med. Chem.* **1988**, *31*, 1847, and the references cited therein.
140. Das, J.; Vu, T.; Harris, D.; Ogletree, M. *J. Med. Chem.*, **1988**, *31*, 930.
141. Hall, S.; Han, W. C.; Harris, D.; Hedbery, A.; Ogletree. *J. Med. Chem.*, **1989**, *32*, 974.
142. Wasserman, A. *Diels-Alder Reaction*. Elsevier, New York. **1965**.
143. (a) Lipshutz, B. H. *Chem. Rev.* **1986**, *86*, 795. (b) Klein, L. L. *J. Am. Chem. Soc.* **1985**, *107*, 2573. (c) Klein, L. L.; Shanklin, M. S. *J. Org. Chem.* **1988**, *53*, 5202. (d) Ashton P. R. *J. Am. Chem. Soc.* **1992**, *114*, 6330. (e) Löffler, M.; Schllter, A.-D.; Gessler, K.; Saenger, W.; Toussaint, J.-M.; Brédas, J.-L. *Angew. Chem.* **1994**, *106*, 2281; *Angew. Chem. Int. Ed. Engl.* **1994**, *33*, 2209. (f) Valdés, C.; Spitz, U. P.; Kubik, Rebek, Jr. *J. Angew. Chem.* **1995**, *107*, 2031; *Angew. Chem. Int. Ed. Engl.* **1995**, *34*, 1885.
144. (a) Katritzky, A. R.; Rees, C. W.; Bird, C. W.; Cheeseman, G. W. H. Eds.;

- Comprehensive Heterocyclic Chemistry*; Pergamon: Oxford, U. K., **1984**, vol. 4.
- (b) Katritzky, A. R.; Rees, C. W.; Scriven, E. F. V.; Bird, C. W. Eds.; *Comprehensive Heterocyclic Chemistry II*; Pergamon: Oxford, U. K., **1996**, vol. 2.
145. (a) Kappe, C. O.; Murphree, S. S.; Padwa, A. *Tetrahedron* **1997**, *53*, 14179. (b) Vogel, P.; Cossy, J.; Plumet, J.; Arjona, O. *Tetrahedron* **1999**, *55*, 13521.
146. (a) Bosshard, P.; Eugster, C. H. *Adv. Heterocycl. Chem.* **1966**, *7*, 377. (b) Dean, F. M. *Adv. Heterocycl. Chem.* **1982**, *31*, 237.
147. (a) Anet, F. A. L. *Tetrahedron Lett.* **1962**, 1219. (b) Schuda, P. F.; Bennett, J. M. *Tetrahedron Lett.* **1982**, *23*, 5525. (c) Balthazor, T. M.; Gaede, B.; Korte, D. E.; Shieh, H. S. *J. Org. Chem.* **1984**, *49*, 4547. (d) Riera, A.; Martí, M.; Moyano, A.; Pericàs, M. A.; Santamaría, J. *Tetrahedron Lett.* **1990**, *31*, 2173. (e) Leroy, J. *Tetrahedron Lett.* **1992**, *33*, 2969. (f) Braverman, S.; Lior, Z. *Tetrahedron Lett.* **1994**, *35*, 6725. (g) Cook, M. J.; Cracknell, S. J. *Tetrahedron* **1994**, *50*, 12125. (h) Song, Z. Z.; Ho, M. S.; Wong, H. N. C. *J. Org. Chem.* **1994**, *59*, 3917. (i) Dauben, W. G.; Lam, J. Y. L.; Guo, Z. R. *J. Org. Chem.* **1996**, *61*, 4816.
148. Klein, L. L.; Deeb, T. M. *Tetrahedron Lett.* **1985**, *26*, 3935.
149. Guildford, A. J.; Turner, R. W. *J. Chem. Soc., Chem. Commun.* **1983**, 466.
150. (a) Brion, F. *Tetrahedron Lett.* **1982**, *23*, 5299. (b) Rogers, C.; Keay, B. A. *Tetrahedron Lett.* **1991**, *32*, 6477. (c) Rogers, C.; Keay, B. A. *Can. J. Chem.* **1992**, *70*, 2929. (d) Fraile, J. M.; García, J. I.; Gracia, D.; Mayoral, J. A.; Pires, E. J. *Org. Chem.* **1996**, *61*, 9479.

151. Nicolaou, K. C.; Snyder, S. A.; Montagnon, T.; Vassilikogiannakis, G. *Angew. Chem. Int. Ed. Engl.* **2002**, *41*, 1668.
152. Danishefsky, S.; Bednarski, M. *Tetrahedron Lett.* **1982**, *23*, 5299.
153. Harwood, L. M.; Leeming, S. A.; Isaacs, N. S.; Jones, G.; Pickard, J.; Thomas, R. M.; Watkin, D. *Tetrahedron Lett.* **1988**, *29*, 5017.
154. Corey, E. J.; Loh, T. P. *Tetrahedron Lett.* **1993**, *34*, 3979.
155. Yamamoto, I.; Narasaka, K. *Chem. Lett.* **1995**, 1129.
156. Hayashi, Y.; Nakamura, M.; Nakao, S.; Inoue, T.; Shoji, M. *Angew. Chem. Int. Ed. Engl.* **2002**, *41*, 4079.
157. Yeo, W. C.; Vittal, J. J.; White, A. J. P.; Williams, D. J.; Leung, P. H. *Organometallics* **2001**, *20*, 2167.
158. Yeo, W.C.; Vittal, J. J.; Koh, L. L.; Tan, G. K.; Leung, P. H. *Organometallics* **2004**, *23*, 3474.
159. Ma, M.; Pullarkat, S. A.; Li, Y.; Leung, P. H. *Inorg. Chem.* **2007**, *46*, 9488.
160. He, G.; Qin, Y.; Mok, K. F.; Leung, P. H. *J. Chem. Soc., Chem. Commun.* **2000**, 167.
161. Aw, B. H.; Hor, T. S. A.; Selvaratnam, S.; Mok, K. F.; White, A. J. P.; Williams, D. J.; Rees, N. H.; McFarlane, W.; Leung, P. H. *Inorg. Chem.* **1997**, *36*, 2138.
162. (a) Dunina, V. V.; Golovan, E. B.; Gulyukina, N. S.; Buyevich, A. V. *Tetrahedron: Asymmetry* **1995**, *6*, 2731. (b) Albert, J.; Bosque, R.; Cadena, J. M.; Delgado, S.; Granell, J. J. *Organomet. Chem.* **2001**, *634*, 83.
163. Nawara, A. J.; Shima, T.; Hampel, F.; Gladysz, J. A. *J. Am. Chem. Soc.* **2006**,

- 128, 4962.
164. Berlin, K. D.; Butler, G. B. *J. Org. Chem.* **1961**, *26*, 2537.
165. Song, Y.; Mok, K. F.; Leung, P. H. *Inorg. Chem.* **1998**, *37*, 6399.
166. Maier, L.; Seyferth, D.; Stone, F. G. A.; Rochow, E. G. *J. Am. Chem. Soc.* **1957**, *79*, 5884.
167. Chooi, S. M. Y.; Ranford, J. D.; Leung, P. H.; Mok, K. F. *Tetrahedron: Asymmetry* **1994**, *5*, 1805.
168. (a) Sargent, M. V.; Dean, F. M. *Comprehensive heterocyclic chemistry*, Pergamon: Oxford, 1984. (b) Carruthers, W. *Some Modern Methods of Organic Synthesis*, 2nd ed.; Cambridge University Press: Cambridge, 1978.
169. Horspool, W. M.; Tedder, J. M.; Din, Z. U. *J. Chem. Soc. (C)* **1969**, 1694.
170. (a) Sugiyama, S.; Tsuda, T.; Mori, A. *Chem. Lett.* **1986**, 1315. (b) Sugiyama, S.; Tsuda, T.; Mori, A.; Takeshita, H.; Kodama, M. *Bull. Chem. Soc. Jpn.* **1987**, *60*, 3633.
171. (a) Wenkert, E.; Moeller, P. D. R.; Piettre, S. R.; *J. Am. Chem. Soc.* **1988**, *110*, 7188. (b) Jung, M. E.; Street, L. J.; Usui, Y. *J. Am. Chem. Soc.* **1986**, *108*, 6810. (c) Raasch, M. S. *J. Org. Chem.* **1980**, *45*, 867.
172. (a) Ghisalberti, E. L.; Jefferies, P. R.; Payne, T. G. *Tetrahedron* **1974**, *30*, 3099. (b) Heller, H. G.; Hughes, D. S.; Hursthouse, M. B.; Levell, J. R. Ottaway. M. J. *J. Chem. Soc., Chem. Commun.* **1995**, 837.
173. (a) Chen, C.-H.; Rao, P. D.; Liao, C.-C. *J. Am. Chem. Soc.* **1998**, *120*, 13254. (b) Rao, P. D.; Chen, C.-H.; Liao, C.-C. *Chem. Commun.* **1999**, 713. (c) Gao, S.-Y.;

- Lin, Y.-L.; Rao, P. D.; Liao, C.-C. *Synlett* **2000**, 421. (d) Gao, S.-Y.; Ko, S.; Lin, Y.-L.; Peddinti, R. K.; Liao, C.-C. *Tetrahedron* **2001**, 57, 297.
174. Mathey, F.; Mercier, F. *C.R. Acad. Sci. Paris, T. 324, Ser IIb*, 1997,701.
175. He, G. S. Ph.D.Thesis, NUS, Singapore, **2001**.
176. (a) Rahn, J. A.; Holt, M. S.; Gray, G. A.; Alcock, N. W.; Nelson, J. H. *Inorg. Chem.* 1989, 28, 217. (b) Liu, X.; Ong, T. K. W.; Selvaratnam, S.; Vittal, J. J.; White, A. J. P.; Williams, D. J.; Leung, P. H. *J. Organomet.Chem.* **2002**, 643, 4.
177. Santini, C. C.; Fischer, J.; Mathey, F.; Mitschler, A. *J. Am. Chem. Soc.* **1980**, 102, 5809.
178. Marinetti, A.; Methey, F.; Jean, F.; Mitschler, A. *J. Chem. Soc., Chem. Commun.* **1982**, 667.
179. Deschamps, B.; Mathey, F. *J. Chem. Soc., Chem. Commun.* **1985**, 1010.
180. Kessler, J. M.; Nelson, J. H.; Jean, F.; De Cian, A.; Bearden, W. H.; Fujii, N. *Inorg. Chem.* **1994**, 33, 4319.
181. Bhaduri, D.; Nelson, J. H.; Jacobson, R. A. *Organometallics* **1994**, 13, 2291.
182. Green, R. L.; Nelson, J. H.; Jean, F. *Organometallics* **1987**, 6, 2256.
183. Rahn, J. A.; Holt, M. S.; Nelson, J. H.; Polyhedron. **1989**, 8, 897.
184. William, L. W.; Jeffrey, A. R.; Nathaniel, W. A.; Jean, F.; Nelson, J. H. *Inorg. Chem.* **1994**, 33, 109.
185. Solujic, L.; Milosavljevic, E. B.; Nelson, J. H. *Inorg. Chem.* **1989**, 28, 3453.
186. Quin, L. D.; Huges, A. N. in: F.R. Hartley (Ed.), *The Chemistry of Organophosphorus Compounds* vol. 1, John Wiley, New York, 1990 (Chapter

- 10).
187. Mercier, F.; Mathey, F.; Fischer, J.; Nelson, J. H. *J. Am. Chem. Soc.* **1984**, *106*, 425.
188. Cahn, R. S.; Ingold, C. K.; Prelog, V. *Angew. Chem., Int. Ed. Engl.* **1966**, *5*, 385.
189. Huffman, M. A.; Smitrovich, J. H.; Rosen, J. D.; Boice, G. N.; Qu, C.; Nelson, T. D.; McNamara, J. M. *J. Org. Chem.* **2005**, *70*, 4409.
190. Breque, A.; Mathey, F.; Savignac P. *Synthesis* **1981**, 983.
191. (a) Newkome, G.R. *Chem. Rev.* **1993**, *93*, 2067. (b) Zhang, Z. Z.; Cheng, H. *Coord. Chem. Rev.* **1996**, *1*, 147. (c) Espinet, P.; Soulantica, K. *Coord. Chem. Rev.* **1999**, *499*, 193. (d) Chelucci, G.; Orru, G.; Pinna, G. A. *Tetrahedron* **2003**, *59*, 9471. (e) Guiry, P. J.; Saunders, C. P. *Adv. Synth. Catal.* **2004**, *346*, 497. (f) Cui, X.; Burgess, K. *Chem. Rev.* **2005**, *105*, 3272.
192. For selected references, see: (a) Abu-Gnim, C.; Amer, I. *J. Chem. Soc., Chem. Commun.* **1994**, 115. (b) Fernanzed, E.; Hooper, M. W.; Knight, F. I.; Brown, J. M. *Chem. Commun.* **1997**, 173. (c) Kwong, F. Y.; Yang, Q.; Mak, T. C. W.; Chan, A. S. C.; Chan, K. S. *J. Org. Chem.* **2002**, *67*, 2769. (d) Tao, B.; Fu, G. C. *Angew. Chem.* **2002**, *41*, 3892. (e) Bunlaksananusorn, T.; Polborn, K.; Knochel, P. *Angew. Chem. Int. Ed.* **2003**, *42*, 3941. (f) Drury III, W. J.; Zimmermann, N.; Keenan, M.; Hayashi, M.; Kaiser, S.; Richard Goddard, R.; Pfaltz, A. *Angew. Chem. Int. Ed.* **2004**, *43*, 70. (g) Kaiser, S.; Smidt, S. P.; Pfaltz, A. *Angew. Chem. Int. Ed.* **2006**, *45*, 5194. (h) Wang, A.; Wüstenberg, B.; and Pfaltz, A. *Angew. Chem. Int. Ed.*

- 2008**, *47*, 2298. (i) Jiang, B.; Lei, Y.; Zhao, X-L. *J. Org. Chem.* **2008**, *73*, 7833. (j) Lai, H.; Huang, Z.; Wu, Q.; Qin, Y. *J. Org. Chem.* **2009**, *74*, 283.
193. (a) Wicht, D. K.; Glueck, D. S. In *Catalytic Hetero-functionalization*; Togni, A., Grutzmacher, H., Eds.; Wiley-VCH: Weinheim, Germany, 2001, Chapter 5; (b) Engel, R.; Cohen, J. L. I. *Synthesis of Carbon–Phosphorus Bonds*, 2nd ed.; CRC Press: Boca Raton, FL, 2003.
194. Bunlaksananusorn, T.; Knochel, P. *Tetrahedron Lett.* **2002**, *43*, 5817, and references cited therein.
195. (a) Hoff, M. C.; Hill, P. *J. Org. Chem.* **1959**, *24*, 356. (b) Ismail, I.; Rios, R.; Vesely, J.; Hammar, P.; Eriksson, L.; Himo, F.; Córdova, A. *Angew. Chem. Int. Ed.* **2007**, *46*, 4507.
196. (a) Therrien, B.; König, A.; Ward, T. R. *Organometallics* **1999**, *18*, 1565. (b) Therrien, B.; Ward, T. R. *Angew. Chem., Int. Ed. Engl.* **1999**, *38*, 405. (c) Trofimov, B. A.; Malysheva, S. F.; Sukhov, B. G.; Belogorlova, N. A.; Schmidt, E.Y.; Sobenina, L. N.; Kuimov, V. A.; Gusarova, N. K. *Tetrahedron Lett.* **2003**, *44*, 2629.
197. (a) Pryde, A.; Shaw, B. L.; Weeks, B. *J. Chem. Soc., Dalton Trans.* **1976**, 322. (b) Zeizinger, M.; Burda, J. V.; Šponer, J.; Kapsa, V.; Leszczynski, J. *J. Phys. Chem. A* **2001**, *105*, 8086. (c) Wu, H-R.; Liu, Y-H.; Peng, S-M.; Liu, S-T. *Eur. J. Inorg. Chem.* **2003**, 3152.
198. (a) Corey, E. J.; Bailar, J. C. *J. Am. Chem. Soc.* **1959**, *81*, 2620. (b) MacNeil, P. A.; Roberts, N. K.; Bosnich, B. *J. Am. Chem. Soc.* **1981**, *103*, 2273.

199. Yeo, W. C.; Tang, L.; Yan, B.; Tee, S. Y.; Koh, L. L.; Geok, K.; Leung, P. H. *Organometallics* **2005**, *24*, 5581.
200. (a) Costa, E.; Pringle, P. G.; Smith, M. B.; Worboys, K. *J. Chem. Soc., Dalton Trans.* **1997**, 4277 and references cited therein. (b) Wicht, D. K.; Kourkine, I. V.; Kovacik, I.; Glueck, D. S.; Concolino, T. E.; Yap, G. P. A.; Incarvito, C. D.; Rheingold, A. L. *Organometallics* **1999**, *18*, 5381. (c) Shulyupin, M. O.; Kazankova, M. A.; Beletskaya, I. P. *Org. Lett.* **2002**, *4*, 761 and references cited therein. (d) Douglass, M. R.; Stern, C. L.; Marks, T. J. *J. Am. Chem. Soc.* **2001**, *123*, 10221. (e) Malisch, W.; Klüpfel, B.; Schumacher, D.; Nieger, M. *J. Organomet. Chem.* **2002**, *661*, 95. (f) Sadow, A. D.; Togni, A. *J. Am. Chem. Soc.* **2005**, *127*, 17012. (g) Kondoh, A.; Yorimitsu, H.; Oshima, K. *J. Am. Chem. Soc.* **2007**, *129*, 4099.
- 201.(a) Gomez, M.; Granell, J.; Martinez, M. *Organometallics* **1997**, *16*, 2539. (b) Lopez, C.; Bosque, R.; Sainz, D.; Font-Bardia, M. *Organometallics* **1997**, *16*, 3261. (c) Gomez, M.; Granell, J.; Martinez, M. *J. Chem. Soc., Dalton Trans.* **1998**, 37.
202. Chooi, S. Y. M.; Leung, P. H.; Lim, C. C.; Mok, K. F.; Quek, G. H.; Sim, K. Y.; Tan, M. K. *Tetrahedron: Asymmetry* **1992**, *3*, 529.
203. Bakó, T.; Bakó, P.; Keglevich, G.; Báthori, N.; Czugler, M.; Tatai, J.; Novák, T.; Parlagh, G.; Töke, L. *Tetrahedron: Asymmetry* **2003**, *14*, 1917.
204. Bull, S. D.; Davies, S. G.; Fox, D. J.; Gianotti, M.; Kelly, P. M.; Camille Pierres, Savory, E. D.; Smith, A. D. *J. Chem. Soc., Perkin Trans. 1*, **2002**, 1858.

205. King, R. B.; Kapoor, P. N. *J. Am. Chem. Soc.* **1971**, *93*, 4158.
206. King, R. B.; Efraty, A. *J. Chem. Soc., Perkin Trans. 1* **1974**, *11*, 1452.
207. Maitra, K.; Catalano, V. J.; Clark, J.; Nelson, J. H. *Inorg. Chem.* **1998**, *37*, 1105.
208. (a) Murrer, B. A.; Brown, J. M.; Chaloner, P. A.; Nicholson, P. N.; Parker, D. *Synthesis* **1979**, 350. (b) Tan, D.-M.; Chan, K. S. *Tetrahedron Lett.* **2005**, *46*, 503. (c) Wang, C. Y.; Tan, D.-M.; Chan, K. S.; Liu, Y.-H.; Peng, S.-M.; Liu, S.-T.; *J. Organomet. Chem.* **2005**, *690*, 4920. (d) Payne, N. C.; Stephan, D. W. *Inorg. Chem.* **1982**, *21*, 182.
209. Liu, F.; Pullarkat, S. A.; Li, Y.; Chen, S.; Yuan, M.; Lee, Z.; Leung, P. H. *Organometallics* **2009**, *28*, 3941.
210. Pauling, L. *The Nature of the Chemical Bond*; Cornell University Press: Ithaca, NY, **1967**.
211. Mann, F. G.; Pragnell, M. J.; *J. Chem. Soc.* **1965**, 4120.
- 212.(a) Reineri, F.; Viale, A.; Giovenzana, G.; Santelia, D.; Dastru, W.; Gobetto, R.; Aime, S. *J. Am. Chem. Soc.* **2008**, *130*, 15047. (b) Adams, R. D.; Qu, B.; Smith, M. D. *Organometallics* **2002**, *21*, 4847. (c) Hintermann, L.; Dang, T. T.; Labonne, A.; Kribber, T.; Xiao, L.; Naumov, P. *Chem. Eur J.* **2009**, *15*, 7167. (d) Iwadate, N.; Suginome, M. *Org. Lett.* **2009**, *11*, 1899.
- 213.(a) Mann, F. G.; Millar, I. T. *J. Chem. Soc.* **1952**, 4453. (b) Aguiar, A. M.; Archibald, T. G. *Tetrahedron Lett.* **1966**, 5471. (c) Weiner, M. A.; Pasternack, G. J. *Org. Chem.* **1969**, *34*, 1130. (d) Delacroix, O.; Gaumont, A.C. *Current Organic Chemistry* **2005**, *9*, 1851.

214. Dombek, B. D. *J. Org. Chem.* **1978**, *43*, 3408.
215. (a) King, R. B. *Acc. Chem. Res.* **1972**, *5*, 177 and refs therein. (b) Bookham, J. L.; McFarlane, W.; Thornton-Pett, M.; Jones, S. *J. Chem. Soc., Dalton Trans.* **1990**, 3621. (c) Bookham, J. L.; Smithies, D. M.; Wright, A.; Thornton-Pett, M.; McFarlane, W. *J. Chem. Soc., Dalton Trans.* **1998**, 811. (d) Bunlaksananusorn, T.; Knochel, P. *Tetrahedron Lett.* **2002**, *43*, 5817.
216. (a) DuBois, D. L.; Miedaner, A.; Haltiwanger, R. C. *J. Am. Chem. Soc.* **1991**, *113*, 8753. (b) Deprèle, S.; Montchamp, J. L. *J. Org. Chem.* **2001**, *66*, 6745. (c) Trofimov, B. A.; Malysheva, S. F.; Sukhov, B. G.; Belogorlova, N. A.; Schmidt, E. Y.; Sobenina, L. N.; Kuimov, V. A.; Gusarova, N. K. *Tetrahedron Lett.* **2003**, *44*, 2629.
217. (a) Takaki, K.; Takeda, M.; Koshoji, G.; Shishido, T.; Takehira, K. *Tetrahedron Lett.* **2001**, *42*, 6357. (b) Takaki, K.; Komeyama, K.; Takehira, K. *Tetrahedron* **2003**, *59*, 10381. (c) Takaki, K.; Koshoji, G.; Komeyama, K.; Takeda, M.; Shishido, T.; Kitani, A.; Takehira, K. *J. Org. Chem.* **2003**, *68*, 6554.
218. (a) Kazankova, M. A.; Efimova, I. V.; Kochetkov, A. N.; Afanas'ev, V. V.; Beletskaya, I. P.; Dixneuf, P. H. *Synlett* **2001**, 497. (b) Kazankova, M. A.; Efimova, I. V.; Kochetkov, A. N.; Afanas'ev, V. V.; Beletskaya, I. P. *Russ. J. Org. Chem.* **2002**, *38*, 1465.
219. Treichel, P. M.; Wong, W. K. *J. Organomet. Chem.* **1978**, *157*, C5.
220. Roberts, N.; Wild, S. B. *J. Am. Chem. Soc.* **1979**, *101*, 6254.
221. Carty, A. J.; Hota, N. K.; Patel, H. A.; O'Connor, T. J. *Can. J. Chem.* **1971**, *49*,

2707.

## Publications

1. Kien-Wee Tan, **Fengli Liu**, Yongxin Li, Geok-Kheng Tan, Pak-Hing Leung\*, Asymmetric synthesis of a chiral arsinophosphine via a metal template promoted asymmetric Diels-Alder reaction between diphenylvinylphosphine and 2-furyldiphenylarsine *Journal of Organometallic Chemistry* **2006**, 691, 22, 4753.
2. **Fengli Liu**, Sumod A. Pullarkat, Yongxin Li, Shuli Chen, Mingjun Yuan, Zhi-Yi Lee, Pak-Hing Leung\*, “Highly Enantioselective Synthesis of (2-Pyridyl)phosphine based C-chiral Unsymmetrical P,N-Ligands Using a Chiral Palladium Complex” *Organometallics* **2009**, 28,13,3941.
3. **Fengli Liu**, Sumod A. Pullarkat, Yongxin Li, Shuli Chen, Pak-Hing Leung\*, “A Novel Enantioselective Synthesis of Functionalized Pyridylarsanes by a Chiral Palladium Template Promoted Asymmetric Hydroarsanation Reaction” *European Journal of Inorganic Chemistry* **2009**. 4134.
4. **Fengli Liu**, Sumod A. Pullarkat, Kien-Wee Tan, Yongxin Li, Pak-Hing Leung\* “Organoplatinum Complex Promoted the Asymmetric Endo Stereochemically Controlled Diels-Alder Reaction between 3-Diphenylphosphinofuran and Diphenylvinylphosphine” *Inorganic Chemistry*, accepted.
5. **Fengli Liu**, Sumod A. Pullarkat, Kien-Wee Tan, Yongxin Li, Pak-Hing Leung\* “Enantioselective Diels-Alder reaction of 3-Diphenylphosphinofuran with 1-Phenyl-3,4-dimethylphosphole and Subsequent Synthetic Manipulations of the Cycloadduct” *Organometallics*, accepted.

## Appendix

**Table A1. Crystal Data and Structure Refinement for *endo-114***

Empirical formula	C <sub>30</sub> H <sub>26</sub> Cl <sub>2</sub> O P <sub>2</sub> Pt
Formula weight	730.44
Temperature	173(2) K
Wavelength	0.71073 Å
Crystal system	Monoclinic
Space group	P2(1)
Unit cell dimensions	a = 11.1119(5) Å      α = 90°. b = 17.0141(6) Å      β = 90.983(2)°. c = 14.4999(6) Å      γ = 90°.
Volume	2740.93(19) Å <sup>3</sup>
Z	4
Density (calculated)	1.770 Mg/m <sup>3</sup>
Absorption coefficient	5.454 mm <sup>-1</sup>
F(000)	1424
Crystal size	0.25 x 0.20 x 0.15 mm <sup>3</sup>
Theta range for data collection	1.40 to 28.00°
Index ranges	-14 ≤ h ≤ 14, -22 ≤ k ≤ 22, -19 ≤ l ≤ 19
Reflections collected	48195
Independent reflections	12971 [R(int) = 0.0286]
Completeness to theta = 28.00°	100.0 %
Absorption correction	Semi-empirical from equivalents
Max. and min. transmission	0.4951 and 0.3426
Refinement method	Full-matrix least-squares on F <sup>2</sup>
Data / restraints / parameters	12971 / 85 / 649
Goodness-of-fit on F <sup>2</sup>	0.947
Final R indices [I > 2σ(I)]	R1 = 0.0181, wR2 = 0.0381
R indices (all data)	R1 = 0.0198, wR2 = 0.0388
Absolute structure parameter	0.003(2)
Largest diff. peak and hole	0.794 and -0.590 e.Å <sup>-3</sup>

**Table A2. Crystal Data and Structure Refinement for *endo-116b***

Empirical formula	C <sub>45</sub> H <sub>44</sub> Cl <sub>3</sub> N O <sub>5</sub> P <sub>2</sub> Pt	
Formula weight	1042.19	
Temperature	296(2) K	
Wavelength	0.71073 Å	
Crystal system	Orthorhombic	
Space group	P2(1)2(1)2(1)	
Unit cell dimensions	a = 10.0786(17) Å	α = 90°.
	b = 10.2927(15) Å	β = 90°.
	c = 42.255(7) Å	γ = 90°.
Volume	4383.4(12) Å <sup>3</sup>	
Z	4	
Density (calculated)	1.579 Mg/m <sup>3</sup>	
Absorption coefficient	3.502 mm <sup>-1</sup>	
F(000)	2080	
Crystal size	0.20 x 0.20 x 0.16 mm <sup>3</sup>	
Theta range for data collection	0.96 to 27.00°	
Index ranges	-12 ≤ h ≤ 12, -7 ≤ k ≤ 13, -53 ≤ l ≤ 53	
Reflections collected	31320	
Independent reflections	9507 [R(int) = 0.0617]	
Completeness to theta = 27.00°	99.4 %	
Absorption correction	Semi-empirical from equivalents	
Max. and min. transmission	0.6042 and 0.5410	
Refinement method	Full-matrix least-squares on F <sup>2</sup>	
Data / restraints / parameters	9507 / 191 / 517	
Goodness-of-fit on F <sup>2</sup>	1.153	
Final R indices [I > 2σ(I)]	R1 = 0.0441, wR2 = 0.0996	
R indices (all data)	R1 = 0.0606, wR2 = 0.1324	
Absolute structure parameter	0.045(10)	
Largest diff. peak and hole	0.830 and -1.801 e.Å <sup>-3</sup>	

**Table A3. Crystal Data and Structure Refinement for *endo*-119**

Empirical formula	C <sub>33</sub> H <sub>30</sub> I <sub>2</sub> O <sub>3</sub> P <sub>2</sub> Pt
Formula weight	985.40
Temperature	296(2) K
Wavelength	0.71073 Å
Crystal system	Orthorhombic
Space group	P2(1)2(1)2(1)
Unit cell dimensions	a = 10.7290(3) Å      α = 90°. b = 17.1175(4) Å      β = 90°. c = 17.8711(4) Å      γ = 90°.
Volume	3282.09(14) Å <sup>3</sup>
Z	4
Density (calculated)	1.994 Mg/m <sup>3</sup>
Absorption coefficient	6.286 mm <sup>-1</sup>
F(000)	1864
Crystal size	0.28 x 0.26 x 0.24 mm <sup>3</sup>
Theta range for data collection	1.65 to 30.61°
Index ranges	-13 ≤ h ≤ 15, -24 ≤ k ≤ 24, -25 ≤ l ≤ 25
Reflections collected	61823
Independent reflections	10064 [R(int) = 0.0346]
Completeness to theta = 30.61°	99.9 %
Absorption correction	Semi-empirical from equivalents
Max. and min. transmission	0.3138 and 0.2720
Refinement method	Full-matrix least-squares on F <sup>2</sup>
Data / restraints / parameters	10064 / 64 / 391
Goodness-of-fit on F <sup>2</sup>	1.034
Final R indices [I > 2σ(I)]	R1 = 0.0252, wR2 = 0.0508
R indices (all data)	R1 = 0.0394, wR2 = 0.0557
Absolute structure parameter	-0.003(3)
Largest diff. peak and hole	0.803 and -1.272 e.Å <sup>-3</sup>

**Table A4. Crystal Data and Structure Refinement for *endo-122a***

Identification code	leung232	
Empirical formula	C <sub>40</sub> H <sub>40</sub> BF <sub>4</sub> NO <sub>2</sub> P <sub>2</sub> Pt · 0.75CH <sub>2</sub> Cl <sub>2</sub> · H <sub>2</sub> O	
Formula weight	976.28	
Temperature	173(2) K	
Wavelength	0.71073 Å	
Crystal system	Monoclinic	
Space group	C2	
Unit cell dimensions	a = 41.4687(15) Å	α = 90°.
	b = 10.2502(4) Å	β = 93.778(2)°.
	c = 18.7603(7) Å	γ = 90°.
Volume	7957.0(5) Å <sup>3</sup>	
Z	8	
Density (calculated)	1.630 Mg/m <sup>3</sup>	
Absorption coefficient	3.763 mm <sup>-1</sup>	
F(000)	3884	
Crystal size	0.25 x 0.20 x 0.10 mm <sup>3</sup>	
Theta range for data collection	1.97 to 30.50°	
Index ranges	-57 ≤ h ≤ 58, -14 ≤ k ≤ 14, -26 ≤ l ≤ 26	
Reflections collected	60390	
Independent reflections	22703 [R(int) = 0.0328]	
Completeness to theta = 30.50°	99.6 %	
Absorption correction	Semi-empirical from equivalents	
Max. and min. transmission	0.7047 and 0.4530	
Refinement method	Full-matrix least-squares on F <sup>2</sup>	
Data / restraints / parameters	22703 / 3 / 966	
Goodness-of-fit on F <sup>2</sup>	1.011	
Final R indices [I > 2σ(I)]	R1 = 0.0311, wR2 = 0.0705	
R indices (all data)	R1 = 0.0377, wR2 = 0.0727	
Absolute structure parameter	-0.012(3)	
Largest diff. peak and hole	2.121 and -1.381 e.Å <sup>-3</sup>	

**Table A5. Crystal Data and Structure Refinement for *endo*-123**

Empirical formula	C <sub>26</sub> H <sub>24</sub> Cl <sub>2</sub> O P <sub>2</sub> Pt
Formula weight	680.38
Temperature	173(2) K
Wavelength	0.71073 Å
Crystal system	Monoclinic
Space group	P2(1)
Unit cell dimensions	a = 7.8064(2) Å      α = 90°. b = 19.7736(6) Å      β = 110.3940(10)°. c = 8.4846(3) Å      γ = 90°.
Volume	1227.59(7) Å <sup>3</sup>
Z	2
Density (calculated)	1.841 Mg/m <sup>3</sup>
Absorption coefficient	6.081 mm <sup>-1</sup>
F(000)	660
Crystal size	0.25 x 0.25 x 0.20 mm <sup>3</sup>
Theta range for data collection	2.56 to 30.57°
Index ranges	-11 ≤ h ≤ 11, -28 ≤ k ≤ 25, -12 ≤ l ≤ 12
Reflections collected	22218
Independent reflections	6879 [R(int) = 0.0302]
Completeness to theta = 30.57°	99.4 %
Absorption correction	Semi-empirical from equivalents
Max. and min. transmission	0.3760 and 0.3117
Refinement method	Full-matrix least-squares on F <sup>2</sup>
Data / restraints / parameters	6879 / 1 / 289
Goodness-of-fit on F <sup>2</sup>	1.158
Final R indices [I > 2σ(I)]	R1 = 0.0243, wR2 = 0.0529
R indices (all data)	R1 = 0.0258, wR2 = 0.0549
Absolute structure parameter	0.037(5)
Largest diff. peak and hole	2.082 and -1.196 e.Å <sup>-3</sup>

**Table A6. Crystal Data and Structure Refinement for *endo*-126**

Empirical formula	C <sub>26</sub> H <sub>24</sub> Cl <sub>2</sub> O P <sub>2</sub> Pt	
Formula weight	680.38	
Temperature	273(2) K	
Wavelength	0.71073 Å	
Crystal system	Monoclinic	
Space group	P2(1)/n	
Unit cell dimensions	a = 10.9588(5) Å	α = 90°.
	b = 14.6679(7) Å	β = 95.564(3)°.
	c = 15.2178(6) Å	γ = 90°.
Volume	2434.62(19) Å <sup>3</sup>	
Z	4	
Density (calculated)	1.856 Mg/m <sup>3</sup>	
Absorption coefficient	6.132 mm <sup>-1</sup>	
F(000)	1320	
Crystal size	0.24 x 0.22 x 0.16 mm <sup>3</sup>	
Theta range for data collection	2.19 to 30.53°	
Index ranges	-15 ≤ h ≤ 14, -20 ≤ k ≤ 20, -21 ≤ l ≤ 21	
Reflections collected	34391	
Independent reflections	7064 [R(int) = 0.0325]	
Completeness to theta = 25.00°	97.5 %	
Absorption correction	Semi-empirical from equivalents	
Max. and min. transmission	0.4404 and 0.3208	
Refinement method	Full-matrix least-squares on F <sup>2</sup>	
Data / restraints / parameters	7064 / 0 / 289	
Goodness-of-fit on F <sup>2</sup>	1.037	
Final R indices [I > 2σ(I)]	R1 = 0.0178, wR2 = 0.0394	
R indices (all data)	R1 = 0.0218, wR2 = 0.0405	
Largest diff. peak and hole	0.493 and -1.288 e.Å <sup>-3</sup>	

**Table A7. Crystal Data and Structure Refinement for(R)-127**

Empirical formula	C <sub>28</sub> H <sub>27</sub> Cl N O <sub>2</sub> P Pt	
Formula weight	671.02	
Temperature	173(2) K	
Wavelength	0.71073 Å	
Crystal system	Orthorhombic	
Space group	P2(1)2(1)2(1)	
Unit cell dimensions	a = 12.7754(6) Å	α = 90°.
	b = 13.0064(5) Å	β = 90°.
	c = 15.4619(7) Å	γ = 90°.
Volume	2569.18(19) Å <sup>3</sup>	
Z	4	
Density (calculated)	1.735 Mg/m <sup>3</sup>	
Absorption coefficient	5.653 mm <sup>-1</sup>	
F(000)	1312	
Crystal size	0.25 x 0.25 x 0.20 mm <sup>3</sup>	
Theta range for data collection	2.05 to 30.50°	
Index ranges	-17 ≤ h ≤ 18, -18 ≤ k ≤ 16, -22 ≤ l ≤ 16	
Reflections collected	18258	
Independent reflections	7735 [R(int) = 0.0317]	
Completeness to theta = 30.50°	99.4 %	
Absorption correction	Semi-empirical from equivalents	
Max. and min. transmission	0.3977 and 0.3322	
Refinement method	Full-matrix least-squares on F <sup>2</sup>	
Data / restraints / parameters	7735 / 18 / 310	
Goodness-of-fit on F <sup>2</sup>	0.932	
Final R indices [I > 2σ(I)]	R1 = 0.0267, wR2 = 0.0565	
R indices (all data)	R1 = 0.0317, wR2 = 0.0578	
Absolute structure parameter	0.022(5)	
Largest diff. peak and hole	1.044 and -0.626 e.Å <sup>-3</sup>	

**Table A8. Crystal Data and Structure Refinement for *endo*-129**

Empirical formula	C <sub>28</sub> H <sub>24</sub> I <sub>2</sub> O <sub>2</sub> P <sub>2</sub> Pt
Formula weight	903.30
Temperature	173(2) K
Wavelength	0.71073 Å
Crystal system	Orthorhombic
Space group	P2(1)2(1)2
Unit cell dimensions	a = 14.1983(6) Å      α = 90°. b = 21.4240(10) Å     β = 90°. c = 9.2044(4) Å        γ = 90°.
Volume	2799.8(2) Å <sup>3</sup>
Z	4
Density (calculated)	2.143 Mg/m <sup>3</sup>
Absorption coefficient	7.355 mm <sup>-1</sup>
F(000)	1688
Crystal size	0.26 x 0.18 x 0.08 mm <sup>3</sup>
Theta range for data collection	1.72 to 31.18°
Index ranges	-20 ≤ h ≤ 19, -30 ≤ k ≤ 29, -13 ≤ l ≤ 13
Reflections collected	32074
Independent reflections	8991 [R(int) = 0.0492]
Completeness to theta = 31.18°	99.4 %
Absorption correction	Semi-empirical from equivalents
Max. and min. transmission	0.5907 and 0.2508
Refinement method	Full-matrix least-squares on F <sup>2</sup>
Data / restraints / parameters	8991 / 225 / 362
Goodness-of-fit on F <sup>2</sup>	1.045
Final R indices [I > 2σ(I)]	R1 = 0.0334, wR2 = 0.0927
R indices (all data)	R1 = 0.0410, wR2 = 0.1123
Absolute structure parameter	0.043(6)
Largest diff. peak and hole	1.650 and -2.451 e.Å <sup>-3</sup>

**Table A9. Crystal Data and Structure Refinement for (R<sub>C</sub>,S<sub>P</sub>)-138b**

Empirical formula	C <sub>43.50</sub> H <sub>45</sub> Cl <sub>4</sub> N O <sub>5</sub> P <sub>2</sub> Pt	
Formula weight	1060.64	
Temperature	173(2) K	
Wavelength	0.71073 Å	
Crystal system	Orthorhombic	
Space group	P2(1)2(1)2(1)	
Unit cell dimensions	a = 10.2693(4) Å	α = 90°.
	b = 18.0459(8) Å	β = 90°.
	c = 25.1613(11) Å	γ = 90°.
Volume	4662.9(3) Å <sup>3</sup>	
Z	4	
Density (calculated)	1.511 Mg/m <sup>3</sup>	
Absorption coefficient	3.349 mm <sup>-1</sup>	
F(000)	2116	
Crystal size	0.20 x 0.10 x 0.10 mm <sup>3</sup>	
Theta range for data collection	2.14 to 30.54°	
Index ranges	-11 ≤ h ≤ 14, -25 ≤ k ≤ 25, -34 ≤ l ≤ 35	
Reflections collected	37115	
Independent reflections	14107 [R(int) = 0.0344]	
Completeness to theta = 30.54°	99.3 %	
Absorption correction	Semi-empirical from equivalents	
Max. and min. transmission	0.7306 and 0.5539	
Refinement method	Full-matrix least-squares on F <sup>2</sup>	
Data / restraints / parameters	14107 / 3 / 528	
Goodness-of-fit on F <sup>2</sup>	0.989	
Final R indices [I > 2σ(I)]	R1 = 0.0363, wR2 = 0.0706	
R indices (all data)	R1 = 0.0529, wR2 = 0.0751	
Absolute structure parameter	0.002(4)	
Largest diff. peak and hole	1.126 and -0.436 e.Å <sup>-3</sup>	

**Table A10. Crystal Data and Structure Refinement for (S<sub>P</sub>)-139**

Empirical formula	C <sub>28</sub> H <sub>26</sub> Cl <sub>2</sub> O P <sub>2</sub> Pt
Formula weight	706.42
Temperature	296(2) K
Wavelength	0.71073 Å
Crystal system	Orthorhombic
Space group	P2(1)2(1)2(1)
Unit cell dimensions	a = 9.8151(3) Å      α = 90°. b = 12.5262(4) Å      β = 90°. c = 22.0264(7) Å      γ = 90°.
Volume	2708.06(15) Å <sup>3</sup>
Z	4
Density (calculated)	1.733 Mg/m <sup>3</sup>
Absorption coefficient	5.516 mm <sup>-1</sup>
F(000)	1376
Crystal size	0.14 x 0.10 x 0.08 mm <sup>3</sup>
Theta range for data collection	2.27 to 30.59°
Index ranges	-14 ≤ h ≤ 14, -17 ≤ k ≤ 17, -31 ≤ l ≤ 31
Reflections collected	66946
Independent reflections	8285 [R(int) = 0.0320]
Completeness to theta = 30.59°	99.6 %
Absorption correction	Semi-empirical from equivalents
Max. and min. transmission	0.6666 and 0.5122
Refinement method	Full-matrix least-squares on F <sup>2</sup>
Data / restraints / parameters	8285 / 0 / 309
Goodness-of-fit on F <sup>2</sup>	0.964
Final R indices [I > 2σ(I)]	R1 = 0.0166, wR2 = 0.0289
R indices (all data)	R1 = 0.0210, wR2 = 0.0297
Absolute structure parameter	-0.007(2)
Largest diff. peak and hole	0.639 and -0.271 e.Å <sup>-3</sup>

**Table A11. Crystal Data and Structure Refinement for (S<sub>P</sub>)-140**

Empirical formula	C <sub>30</sub> H <sub>30</sub> Cl <sub>8</sub> O <sub>2</sub> P <sub>2</sub> Pt
Formula weight	963.17
Temperature	173(2) K
Wavelength	0.71073 Å
Crystal system	Orthorhombic
Space group	P2(1)2(1)2(1)
Unit cell dimensions	a = 13.6338(5) Å      α = 90°. b = 14.5439(5) Å      β = 90°. c = 17.8652(7) Å      γ = 90°.
Volume	3542.5(2) Å <sup>3</sup>
Z	4
Density (calculated)	1.806 Mg/m <sup>3</sup>
Absorption coefficient	4.683 mm <sup>-1</sup>
F(000)	1880
Crystal size	0.30 x 0.20 x 0.20 mm <sup>3</sup>
Theta range for data collection	1.81 to 30.60°
Index ranges	-19 ≤ h ≤ 19, -20 ≤ k ≤ 20, -25 ≤ l ≤ 25
Reflections collected	28061
Independent reflections	10641 [R(int) = 0.0296]
Completeness to theta = 30.60°	99.5 %
Absorption correction	Semi-empirical from equivalents
Max. and min. transmission	0.4544 and 0.3340
Refinement method	Full-matrix least-squares on F <sup>2</sup>
Data / restraints / parameters	10641 / 0 / 391
Goodness-of-fit on F <sup>2</sup>	1.040
Final R indices [I > 2σ(I)]	R1 = 0.0368, wR2 = 0.0975
R indices (all data)	R1 = 0.0461, wR2 = 0.1075
Absolute structure parameter	0.024(6)
Largest diff. peak and hole	1.750 and -1.416 e.Å <sup>-3</sup>

**Table A12. Crystal Data and Structure Refinement for (S<sub>P</sub>)-142**

Empirical formula	C <sub>35</sub> H <sub>32</sub> I <sub>2</sub> O <sub>3</sub> P <sub>2</sub> Pt
Formula weight	1011.44
Temperature	173(2) K
Wavelength	0.71073 Å
Crystal system	Orthorhombic
Space group	P2(1)2(1)2(1)
Unit cell dimensions	a = 12.3171(2) Å      α = 90°. b = 14.4668(2) Å      β = 90°. c = 18.6833(3) Å      γ = 90°.
Volume	3329.16(9) Å <sup>3</sup>
Z	4
Density (calculated)	2.018 Mg/m <sup>3</sup>
Absorption coefficient	6.200 mm <sup>-1</sup>
F(000)	1920
Crystal size	0.30 x 0.16 x 0.16 mm <sup>3</sup>
Theta range for data collection	2.17 to 35.22°
Index ranges	-19 ≤ h ≤ 19, -23 ≤ k ≤ 22, -30 ≤ l ≤ 30
Reflections collected	47363
Independent reflections	14708 [R(int) = 0.0340]
Completeness to theta = 35.22°	99.8 %
Absorption correction	Semi-empirical from equivalents
Max. and min. transmission	0.4370 and 0.2578
Refinement method	Full-matrix least-squares on F <sup>2</sup>
Data / restraints / parameters	14708 / 0 / 390
Goodness-of-fit on F <sup>2</sup>	1.023
Final R indices [I > 2σ(I)]	R1 = 0.0293, wR2 = 0.0637
R indices (all data)	R1 = 0.0407, wR2 = 0.0826
Absolute structure parameter	-0.002(3)
Largest diff. peak and hole	1.126 and -1.715 e.Å <sup>-3</sup>

**Table A13. Crystal Data and Structure Refinement for (R)-146**

Empirical formula	C <sub>26</sub> H <sub>22</sub> Cl <sub>2</sub> N O P Pd
Formula weight	572.72
Temperature	173(2) K
Wavelength	0.71073 Å
Crystal system	Orthorhombic
Space group	P2(1)2(1)2(1)
Unit cell dimensions	a = 8.9444(2) Å      α = 90°. b = 10.3498(3) Å      β = 90°. c = 25.0386(7) Å      γ = 90°.
Volume	2317.89(11) Å <sup>3</sup>
Z	4
Density (calculated)	1.641 Mg/m <sup>3</sup>
Absorption coefficient	1.120 mm <sup>-1</sup>
F(000)	1152
Crystal size	0.20 x 0.20 x 0.18 mm <sup>3</sup>
Theta range for data collection	3.01 to 36.49°
Index ranges	-14 ≤ h ≤ 14, -10 ≤ k ≤ 17, -40 ≤ l ≤ 40
Reflections collected	38018
Independent reflections	10761 [R(int) = 0.0318]
Completeness to theta = 36.49°	97.9 %
Absorption correction	Semi-empirical from equivalents
Max. and min. transmission	0.8238 and 0.8070
Refinement method	Full-matrix least-squares on F <sup>2</sup>
Data / restraints / parameters	10761 / 0 / 289
Goodness-of-fit on F <sup>2</sup>	1.059
Final R indices [I > 2σ(I)]	R1 = 0.0275, wR2 = 0.0551
R indices (all data)	R1 = 0.0313, wR2 = 0.0564
Absolute structure parameter	-0.023(12)
Largest diff. peak and hole	0.774 and -0.698 e.Å <sup>-3</sup>

**Table A14. Crystal Data and Structure Refinement for (R<sub>C</sub>, S<sub>C</sub>)-148**

Empirical formula	C <sub>45</sub> H <sub>42</sub> Cl <sub>3</sub> N <sub>2</sub> O <sub>5</sub> P Pd	
Formula weight	934.53	
Temperature	296(2) K	
Wavelength	0.71073 Å	
Crystal system	Monoclinic	
Space group	C2	
Unit cell dimensions	a = 23.971(3) Å	α = 90°.
	b = 10.7414(14) Å	β = 117.146(7)°.
	c = 19.357(3) Å	γ = 90°.
Volume	4435.1(10) Å <sup>3</sup>	
Z	4	
Density (calculated)	1.400 Mg/m <sup>3</sup>	
Absorption coefficient	0.681 mm <sup>-1</sup>	
F(000)	1912	
Crystal size	0.32 x 0.28 x 0.10 mm <sup>3</sup>	
Theta range for data collection	1.73 to 25.00°	
Index ranges	-28 ≤ h ≤ 28, -12 ≤ k ≤ 12, -21 ≤ l ≤ 23	
Reflections collected	25750	
Independent reflections	7730 [R(int) = 0.0591]	
Completeness to theta = 25.00°	99.2 %	
Absorption correction	Semi-empirical from equivalents	
Max. and min. transmission	0.9350 and 0.8116	
Refinement method	Full-matrix least-squares on F <sup>2</sup>	
Data / restraints / parameters	7730 / 52 / 518	
Goodness-of-fit on F <sup>2</sup>	1.071	
Final R indices [I > 2σ(I)]	R1 = 0.0528, wR2 = 0.1179	
R indices (all data)	R1 = 0.0909, wR2 = 0.1535	
Absolute structure parameter	-0.03(4)	
Largest diff. peak and hole	0.701 and -1.168 e.Å <sup>-3</sup>	

**Table A15. Crystal Data and Structure Refinement for ( $R_C$ ,  $S_C$ )-151**

Empirical formula	C40 H40 Cl5 N2 O5 P Pd S
Formula weight	975.42
Temperature	173(2) K
Wavelength	0.71073 Å
Crystal system	Orthorhombic
Space group	P2(1)2(1)2(1)
Unit cell dimensions	a = 10.5379(3) Å $\alpha = 90^\circ$ . b = 14.9811(5) Å $\beta = 90^\circ$ . c = 27.5202(9) Å $\gamma = 90^\circ$ .
Volume	4344.6(2) Å <sup>3</sup>
Z	4
Density (calculated)	1.491 Mg/m <sup>3</sup>
Absorption coefficient	0.863 mm <sup>-1</sup>
F(000)	1984
Crystal size	0.40 x 0.12 x 0.10 mm <sup>3</sup>
Theta range for data collection	1.48 to 30.79°
Index ranges	-14 ≤ h ≤ 15, -21 ≤ k ≤ 21, -39 ≤ l ≤ 39
Reflections collected	47748
Independent reflections	13422 [R(int) = 0.0530]
Completeness to theta = 30.79°	98.9 %
Absorption correction	Semi-empirical from equivalents
Max. and min. transmission	0.9186 and 0.7239
Refinement method	Full-matrix least-squares on F <sup>2</sup>
Data / restraints / parameters	13422 / 118 / 554
Goodness-of-fit on F <sup>2</sup>	1.068
Final R indices [I > 2σ(I)]	R1 = 0.0532, wR2 = 0.1384
R indices (all data)	R1 = 0.0777, wR2 = 0.1602
Absolute structure parameter	-0.04(3)
Largest diff. peak and hole	1.139 and -0.885 e.Å <sup>-3</sup>

**Table A16. Crystal Data and Structure Refinement for ( $R_C$ ,  $S_C$ )-154**

Empirical formula	C <sub>36</sub> H <sub>37</sub> Cl <sub>4</sub> N <sub>2</sub> O <sub>6</sub> P Pd	
Formula weight	872.85	
Temperature	173(2) K	
Wavelength	0.71073 Å	
Crystal system	Triclinic	
Space group	P1	
Unit cell dimensions	a = 9.7638(3) Å	$\alpha = 84.9060(10)^\circ$ .
	b = 9.9971(3) Å	$\beta = 73.042(2)^\circ$ .
	c = 10.0920(3) Å	$\gamma = 66.7710(10)^\circ$ .
Volume	938.04(5) Å <sup>3</sup>	
Z	1	
Density (calculated)	1.545 Mg/m <sup>3</sup>	
Absorption coefficient	0.869 mm <sup>-1</sup>	
F(000)	444	
Crystal size	0.30 x 0.22 x 0.12 mm <sup>3</sup>	
Theta range for data collection	2.83 to 36.57°	
Index ranges	-16 ≤ h ≤ 16, -16 ≤ k ≤ 16, -16 ≤ l ≤ 16	
Reflections collected	42144	
Independent reflections	15882 [R(int) = 0.0295]	
Completeness to theta = 36.57°	99.2 %	
Absorption correction	Semi-empirical from equivalents	
Max. and min. transmission	0.9029 and 0.7805	
Refinement method	Full-matrix least-squares on F <sup>2</sup>	
Data / restraints / parameters	15882 / 3 / 455	
Goodness-of-fit on F <sup>2</sup>	1.010	
Final R indices [I > 2σ(I)]	R1 = 0.0331, wR2 = 0.0657	
R indices (all data)	R1 = 0.0376, wR2 = 0.0686	
Absolute structure parameter	-0.011(9)	
Largest diff. peak and hole	0.438 and -0.706 e.Å <sup>-3</sup>	

**Table A17. Crystal Data and Structure Refinement for ( $R_C$ ,  $S_C$ )-157**

Empirical formula	C <sub>44</sub> H <sub>40</sub> Cl N <sub>2</sub> O <sub>5</sub> P Pd	
Formula weight	849.60	
Temperature	296(2) K	
Wavelength	0.71073 Å	
Crystal system	Orthorhombic	
Space group	P2(1)2(1)2(1)	
Unit cell dimensions	a = 9.877(3) Å	$\alpha = 90^\circ$ .
	b = 19.319(7) Å	$\beta = 90^\circ$ .
	c = 20.743(6) Å	$\gamma = 90^\circ$ .
Volume	3958(2) Å <sup>3</sup>	
Z	4	
Density (calculated)	1.426 Mg/m <sup>3</sup>	
Absorption coefficient	0.625 mm <sup>-1</sup>	
F(000)	1744	
Crystal size	0.32 x 0.26 x 0.20 mm <sup>3</sup>	
Theta range for data collection	1.44 to 25.08°	
Index ranges	-11 ≤ h ≤ 11, -22 ≤ k ≤ 22, -24 ≤ l ≤ 24	
Reflections collected	19776	
Independent reflections	6954 [R(int) = 0.0466]	
Completeness to theta = 25.08°	99.3 %	
Absorption correction	Semi-empirical from equivalents	
Max. and min. transmission	0.8853 and 0.8252	
Refinement method	Full-matrix least-squares on F <sup>2</sup>	
Data / restraints / parameters	6954 / 174 / 539	
Goodness-of-fit on F <sup>2</sup>	1.107	
Final R indices [I > 2σ(I)]	R1 = 0.0400, wR2 = 0.1065	
R indices (all data)	R1 = 0.0532, wR2 = 0.1332	
Absolute structure parameter	-0.03(4)	
Largest diff. peak and hole	0.616 and -0.875 e.Å <sup>-3</sup>	

**Table A18. Crystal Data and Structure Refinement for (R)-161**

Empirical formula	C <sub>26</sub> H <sub>22</sub> As Cl <sub>2</sub> N O Pd
Formula weight	616.67
Temperature	173(2) K
Wavelength	0.71073 Å
Crystal system	Orthorhombic
Space group	P2(1)2(1)2(1)
Unit cell dimensions	a = 8.9848(4) Å      α = 90°. b = 10.5337(5) Å      β = 90°. c = 25.0414(12) Å      γ = 90°.
Volume	2370.00(19) Å <sup>3</sup>
Z	4
Density (calculated)	1.728 Mg/m <sup>3</sup>
Absorption coefficient	2.414 mm <sup>-1</sup>
F(000)	1224
Crystal size	0.26 x 0.20 x 0.20 mm <sup>3</sup>
Theta range for data collection	1.63 to 32.00°
Index ranges	-5 ≤ h ≤ 13, -15 ≤ k ≤ 15, -37 ≤ l ≤ 37
Reflections collected	29480
Independent reflections	8228 [R(int) = 0.0330]
Completeness to theta = 32.00°	100.0 %
Absorption correction	Semi-empirical from equivalents
Max. and min. transmission	0.6439 and 0.5726
Refinement method	Full-matrix least-squares on F <sup>2</sup>
Data / restraints / parameters	8228 / 0 / 289
Goodness-of-fit on F <sup>2</sup>	1.121
Final R indices [I > 2σ(I)]	R1 = 0.0245, wR2 = 0.0556
R indices (all data)	R1 = 0.0310, wR2 = 0.0740
Absolute structure parameter	0.020(7)
Largest diff. peak and hole	0.650 and -0.697 e.Å <sup>-3</sup>

**Table A19. Crystal Data and Structure Refinement for (R)-164**

Empirical formula	C <sub>30</sub> H <sub>24</sub> AsCl <sub>2</sub> NOPd
Formula weight	666.72
Temperature	296(2) K
Wavelength	0.71073 Å
Crystal system	Orthorhombic
Space group	P2(1)2(1)2(1)
Unit cell dimensions	a = 9.1122(4) Å      α = 90°. b = 10.6490(4) Å      β = 90°. c = 27.6610(12) Å      γ = 90°.
Volume	2684.11(19) Å <sup>3</sup>
Z	4
Density (calculated)	1.650 Mg/m <sup>3</sup>
Absorption coefficient	2.138 mm <sup>-1</sup>
F(000)	1328
Crystal size	0.30 x 0.26 x 0.24 mm <sup>3</sup>
Theta range for data collection	2.92 to 27.50.
Index ranges	-9 ≤ h ≤ 11, -13 ≤ k ≤ 13, -33 ≤ l ≤ 35
Reflections collected	19937
Independent reflections	6118 [R(int) = 0.0334]
Completeness to theta = 27.50°	99.7 %
Absorption correction	Semi-empirical from equivalents
Max. and min. transmission	0.6279 and 0.5664
Refinement method	Full-matrix least-squares on F <sup>2</sup>
Data / restraints / parameters	6118 / 0 / 325
Goodness-of-fit on F <sup>2</sup>	1.233
Final R indices [I > 2σ(I)]	R1 = 0.0548, wR2 = 0.1150
R indices (all data)	R1 = 0.0676, wR2 = 0.1218
Absolute structure parameter	0.041(19)
Largest diff. peak and hole	0.912 and -1.272 e.Å <sup>-3</sup>

**Table A20. Crystal Data and Structure Refinement for (R<sub>C</sub>, S<sub>C</sub>)-166**

Empirical formula	C <sub>36</sub> H <sub>38</sub> AsCl <sub>3</sub> N <sub>2</sub> O <sub>6</sub> Pd	
Formula weight	882.35	
Temperature	296(2) K	
Wavelength	0.71073 Å	
Crystal system	Monoclinic	
Space group	P2(1)	
Unit cell dimensions	a = 10.0428(6) Å	α = 90°.
	b = 17.9964(11) Å	β = 94.719(3)°.
	c = 10.3669(6) Å	γ = 90°.
Volume	1867.30(19) Å <sup>3</sup>	
Z	2	
Density (calculated)	1.569 Mg/m <sup>3</sup>	
Absorption coefficient	1.637 mm <sup>-1</sup>	
F(000)	892	
Crystal size	0.30 x 0.30 x 0.10 mm <sup>3</sup>	
Theta range for data collection	1.97 to 30.58°	
Index ranges	-14 ≤ h ≤ 14, -25 ≤ k ≤ 25, -14 ≤ l ≤ 14	
Reflections collected	28535	
Independent reflections	11419 [R(int) = 0.0356]	
Completeness to theta = 30.58°	99.8 %	
Absorption correction	Semi-empirical from equivalents	
Max. and min. transmission	0.8534 and 0.6394	
Refinement method	Full-matrix least-squares on F <sup>2</sup>	
Data / restraints / parameters	11419 / 31 / 446	
Goodness-of-fit on F <sup>2</sup>	1.041	
Final R indices [I > 2σ(I)]	R1 = 0.0414, wR2 = 0.0966	
R indices (all data)	R1 = 0.0675, wR2 = 0.1254	
Absolute structure parameter	0.009(10)	
Largest diff. peak and hole	1.104 and -0.699 e.Å <sup>-3</sup>	

**Table A21. Crystal Data and Structure Refinement for (R<sub>C</sub>,S<sub>P</sub>)-173**

Empirical formula	C <sub>36.50</sub> H <sub>39</sub> Cl <sub>2</sub> N O <sub>4</sub> P <sub>2</sub> Pd	
Formula weight	794.93	
Temperature	173(2) K	
Wavelength	0.71073 Å	
Crystal system	Monoclinic	
Space group	C2	
Unit cell dimensions	a = 23.872(4) Å	α = 90°.
	b = 10.2793(15) Å	β = 104.126(16)°.
	c = 15.057(4) Å	γ = 90°.
Volume	3583.1(12) Å <sup>3</sup>	
Z	4	
Density (calculated)	1.474 Mg/m <sup>3</sup>	
Absorption coefficient	0.796 mm <sup>-1</sup>	
F(000)	1628	
Crystal size	0.30 x 0.28 x 0.10 mm <sup>3</sup>	
Theta range for data collection	1.39 to 30.73°	
Index ranges	-34 ≤ h ≤ 33, -14 ≤ k ≤ 14, -21 ≤ l ≤ 21	
Reflections collected	36284	
Independent reflections	10643 [R(int) = 0.0616]	
Completeness to theta = 30.73°	99.1 %	
Absorption correction	Semi-empirical from equivalents	
Max. and min. transmission	0.9246 and 0.7962	
Refinement method	Full-matrix least-squares on F <sup>2</sup>	
Data / restraints / parameters	10643 / 1 / 425	
Goodness-of-fit on F <sup>2</sup>	1.128	
Final R indices [I > 2σ(I)]	R1 = 0.0413, wR2 = 0.0938	
R indices (all data)	R1 = 0.0579, wR2 = 0.1251	
Absolute structure parameter	0.05(2)	
Largest diff. peak and hole	0.660 and -1.464 e.Å <sup>-3</sup>	

**Table A22. Crystal Data and Structure Refinement for (S<sub>P</sub>)-174**

Empirical formula	C <sub>22.50</sub> H <sub>23</sub> Cl <sub>3</sub> P <sub>2</sub> Pd
Formula weight	568.10
Temperature	173(2) K
Wavelength	0.71073 Å
Crystal system	Orthorhombic
Space group	P2(1)2(1)2(1)
Unit cell dimensions	a = 8.6265(2) Å      α = 90°. b = 13.1695(3) Å      β = 90°. c = 22.0432(5) Å      γ = 90°.
Volume	2504.26(10) Å <sup>3</sup>
Z	4
Density (calculated)	1.507 Mg/m <sup>3</sup>
Absorption coefficient	1.196 mm <sup>-1</sup>
F(000)	1140
Crystal size	0.20 x 0.20 x 0.18 mm <sup>3</sup>
Theta range for data collection	1.80 to 30.62°
Index ranges	-12 ≤ h ≤ 11, -18 ≤ k ≤ 18, -31 ≤ l ≤ 29
Reflections collected	24409
Independent reflections	7555 [R(int) = 0.0561]
Completeness to theta = 30.62°	98.1 %
Absorption correction	Semi-empirical from equivalents
Max. and min. transmission	0.8135 and 0.7959
Refinement method	Full-matrix least-squares on F <sup>2</sup>
Data / restraints / parameters	7555 / 2 / 273
Goodness-of-fit on F <sup>2</sup>	1.221
Final R indices [I > 2σ(I)]	R1 = 0.0615, wR2 = 0.1784
R indices (all data)	R1 = 0.0748, wR2 = 0.2090
Absolute structure parameter	-0.04(5)
Largest diff. peak and hole	1.902 and -2.692 e.Å <sup>-3</sup>

**Table A23. Crystal Data and Structure Refinement for (R<sub>P</sub>,R<sub>P</sub>)-177**

Empirical formula	C <sub>19</sub> H <sub>20</sub> Cl <sub>2</sub> P <sub>2</sub> Pd
Formula weight	487.59
Temperature	173(2) K
Wavelength	0.71073 Å
Crystal system	Orthorhombic
Space group	P2(1)2(1)2(1)
Unit cell dimensions	a = 10.0605(3) Å      α = 90°. b = 13.6842(5) Å      β = 90°. c = 14.8086(4) Å      γ = 90°.
Volume	2038.70(11) Å <sup>3</sup>
Z	4
Density (calculated)	1.589 Mg/m <sup>3</sup>
Absorption coefficient	1.328 mm <sup>-1</sup>
F(000)	976
Crystal size	0.22 x 0.12 x 0.10 mm <sup>3</sup>
Theta range for data collection	2.03 to 30.59°
Index ranges	-12 ≤ h ≤ 14, -18 ≤ k ≤ 19, -21 ≤ l ≤ 21
Reflections collected	20695
Independent reflections	6244 [R(int) = 0.0564]
Completeness to theta = 30.59°	99.7 %
Absorption correction	Semi-empirical from equivalents
Max. and min. transmission	0.8787 and 0.7588
Refinement method	Full-matrix least-squares on F <sup>2</sup>
Data / restraints / parameters	6244 / 0 / 220
Goodness-of-fit on F <sup>2</sup>	1.114
Final R indices [I > 2σ(I)]	R <sub>1</sub> = 0.0388, wR <sub>2</sub> = 0.1007
R indices (all data)	R <sub>1</sub> = 0.0469, wR <sub>2</sub> = 0.1148
Absolute structure parameter	-0.08(3)
Largest diff. peak and hole	1.266 and -0.981 e.Å <sup>-3</sup>